THE EFFECTS OF THE HUMAN OOCYTE VESTMENTS AND FOLLICULAR FLUID ON SPERMATOZOA

by

REBECCA LOUISE FRETTSOME

A thesis submitted to

The University of Birmingham

For the degree of

DOCTOR OF PHILOSOPHY

College of Medical and Dental Sciences

School of Clinical and Experimental Medicine

September 2011

ABSTRACT

Our knowledge of the released human ovulatory components, the cumulus-oocyte complex (COC) and follicular fluid, and their physiological effects on spermatozoa and roles in fertilisation remain poorly characterised. The aim of this study was to use a multi-pronged approach to begin to unravel these interactions and their relation to fertilisation success.

Experiments designed to better replicate the physiological environment of the female tract showed environmental modulation of sperm motility. Mean sperm velocity values VSL, VAP and VCL increased by 12.4%, 15%, 16.5% respectively, when exposed to cumulus cells from pregnancy-positive donors, compared to pregnancy-negative donors.

Follicular fluid elicited a $[Ca^{2+}]_i$ response in spermatozoa that was independent of treatment outcome. The response of spermatozoa exposed to follicular fluid at a 50% (v/v) dilution was a large spike on the front of the 'classical' progesterone transient response, which has not been previously reported.

Human sperm-zona binding (SZB) studies are hampered by the shortage of oocytes, and thus zona pellucida (ZP) available for research. As a possible source of ZP this study investigates the development of an *in vitro* model for oogenesis, utilising follicular fluid and cumulus cell co-culture with human embryonic stem cells. The feasibility of SPR technology, using both native and recombinant sources of ZP, to measure SZB and identify possible binding candidates is also assessed.

The data in this study addresses just some of the potential effects of the COC and follicular fluid on spermatozoa. Further developments within this area may lead to better diagnostics and treatments for patients undergoing ART, in addition to providing targets for novel contraceptives.

DEDICATION

To my Family

ACKNOWLEDGMENTS

I firstly would like to thank my supervisor Dr. Sarah Conner for all her help and support throughout my PhD. I also have to thank Dr. Jackson Kirkman-Brown for his input over the last 4 years in addition to all the members of RBG (both old and new) with special mention to Dr Linda Lefievre, Dr David Foo Joao Correia, Qamar Walayat and Kate Nash,

I also want mention Dr. Stephen Young and Dr. Ashley Martin, thank you, your help and advice was invaluable. Also I would like to say thank you to Dr. Angela Taylor and Dr. Wiebke Arlt for their contribution to this study.

I have to say thank you to the staff at the Assisted Conception Unit, Birmingham Women's Hospital, and all patients and donors that made this work possible.

I am truly grateful for all the support I have received from my friends over the years, but I have to give a very special mention to Alexis Barnett, Thomas Connolly, Leanne, Daniel (and Ella!) Stones, you all have offered me more love and support I could ever ask for and I truly value your lifelong friendship.

Finally I have to thank my family: my Grandparents, Auntie Tracey, Auntie Dawn, Uncle David, Emily and Joseph and especially my wonderful Mum. Without any of you I wouldn't have achieved what I have. I love you all.

CONTENTS

LIST OF FIGURES

LIST OF TABLES

ABBREVIATIONS

$[Ca^{2+}]_i$	Intracellular calcium
ACU	Assisted Conception Unit
ALH	Lateral head displacement
AR	Acrosome reaction
ART	Assisted reproduction technique
BCF	Beat cross frequency
bFGF	Basic fibroblast growth factor
BSA	Bovine serum albumin
Ca^{2+}	Calcium ion
cAMP	Cyclic adenosine monophosphate
CASA	Computer aided sperm analysis
CHO	Chinese hamster ovary
COC	Cumulus oocyte complex
cP	Centipoise
CV	Column volume
ddH_2O	Double distilled water
DMEM	Dulbecco's modified eagle medium
DMSO	Dimethylsulphoxide
DNA	Deoxyribonucleic acid
DTT	Dithiothreitol
EB	Embryoid body
EBSS	Earles balanced salt solution
EDC	1-ethyl-3-(3-dimethylaminopropyl) carbodiimide
EDTA	Sodium ethylene tetraacetate
ES	Embryonic stem
FBS	Fetal bovine serum

FITC	Fluorescein isothiocynate
FSH	Follicle stimulating hormone
GFP	Green fluorescent protein
HBS	HEPES buffered saline
HBSS	HEPES buffered sucrose solution
HEPES	4-(2-hydroxyethyl)-1-piperazineethanesulfonic acid
hESCs	Human embryonic stem cells
HFEA	Human Fertilization and Embryology Authority
hff	Human foreskin fibroblasts
hZP	Human zona pellucida
hZP1	Human zona pellucida protein 1
hZP2	Human zona pellucida protein 2
hZP3	Human zona pellucida protein 3
hZP4	Human zona pellucida protein 4
ICM	Inner cell mass
ICSI	Intracytoplasmic sperm injection
IMDM	Iscove's modified Dulbecco's medium
IP_3	Inositol triphosphate
IP_3R	Inositol triphosphate receptors
IVF	*In vitro* fertilization
LB	Luria-Bertani
LH	Luteinising hormone
mESC	Mouse embryonic stem cell
mZP	Mouse zona pellucida
NEAA	Non essential amino acids
NHS	*N*-Hydroxysuccinimide
NO	Nitric oxide

NTA	Nitrilotriacetic acid
NTA-NH2	(S)-N-(5-Amino-1-Carboxypentyl)iminodiacetic acid
OD	Optical density
PBS	Phosphate buffered saline
PCR	Polymerase chain reaction
PGC	Primordial germ cell
PKA	Protein kinase A
rhZP2	Recombinant human zona pellucida protein 2
rhZP3	Recombinant human zona pellucida protein 3
rhZP4	Recombinant human zona pellucida protein 4
RNA	Ribonucleic acid
RT	Reverse transcription
RU	Resonance units
SDS	Sodium dodecyl sulfate
sEBBS	Supplement Earles balanced salt solution
SPR	Surface plasmon resonance
SZB	Spermatozoa-zona binding
TAE	Tris-Acetate EDTA buffer
TEMED	Tetramethylethylenediamine
TRIS	2-Amino-2-(hydroxymethyl)-1,3-propanediol
TTBS	Tris-buffered saline
Tween-20	Polyoxyethylenesorbitan monolaurate
v/v	Ratio of volume per volume
VAP	Average path velocity
VCL	Curvilinear velocity
VSL	Straight line velocity
w/v	Ratio of weight per volume

WHO	World Health Organization
ZP	Zona pellucida

CHAPTER 1

Introduction

1.1 Foreword to Chapter One

The interplay between human gametes and their environment is now recognised as being important in order to deliver a successful fertilisation outcome. This chapter gives a broad overview of key events in the development, transport and environmental interactions of both male and female human gametes.

1.2 Early gametogenesis

The formation and development of both male and female mature gametes capable of undergoing fertilisation is a long process which starts in the early embryo and continues throughout adulthood. Much of our understanding of the mechanisms of early human germ cell development is based on mouse models due to the inaccessibility of human germ cells during fetal development.

1.2.1 Mammalian primordial germ cell (PGC) specification

The specification of the early gamete precursors, known as primordial germ cells (PGCs) is a significant event marking the definitive separation of somatic and germ cell lineages. PGCs are first identifiable during early embryonic development where they arise independently from the primitive gonads in the wall of the yolk sac, near the developing allantois (Ginsburg et al. 1990). Although there is limited information regarding the specification of PCGs in human embryos, a PGC population of approximately 50-90 cells can be observed at approximately 21-22 days gestation (Falin. 1969).

Unlike non-mammalian species which rely on the asymmetric localisation of germplasm to induce PGC specification (Ikenishi. 1998), mammals rely on a series of induction signals released by the extraembryonic ectoderm and the visceral endoderm, promoting PGC differentiation in cells within the epiblast (Chuva de Sousa Lopes et al. 2008). Although these signals have not been fully characterised it is known that members of the bone morphogenetic protein (BMP) family are major extrinsic factors in the specification of PGC (de Sousa Lopes et al. 2007). Secretions of BMP4 and BMP8b from extraembryonic ectoderm

(Lawson et al. 1999;Ying et al. 2000) and BMP2 from visceral endoderm (Ying and Zhao. 2001) initiate a receptor cascade of SMAD phosphorylation; both SMAD1 and SMAD5 in conjunction with SMAD4 (Chang and Matzuk. 2001;Tremblay et al. 2001;Hayashi et al. 2002;Chu et al. 2004).

This complex cascade of signals regulates many important genes in PGCs such as the up-regulation of the transcriptional regulator *Blimp1*, which itself both down-regulates somatic genes such as particular members of the Hox gene family and up-regulates pluripotent genes *Nanog*, *Stella* and *Nanos3* (Saitou et al. 2002;Ohinata et al. 2005;Vincent et al. 2005). An early gene expressed in PGCs is *Fragilis*, and although identified as an early marker of PGC specification, is not thought to be functionally important. Similarly, PCGs express characteristic alkaline phosphatase activity, stained as small spots within the cytoplasm. (Ginsburg, Snow and McLaren. 1990) and although this is characteristic of PCGs, experiments mutating alkaline phosphatase liver/bone/kidney (ALPL) have indicated that ALPL is only a marker and is not essential for PGC specification or proliferation (MacGregor et al. 1995).

1.2.2 Mammalian primordial germ cell migration

After specification PGC cells must migrate from the base of the yolk sac along the hindgut to the genital ridges where the somatic gonad precursors reside (Seki et al. 2007). Migrating cells exhibit a directional polarity, with a front leading edge that promotes movement through protrusion and adhesion, and a back lagging edge that retracts. The process is regulated by transmembrane receptors that are sensitive to external chemoattractant signals that induce phospholipids and small GTPases to create cytoskeletal changes. Very little is known about human PGC migration; much of what is understood is based on

research on the model organisms *Drosophila melanogaster*, zebrafish and mice which is reviewed in Richardson and Lehmann. 2010.

1.3 The spermatozoon

1.3.1 Spermatogenesis

Spermatogenesis is a key and complex biological process, leading to the formation of the mature male gamete, a spermatozoon, a motile, haploid cell that is capable of fertilising the female oocyte. After decades of investigation, there is too much information to be discussed within this chapter, however for an extensive review see Hermo et al. 2010a;Hermo et al. 2010b;Hermo et al. 2010c;Hermo et al. 2010d;Hermo et al. 2010e.

The site of spermatogenesis, the adult testis, has two major functions; the production of spermatozoa and the synthesis of important steroids. These two functions are completed in distinct and physically separate areas of the testes. Spermatozoa develop within the seminiferous tubules, numerous coiled hairpin-like structures (Huckins and Clermont. 1968). The epithelium lining of these tubules composing of germ cells and a corresponding Sertoli cell, which supports the development of the spermatozoa (Fawcett. 1975a). Interstitial spaces between seminiferous tubules harbour androgen-producing Leydig cells in addition to macrophages, blood, lymphatic channels and nerves (Hermo et al. 2010a). The Leydig and Sertoli cells work together to regulate spermatogenesis (Cheng and Mruk. 2002;Mruk and Cheng. 2004).

During spermatogenesis the more developed germ cells occupy successive layers in the seminiferous tubules. The first phase involves the continuous mitotic proliferation of diploid

(2n) spermatogonia at the basal compartment of the seminiferous tubule. The second phase, the initiation of meiotic division, forms haploid (n) spermatids. Finally the cytodifferentiation phase focuses on the elongation and development of the spermatids forming spermatozoa that have an acrosome, condensed hetrochromatin, mitochondria-containing midpiece, and a flagellum (Johnson. 2007b).

Throughout spermatogenesis, the developing germ cells are dependent on interactions with the Sertoli cells via cell-cell junctions and with other developing germ cells via cytoplasmic bridges. Once spermatogenesis is completed these attachments are terminated and immature spermatozoa are released into the lumen of the seminiferous tubule (Guraya. 1995) (figure 1.1).

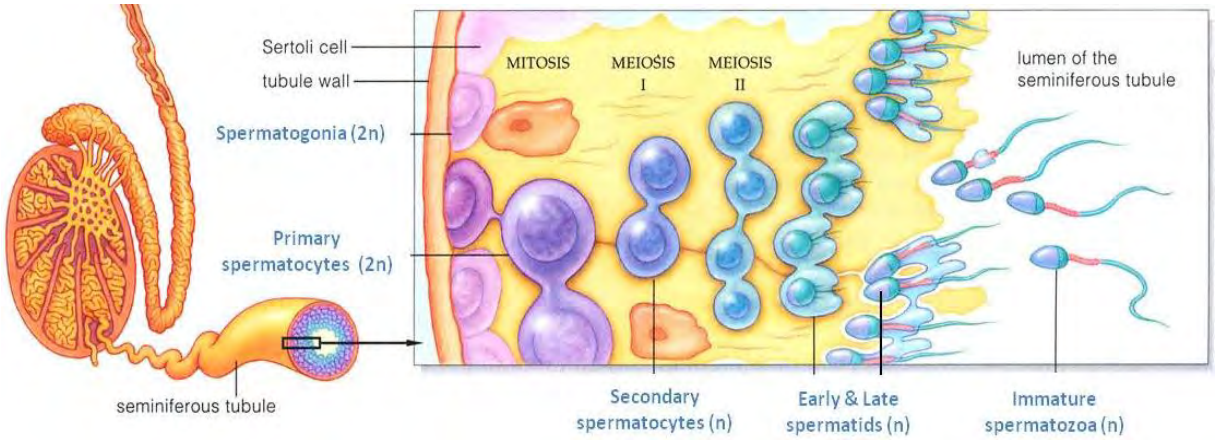

Figure 1.1: Spermatogenesis.

Image modified from (Hammack's universe of ideas. 2011).

1.3.2 The structure of mature spermatozoa

The primary function of spermatozoa is to deliver a haploid set of chromosomes to the female gamete, the oocyte. All mammalian spermatozoa share the fundamental basic sperm

structure composing of a head and tail (flagellum) (figure 1.2) whose structural features reflect their functional roles.

The majority of mammalian spermatozoa, including human have spatulate-shaped heads, with the exception of rodents which have heads that resemble a sickle shape (Yanagimachi. 1981). Each spermatozoa head contains an individual membrane-enclosed nucleus and acrosome (Mortimer. 1997).

The nucleus, as a result of the complete reorganisation mid-spermiogenesis has highly condensed chromatin (extensively reviewed in Dadoune. 2003). This is due to the nucleosomal histones of the meiotic germ cells being replaced with intermediate proteins and protamines, which are low molecular weight highly basic proteins that associate with DNA (Wouters-Tyrou et al. 1998). This nuclear hypercondensation gives spermatozoa the hydrodynamic shape to permit sperm motility and penetration through the oocyte vestments (Brewer et al. 2002). The nuclear envelope is protected by the perinuclear theca, which is stabilised by disulfide bonds (Oko and Maravei. 1995).

Located in the sperm head there is also the acrosome, a highly specialised Golgi-derived membrane-bound vesicle, which overlays the anterior of the spermatozoa nucleus and believed to have an important role in spermatozoa-zona binding (SZB) during fertilisation. The formation of the acrosome happens during early spermiogenesis (for further information see Yoshinaga and Toshimori. 2003). The acrosomal contents include a variety of hydrolytic enzymes, acid glycohydrolases, proteinases, phosphatases, esterases and aryl sulfatases (Yanagimachi. 1994;Tulsiani et al. 1998).

The spermatozoon flagellum is composed of four regions, the connecting piece, the midpiece, the principal piece and the end piece (Fawcett. 1965). The ultra-structure of the flagellum is critical for its function, to provide propulsion to the cell. The connecting piece joins the sperm head to the rest of the flagellum from which the axoneme extends along the length of the flagellum. The axoneme is a ring of nine microtubule doublets that surround a central doublet pair. Dynein arms project and link the microtubule doublets and are responsible for the motive propulsions generated by the flagellum (Fawcett. 1975b;Clermont et al. 1990). In the midpiece region, the axoneme is surrounded by a ring of nine outer dense fibres. Both structures are then enclosed in a mitochondrial sheath which is exclusive to the midpiece region. The annulus signals the termination of the midpiece and the start of the principle piece of the flagellum. From this point, two outer dense fibres are replaced with two longitudinal columns of fibrous sheath. Towards the end of the principle piece the fibrous sheath and longitudinal columns terminate leaving only the axoneme surrounded by plasma membrane to form the end piece region of the flagellum (Turner. 2006) (figure 1.2).

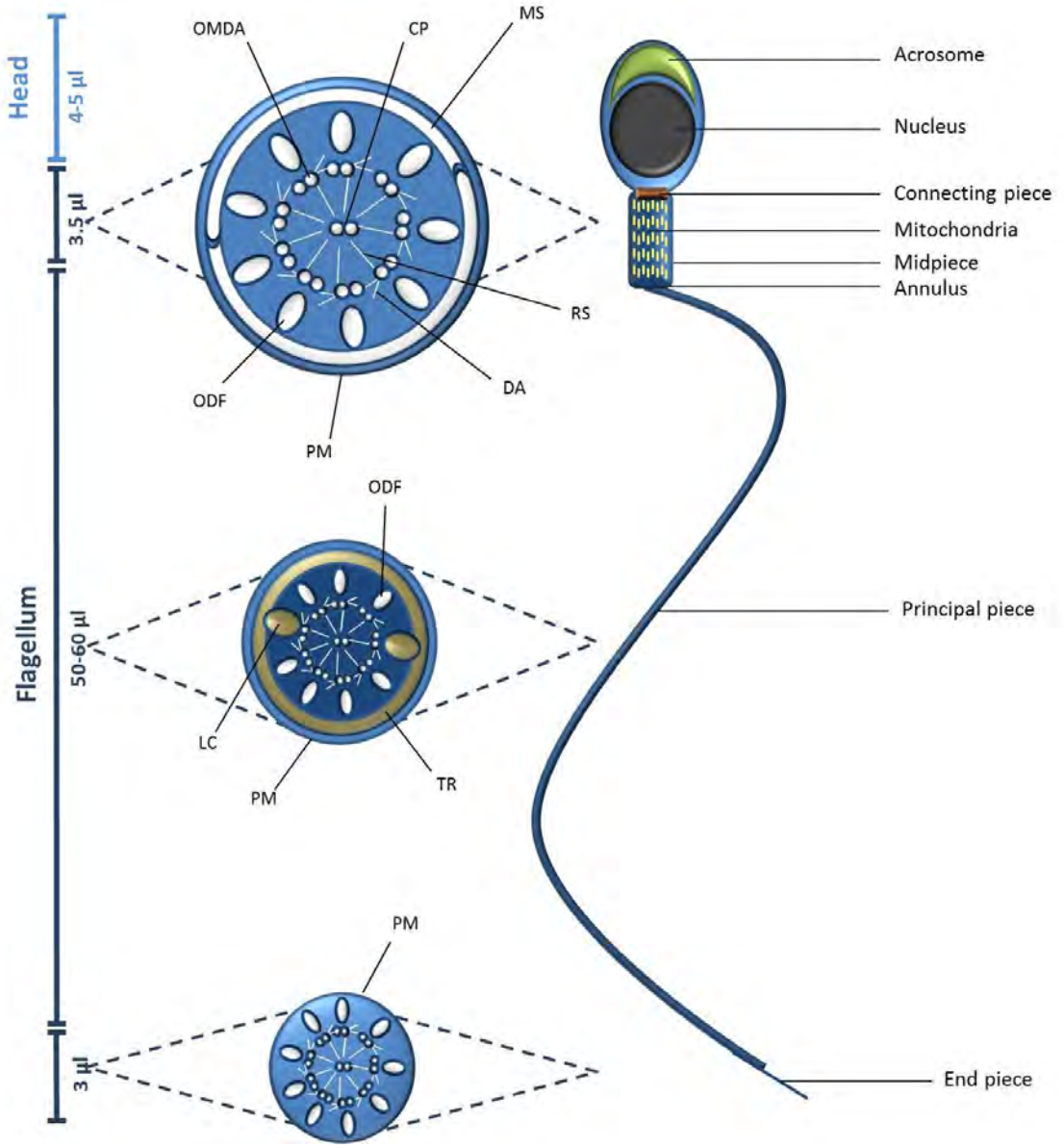

Figure 1.2: The mature human spermatozoa.

Schematic representation of mature human spermatozoa and ultrastructure of the flagellum. **OMDA**: Outer microtubule doublets of the axoneme, **PM**: Plasma membrane, **MS**: Mitochondrial sheath, **ODF**: Outer dense fibres, **RS**: Radial spokes, **DA**: Dynein arms, **CP**: Central pair of microtubule doublets, **TR**: Transverse ribs, **LC**: Longitudinal columns. Figure adapted from (Turner. 2006).

1.3.3 Epididymal storage and transport

Once spermatozoa are released into the lumen of seminiferous tubules the morphologically mature but functionally incompetent spermatozoa leave the testes and are transported into the epididymis (Cornwall. 2009). The epididymis which transports spermatozoa from the testes to the vas deferens is a single duct, composed of three anatomical regions: the caput, the corpus and the cauda. The movement of spermatozoa through the caput to cauda relies on smooth muscle contractions by the epididymal wall (Reid et al. 2011). Exposure to the complex environmental milieu initiates a rapid process of membrane remodelling and protein acquisition (Nikolopoulou et al. 1985;Haidl and Opper. 1997;Aitken et al. 2007;Jones et al. 2007;Cornwall. 2009). This produces progressively motile spermatozoa which have further gained the capacity for fertilisation (Bedford. 1963;Bedford. 1965;Horan and Bedford. 1972;Saling. 1982).

1.3.4 Seminal components and ejaculation

Spermatozoa are expelled from the male via the urethra in a process termed ejaculation. A minimal value from a typical fertile human male ejaculate is 1.5 ml in volume, containing 39 million spermatozoa (Cooper et al. 2010). Spermatozoa are not the only component of the ejaculate, with estimates of spermatozoa only forming 1-5% of the total ejaculate volume (Mortimer. 1994). During ejaculation spermatozoa are mixed with seminal plasma secreted by the accessory sex glands which, together with spermatozoa forms a substance termed semen.

There is incomplete mixing of these secretions leading to semen being a non-homogenous mixture. The initial 5% of semen volume is secretions from both the Cowper and Littre

glands. A further 15-30% of semen volume is derived from prostate secretions composing of acid phosphatase, citric acid, inositol, calcium, zinc and magnesium. Fructose is found in a small volume of secretion from the epididymis. The largest volume is secreted by the seminal vesicles, which secrete large amounts of fructose, ascorbic acid and prostaglandins (Owen and Katz. 2005).

A full comprehensive review of seminal components has been undertaken by Owen & Katz. 2005.

1.4 The oocyte

1.4.1 Oogenesis

Like the production of the male gamete, female gametes must undergo stages of mitotic proliferation and meiotic division to create a haploid oocyte (figure 1.3). In comparison to spermatogenesis which occurs in continual cycles throughout adulthood, oogenesis is an episodic process, with stages of divisional arrest which can last for long periods of time. The stages of oogenesis are closely linked with development of the follicle, which will be discussed in section 1.4.2.

In the embryonic gonads PCGs mitotically proliferate into oogonia, forming a synctium, a cluster of oogonium attached by their cell membranes. The cytoplasmic bridges are as a result of incomplete cytokinesis during cell division. It is believed that the formation of the synctium helps synchronise molecular signals initiating meiosis (Baltus et al. 2006). With the rapid rate of mitosis the number of oogonia peaks at week 20 of gestation, at approximately

6 million, however this then follows a period of oogonial atresia which continues throughout the female's lifetime (Oktem and Oktay. 2008).

As oogonia enter the first stages of meiosis I, they soon arrest at the prophase I stage (Miyazaki. 1995;Hassold and Hunt. 2001;Conti et al. 2002), which is fairly stable allowing for long periods of storage and development of the oocyte (Smith. 1989;Conti et al. 2002;Voronina and Wessel. 2003). The regulation and maintenance of this meiotic arrest seems dependent on a mixture of phosphorylation of cyclin-dependant kinase I and anaphase-promoting complex mediation of cyclin B levels (Solc et al. 2010;Tripathi et al. 2010). The immature female gametes are now termed primary oocytes and by birth only 1 million remain (Oktem & Oktay. 2008).

By the onset of puberty only 3000-4000 primary oocytes remain and resumption of oocyte meiosis occurs (Oktem and Oktay. 2008). Prior to ovulation as a result of the Luteinising hormone (LH) surge, the nuclear membrane surrounding the chromosomes breaks down and the oocyte resumes meiotic division (Neal and Baker. 1975;Lei et al. 2001) and completes meiosis I. The primary oocyte undergoes an asymmetric division, resulting in two structures, the secondary oocyte and first polar body, which although both haploid, are unequal in cytoplasmic content. The secondary oocyte progresses to metaphase II, where it arrests for a second time. The meiotic mechanisms have been recently reviewed (Brunet and Verlhac. 2011;Fabritius et al. 2011).

The second arrest is maintained by inhibition of an anaphase promoting complex (APC), which in turn promotes the degradation of maturation promoting factors (MPC) (Tunquist and Maller. 2003). Upon fertilisation by a spermatozoon the oocyte is subjected to an influx

of Ca^{2+}, this promotes the completion of meiosis before pronuclear formation (Machaca. 2010).

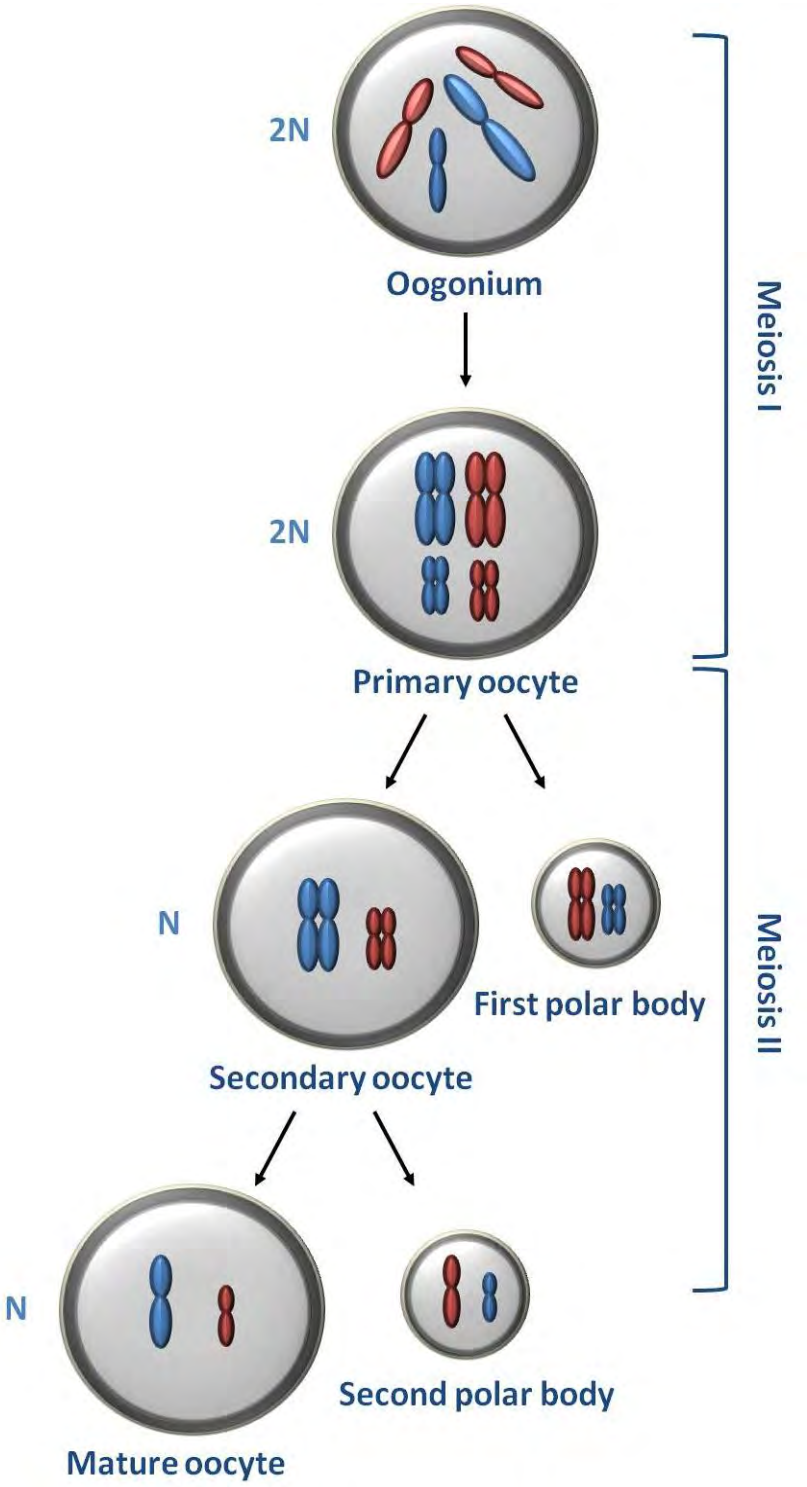

Figure 1.3: Oogenesis.

1.4.2 Folliculogenesis

The immature oocyte is surrounded by specialised somatic cells within the female ovary in structures known as follicles. The follicles that are formed around the immature oocyte create an essential microenvironment critical to the growth and development of the oocyte.

Primordial follicle

The first follicles (the primordial follicles) can be identified at 15 weeks gestation and their formation is completed by 6 months (Baker. 1963;McGee and Hsueh. 2000;Maheshwari and Fowler. 2008). The primordial follicle contains a primary oocyte which is surrounded by squamous pre-granulosa cells, encapsulated by a basal membrane and surrounding stromal cells (figure 1.4).

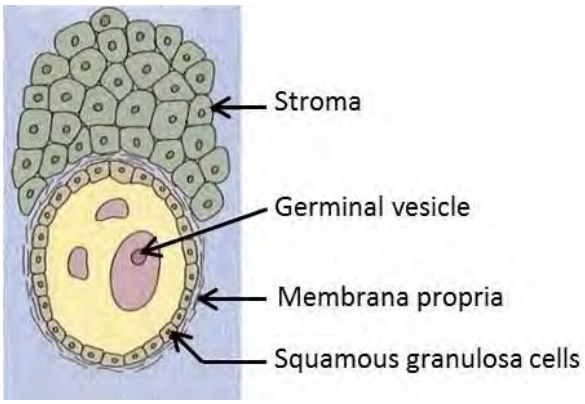

Figure 1.4: Primordial follicle.

Image from (Johnson. 2007a).

Primary oocytes can reside in primordial follicles for decades and a complex set of inhibitory signals maintain their dormant state. Studies in mice have shown that the loss of certain factors such as tumour suppressor tuberous sclerosis complex 1 (Tsc-1), phosphatase and

tensin homolog deleted on chromosome 10 (PTEN), Foxo3a, p27kip1 and Foxl2 leads to the resumption of follicle development (Castrillon et al. 2003;Rajareddy et al. 2007;Reddy et al. 2008;Adhikari et al. 2010). Anti-Mullerian hormone (AMH), which is expressed from granulosa cells in growing follicles, also plays a role in suppressing follicle transition, once recruitment has been initiated, creating a steady continuous stream of follicle recruitment and development (Durlinger et al. 1999;Durlinger et al. 2002).

Primary follicle

The transition between primordial follicles and primary follicles appears reliant on a myriad of environmental factors secreted by the surrounding somatic cells (O'Brien et al. 2003). Recruitment seems independent from the gonadotropin, follicle stimulating hormone (FSH), as no FSH receptors have been found in primordial follicles (Oktay et al. 1997). Members of the TGF-β family, BMP4 and BMP7 expressed by the stromal and theca cells (Nilsson and Skinner. 2003;Lee et al. 2004), GDF9 (Dong et al. 1996;Carabatsos et al. 1998; Vitt et al. 2000) and Figla (Soyal et al. 2000) expressed by the oocyte itself have been shown to be among the factors that play a critical role in primary follicle formation. Figla is also the transcription factor controlling zona pellucida protein expression and along with ZP3 has been shown to be expressed prior to follicle formation (Soyal et al. 2000;Tormala et al. 2008). Other factors that promote follicle transition are further reviewed in (Oktem and Urman. 2010).

As a result of exposure to these factors morphological changes occur within the primary follicle and the stroma cells begin to condense near the basal membrane to form a theca cell

layer. The granulosa cells begin proliferate and become cuboidal (Johnson. 2007a) (figure 1.5).

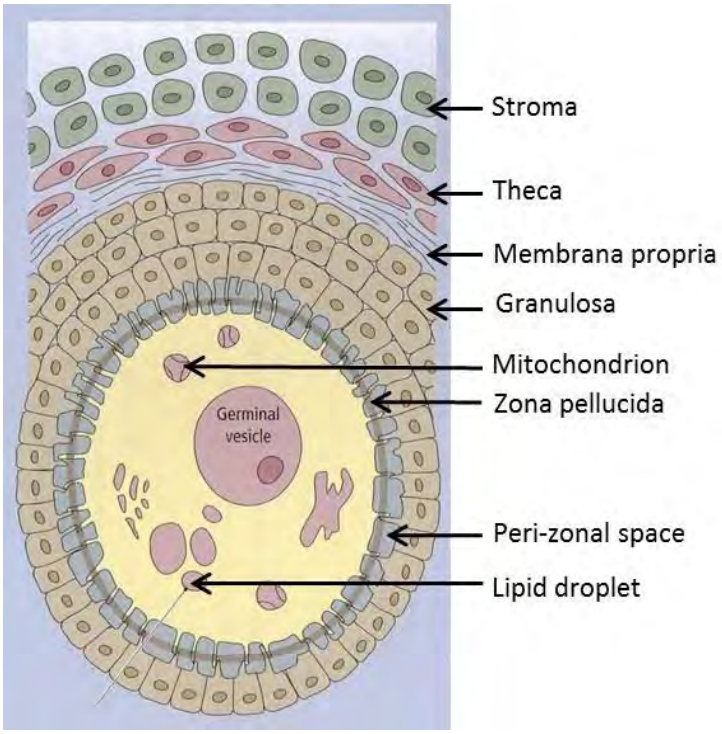

Figure 1.5: Primary follicle.

Image from (Johnson. 2007a).

Secondary follicle

As the surrounding granulosa cells proliferate, they create ever increasing layers around the oocyte. This signals the long progression of the follicle to the secondary follicle stage (figure 1.6), which develops over a period of several months. The follicle and oocyte increase in size and there is increasing vascularisation, which results in the formation of follicular fluid (section 1.4.3). Like the primary follicle stage, development of the secondary follicle is reliant on factors such as members of the TGF-β family (BMP4, BMP7 and BMP17), GDF9 and

activins produced by the surrounding granulosa, theca and the oocyte itself (Oktem and Urman. 2010). Although secondary follicles express FSH receptors the role of FSH in follicle maturation is debated (Goldenberg et al. 1976;McGee et al. 1997;Oktay et al. 1998).

Intimate connections form between the oocyte and the surrounding granulosa cells. The granulosa cells form a network of gap junctions. The junctions are composed of connexin proteins arranged in a hexameric configuration, providing not only an ability to communicate with the neighbouring cell but also an ability to exchange metabolites with each other. The gap junctions also extent through the zona pellucida and connects the granulosa cells with the oocyte (Oktem and Urman. 2010). A bi-directional communication appears to develop with an exchange of small ions, amino acids, metabolites and regulating factors, this is further reviewed in Gilchrist et al. 2004.

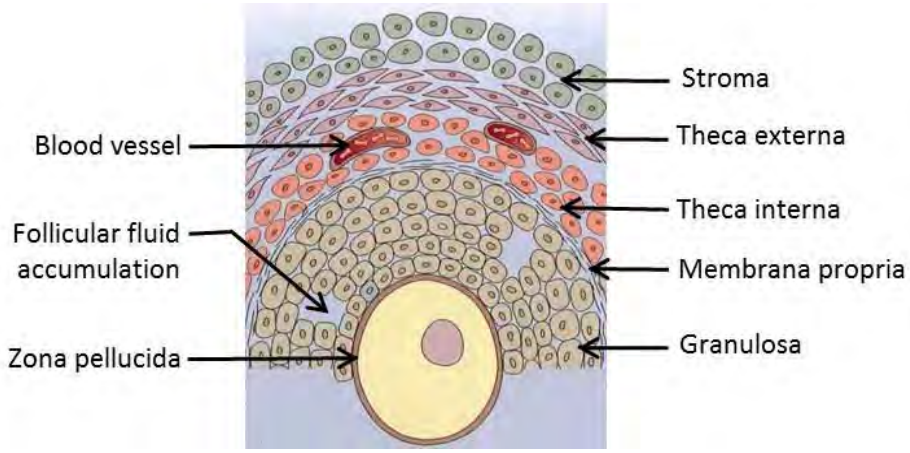

Figure 1.6: Secondary follicle.

Image from (Johnson. 2007a).

Tertiary follicle and Ovulation

In order for follicles to progress and release their oocyte, a combination of signals selects for a dominant follicle. Only a follicle with the correct expression of FSH and LH receptors and FSH aromatase activity will result in follicle dominance and avoid follicle atresia. The factors involved in the selection of dominant follicles were reviewed by Oktem and Urman. 2010. The oocyte is released at the end of the follicular phase of the female menstrual cycle (approximately day 14). Prior to ovulation a surge of the gonadotropin, LH, results in increased oestrogen expression from the tertiary follicle via a positive feedback loop. LH activates a number of signalling cascades such as PKA, PI3K/AKT and RAS, which initiates the process of ovulation. In the final stages, oocyte meiosis resumes and cumulus expansion occurs (section 1.4.1). The follicle becomes increasingly vascularised, increasing the volume of follicular fluid accumulating within the follicle (figure 1.7).

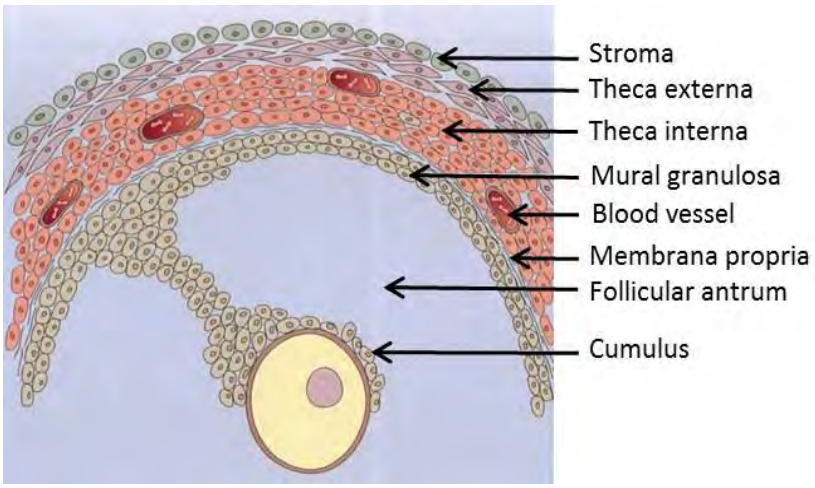

Figure 1.7: Tertiary follicle.

Image from (Johnson. 2007a).

The rapid follicle expansion results in the thinning of the peripheral rim of mural granulosa cells, membrane and theca cells and the remaining connective tissue is broken down by a number of proteases such as matrix metalloproteinases. This process forces the follicle to rupture (Johnson. 2007a;Richards and Pangas. 2010).

1.4.3 Follicular fluid

Follicular fluid forms a supportive microenvironment for oocytes during maturation; it reflects not only the secretory activities of the surrounding granulosa and cumulus cells (Nayudu et al. 1989;Fortune. 1994), but also oocyte quality (Andersen. 1993;Mendoza et al. 1999;Lamb et al. 2010).

The proportion of the follicle filled with follicular fluid appears to be species related, with larger animals such as human, bovine and porcine having larger accumulation. For instance in bovine, >95% of follicular volume is reportedly comprised of follicular fluid (Rodgers et al. 2001). The mechanisms behind follicular fluid accumulation as of yet have not been fully elucidated, however it is hypothesised that follicular fluid is derived from the blood (van Wezel and Rodgers. 1996;Herrmann and Spanel-Borowski. 1998) and involves an osmotic gradient during early stages of folliculogenesis (Jiang et al. 2002;Clarke et al. 2006). In larger species theca capillaries form multilayers around follicles to increase the vascularisation and blood flow (Yamada et al. 1995). Differences in the vascularisation of the follicle have been associated with the dominance or subordinance of the follicle and oocyte quality (Huey et al. 1999;Berisha and Schams. 2005;Acosta. 2007;Rodgers and Irving-Rodgers. 2010a).

Researchers using transgenic mice have identified genes that exhibit abnormal follicular fluid accumulation. Mice null for *Gdf9* (Dong et al. 1996), *Fshb* (Kumar et al. 1997), *Fshr* (Abel et

al. 2000) and *Igf1* (Zhou et al. 1997) exhibit small defective follicles whereas *αEsrl* (Lubahn et al. 1993) and *Cyp19A1* (Britt et al. 2000) null mice exhibit large cystic follicles. Further investigation is needed to establish whether these genes are important for overall follicle development or they are directly involved in the regulation of follicular fluid accumulation.

There appears to be close relationship between follicular fluid formation and the granulosa cells. Abnormal basal granulosa cells and follicular basal lamina in bovine follicles exhibit different rates of antrum expansion (Rodgers and Irving-Rodgers. 2010b). It has been hypothesised that as a result of certain factors, granulosa and cumulus cell types within the follicle secrete osmotically active molecules or factors that facilitate fluid movement, resulting in the accumulation of follicular fluid (Rodgers and Irving-Rodgers. 2010a).

Due to the complexity of follicular fluid, the complete composition profile has yet to be completed. One study however identified 69 proteins in human follicular fluid, the majority of which were blood plasma proteins. Follicular fluid also contains an array of steroids including progesterone, oestradiol and testosterone (Hanrieder et al. 2008).

1.4.4 The cumulus oocyte complex (COC)

At ovulation the secondary oocyte, which is arrested in metaphase of meiosis II, is released from the ovarian follicle into the peritoneal or bursal cavity surrounded by an elaborate structure consisting of the zona pellucida (ZP) and cumulus cells embedded in a viscous matrix, together they are termed the cumulus oocyte complex (COC) (figure 1.8). The COC is transferred into the ampullar region of the female reproductive tract via the infundibulum where it awaits possible fertilisation.

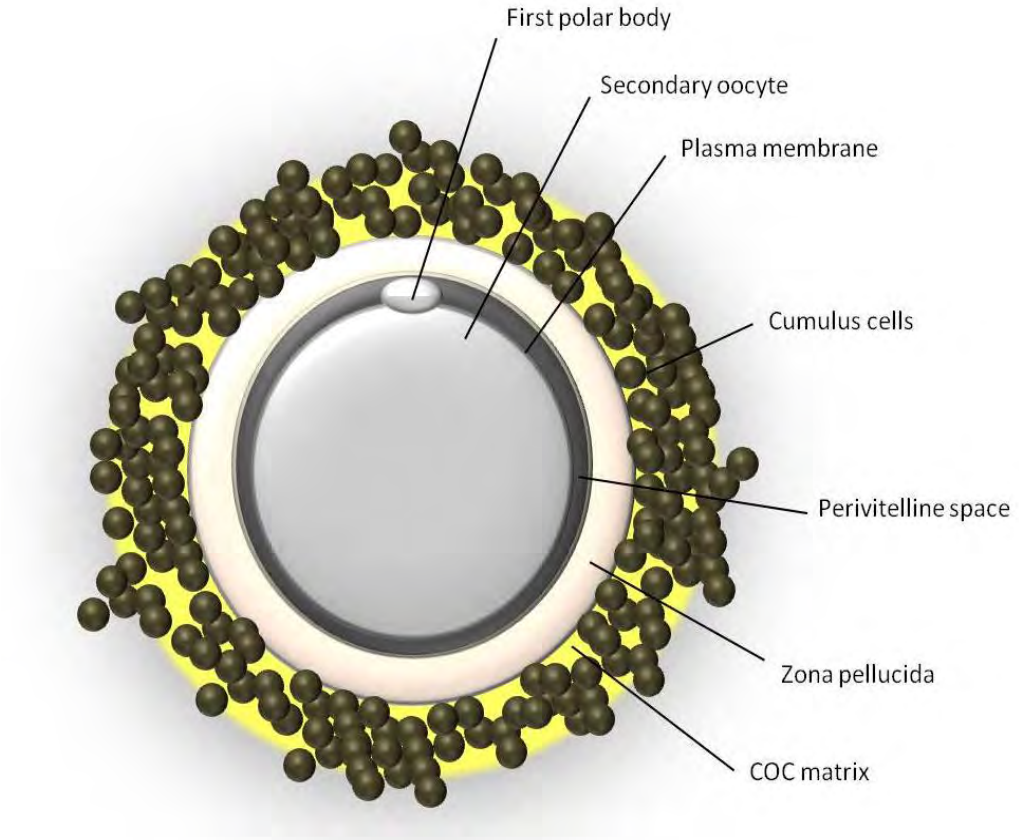

Figure 1.8: The cumulus oocyte complex (COC).

1.4.5 The cumulus matrix

Following the LH surge the cumulus cells surrounding the oocyte expand, and the components of the follicular fluid are incorporated into the COC matrix. Although not fully characterised, the viscous extracellular matrix appears to be mainly composed of hyaluronic acid, a polymer of repeating disaccharide units of N-acetyl-D-glucosamine and D-glucuronic acid (Laurent and Fraser. 1992;Harper. 1994) along with versican (Russell et al. 2003), dermatin sulphate proteoglycan (Camaioni et al. 1996) and inter-α-trypsin inhibitor (Chen et al. 1996;Nagyova et al. 2004). The gel viscosity is created as a result of the multimeric interactions between hyaluronic acid and complexes of pentraxin 3 and TNFAIP6 (Salustri et

al. 2004). After the COC is ovulated the links created between the oocyte and the surrounding cumulus cells, through the ZP matrix, during folliculogenesis are thought to be lost or at least greatly reduced (Gregory et al. 1994;Motta et al. 1994;Motta et al. 1995).

1.4.6 The zona pellucida

The zona pellucida (ZP) is an extracellular matrix that surrounds all vertebrate oocytes and remains around the early embryo. The ZP matrix in humans is composed of four individual glycoproteins (hZP1,hZP2, hZP3 and hZP4) (Lefievre et al. 2004) and they are involved in several important roles within fertilisation process. The ZP is thought to mediate spermatozoa binding in a species-specific manner, induce spermatozoa to undergo the acrosome reaction, be involved in the prevention of polyspermy and protect the zygote until implantation (Conner et al. 2005).

1.4.7 Secondary structure of the zona pellucida proteins

Although all four human zona glycoproteins have their own distinct structure, they share certain functional motifs which are conserved not only between themselves but also with their mammalian homologues (Rankin and Dean. 2000) (figure 1.9).

ZP domain

All ZP proteins share a conserved structural element, the ZP domain, which was first identified in mice by Bork and Sander (Bork and Sander. 1992). Since then the ZP domain has been found in hundreds of different eukaryotic proteins that have a wide range of structural architecture and function (Jovine et al. 2005). The ZP domain resides close the C-terminal end of the protein and consist of approximately 260 amino acids with 8 conserved cysteine

(Cys) residues (Wassarman et al. 2001). It is a bipartite structure consisting of two sub-domains, ZP-N and ZP-C consisting of approximately 120-130 amino acids respectively with each sub-domain containing 4 conserved cysteine (Cys) residues (figure 1.10 a). The two sub-domains are separated by a protease-sensitive linker (Jovine et al. 2004). The ZP-N motif has been implicated as the basic building block of the ZP filaments, whereas ZP-C has been suggested as the mediator between the protein interactions (Sasanami et al. 2006;Kanai et al. 2008).

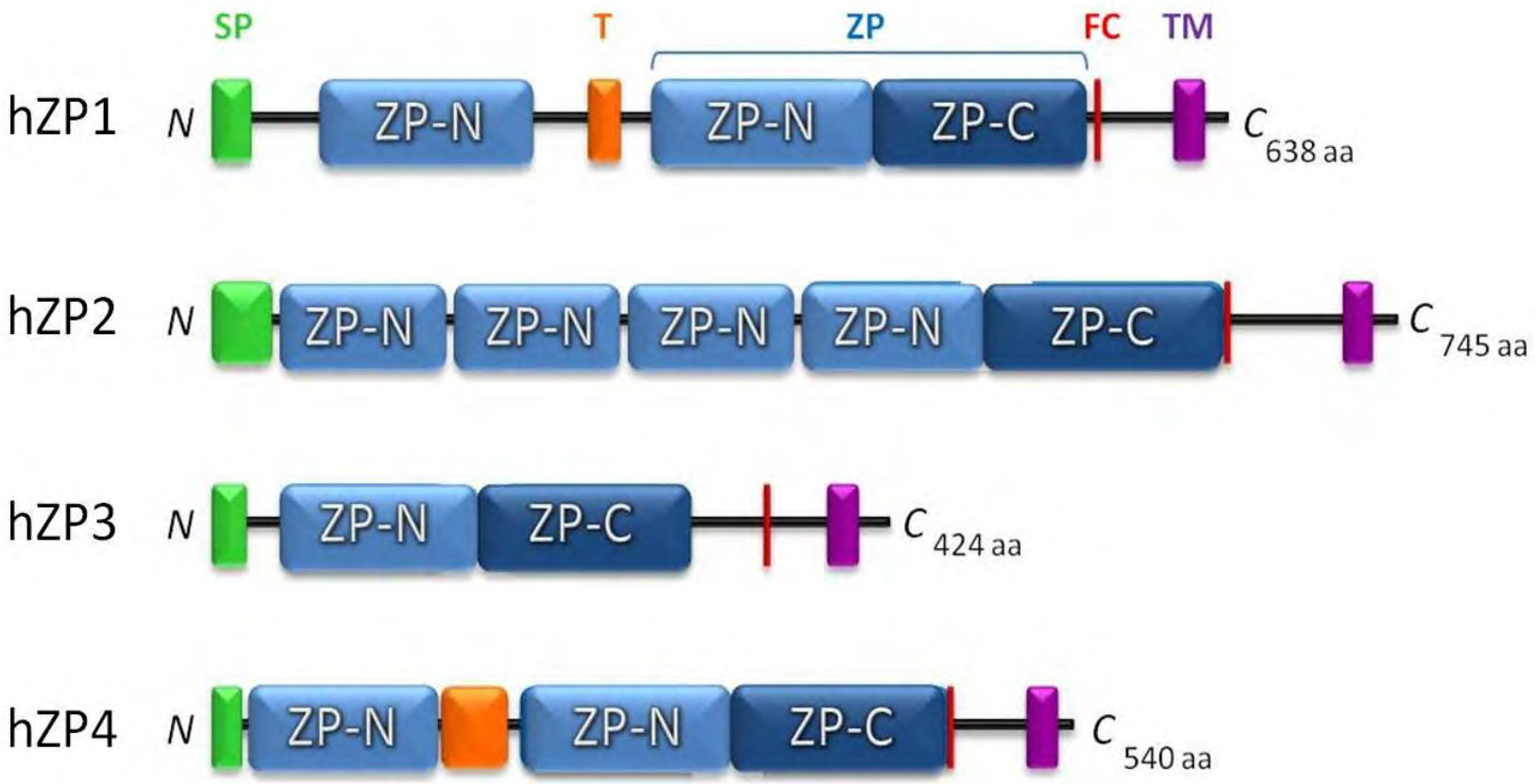

Figure 1.9: Schematic representation of key structural motifs in human zona pellucida proteins.

All zona proteins have an N-terminal signal peptide (**SP**), a C-terminal transmembrane domain (**TM**) which is preceded by a conserved furin cleavage site (**FC**) and a ZP domain (**ZP**). Human ZP1 and ZP4 also share an additional structural motif, a conserved trefoil domain (**T**). All protein sizes are given in the number of amino acid residues (aa) (Callabaut et al. 2007). Adapted from (Conner et al. 2005).

The conserved Cys residues form disulfide bonds within the ZP domain itself. The connectivity of the Cys residues within the ZP-N motif is identical (1-4, 2-3) in all ZP proteins, however differences exist in the connectivity of the Cys residues in ZP-C motif, taking either a type I or type II form. A type I ZP-C motif is found in ZP1, ZP2 and ZP4 proteins which have Cys-Cys connectivity of 5-6, 7-8, whereas a type II motif is found in ZP3 with bond between Cys 5-7 and 6-8. These disulfide bonds are thought to be crucial for the three dimensional folding of the proteins (Jovine et al. 2005) (figure 1.10 b, c).

ZP-N repeats

With the exception of hZP3, the other hZP proteins have N-terminal extensions formed of divergent copies of ZP-N domain, with hZP1 and hZP4 having one copy and hZP2 having 3. This has raised the debate whether the ZP proteins evolved around the common ZP-N motif (Callebaut et al. 2007).

Transmembrane domain and furin cleavage site

In addition, each ZP protein has an N-terminal signal peptide and a C-terminal transmembrane (TM) domain preceded by a conserved furin cleavage (FC) recognition sequence (RXK/RR) (Rankin and Dean. 2000). While it is generally accepted that the ZP proteins are cleaved at the FC site during proteolytic processing, some studies in mice have suggested that the FC site might not be essential for intracellular trafficking, post-translational processing or secretion of the ZP proteins (Zhao et al. 2002).

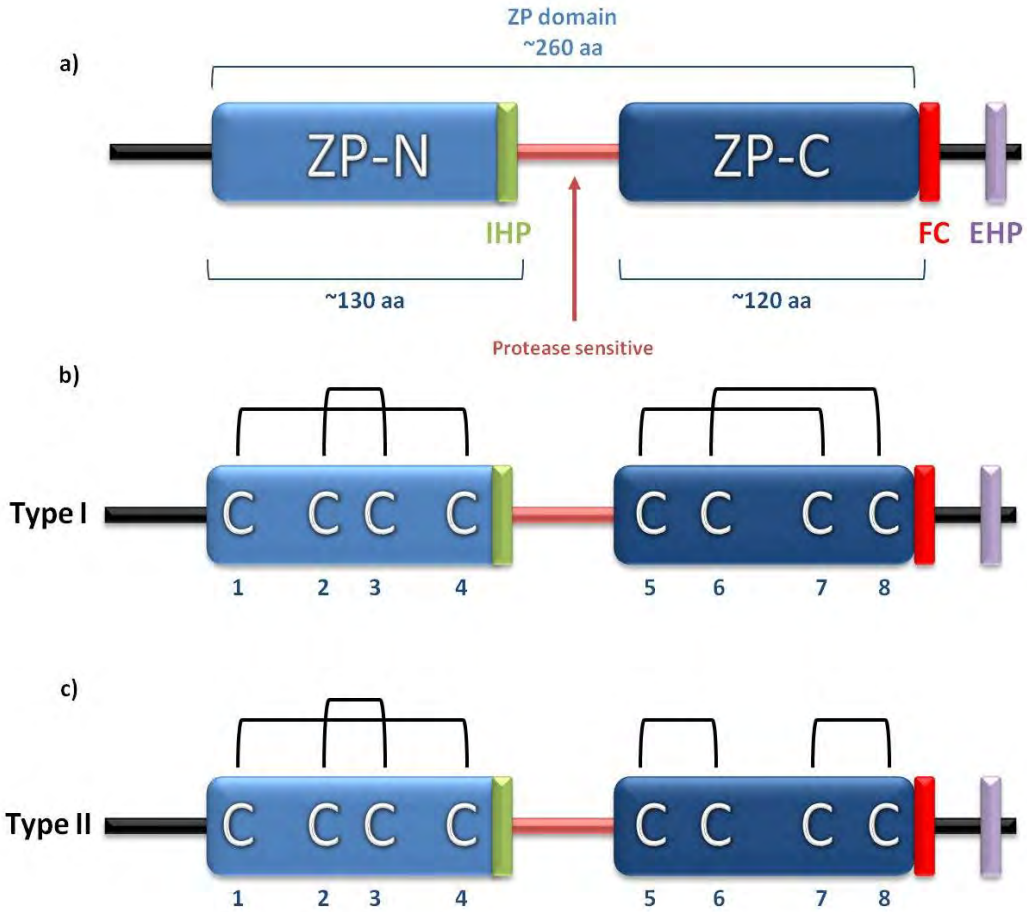

Figure 1.10: The subunits and cysteine residues of the ZP domain.

The ZP domain is bipartite structure composed of two motifs ZP-N and ZP-C. It also contains: an internal hydrophobic patch (IHP); an external hydrophobic patch (EHP) and a furin cleavage site (FC) (**a**). The formation of type I (ZP3 like) cysteine disulfide bonds (**b**). The formation of type II (ZP1, ZP2 and ZP4 like) cysteine disulfide bonds (**c**). Figure adapted from (Jovine et al. 2005).

Internal and external hydrophobic patches

Two short hydrophobic motifs are also conserved, an internal hydrophobic patch (IHP) resides after the 4 conserved cysteines within the ZP-N region of the ZP domain and an external hydrophobic patch (EHP) which is located between the FC site and the TM domain. The EHP is conserved in all ZP domain-containing proteins (Jovine et al. 2004). Both the IHP and EHP are thought to be important in the proteolytic processing of ZP proteins (Jovine et al. 2003).

Trefoil domain

ZP1 and ZP4 contain an additional structural motif, a trefoil domain, which forms a three loop structure of approximately 40 residues and like the ZP domain has six conserved cysteine residues (Braun et al. 2009).

1.4.8 3D structure of the zona pellucida

Recent studies by Jovine et al., have attempted to elucidate the three dimensional structure of the ZP proteins. Crystal structures of both the mouse ZP3 (mZP3) ZP-N domain (Monne and Jovine. 2011) and full length chicken ZP3 (Han et al. 2010) established that both ZP-N and ZP-C form immunoglobulin (Ig) like folds, which consist of two β sheets that enclose a hydrophobic core (Halaby et al. 1999).

The ZP-N can be defined as a new subtype of the Ig superfamily of proteins due to its characteristic E'-strand within an E'-F-G β sheet that extends from the hydrophobic core, in addition to two enclosed disulfide bonds that secure both sides of the β sandwich (Han et al. 2010;Monne and Jovine. 2011).

Additional structural information can be found in their most recent review (Monne and Jovine. 2011).

1.4.9 Secretion of the zona pellucida

The secretion and formation of the ZP matrix appears to rely on the presence and possible interaction of the IHP and EHP (Jovine et al. 2004). The formation of the ZP matrix appears to happen outside of the oocyte with ZP proteins being secreted in a monomeric form. The IHP and EHP create a hydrophobic core, which is the key interaction between the ZP-N and ZP-C motifs of the ZP domain. The position of the EHP is important as it appears to be critical in correct secretion and preventing premature polymerisation within the oocyte (Jovine et al. 2004;Han et al. 2010) (figure 1.11 a). Cleavage of the exposed FC site on the cell surface causes a conformational change separating the IHP and EHP and exposing the IHP (figure 1.11 b), resulting in polymerisation events to form the ZP filaments (Monne and Jovine. 2011) (figure 1.11 c).

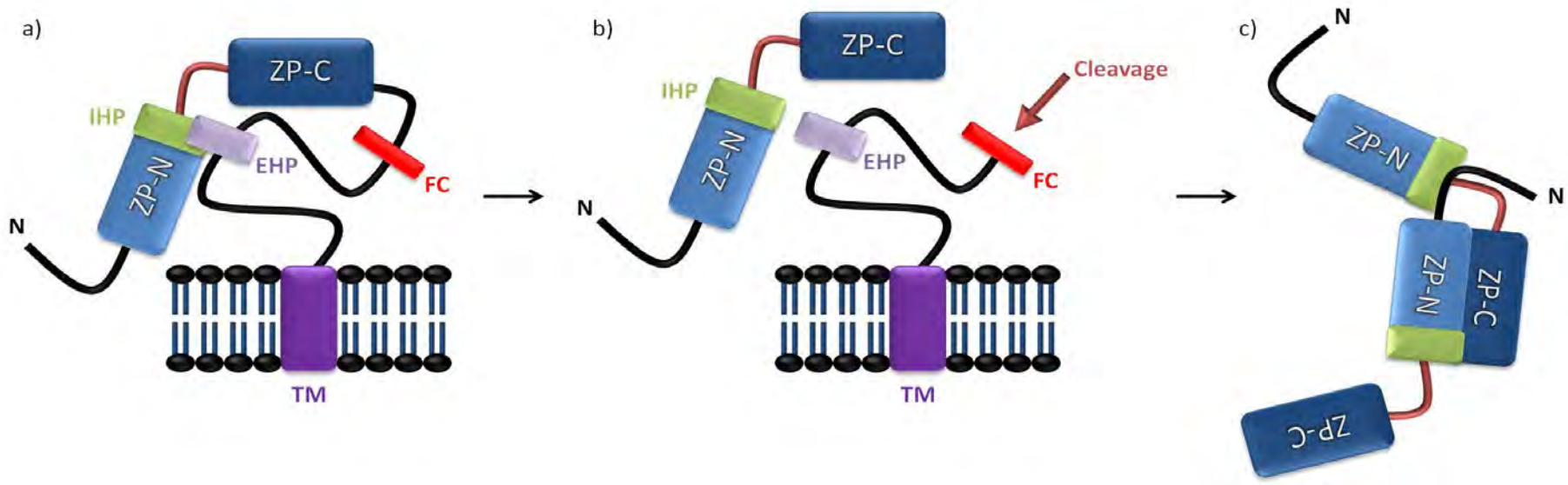

Figure 1.11: Assembly model for zona pellucida proteins.

The interaction between the IHP and the EHP avoids the premature polymerisation of ZP proteins (**a**). On the cell surface cleavage occurs causing a conformational change and exposure of IHP (**b**). This IHP exposure allows polymerisation of the ZP proteins into filaments (**c**). Internal hydrophobic patch (**IHP**); external hydrophobic patch (**EHP**); furin cleavage site (**FC**) and transmembrane domain (**TM**). (Jovine et al. 2005).

1.5 The spermatozoon's journey to fertilisation

1.5.1 Capacitation

Ejaculated spermatozoa have to undergo a further and final maturation process, termed capacitation, before they are capable of fertilising the oocyte (Austin. 1951;Chang. 1951;Austin. 1952). The process of capacitation is mediated by factors expressed by the female reproductive tract and it is a distinctive process of plasma membrane lipid remodelling, increases in intracellular pH and induction of signalling pathways within the spermatozoa (Visconti et al. 1995;Aitken et al. 1998;Baldi et al. 2000;Salicioni et al. 2007). The precise molecular mechanisms of capacitation have yet to be elucidated however some of the key molecular events are summarised in table 1.1 and for further information spermatozoa capacitation has been reviewed (Shivaji et al. 2007;Fraser 2010;Visconti et al. 2011).

Key event	Information	Reference
Cholesterol efflux	• Substantial efflux of cholesterol from spermatozoa plasma membrane. • Caused by exposure to cholesterol sinks e.g. human follicular fluid. • Loss of cholesterol induces transmembrane signalling pathways. • Cholesterol efflux also creates an increased fluidity of the spermatozoa plasma membrane allowing movement of integral membrane proteins.	(Davis. 1981;Langlais et al. 1988;Martinez and Morros. 1996; Visconti and Kopf. 1998;Visconti et al. 1999)
Bicarbonate ion influx	• Influx disrupts and destabilises spermatozoon plasma membrane, rendering it more fusogenic. • This is due to activation of phospholipid scramblases. • It also activates signal transduction pathways which lead to an increase in tyrosine phosphorylation that can induce hyperactivated motility.	(Visconti et al. 1995;Aitken et al. 1998) (Gadella and Harrison. 2000;Harrison and Gadella. 2005)
Loss of de-capacitation factors	• The loss of factors acquired by spermatozoa from the epididymis and seminal components, which makes spermatozoa capable of fertilisation. • Factors such as HongrES1, DF glycoprotein and phosphatidylethanolamine binding protein 1.	(Fraser. 1984;Fraser. 1998;Gibbons et al. 2005;Ni et al. 2009)
Protein and lipid raft remodelling and movement	• Spermatozoa are transcriptionally inactive so rely on post-translational modifications to aid remodelling. • Lipid raft movement may act as platforms for functional molecules to aggregate.	(Nixon et al. 2009;Jones et al. 2010)

Table 1.1: The key biochemical and molecular events that happen during sperm capacitation.

Table modified from (Reid et al. 2011).

1.5.2 Sperm motility

Motility is critical for the mammalian spermatozoon. Motility is achieved through the specialised structure the flagellum, however it is a process that is acquired under the regulation of many extrinsic and intrinsic factors (Turner. 2006).

The motility pattern displayed by spermatozoa differs between ejaculated spermatozoa and spermatozoa that are recovered from the site of fertilisation (Katz and Vanagimachi. 1980;Chevrier and Dacheux. 1987;Suarez and Osman. 1987). Freshly deposited spermatozoa within the female reproductive tract exhibit a symmetrical, low amplitude flagellar wave which gives spermatozoa a progressive trajectory when observed in aqueous medium (Katz and Vanagimachi. 1980;Suarez. 2008). It is believed that this enables spermatozoa to traverse the early anatomical regions of the female reproductive tract (Turner. 2006). However as spermatozoa progress to the site of fertilisation they exhibit an asymmetric, higher amplitude flagellar wave, which gives them a characteristic circular figure-of-eight movement when observed in aqueous medium (Yanagimachi. 1970;Yanagimachi. 1994). This pattern of motility is termed hyperactivation and although such spermatozoa exhibit characteristic movements in an aqueous environment, recent evidence suggests that within the viscous *in vivo* environment of the female reproductive tract (Smith et al. 2009) this hyperactivated movement allows spermatozoa to have a progressive trajectory through the oviduct and also facilitate the penetration of the COC (Ho and Suarez. 2001;Turner. 2006). The hyperactivated motility is observed to coincide with the completion of capacitation which may be important *in vivo*, although studies have demonstrated that they arise independently (Olds-Clarke. 1989;Marquez and Suarez. 2004).

Sperm motility appears to be regulated by a number of different signalling pathways (White and Aitken. 1989;Brokaw. 1991;Yanagimachi. 1994;Ho and Suarez. 2003;Wang et al. 2003). The two main signalling pathways have been identified as cyclic AMP (cAMP)/protein kinase A (PKA) and Ca^{2+} signalling. An influx of bicarbonate ions (HCO_3^-) results in the cAMP-dependent phosphorylation of downstream flagellar proteins such as tyrosine (Turner. 2006). Extracellular Ca^{2+} signalling has been identified as regulating both activated and hyperactivated sperm motility patterns (Yanagimachi. 1994;Ho et al. 2002;Darszon et al. 2006). Ca^{2+} influx is required for HCO_3^- induction of 'soluble' adenylyl cyclase (sAC) which promotes the cAMP activation of PKA (Carlson et al. 2007). Calcium can also act as part of a positive feedback loop with cAMP stimulating calcium influx via cyclic nucleotide-gated Ca^{2+} or CatSper channels activation (Xia et al. 2007). The increase in $[Ca^{2+}]_i$ observed in spermatozoa may also involve $[Ca^{2+}]_i$ stores, however the mechanisms are not fully elucidated (Ho and Suarez. 2003).

Although discussed briefly, the mechanisms and regulation of sperm motility are highly complex which far reaches beyond the scope of this thesis, however there are many reviews that provide further details (Ford. 2006;Turner. 2006;Bedu-Addo et al. 2008; Publicover et al. 2008;Hung and Suarez. 2010).

1.5.3 Sperm selection and migration

Once deposited in the vagina of the female reproductive tract, spermatozoa must traverse multiple selective obstacles to reach the ovulated oocyte.

The cervix and cervical mucus

The initial barrier that spermatozoa must penetrate is the cervix, a narrow structure which connects the vagina to the uterus. Numerous glands residing in the cervix produce a viscous secretion, cervical mucus. Cervical mucus is a highly viscoelastic gel composed of long hydrated glycoproteins called mucins (Brunelli et al. 2007). The physical, chemical and hydrodynamic properties of cervical mucus change in response to ovarian hormone changes through the female menstrual cycle. Outside the ovulatory phase of the cycle cervical mucus is thick and viscous, limiting the spermatozoon's ability to penetrate. However during ovulation cervical mucus thins, becoming penetrable to only highly motile spermatozoa (Mortimer and Templeton. 1982;Katz et al. 1997). There is evidence to suggest that a protein acquired during the epididymal maturation of spermatozoa aids cervical mucus transit (Tollner et al. 2008). Studies *in vivo* have observed that spermatozoa lose lipid species after migration through cervical mucus (Feki et al. 2004), suggesting that cervical mucus may play a role in remodelling of sperm surface plasma membranes (Baldi et al. 2000).

The utero-tubal junction (UTJ)

The UTJ connects the uterus and the oviduct by intersecting the distal portion of the oviduct and it is another barrier to sperm migration. Like the cervix, the UTJ lumen has been found to contain mucus during the periovulatory period, inhibiting sperm migration into the oviduct (Jansen. 1980). In addition to physical barriers, studies using transgenic mice have shown that the process of sperm migration through the UTJ is biologically regulated. Mice spermatozoa lacking in Clgn, Ace, Adam1a, Adam2 or Adam3 cannot traverse the UTJ, even

though motility is not impaired (Cho et al. 1998;Hagaman et al. 1998;Ikawa et al. 2001;Nishimura et al. 2004;Yamaguchi et al. 2009).

Interactions with the oviduct

Interactions between both male and female gametes and oviductal epithelial cells and their products play an important role in fertilisation.

Spermatozoa can bind to cells in the isthmus region of the oviduct, suppressing capacitation for approximately 24 hours (Dobrinski et al. 1997;Murray and Smith. 1997;Connolly. 2011). Prior to ovulation spermatozoa are released from the isthmus allowing progression towards the site of fertilisation within the ampulla region of the oviduct. The mechanisms behind this release are not fully elucidated; however capacitation of the spermatozoa could promote changes within the plasma membrane of spermatozoa, causing them to lose their binding ability (Ignotz et al. 2001). Induction of the hyperactivated motility pattern may also facilitate spermatozoa release (Demott and Suarez. 1992). Recent studies show that interaction between human spermatozoa and cells of the female tract induces Ca^{2+} signalling in both cell types (Connolly. 2011).

Multiple studies have observed gametes and early embryos modifying the transcriptomic and proteomic expression profile of the oviduct (Ellington et al. 1993;Thomas et al. 1995;Lee et al. 2002;Bauersachs et al. 2003;Long et al. 2003;Fazeli et al. 2004;Georgiou et al. 2005;Das et al. 2006;Sostaric et al. 2006;Mack et al. 2006;Georgiou et al. 2007;Kapelnikov et al. 2008;Seytanoglu et al. 2008;Kolle et al. 2010). Spermatozoa exposure in the oviduct of pigs causes an up-regulation in the synthesis of 19 oviductal proteins (Georgiou et al. 2007) and 58 genes have been found to be up-regulated in the mouse (Fazeli et al. 2004). These studies

demonstrate the ability of spermatozoa to create their own microenvironments within the oviduct, which potentially supports spermatozoa maturation, viability and function (reviewed by Holt and Fazeli. 2010).

Chemotaxis

Sperm migration may also rely on chemotaxis as a result of exposure to both follicular fluid and the COC itself (Cohen-Dayag et al. 1995;Sun et al. 2005;Oren-Benaroya et al. 2008). Progesterone has been observed to elicit a chemotactic effect in spermatozoa (Oren-Benaroya et al. 2008). An olfactory receptor (OR1D2) found on spermatozoa has also been implied to play a functional role in sperm migration when exposed to bourgeonal *in vitro*, however the *in vivo* ligand for OR1D2 has not yet been found (Spehr et al. 2003).

1.5.4 Calcium (Ca^{2+}) signalling in spermatozoa

Calcium (Ca^{2+}) is a common signalling molecule important in many cellular processes. The regulation of Ca^{2+} entry into the cytoplasm of the cell initiates the transduction of a series of signalling cascades (figure 1.12 a), resulting in Ca^{2+} and its associated secondary messengers activating functional proteins. Ca^{2+} signalling is known to play a crucial role in sperm function involving many Ca^{2+} channels and pumps and has been reviewed (Jimenez-Gonzalez et al. 2006;Publicover et al. 2007;Bedu-Addo et al.2008) (figure 1.12 b).

Ca^{2+} signalling is reliant on the influx of Ca^{2+} from both extracellular and intracellular sources into the cytoplasm of the spermatozoa. The levels of Ca^{2+} in the cytoplasm are purposely maintained at a lower concentration than either of its Ca^{2+} sources (Publicover et al. 2007).

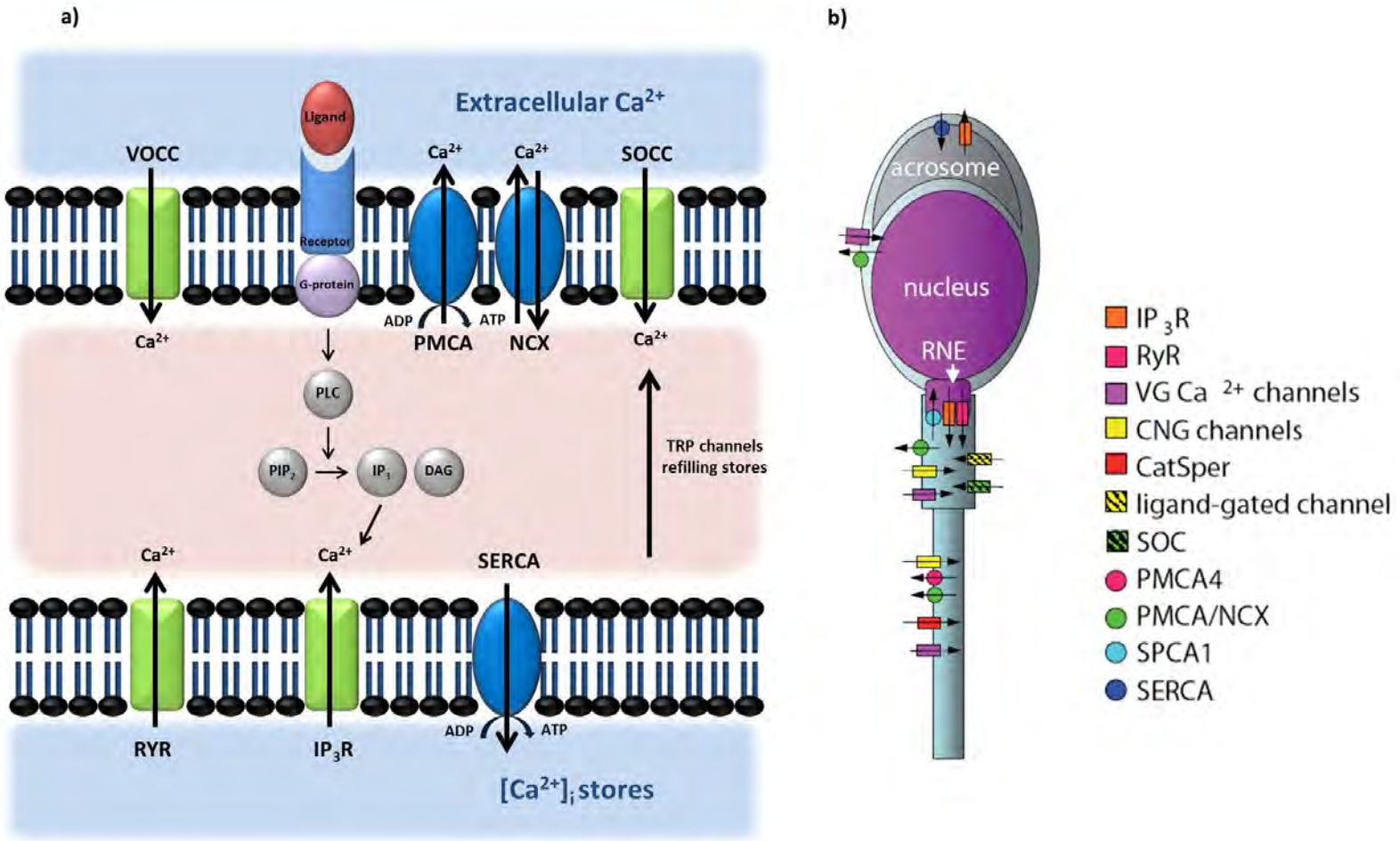

Figure 1.12: Spermatozoa Ca^{2+}signalling.

(**a**) Key routes and molecular cascades in spermatozoa (Image adapted from Connolly. 2011). (**b**) Summary of identified calcium channels (rectangles) and pumps (circles) and their location within the spermatozoa (Image from Bedu-Addo et al. 2008).

Rises in the concentration of extracellular Ca^{2+} increases the membrane potential of the plasma membrane, causing the opening of voltage-operated Ca^{2+} channels (VOCCs) allowing an influx of Ca^{2+} into the cytoplasm (Arnoult et al 1996;Jimenez-Gonzalez 2006). Spermatozoa contain a range of VOCCs, including both L (long lasting) and T (transient) channel types (Goodwin et al. 2000;Jagannathan et al. 2002;Park et al. 2003). As a divalent cation, Ca^{2+} can bind directly to exposed negative and uncharged oxygen atoms on carbonyl groups of peptides, causing a conformational change that can in turn alter the protein function.

Binding of specific ligands to G-coupled membrane receptors results in a phosphoinositide signalling cascade producing the secondary messengers inositol 1,4,5-trisphosphate (IP_3) and diacylglycerol (DAG) (Putney. 2001). IP_3 binds to a receptor (IP_3R) which is located on an intracellular store of Ca^{2+}. In somatic cells the *endoplasmic reticulum* and the *golgi body* act as internal Ca^{2+} stores, however spermatozoa lack these membranous organelles. Currently two intracellular Ca^{2+} stores have been identified in spermatozoa, the acrosome and the redundant nuclear envelope (RNE). IP_3R can be detected in both the acrosome and RNE (Bedu-Addo et al. 2008). Binding of IP_3 to the IP_3R causes Ca^{2+} to be released from the intracellular Ca^{2+} stores, allowing Ca^{2+} to act on other proteins. The process of Ca^{2+} release from intracellular stores appears to be under the control of Ca^{2+} itself with IP_3R activity being inhibited by high levels of Ca^{2+} (Marchant and Parker. 2000). Ryanodine receptors (RYRs) have also been found to empty intracellular Ca^{2+} stores and like IP_3R are also controlled by Ca^{2+} in addition to ATP and cyclic ADP (cADP) (Marks. 1997). The intracellular stores can signal to store-operated Ca^{2+} channels (SOCC) located on the plasma membrane, that open when the $[Ca^{2+}]_i$ stores are depleted (Berridge et al. 2003).

In addition to mechanisms controlling Ca^{2+} influx into spermatozoa, there are also mechanisms controlling Ca^{2+} removal. This process is essential as prolonged exposure to high Ca^{2+} concentration levels can result in cell death. The removal of Ca^{2+} depends on ATP-dependent PMCA and SERCA pumps, which transports Ca^{2+} from the cytoplasm back into the extracellular fluid and pumps cytoplasmic Ca^{2+} back into $[Ca^{2+}]_i$ stores, respectively. The NCX exchanger, found in the plasma membrane can transport Ca^{2+} out into the extracellular fluid (Berridge et al. 2003).

1.6 Fertilisation

1.6 1 Spermatozoa penetration of cumulus

For successful mammalian fertilisation, spermatozoa must penetrate through cumulus matrix in order to reach the oocyte (Myles and Primakoff. 1997;Kim et al. 2008). As the cumulus cells are embedded in an extracellular viscous matrix, comprised mostly of hyaluronic acid, it was believed that the action of sperm hyaluronidase enabled spermatozoa to penetrate the cumulus matrix (Kim et al. 2008). However knockout experiments involving two key hyaluronidases identified on spermatozoa, SPAM1 and HYAL5, showed that null mice were fertile and only SPAM1-null mice showed slightly delayed cumulus matrix penetration (Lin et al. 1994;Baba et al. 2002;Kim et al. 2005;Kimura et al. 2009). A hyaluronidase inhibitor, apigenin also showed no effect on sperm penetration through the cumulus matrix (Kang et al. 2010). Double-knockout mice lacking the serine proteases Acrosin and Tesp5 were unable to traverse the cumulus matrix, suggesting that the joint activity of both Acrosin and Tesp5 seems to be essential for cumulus penetration, at least *in*

vitro. However normal phenotype was partially restored *in vitro* with exposure to uterine fluid (Kawano et al. 2010).

1.6.2 Acrosome reaction (AR)

The exocytosis of the contents of the spermatozoon acrosome is an important pre-requisite for fertilisation, allowing spermatozoa to penetrate through the ZP matrix. The induction of AR only occurs in capacitated spermatozoa (Saling and Storey. 1979;Yanagimachi. 1994). The release of acrosomal contents occurs as a result of the outer acrosomal membrane fusing at multiple points with the spermatozoon outer plasma membrane, exposing the inner acrosomal membrane (Zanetti and Mayorga. 2009). Experiments using murine spermatozoa with an acrosome labelled with a GFP reporter indicated that the AR is a gradual process (figure 1.13), with some acrosomal components such as acrin 1 and acrin 2 remaining attached to the membrane for 15 minutes after AR induction (Nakanishi et al. 1999;Nakanishi et al. 2001).

The *in vivo* stimulant of spermatozoa AR is still not fully elucidated. The ZP has long been thought to have a physiological role in the stimulation of AR as *in vitro* studies showed that solubilised zona induce the AR (Florman and Storey. 1982;Cherr et al. 1986;Bailey and Storey. 1994;Chiu et al. 2008a;). However there are reports that intact ZP does not induce spermatozoa AR (Baibakov et al. 2007). In comparison to the mouse, where only mZP3 appears to induce the spermatozoa AR, three hZPs (hZP1, hZP3 and hZP4) appear to induce the AR (reviewed Gupta and Bhandari. 2011). Both progesterone and 17 α OH-progesterone from human cumulus and follicular fluid have been identified as AR inducers (Osman et al. 1989;Garcia and Meizel. 1999;Patrat et al. 2000). There is also evidence to suggest that *in*

vivo, the cumulus oophorus is the physiological inducer of the mammalian spermatozoa AR (Bedford et al. 2004;Jin et al. 2011). *In vitro* AR can be induced by ionophores which exchange Ca^{2+} for alternate ions, such as H^{+} (Florman. 1994).

Both ZP and progesterone induced AR induction causes a vast signal cascade mediated by an elevation of $[Ca^{2+}]_i$, and have been extensively reviewed (Abou-Haila and Tulsiani. 2000;Kirkman-Brown et al. 2002;Gupta and Bhandari. 2011). Although initial receptors and responses differ, the subsequent signals employ common components. The influx of Ca^{2+} produces a multiphasic response with an initial transient phase that results in plasma membrane depolarisation which activates voltage-operated calcium channels (VOCCs), although it is believed that progesterone-induced AR is not solely reliant on VOCCs (Thomas and Meizel. 1989;Foresta et al. 1993;Aitken et al. 1996). This results in multiple downstream activation, resulting in the emptying of $[Ca^{2+}]_i$ stores (O'Toole et al. 2000). The resulting increase in Ca^{2+} and elevated pH depolymerises the F-actin between the plasma and outer acrosomal membranes in addition to activating phospholipase A_2 which cleaves fatty acids from phospholipids, which promotes the fusion of membranes at multiple sites resulting in vesiculation (Tulsiani et al. 1998;Abou-Haila and Tulsiani. 2000).

There is some evidence to suggest that the AR is stimulated by purely a mechanical force and requires no biological inducer. A study by Baibakov et al. 2007 showed that mouse spermatozoa penetrating 1.2 µM polycarbonate filters, in the absence of known AR inducers (such as ZP or progesterone) induced the AR in 98 ± 5.8% of the sperm population, however this fell to 10-11% when spermatozoa penetrated polycarbonate filters with a larger pore size of ≥ 5 µM.

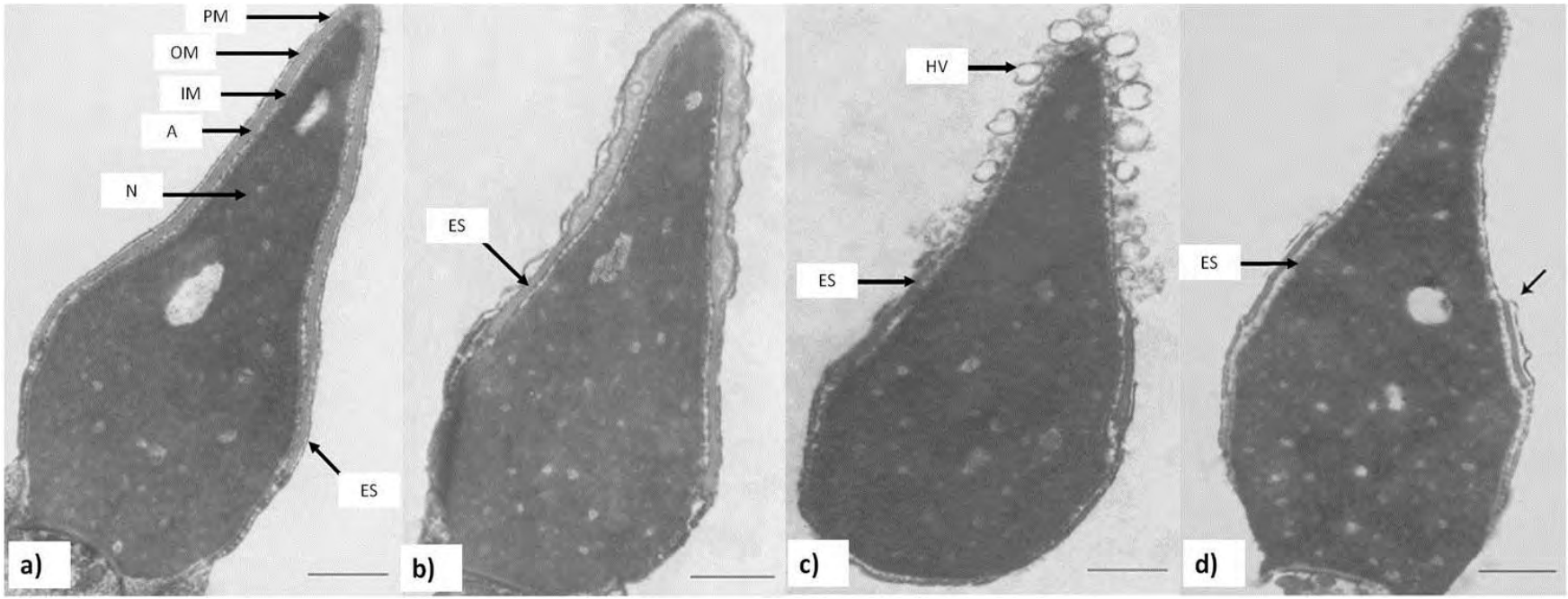

Figure 1.13: Morphological changes during human sperm acrosomal exocytosis.

Spermatozoa acrosomal exocytosis induced by calcium ionophore A22187 incubated for 10 min. Images (**a**) to (**d**) show the gradual vesiculatated acrosome, exposing the inner plasma membrane. Acrosomal exocytosis is restricted to the anterior part of the equatorial segment. (***ES***) equatorial segment, (***N***) nucleus, (***A***) acrosomal contents, (***IM***) inner plasma membrane, (***OM***) outer plasma membrane, (***PM***) plasma membrane, (***HV***) hybrid vesicle. Bars represent 500 nm, images taken from (Zanetti and Mayorga. 2009).

1.6.3 Spermatozoa-zona binding and penetration

In order to fertilise the oocyte, spermatozoa must bind and penetrate the ZP matrix. The mechanisms behind this have not been fully characterised.

There is evidence from using a combination of both native hZP3 and hZP4 (Chiu et al. 2008a;Chiu et al. 2008b) and recombinant human zona (rhZP) proteins that all four, rhZP1 (Ganguly et al. 2010), rhZP2 (Chirinos et al. 2011), rhZP3 and rhZP4 (Chakravarty et al. 2005;Chakravarty et al. 2008) exhibit spermatozoa binding. However the exact interactions and their overall importance to fertilisation have yet to be elucidated. There has been research for many decades looking for the primary zona receptor on spermatozoa, with multiple candidates being put forward, however the true receptor remains elusive. This is further discussed within chapter 4.

Spermatozoa zona penetration may be due to mechanical force generated by flagellar motility and/or dependent on proteolytic hydrolysis by enzymes originating from the acrosome (Yanagimachi. 1994). A number of proteolytic enzymes have been suggested as playing a key role in ZP penetration such as Acrosin and Tesp5, however knockout mouse experiments showed that ZP penetration still occurred, albeit slightly delayed (Baba et al. 1994;Adham et al. 1997;Yamashita et al. 2008). In the case of Tesp5, normal phenotype can be rescued with exposure to uterine fluids.

Other proteins have also been highlighted as important players in ZP penetration. Experiments blocking PSMD4, an essential subunit of a proteasomal 19S complex important in proteasome substrate recognition, show defective ZP penetration with no effect on ZP binding (Yi et al. 2010). DKKL1-null mice exhibit defective ZP penetration *in vitro*, however it

appears that *in vivo* they are completely fertile, whether this is as a result of phenotype rescue by *in vivo* conditions is still under investigation (Kohn et al. 2010).

1.6.4 Sperm-oocyte fusion

Only acrosome reacted spermatozoa can penetrate the ZP matrix and fuse with the oocyte plasma membrane (Bedford 1968;Stein et al. 2004). Although the exact mechanisms behind sperm-oocyte fusion are still not fully elucidated there has been identification of a number of key molecules involved in the process. Both an Ig superfamily, type 1 membrane protein, Izumo1 identified on spermatozoa and a tetraspanin Cd9 identified on the oocyte plasma membrane, have been found to be essential in sperm-oocyte fusion (Kaji et al. 2000;Le et al. 2000;Miyado et al. 2000;Inoue et al. 2005). However no direct interaction between the two molecules has been found, potentially implying that the process involves some sort of multimeric protein interaction or a number of distinct receptors.

1.6.5 Prevention of polyspermy

The successful fusion of the sperm and oocyte plasma membranes initiates the most important event in oocyte activation, the release of intracellular calcium $[Ca^{2+}]_i$. This initial increase in $[Ca^{2+}]_i$ triggers cortical granule exocytosis, which is key in preventing the occurrence of polyspermy (Abbott and Ducibella. 2001).

Polyspermy is an abnormal phenomenon where more than one spermatozoon fertilises the oocyte, introducing more than the desired haploid set of chromosomes. Polyspermy in humans usually results in embryo lethality; although there have been reports of both tetraploid and triploid infants, however they are born with severe abnormalities which result

in an early infant death (Sherard et al. 1986;Roberts et al. 1996;Dean et al. 1997;Hasegawa et al. 1999).

Cortical granules reside beneath the oocyte plasma membrane (Longo. 1985) and exocytosis of their contents in mature oocytes is dependent of the rise in $[Ca^{2+}]_i$ and calcium dependent proteins (Abbott and Ducibella. 2001). The mammalian cortical granule contents which include proteinases, ovoperoxidase and N-acetylglucosaminidase (reviewed by Sun. 2003) initiates cleavage of ZP2 in the second ZP-N repeat which causes conformational change within the ZP matrix (Monne and Jovine. 2011). This prevents further spermatozoa unable to bind and penetrate the ZP, although the identity of the exact molecule that catalyses these changes remains unidentified (Moller and Wassarman. 1989;Familiari et al. 2008;Papi et al. 2010).

1.7 Research aims

This study aims to take a multidirectional approach to investigate the interactions between human spermatozoa and the ovulatory components including follicular fluid, the COC and the ZP, addressing the hypothesis that sperm function is altered by the ovulatory components they encounter, as they approach the oocyte in the female reproductive tract.

Since these modulatory effects would be crucial to fertilisation success we predict that follicular fluid and cumulus cells from patients undergoing ART treatment would differ in their ability to induce these changes according to the treatment outcome of the patient. The modulation of sperm motility parameters caused by cumulus cells and spermatozoa Ca^{2+} signalling induced by follicular fluid will be studied.

In addition the development of novel experimental procedures designed to further our understanding of the interactions of spermatozoa with the ZP will be undertaken, utilising both recombinant and native ZP in SPR technology and also examining a novel *in vitro* oogenesis model via hESC differentiation.

CHAPTER 2

Effect of the cumulus oophorus and follicular fluid on spermatozoa

2.1 Introduction

At the moment of ovulation the contents of the ovarian follicle, comprising of the cumulus oocyte complex (COC) and follicular fluid, are released into the female reproductive tract (Harper. 1994). The milieu created by these follicular components at the time of fertilisation may be critical in the regulation of spermatozoa activity. Although debated (Gur and Breitbart. 2008), spermatozoa are generally regarded as transcriptionally and translationally inactive, due to the absence of ribosomes and endoplasmic reticulum, in addition to having highly condensed nuclear DNA. With this lack of *de novo* protein synthesis, spermatozoa may be sensitive to post translational modifications such as *phosphorylation (Visconti and Kopf. 1998), nitrosylation* (Lefievre et al. 2009) and *carbonylation (El-Taieb et al. 2009),* initiated by environmental factors.

Both the COC and follicular fluid are a major source of potential sperm modulators and are known sources of steroids, particularly the steroid hormone progesterone (Osman et al. 1989;Bar-Ami 1994;Wen et al. 2010). Progesterone has been shown to have an effect on sperm motility by increasing the levels of intracellular Ca^{2+} ($[Ca^{2+}]_i$) (Blackmore et al. 1990;Harper et al. 2004;Giretti and Simoncini. 2008). Such increases in $[Ca^{2+}]_i$ are known to initiate a hyperactivated motility pattern (Marquez and Suarez. 2007), a vigorous 'whiplash' effect characterised by a high amplitude, asymmetrical flagellar bending which is thought to aid penetration through the oocyte vestments (Suarez. 2008). Progesterone stimulation has also been seen to cause sperm populations to undergo the acrosome reaction (AR), which is also linked to a rapid elevation in $[Ca^{2+}]_i$ (Harper et al. 2006). Some evidence suggests that progesterone may have a directional

chemotactic effect on spermatozoa motility (Teves et al. 2006) although this is not without rebuttal (Jaiswal et al. 1999).

Nitric oxide (NO) is another key molecule secreted by cumulus cells and found in follicular fluid (Machado-Oliveira et al. 2008;Vignini et al. 2008;Zhao et al. 2010). Due to its uncharged nature and diffusible properties NO can act as an effective intracellular and extracellular biological messenger (Lancaster. 1997). As with progesterone, NO has been identified as a modulator of sperm motility (Lewis et al. 1996). In addition to protein nitrosylation (Lefievre et al. 2007), NO may also have a role in the final steps of sperm maturation, capacitation and induction of AR (Herrero et al. 1999).

Isoforms of lipocalin glycoproteins have been identified in both follicular fluid and the cumulus oophorous; Glycodelin F, identified from follicular fluid (Chiu et al. 2003b) and Glycodelin C which is converted from endogenous Glycodelin A and F by the cumulus cells (Chiu et al. 2007). The proteins have the same core and only differ in their glycosylation pattern (Yeung et al. 2006). Glycodelin F has been shown to inhibit spermatozoa zona binding (Chiu et al. 2005) and the progesterone-induced acrosome reaction (Chiu et al. 2003a). In contrast, Glycodelin-C appears to promote spermatozoa-zona binding (Chiu et al 2007).

Although there have been a handful of studies, the full proteomes and steroid composition of cumulus oophorus and follicular fluid are as yet uncertain (Memili et al. 2007;Hanrieder et al. 2008;Jarkovska et al. 2010).

There are factors secreted by cumulus cells and/or present in follicular fluid that appear to have an active role in fertilisation success. Studies using animal models *in vitro* have

shown that, although spermatozoa are capable of fertilising the oocyte in the absence of the cumulus oophorus layer, there are decreased levels of spermatozoa/oocyte interaction and lower fertilisation rates (Mattioli et al. 1988). The quality of the resultant embryos is also affected with reduced cleavage rates (Cross and Brinster. 1970) and early embryo development is slowed (Eyestone et al. 1987;Goto et al. 1988). Glucocorticoid production has been highlighted as a further marker for fertilisation success. Decreased activity in granulosa cells of 11β hydroxysteroid dehydrogenase (HSD11β) enzymes, which catalyse the conversion of steroid hormones from 'inert' cortisone to 'active' cortisol or vice versa, and/or increased cortisol:cortisone ratios in follicular fluid have been associated with improved pregnancy outcomes in patients undergoing ART (Michael and Papageorghiou. 2008). The production of steroids has been shown to be important for successful fertilisation, indicating that higher levels of certain steroid hormone levels in follicular fluid relate to fertilisation success in patients undergoing ART (Andersen. 1993;Mendoza et al. 1999;Lamb et al. 2010) (figure 2.1). These studies however focus on oocyte quality and ignore the potential effects these factors could have on sperm function and their fertilising ability.

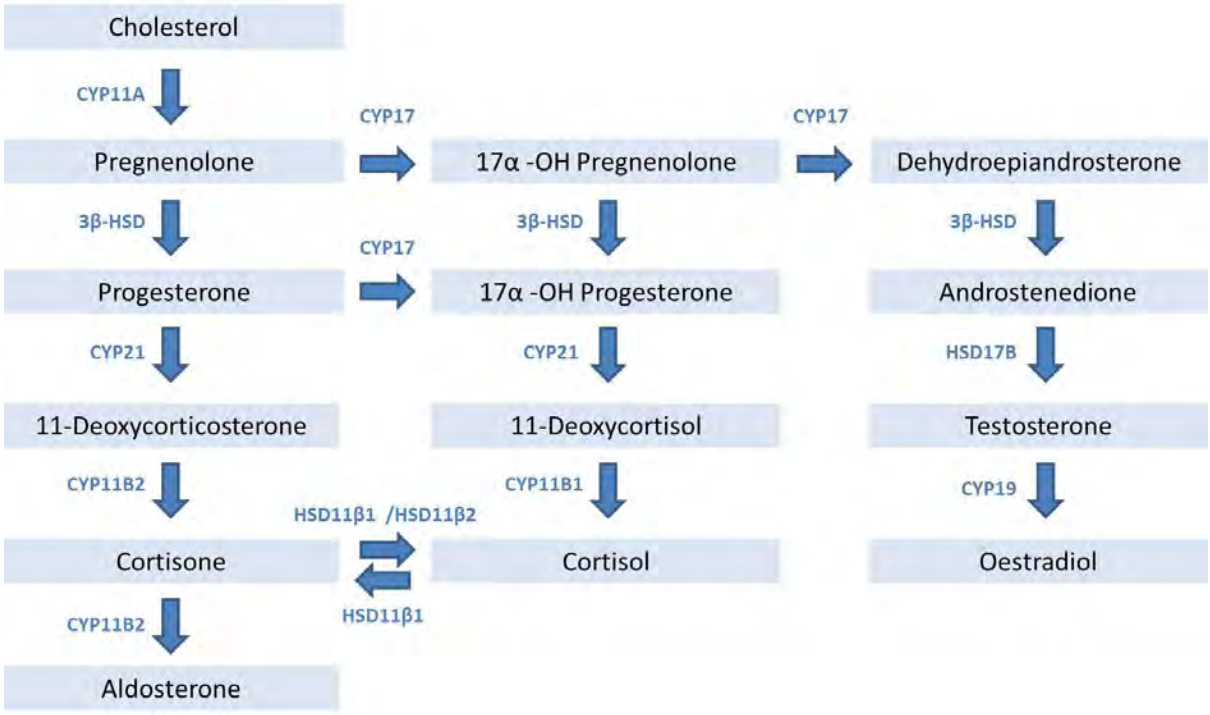

Figure 2.1: Steroidogenic pathway.

Overview of the major steroidogenic pathway. Conversion enzymes are indicated by blue text and steroid products indicated by blue shaded boxes (Holt and Hanley. 2007).

To assess the physiological effects of products exposed to spermatozoa it is important to select the 'correct' sperm population. *In vivo* the population containing the fertilising spermatozoa are selected through viscous barriers within the female reproductive tract. The cervical mucus, which spermatozoa have to penetrate, exhibits a viscoelastic property, contributed by the protein Mucin (Carlstedt and Sheehan. 1984) and has been shown to preferentially select for spermatozoa which have a 'normal' morphology and progressive motility (Hanson and Overstreet. 1981;Katz et al. 1997). Spermatozoa in viscous mediums have been shown to affect flagellar bending and sperm trajectory (Smith et al. 2009). There is also preliminary unpublished data from our laboratory that

shows that penetration through a viscous medium may not only select for progressive spermatozoa, but select for spermatozoa with lower levels of DNA damage (data not shown). There appears a moderate negative correlation between sperm motility and chromatin structure, with sperm populations that exhibit higher percentages of motile cells having lower levels of DNA fragmentation (Giwercman et al. 2003).

There appears to be a complex combination of signals and interaction between spermatozoa and their environment. Many of the molecular mechanisms involved and their effects on spermatozoa are currently unknown. Whether these factors and their ability to elicit the 'correct' response in spermatozoa are important for a pregnancy positive outcome deserves investigation. The work in this chapter looks at the selection of motile spermatozoa through a viscous medium and effect of cumulus cells and follicular fluid collected from patients undergoing assisted reproductive treatment, on spermatozoa motility and $[Ca^{2+}]_i$ influx and whether the results relate to pregnancy outcome.

2.2 Aims

- To develop a physiologically based sperm selection method and compare different sperm preparation techniques.
- To identify any effects on sperm motility exerted by native human cumulus cells.
- To establish the effects of human follicular fluid on spermatozoa $[Ca^{2+}]_i$ responses.

2.3 Materials

2.3.1 Cell Culture reagents

Product Name	Company	Product Number
Bovine Serum Albumin (BSA)	Millipore, Watford, UK	82-002-4
Dimethyl sulfoxide (DMSO)	Sigma, Dorset, UK.	D4540
Dulbecco's Modified Eagle/F-12 Medium (DMEM/F-12)	Invitrogen, Paisley, UK.	21041-033
Fetal Bovine Serum (FBS)	Biosera, Ringmer, UK.	S181X
Non Essential Amino Acids (NEAA)	Invitrogen, Paisley, UK	11140-035
Penicillin/Streptomycin	Invitrogen, Paisley, UK.	15140-122
Supplemented Earle's Balanced Salt Solution (sEBSS)	Geneflow, Fradley, UK.	06-2010-03-1B

2.3.2 Chemicals

Product Name	Company	Product Number
Agarose	Bioline, London, UK.	41025
Deoxynucleoside triphosphates (dNTPs)	Promega, Southampton, UK	C1141
Ethidium bromide	Sigma, Dorset, UK.	160539
Ethylenediaminetetraacetic acid disodium salt dehydrate (EDTA)	Sigma, Dorset, UK	E5134
Glacial acetic acid	Fisher Scientific, Loughborough, UK	A/0400/PB17
Glucose	Sigma, Dorset, UK	G7528
Methylcellulose 4000	Sigma, Dorset, UK	M0512
N-(2-Hydroxyethyl)piperazine-N'-(2-ethanesulfonic acid) (HEPES)	MP Biochemical, Ohio, USA l	194726
Percoll	Sigma, Dorset, UK	P1644
Pluronic F-127 *20% solution in DMSO	Invitrogen, Paisley, UK	P3000MP
Poly D lysine solution	Sigma, Dorset, UK.	P8920

Product Name	Company	Product Number
Potassium chloride	MP Biochemical, Ohio, USA l	194726
Progesterone	Sigma, Dorset, UK.	P0130
Sodium chloride	Sigma, Dorset, UK.	S9888
Tris(hydroxymethyl)aminomethane	Sigma, Dorset, UK	25285-9

2.3.3 Commercial Kits

Product Name	Company	Product Number
Sensiscript Reverse Transcriptase (RT) kit	Qiagen, Crawley, UK.	205211
Total RNA purification kit	Norgen Bioteck Corp	17200

2.3.4 DNA and Protein ladders

Product Name	Company	Product Number
1Kb DNA Step Ladder	Promega, Southampton, UK.	G6941
25bp DNA Step Ladder	Promega, Southampton, UK.	G4511

2.3.5 Dyes

Product Name	Company	Product number
Calcium Green-1 AM	Invitrogen, Paisley, UK	C3012
6X Blue/Orange loading dye	Promega, Southampton, UK.	G1881

2.3.6 Enzymes

Product Name	Company	Product Number
RNase Inhibitor	Bioline, London, UK.	65027
Red Taq DNA Polymerase	Bioline, London, UK	21038

2.4 Methods

2.4.1 Human Spermatozoa preparation

Human sperm donors were recruited and gave their informed consented at the Assisted Conception Unit (ACU), Birmingham Women's Hospital (HFEA Centre 0119) in accordance with the Human Fertilization and Embryology Authority code of practice (The HFEA 2011). The research was reviewed and approved by the Local Ethical Panel (South Birmingham LREC 2003/239). Semen samples were obtained from healthy donors via masturbation after 2-3 days of sexual abstinence. Semen was then allowed to liquify for 30 min at 37°C before preparation.

Dependent on the experimental design, spermatozoa were prepared using either one or all of the following sperm preparation techniques.

Percoll Density Gradient Centrifugation

Percoll was prepared into a 100% isotonic (285-300 mOsm/kg) solution by dilution with 10 X M medium (1.37 M NaCl, 25 mM KCl, 200 mM N-(2-hydroxyethyl)piperazine-N'-(2-ethanesulfonic acid) (HEPES), 100 mM glucose). Percoll fractions of 90% and 45% were prepared by diluting 100% Percoll with 1 X M medium. Liquefied semen (1 ml) was layered over a 90% and 45% gradient (1 ml of each) and centrifuged at 2000 *x g* for 20 min, the spermatozoa pellet was resuspended and left to capacitate in sEBBS + 0.3% (w/v) BSA for a minimum of 3 h and maximum of 4 h, at 37°C, 6% CO_2.

The Direct Swim-up Method

Three hundred microlitre aliquots of liquefied semen were underlaid beneath 1 ml sEBBS + 0.3% (w/v) BSA in round bottomed tubes. Tubes were inclined at a 45° angle and incubated for 1 h at 37°C, 6% CO_2. The upper 0.8 ml of media, containing highly motile spermatozoa, was then collected, and set aside for the spermatozoa to capacitate in sEBBS + 0.3% (w/v) BSA for a minimum of 3 h and of maximum 4 h, at 37°C, 6% CO_2.

Modified Swim-up Method

These experiments were designed to mimic the selective viscous physiological environment of the female reproductive tract. Three hundred microlitre of 1% (w/v) methylcellulose 4000 in sEBBS + 0.3% (w/v) BSA, which had a viscosity of 140 centipoise (cP) was aliquoted into round bottomed tubes. Three hundred microlitre of semen sample was underlaid beneath the methylcellulose. The methylcellulose layer was then overlaid with 250 µl of sEBSS + 0.3% (w/v) BSA. Multiple tubes were inclined at a 45° angle and incubated for 1 h at 37°C, 6% CO_2. Penetrating spermatozoa were collected, pooled and left to capacitate in sEBBS + 0.3% (w/v) BSA for a minimum of 3 h and maximum of 4 h, at 37°C, 6% CO_2 (figure 2.2).

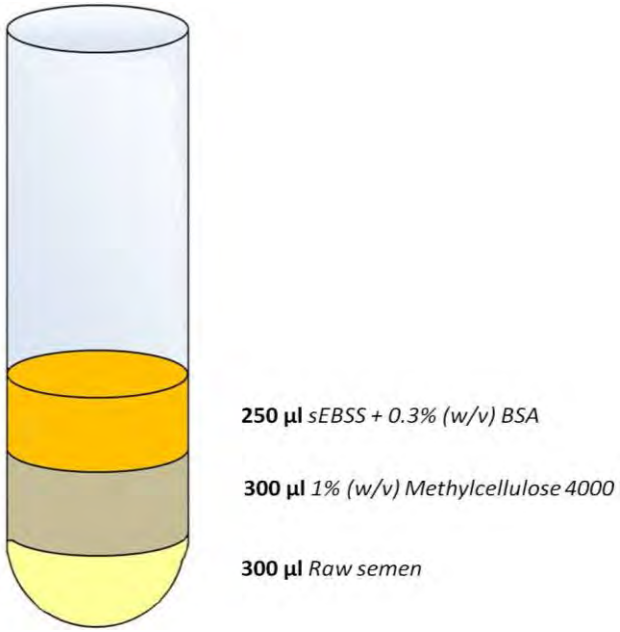

Figure 2.2: Modified swim-up sperm preparation method.

2.4.2 Spermatozoa preparation technique comparison

For comparison between sperm preparation techniques, each sample was prepared using all three preparation techniques. The motility of the spermatozoa was assessed both before and after preparation.

Analysis of motility

Sperm motility was assessed using Computer Aided Sperm Analysis (CASA) software on a Hamilton-Thorne IVOS Version 10.9i. The CASA equipment was operated using the standard setup parameters (37°C working temperature; cell depth 20 µm; frame rate 60 Hz; average path velocity low cutoff 5 µm/s and high cutoff 25 µm/s) (Björndahl et al. 2006). Each assessment of motility was an average of 10 fields of view per chamber with two chambers used per treatment to obtain a reliable evaluation of sperm motility. The

percentage of motile and progressive sperm was recorded. Statistical analysis (one-way analysis of variance (ANOVA)) was completed using SPSS 14.0.

2.4.3 Human Cumulus Cell, Follicular Fluid and Granulosa cell preparation

Patients undergoing either *in vitro* fertilisation (IVF) or intracytoplasmic sperm injection (ICSI) treatment were recruited and gave their informed consent at the Assisted Conception Unit (ACU), Birmingham Women's Hospital (HFEA Centre 0119) in accordance with the Human Fertilization and Embryology Authority code of practice (Ethical approval number 2003/239). The patients had been treated hormonally to induce multiple follicle development prior to oocyte retrieval; briefly the female cycle was down regulated with Buserelin acentate, followed by long protocol stimulation with urinary follicle stimulating hormone (FSH). A transvaginal ultrasound-guided puncture was used to aspirate the follicles recovering the cumulus oocyte complexes (COC) and follicular fluid. In some cases a 'flushing' medium, containing Hartmann's solution with heparin was used to aspirate the follicle. Samples of follicular fluid from individual follicles were separated and pooled depending on whether a "flushing" medium was used.

Preparation of Cumulus cells

The cumulus cells were removed from the COC by exposure to hyaluronidase, either before ICSI was performed or post-fertilisation of the oocyte in IVF. The cells collected were centrifuged at 600 *x g* for 10 min, the cell pellet was resuspended in Dulbecco's modified Eagle's medium F-12 (DMEM/F-12) supplemented with 10% (v/v) FBS, 1% (v/v)

NEAA and 100 IU/ml (each) Penicillin and Streptomycin and incubated at 37°C, 6% CO_2. Cumulus cultures were kept for a maximum of 3 days.

Preparation of Follicular Fluid

Only recovered follicular fluid from follicles not "flushed" was used, to avoid "flushing" medium contamination. Follicular fluid was centrifuged at 3500 *x g* for 30 min to remove any cell debris. The supernatant was then aliquoted and frozen at -20°C until required.

Preparation of Granulosa Cells

Mural granulosa cells dislodged from the follicles by the aspiration process were collected from the follicular fluid by centrifugation. The cell pellet was layered over a 90%/45% Percoll density gradient and centrifuged at 2000 *x g* for 20 min to allow separation of granulosa cells from red blood cells. The granulosa cells were collected and further centrifuged at 600 *x g* for 10 min to remove Percoll contamination. The cell pellet was resuspended in Dulbecco's modified Eagle's medium F-12 (DMEM/F-12) supplemented with 10% (v/v) FBS, 1% (v/v) NEAA and 100 IU/ml (each) Penicillin and Streptomycin and incubated at 37°C, 6% CO_2, cells were in culture for a maximum of 3 days.

2.4.4 Immortalised Human Granulosa cell line (COV434) cell culture.

An immortalised human granulosa cell line (COV434) (derived from a primary human granulosa cell tumour) was donated by Dr. P.I.Schrier of the Department of Oncology, University of Leiden, Netherlands (van den Berg-Bakker et al. 1993). The granulosa cells were cultured in Dulbecco's modified Eagle's medium F-12 (DMEM/F-12) supplemented

with 10% (v/v) FBS, 1% (v/v) NEAA and 100 IU/ml (each) Penicillin and Streptomycin and incubated at 37°C, 6% CO_2 (Zhang et al. 2000). Culture media was replaced every 3-4 days.

Once the COV434 cells were confluent they were subcultured. Cell scrapers were used to dislodge the COV434 cells from the culture flask and cells were recovered in complete growth medium and centrifuged for 5 min at 500 *x g.* Cells were resuspended in culture medium at a typical subcultivation ratio of 1:3.

For storage, frozen aliquots of COV434 cells in cryoprotectant medium (90% (v/v) FBS, 10% (v/v) DMSO) were stored in liquid nitrogen. When required, frozen aliquots of COV434 cells were thawed in a 37°C water-bath and slowly mixed with complete growth medium in order to avoid osmotic shock. Cells were then centrifuged for 5 min at 500 x *g,* then seeded in an appropriate volume of culture medium.

2.4.5 Investigation of the interaction between Spermatozoa and Cumulus cells

After preparing semen by the modified swim-up technique (section 2.4.1) selected and capacitated spermatozoa were split into 300 µl aliquots and placed in round bottomed tubes. Layers of 300 µl 1% (w/v) methylcellulose 4000 in sEBSS + 0.3% (w/v) BSA containing suspensions of either native human cumulus cell, COV434 cells or cell-less controls were pipetted over the spermatozoa. The methylcellulose layer was then overlaid with 250 µl of sEBSS. + 0.3% (w/v) BSA, (figure 2.3). Tubes were inclined at a 45° angle and incubated for 1 h at 37°C, 6% CO_2. Penetrating spermatozoa were collected and analysed.

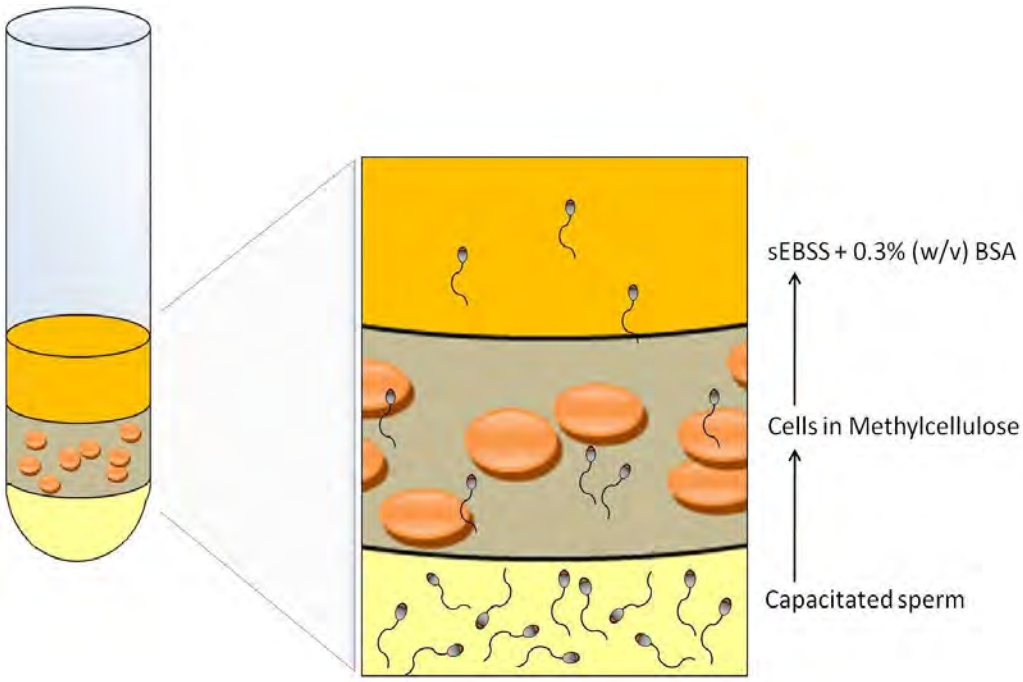

Figure 2.3: Cartoon illustrating the spermatozoa and cumulus cell interaction swim-up experiment.

Analysis of motility

Sperm motility parameters (see table 2.1) were assessed using Computer Aided Sperm Analysis (CASA) software on a Hamilton-Thorne IVOS Version 10.9i. The CASA equipment was operated using the standard setup parameters (37°C working temperature; cell depth 20 µm; frame rate 60 Hz; average path velocity low cutoff 5 µm/s and high cutoff 25 µm/s) (Björndahl et al. 2006). Each assessment of motility was an average of 10 fields of view per chamber with two chambers used per treatment to obtain a reliable evaluation of sperm motility.

Sperm motility parameters were normalised to sperm motility parameters from control experiments containing no cumulus cells (expressed as percentage change (Δ%)). Statistical analysis (student's independent t-test) was completed using SPSS 14.0.

Motility parameter	Abbreviation	Unit	Definition
Straight line velocity	VSL	µm/s	The total straight line distance travelled, measured from the first to the last point of trajectory.
Average path velocity	VAP	µm/s	The distance travelled in the average direction of movement.
Curvilinear velocity	VCL	µm/s	The distance that the head of the sperm travels.
Lateral head displacement	ALH	µm	The width of the lateral movement of the head, calculated as the total width of the head trajectory
Beat cross frequency	BCF	Hz	The number of times the sperm head crosses the direction of movement, which is related to the development of another flagellar wave.

Table 2.1: CASA motility parameters.

(Mortimer. 2000b)

2.4.6 Analysis of Steroidogenic enzyme gene expression.

Total RNA was extracted from a number of donated cumulus cell samples using the Total RNA purification kit in accordance to the manufacturers' protocol, once extracted RNA was stored at -80°C.

Reverse transcription was carried out with Sensiscript Reverse Transcriptase (RT) kit according to manufacturers' protocol. Briefly reactions contained; 1 µM oligo-dT primer, 1 X buffer, 0.5 mM (each) dNTPs , 10 U RNase inhibitor, 1 µl Sensiscript Reverse Transcriptase enzyme and 50 ng of RNA template. Reactions were incubated at 37°C for 1 h, and then stored at -20°C.

Primers were designed to screen for expression of steroidogenic enzymes, using the NCBI Primer-BLAST online tool. Primers used in PCR amplifications were obtained from Eurogentec, Southampton, UK. Oligonucleotide sequences are indicated in table 2.2.

PCR reactions contained 1 U Taq DNA polymerase, 0.5 µM (each) appropriate reverse and forward primers, 0.5 mM (each) dNTPs, 2 mM $MgCl_2$ and 2 µl of RT Sensiscript reaction. Each PCR reaction had a corresponding negative water control to ensure no contamination was present. Reactions were performed under the following conditions: 95°C, 2 min; 35 cycles of 95°C, 30 s; 52°C, 30 s; 72°C, 1 min and one cycle of 72°C, 5 min.

Primer	Oligonucleotide sequence (5'-3')
GAPDH - Forward	CAATGACCCCTTCATTGACC
GAPDH - Reverse	TTGATTTTGGAGGGATCTCG
CYP19 - Forward	TCACTGGCCTTTTTCTCTTGGT
CYP19- Reverse	GGGTCCAATTCCCATGCA
CYP17 - Forward	CATGCTGGACACACTGATGC
CYP17 - Reverse	GGGTTGTATCTCTAAATCTGTG
3β HSD - Forward	GTGTGCCAGTCTTCATCTAC
3β HSD - Reverse	CAGGGTTAAAGGAAGGCTCC
HSD11B2 - Forward	CTGGCTGCTTCAAGACAGAGT
HSD11B2 - Reverse	AGGCAGGTAGTAGTGGATGAA

Table 2.2: Steriodogenic enzyme oligonucleotide sequences.

2.4.7 Agarose gel electrophoresis.

Dependent on the expected size of the PCR product, agarose gels were prepared at various concentrations from 1% to 2.5% (w/v) agarose (table 2.3) in 1 X TAE buffer (0.04 M tris-acetate, 0.001 M EDTA) supplemented with 0.5 µg/ml ethidium bromide. Five microlitres of an appropriate DNA ladder and 20 µl of PCR product were loaded. Gels were visualised using a UV-Transilluminator.

Amount of agarose in gel (%)	Range of separation of linear DNA (Kb)
1.0	3 – 0.1
2.0	6 – 0.4

Table 2.3: DNA separation of different (w/v) percentages agarose gels.

(Maniatis et al. 1982).

2.4.8 Single Cell Imaging.

After preparing semen by direct swim-up technique (section 2.4.1), capacitated spermatozoa at 6 million cells/ml were labelled with Calcium Green-1 AM, diluted in Pluronic F-127 *20% solution in DMSO, to a final concentration of 7.5 µM and incubated for 45 min at 37°C, 6% CO_2. After incubation approximately 100 µl of labelled spermatozoa were introduced into a purpose-built, perfusable, imaging chamber. Chambers were then incubated at 37°C, 6% CO_2 for 5-10 min, to allow spermatozoa to become fully immobilised to the lower surface of the imaging chamber, a 0.01% (v/v) poly-D-lysine coated coverslip.

The chamber was placed on the stage of the imaging system (Cairn Imaging System – in brief comprising Nikon TE3000 with LED excitation controlled by Cairn Optomorph software) and perfused with sEBSS + 0.3% (w/v) of BSA for 5 min at the standard perfusion rate (0.4 ml/min) to remove all traces of extracellular dye. Cells were imaged using an x40 Plan Fl objective. Experiments were carried out at room temperature.

Experiments consisted of an initial 5 min control perfusion of sEBSS + 0.3% (w/v) BSA followed by sequential repeats of exposure to follicular fluid for 50 s followed by either 5 or 10 min control perfusion with sEBSS + 0.3% (w/v) BSA. Experiments were ended with a final exposure of 3.2 µM progesterone diluted in sEBSS supplemented with 0.3% (w/v) BSA. Images were captured at intervals of 2.5 s. Follicular fluid samples from a variety of patients were used at different concentrations (see table 2.4).

Exposure number	Donor number	Dilution (v/v)	Pregnancy outcome	Procedure	Reason for infertility
1	119ECF04	10%	Positive	IVF	Unexplained
2	119ECF08	10%	Negative	IVF	Age related factors
3	119ECF25	10%	Positive	ICSI	Male infertility
4	119ECF21	10%	Negative	ICSI	Endometriosis
5	119ECF04	10%	Positive	IVF	Unexplained
6	119ECF04	50%	Positive	IVF	Unexplained
7	119ECF25	10%	Positive	ICSI	Male infertility
8	119ECF25	50%	Positive	ICSI	Male infertility

Table 2.4: Human follicular fluid samples used in imaging experiments.

Human follicular fluid was diluted to the desired concentration in sEBSS + 0.3% (w/v) BSA. Donors were assigned an individual code, ensuring anonymity. Information regarding their clinical diagnosis and pregnancy outcome was taken from their clinical medical records.

2.4.9 Data processing and analysis.

Data was processed offline using Image ProPlus 7.0 software. A region of interest was manually drawn around the head of each spermatozoon in the field of view. For each cell the average intensity within the head was obtained for every image in the series and plotted against time. Data from cells that moved significantly during the experiment were not included in analysis.

Raw intensity values were imported into Microsoft Excel and normalised using the equation:

$$R = [(F - F_{rest})/F_{rest}] \times 100\%$$

R is normalised fluorescence intensity, F is Fluorescence intensity at time t and F_{rest} is the mean of at least 20 determinations of F taken during the control period.

At each time point the normalised fluorescence intensity values (R) for each cell were compiled to generate average normalised head fluorescence (R_{tot}). The total series of R_{tot} were then plotted to give the mean normalised response of head fluorescent intensity for that experiment.

To assess if cells were exhibiting a significant $[Ca^{2+}]_i$ response to the follicular fluid and progesterone treatments Microsoft Excel was used to calculate the mean and 95% confidence interval of fluorescent intensity for 20 images during the control periods taken prior to individual treatments ($C \pm c$) and 20 images during exposure to treatments ($T \pm t$) (figure 2.4) . An increase in fluorescence was considered significant if,

$$T - t > C + c$$

Where ‘T’ and ‘t’ are the mean and 95% confidence interval for the treatment periods and ‘C’ and ‘c’ the mean and 95% confidence interval for the control period. Cells were categorised as either a responder or non-responder. Data from each experiment was pooled to calculate the frequency of each response to the different treatments and expressed as mean ± SEM. SPSS 14.0 was used to analyse for statistical significance.

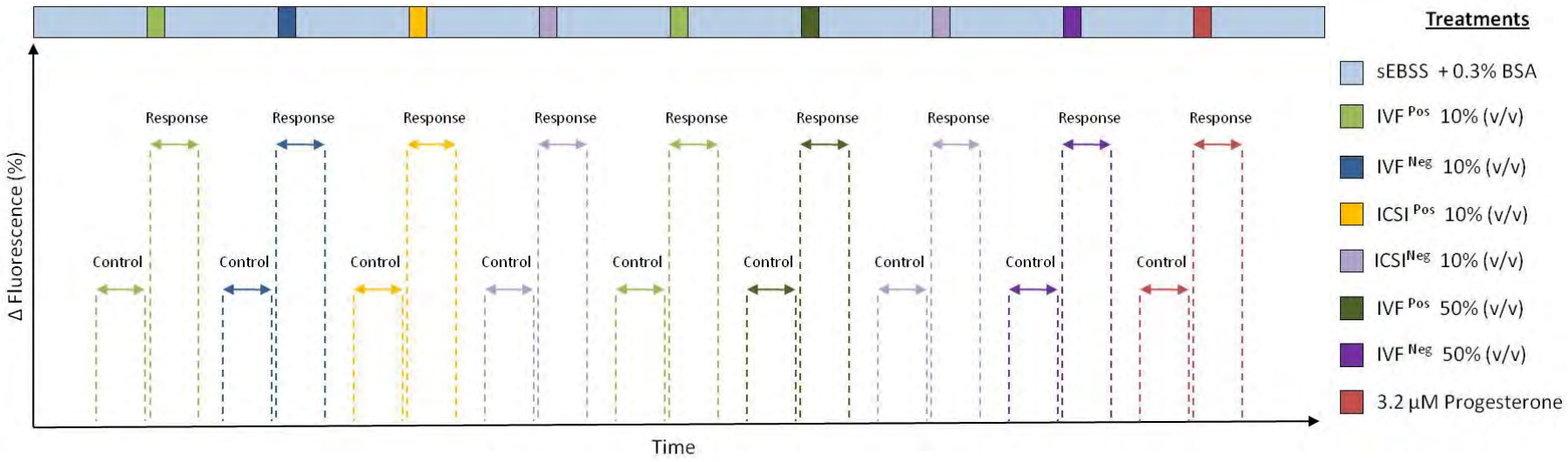

Figure 2.4: Assessment of sperm responses to treatments.

To analyse spermatozoa for statistically significant $[Ca^{2+}]_i$ responses upon exposure to human follicular fluid and progesterone, normalised fluorescence values (Δ Fluorescence (%)) during response periods (50 s) were compared to responses during control periods (50 s) prior to treatment exposure.

2.5 Results

2.5.1 Modified swim-up method viability

To assess the ability of the modified swim up to select motile and progressive spermatozoa in comparison to more established sperm preparation techniques: Percoll density centrifugation and aqueous direct swim-up, data was collected and CASA analysed from 16 sperm donors. The percentage of motile and progressively motile sperm in raw semen samples was assessed using CASA (section 2.4.2). Samples were then split equally and prepared using the three sperm preparation methods (section 2.4.1) and again analysed by CASA to determine the percentage of motile and progressive spermatozoa present.

All three preparation methods effectively selected motile and progressive sperm populations from raw semen, increasing the percentage of motile spermatozoa by 5-8% and progressive spermatozoa by 13-15% dependent on preparation method. No statistical difference in the percentage of motile and progressive spermatozoa was found between the three preparation methods (figure 2.5).

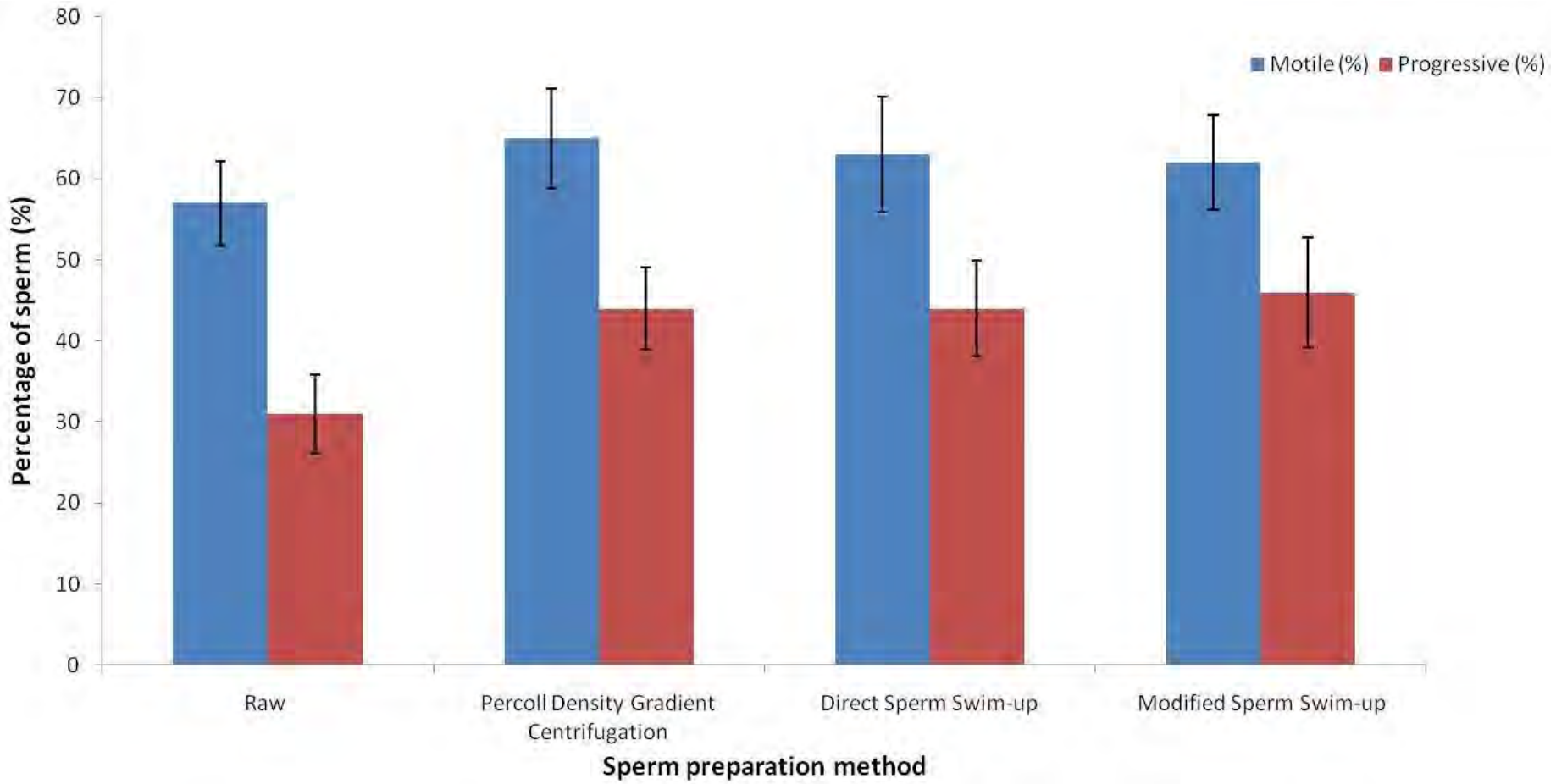

Figure 2.5: Mean (%) of motile and progressive spermatozoa recovered after different sperm preparation techniques.

The motile and progressive percentages (%) of spermatozoa were recorded by CASA before and after spermatozoa preparation. Samples were equally split between the three preparation techniques. Bars represent the mean (%) ± SEM, n = 16.

2.5.2 Modulation of sperm motility by native cumulus

To investigate whether cumulus cells play an active role in the modulation of sperm motility, the modified swim-up technique was utilised to facilitate an interaction between human spermatozoa with either: cumulus cells removed from pre-fertilisation COCs from patients undergoing ICSI treatment; cumulus cells removed from post-fertilisation COCs from patients undergoing IVF treatment; or an immortalised human granulosa cell line (COV434). Cumulus cells were suspended in a 1% methylcellulose layer which allowed spermatozoa to interact in a more physiological viscous environment (section 2.4.5). Motility parameters were analysed using CASA (section 2.4.2).

The data presented by cell type (IVF cumulus; ICSI cumulus; COV434 cells) shows that after exposure to different cumulus cell types the straight line velocity (VSL), the straight line distance between the first and last points of spermatozoa trajectory, and the average path velocity (VAP), the distance the spermatozoa has travelled in the average direction of movement, both decrease, with no statistical difference between cell types ($P>0.05$) (figure 2.6 a, 2.7 a). The curvilinear velocity (VCL), the total distance that the spermatozoa covers, the highest of the three sperm velocity values, increases, but again shows no statistical difference between cell type ($P>0.05$) (figure 2.8 a). The amplitude of lateral head displacement (ALH), the total width of the lateral movement of the spermatozoa head trajectory, increases, but no statistical difference could be identified between cell types ($P>0.05$) (figure 2.9 a). Finally beat cross frequency (BCF), the number of times the sperm head crosses the direction movement which is related to the formation of the flagellar wave,

decreases, but no statistical difference could be identified between cell types (P>0.05) (figure 2.10 a).

Data was also separated according to the cumulus cell donors' fertility treatment outcome. This identified some interesting trends. VSL values for spermatozoa exposed to cumulus from donors that had a pregnancy-positive outcome increased with a mean percentage change (Δ%) of 4.7 ± 6.5% as compared to cumulus with a pregnancy-negative outcome that decreased by 7.7 ± 3.3%. Statistical analysis identified no significant difference, however the P value was 0.086 (figure 2.6 b). As with the case of VSL, VAP showed a clear difference between spermatozoa exposed to cumulus from donors with either a pregnancy-positive or pregnancy-negative outcome. In the presence of pregnancy-positive cumulus cells spermatozoa VAP values increased by 10.1 ± 6.9%, whereas with pregnancy-negative cumulus VAP values decreased by 4.9 ± 3.5%. Again statistical analysis showed no significant difference, however the P value was 0.054 (figure 2.7 b). Spermatozoa that were exposed to pregnancy-positive and pregnancy-negative cumulus cells, are found to have increased levels of VCL, 22.3 ± 9.7%, 5.8 ± 6.7% (respectively). However the large standard error of the data made it hard to determine accurate trends, with no statistical significance being identified (P>0.05) (figure 2.8 b). Cumulus cells from both pregnancy-positive and pregnancy negative groups caused a similar increase in spermatozoa ALH values with and no differential effect between pregnancy-positive cumulus (68.1 ± 30.9%) and pregnancy-negative cumulus (63.9 ± 37.0%) (figure 2.9 b). Finally spermatozoa BCF decreased when exposed to cumulus cells from both patient groups. However spermatozoa exposed to pregnancy-positive cumulus had a much smaller decrease (4.2 ± 2.0%) as compared to that of BCF from spermatozoa

exposed to pregnancy-negative cumulus (13.9 ± 1.6%), which exhibits an almost statistically different significance (P = 0.06) (figure 2.10 b).

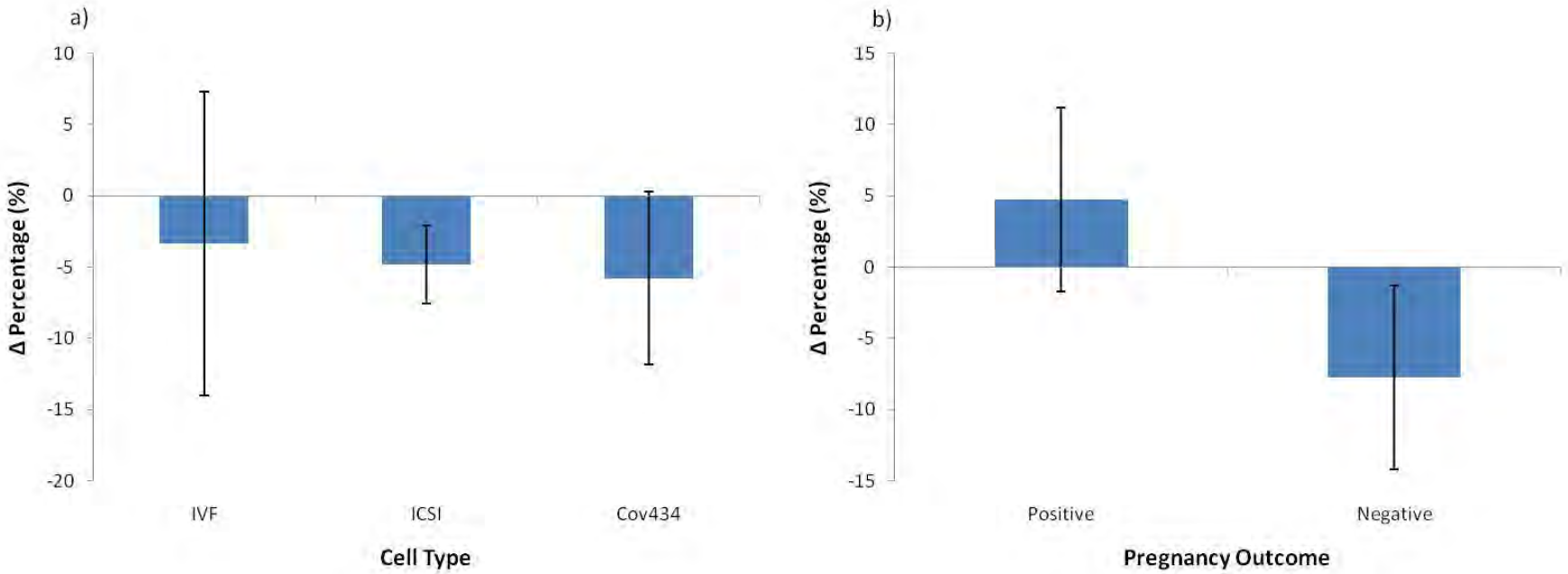

Figure 2.6: Mean percentage change (Δ%) of spermatozoa straight line velocity (VSL) after cumulus interaction.

Bars represent the mean percentage change from prepared spermatozoa (Δ%) of VSL values after interaction with either native human cumulus or an immortalised granulosa (COV434) cell line suspended in 1% methylcellulose made with sEBSS + 0.3% (w/v) BSA. Samples were analysed using CASA and normalised to cell-free controls. Errors bars represent SEM. (**a**) Shows data separated by assisted reproductive technique (IVF or ICSI) in addition to COV434 cell line (**b**) Shows data separated by pregnancy outcome of cumulus cell donors.

	IVF	ICSI	COV434
N number	4	11	8
Mean VSL (Δ%) ± SEM	-3.4 ± 10.6	-4.8 ± 2.7	-5.8 ± 6.1

	Positive	Negative
N number	4	11
Mean VSL (Δ%) ± SEM	4.7 ± 6.5	-7.7 ± 3.3

Table 2.5: Summary data for figure 2.6.

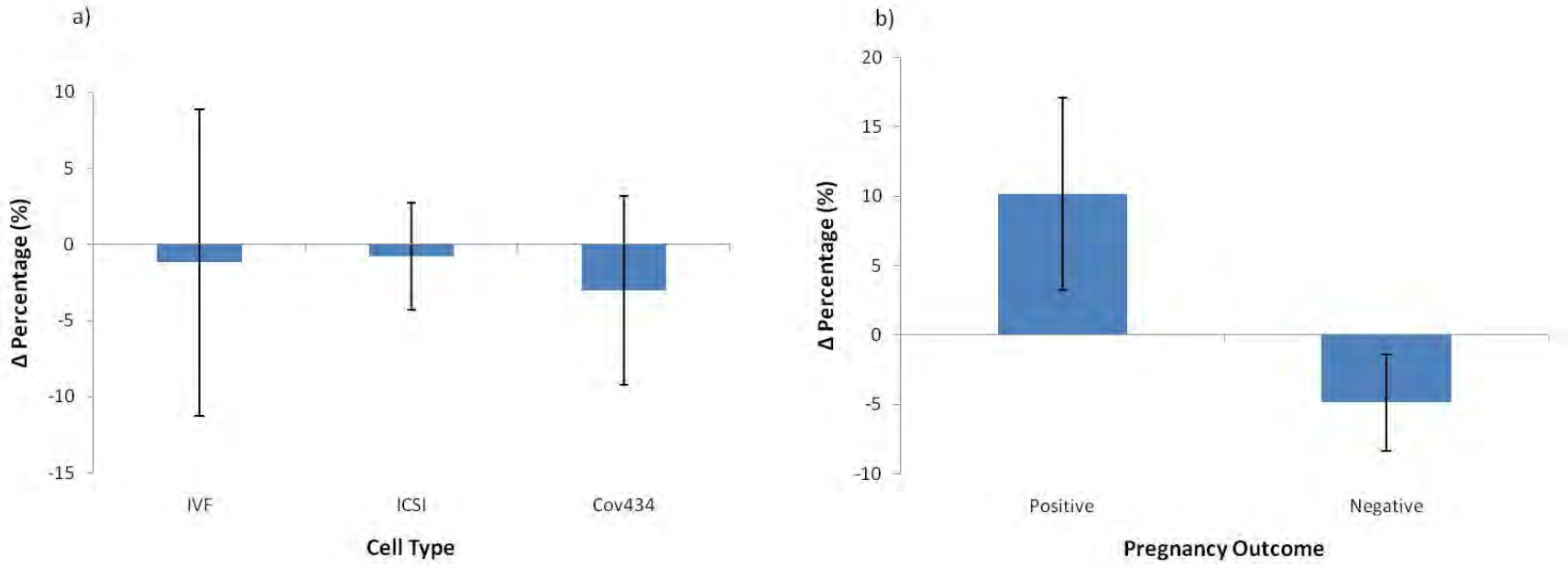

Figure 2.7: Mean percentage change (Δ%) of spermatozoa average path velocity (VAP) after cumulus interaction.

Bars represent the mean percentage change from prepared spermatozoa (Δ%) of VAP values after interaction with either native human cumulus or an immortalised granulosa (COV434) cell line suspended in 1% methylcellulose made with sEBSS + 0.3% (w/v) BSA. Samples were analysed using CASA and normalised to cell-free controls. Errors bars represent SEM. (**a**) Shows data separated by assisted reproductive technique (IVF or ICSI) in addition to COV434 cell line (**b**) Shows data separated by pregnancy outcome of cumulus cell donors.

	IVF	ICSI	COV434
N number	4	11	8
Mean VAP (Δ%) ± SEM	-1.2 ± 10.1	-0.8 ± 3.5	-3.0 ± 6.2

	Positive	Negative
N number	4	11
Mean VAP (Δ%) ± SEM	10.1 ± 6.9	-4.9 ± 3.5

Table 2.6: Summary data for figure 2.7.

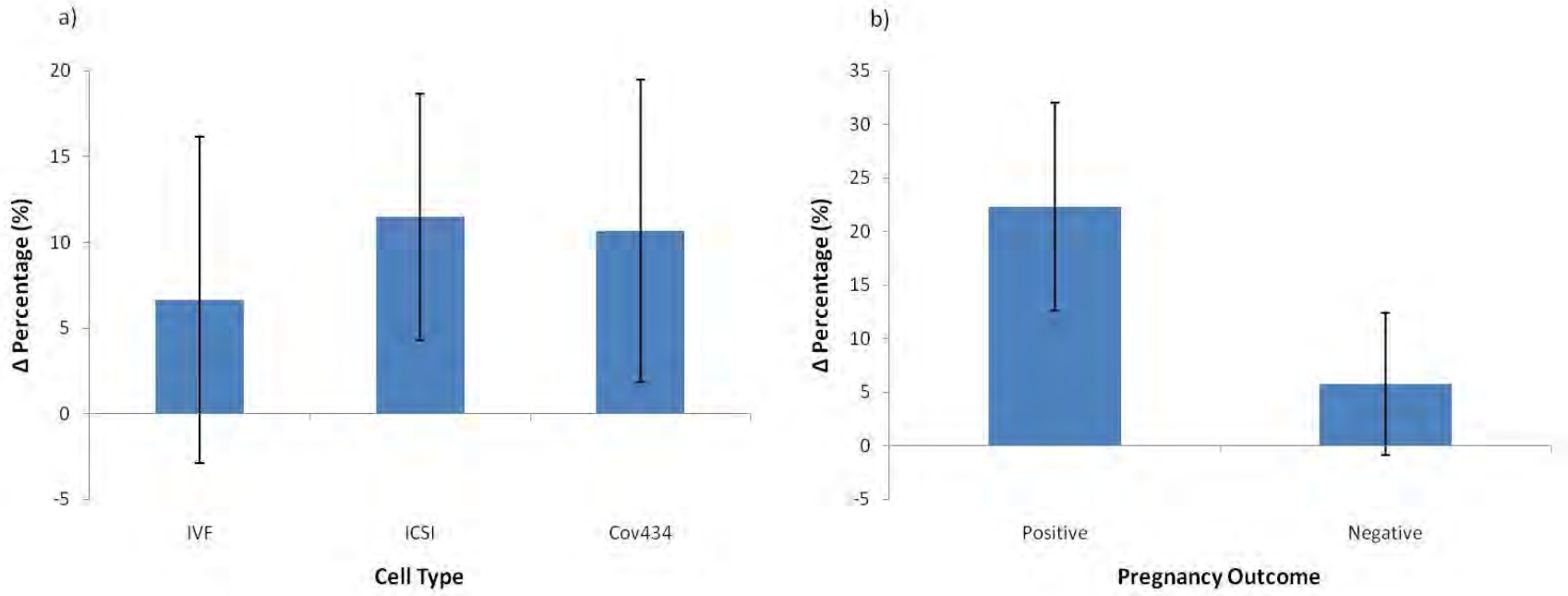

Figure 2.8: Mean percentage change (Δ%) of spermatozoa curvilinear velocity (VCL) after cumulus interaction.

Bars represent the mean percentage change from prepared spermatozoa (Δ%) of VCL values after interaction with either native human cumulus or an immortalised granulosa (COV434) cell line suspended in 1% methylcellulose made with sEBSS + 0.3% (w/v) BSA. Samples were analysed using CASA and normalised to cell-free controls. Errors bars represent SEM. (**a**) Shows data separated by assisted reproductive technique (IVF or ICSI) in addition to COV434 cell line (**b**) Shows data separated by pregnancy outcome of cumulus cell donors.

	IVF	ICSI	COV434
N number	4	11	8
Mean VCL (Δ%) ± SEM	6.6 ± 9.5	11.5 ± 7.2	10.7 ± 8.8

	Positive	Negative
N number	4	11
Mean VCL (Δ%) ± SEM	22.3 ± 9.7	5.8 ± 6.7

Table 2.7: Summary data for figure 2.8.

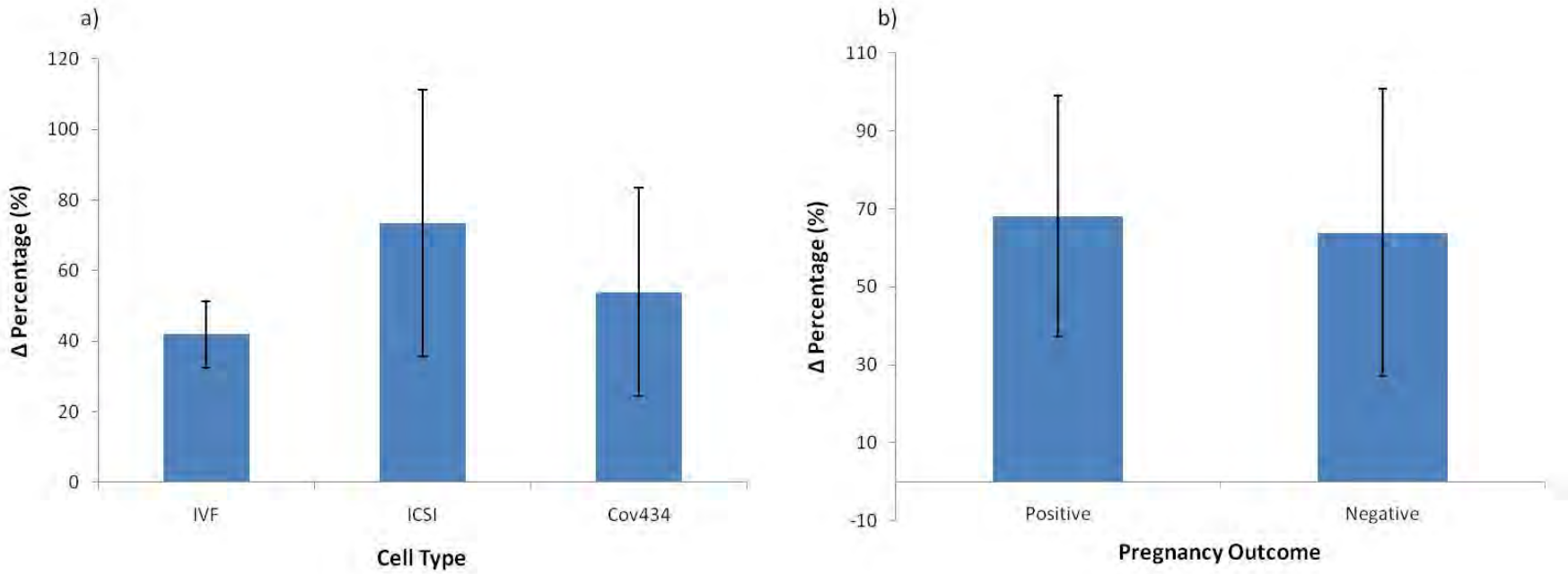

Figure 2.9: Mean percentage change (Δ%) of spermatozoa amplitude of lateral head displacement (ALH) after cumulus interaction.

Bars represent the mean percentage change from prepared spermatozoa (Δ%) of ALH values after interaction with either native human cumulus or an immortalised granulosa (COV434) cell line suspended in 1% methylcellulose made with sEBSS + 0.3% (w/v) BSA. Samples were analysed using CASA and normalised to cell-free controls. Errors bars represent SEM. (**a**) Shows data separated by assisted reproductive technique (IVF or ICSI) in addition to COV434 cell line (**b**) Shows data separated by pregnancy outcome of cumulus cell donors.

	IVF	ICSI	COV434
N number	4	11	8
Mean ALH (Δ%) ± SEM	42.0 ± 9.3	73.4 ± 37.6	53.8 ± 29.6

	Positive	Negative
N number	4	11
Mean ALH (Δ%) ± SEM	68.1 ± 30.9	63.9 ± 37.0

Table 2.8: Summary data for figure 2.9.

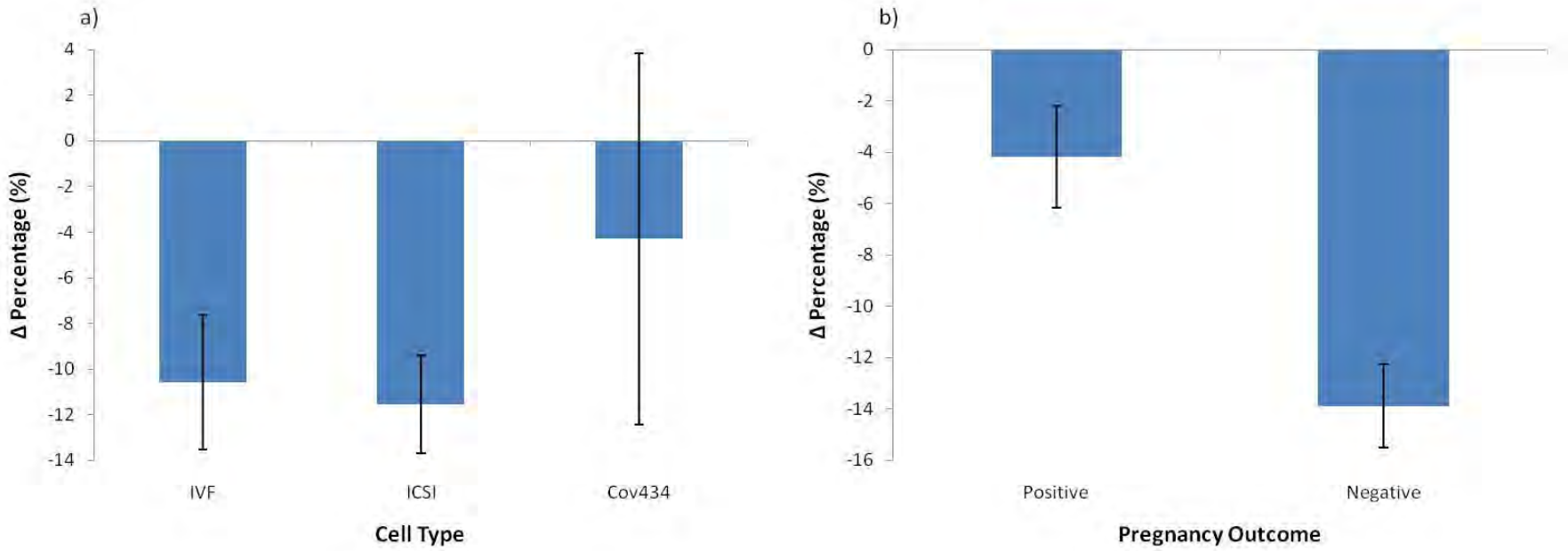

Figure 2.10: Mean percentage change (Δ%) of spermatozoa beat cross frequency (BCF) after cumulus interaction.

Bars represent the mean percentage change from prepared spermatozoa (Δ%) of BCF values after interaction with either native human cumulus or an immortalised granulosa (COV434) cell line suspended in 1% methylcellulose made with sEBSS + 0.3% (w/v) BSA. Samples were analysed using CASA and normalised to cell-free controls. Errors bars represent SEM. (**a**) Shows data separated by assisted reproductive technique (IVF or ICSI) in addition to COV434 cell line (**b**) Shows data separated by pregnancy outcome of cumulus cell donors.

	IVF	ICSI	COV434
N number	4	11	8
Mean BCF (Δ%) ± SEM	-10.6 ± 2.9	-11.6 ± 2.1	-4.3 ± 8.1

	Positive	Negative
N number	4	11
Mean BCF (Δ%) ± SEM	-4.2 ± 2.0	-13.9 ± 1.6

Table 2.9: Summary data for figure 2.10.

2.5.3 Expression of steroidogenic enzymes in cumulus cells

Cumulus cells from ICSI and IVF patients (section 2.4.3) were analysed for expression of enzymes involved in steroidogenesis and to see if expression of the conversion enzyme HSD11β related to pregnancy outcome as previously reported (Michael et al. 1993). RT-PCR (section 2.4.6) identified expression of 3β-HSD and CYP19 in all samples, while CYP17 was not detected at all. HSD11β2 expression was found in all samples tested except patient: IVF #4, which was the only sample that came from a patient with positive pregnancy outcome (figure 2.11).

Expression was also tested in the mural granulosa cells, dislodged from the follicle during the oocyte aspiration procedure (section 2.4.3). As with the cumulus cells, 3β-HSD and CYP19 were expressed in all samples, however unlike cumulus cell samples there was a positive result for CYP17 expression. HSD11β2 was also present in all samples. All mural granulosa cell samples were recovered from patients with a negative pregnancy outcome (figure 2.11).

.

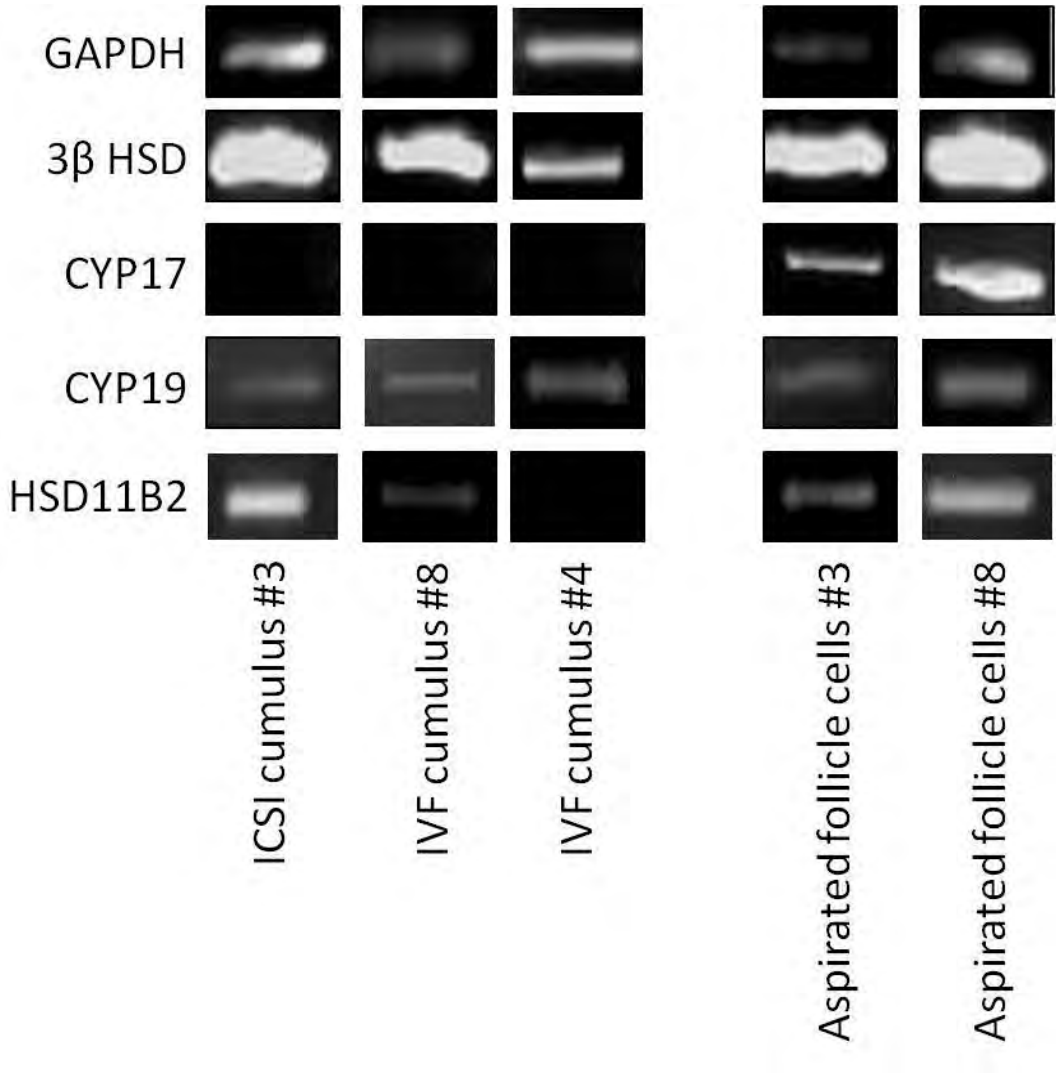

Figure 2.11: Expression of steroidogenic enzyme genes in human cumulus and granulosa cells.

Cells donated by patients undergoing either IVF or ICSI treatment are indicated by individual anonymised sample numbers. Shown are PCR products separated by gel electrophoresis, performed on the following genes: Positive RT-PCR control GAPDH; 3β HSD; CYP17; CYP19 and HSD11β2.

2.5.4 Sperm calcium response to human follicular fluid

Single cell $[Ca^{2+}]_i$ imaging was used to investigate if follicular fluid from patients undergoing ART could generate a Ca^{2+} response in spermatozoa.

Immobilised spermatozoa were exposed by constant perfusion to sequential repeats of either 5-10 min control periods of sEBSS + 0.3% (w/v) BSA followed by 50 s exposure to follicular fluid samples. The follicular fluid samples used in these experiments were selected based on patients' ART procedure and their treatment outcome. The two follicular fluid samples from patients with a pregnancy-positive outcome were exposed to spermatozoa at two differing dilutions (10% and 50% (v/v)). As a positive control spermatozoa were exposed to 3.2 µM progesterone (Kirkman-Brown et al. 2000). In total 206 cells over 3 replicate experiments were individually analysed for increases in $[Ca^{2+}]_i$.

Spermatozoa had a significant increase in $[Ca^{2+}]_i$ upon exposure to human follicular and progesterone This can be seen on an individual single cell level in single cellular normalised fluorescent intensity traces and pseudocolour images (figure 2.12, figure 2.13) as well as a universal population level by analysis of the mean normalised fluorescent intensity values (R_{tot}) of 206 spermatozoa cells over 3 individual replicate experiments (figure 2.14).

The mean percentage of the sperm population responses to the different follicular fluid samples showed a high population response ranging from 88.5 ± 7.9% to 98.4 ± 1.7% (figure 2.15), with no statistical difference identified between population responses to different follicular fluid samples. Progesterone however, initiated a mean population response of only 85.3 ± 4.1% and when compared to the follicular fluid population responses to all three IVF^{Pos} applications it showed a statistically significant difference: IVF^{Pos} 10% (v/v) 1st

application (P = 0.039); IVF^{Pos} 10% (v/v) 2nd application (P = 0.042); IVF^{Pos} 50% (v/v) (P = 0.039). A significant difference was also identified between the progesterone and $ICSI^{Pos}$ 50% (v/v) (P = 0.039). The initial application of $ICSI^{Pos}$ 10% (v/v) was almost significant with a P value of 0.058 (figure 2.15).

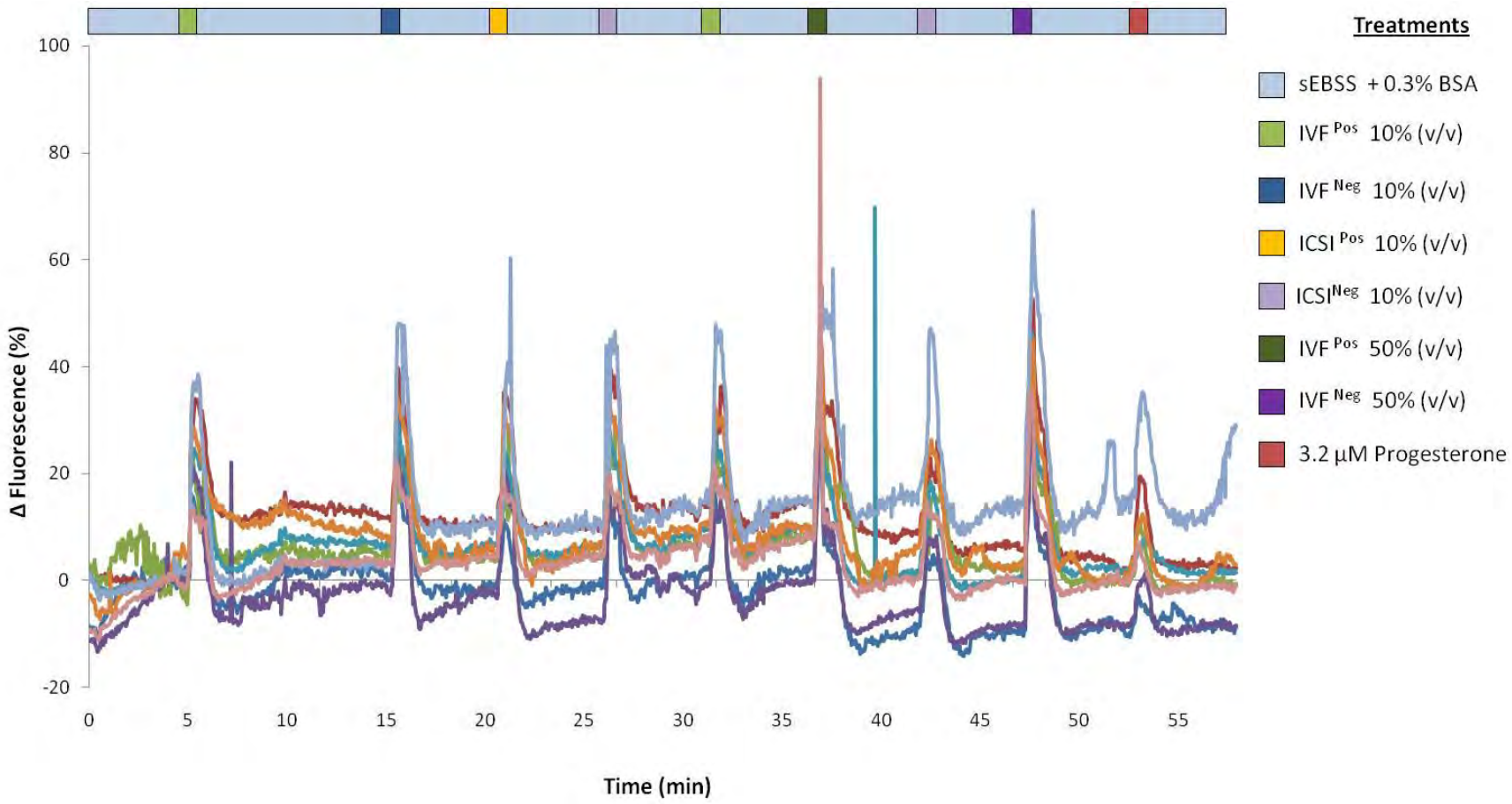

Figure 2.12: Single cell traces of human follicular fluid and progesterone induced $[Ca^{2+}]_i$ responses in spermatozoa.

Representative single cell traces of 8 cells from an individual experiment. Treatment bar gives a schematic representation of time periods when cells were exposed via constant perfusion to a sequential exposure of different preparations of human follicular fluid and 3.2 µM progesterone, all separated by control periods of sEBSS + 0.3% (w/v) BSA for either 5 or 10 min.

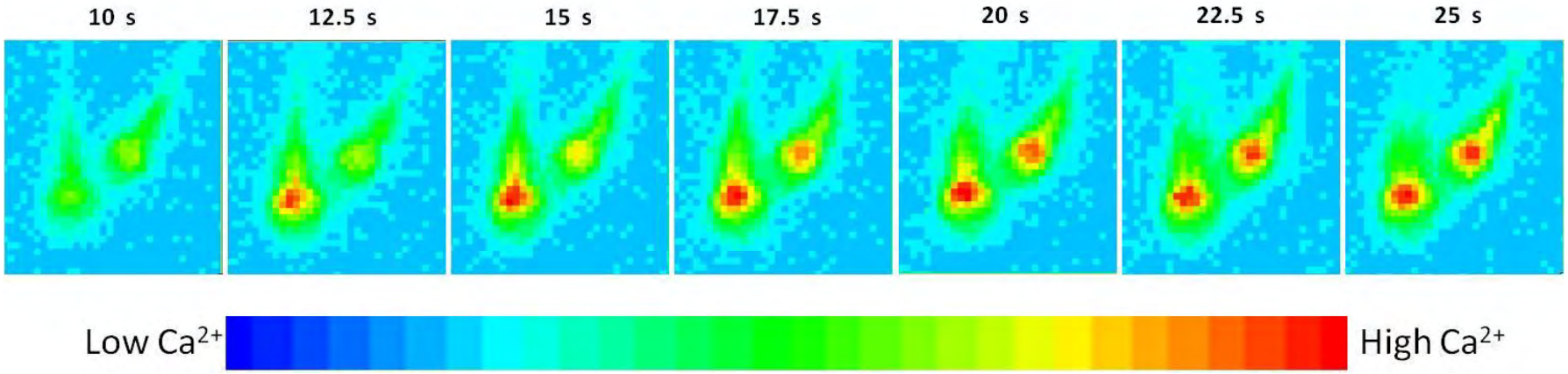

Figure 2.13: Series of representative pseudo-colour images of two spermatozoa undergoing a Ca^{2+} response to follicular fluid.

High $[Ca^{2+}]_i$ (indicated by warm colours) was observed when spermatozoa were exposed to human follicular fluid (IVF^{Pos} 10% (v/v)1^{st} application) (labelled with Calcium Green-1AM). Numbers show time in seconds (s) after perfusion was initiated.

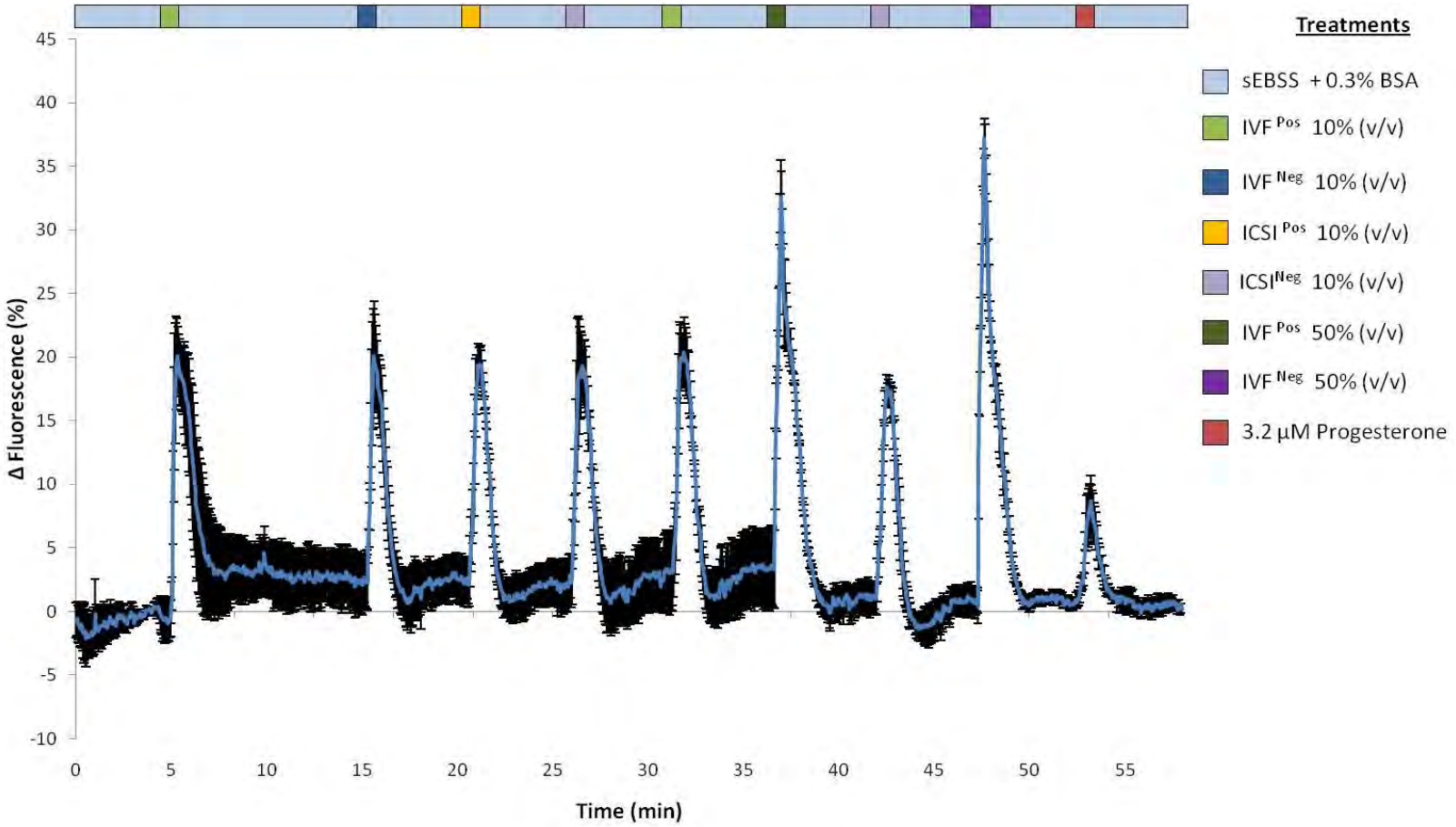

Figure 2.14: Mean response (R_{tot}) trace of Human follicular fluid and Progesterone induced $[Ca^{2+}]_i$ response in spermatozoa.

Mean response (R_{tot}) trace of normalised Δ fluorescence (%) in 206 spermatozoa cells over 3 replicate experiments. Treatment bar gives a schematic representation of time periods when cells were exposed via constant perfusion to a sequential exposure of different preparations of human follicular fluid and 3.2 µM progesterone, all separated by control periods of sEBSS + 0.3% (w/v) BSA for either 5 or 10 min. Error bars represent + SEM.

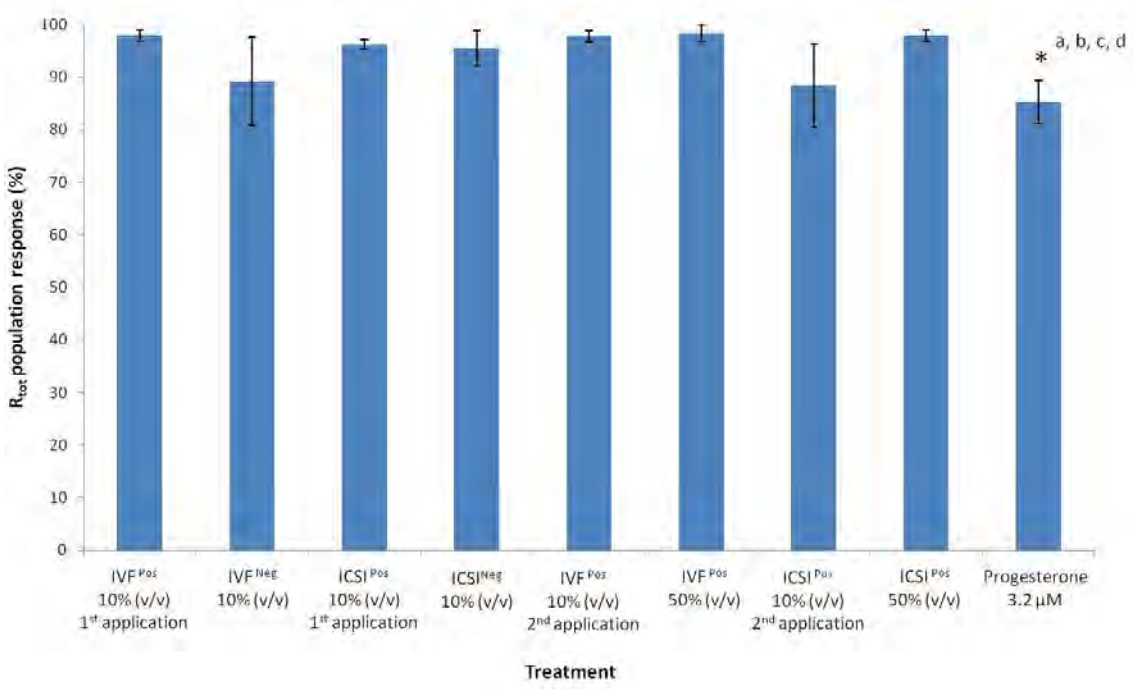

Figure 2.15: Mean percentage (%) of sperm population that elicit a significant $[Ca^{2+}]_i$ response upon exposure to different follicular fluid preparations and 3.2 µM progesterone.

R_{tot} values from 3 replicate experiments analysing 206 cells. Asterisk denotes statistical significant (P<0.05) when compared to [a] IVF^{Pos} 10% (v/v) 1st application; [b] IVF^{Pos} 10% (v/v) 2nd application; [c] IVF^{Pos} 50% (v/v), [d] $ICSI^{Pos}$ 10% (v/v). Error bars represent ± SEM.

	IVF^{Pos} 10% (v/v) #1	IVF^{Neg} 10% (v/v)	$ICSI^{Pos}$ 10% (v/v) #1	$ICSI^{Neg}$ 10% (v/v)	IVF^{Pos} 10% (v/v) #2	IVF^{Pos} 50% (v/v)	$ICSI^{Pos}$ 10% (v/v) #2	$ICSI^{Pos}$ 50% (v/v)	Progesterone 3.2 µM
N number	3	3	3	3	3	3	3	3	3
Number of cells	206	206	206	206	206	206	206	206	206
Mean population response (%) ± SEM	98.0 ± 1.1	89.3 ± 8.3	96.2 ± 0.8	96.0 ± 3.3	97.8 ± 1.1	98.4 ± 1.7	88.5 ± 7.9	98.0 ± 1.1	85.3 ± 4.1

Table 2.10: Summary data for figure 2.15.

2.5.5 Peak kinetics of $[Ca^{2+}]_i$ in response to human follicular fluid

To identify significant variations in $[Ca^{2+}]_i$ when spermatozoa were exposed to multiple human follicular fluid samples, the mean normalised fluorescent intensities (R_{tot}) of peaks initiated by follicular fluid samples from patients undergoing different assisted reproduction procedures and with different pregnancy outcomes were aligned by the initiation of the rising phase and compared.

Initial exposure to follicular fluid from an IVF^{Pos} patient initiated a maximum peak of 20.1 ± 2.3% which had a duration of approximately 140 s. The peak had a distinctive shoulder on the descent and the proceeding control perfusion saw responses stay above that of the initial fluorescent intensity baseline (figure 2.16). As this was different to subsequent peaks caused by other patient samples, it had to be established if the peak was patient specific. The same follicular fluid sample was perfused for a second time period; this peak was more like the subsequent peaks after the initial exposure (figure 2.17). The peak had a slightly decreased maximum height, 17.6 ± 1.0% with duration of approximately 90 s. Intensity values returned to pre-exposure values. The same sample was also applied to spermatozoa at a higher concentration (50% (v/v)) and initiated a higher maximum peak (32 ± 2.9%) compared to the 10% (v/v) dilutions. The duration of the peak was similar at approximately 100 s and intensity values returned to pre-stimulation baseline levels (figure 2.16). However what was very notable was that the peak gained a very clear two phase appearance, with an initial rise to a much higher level, looking like a spike, then dropping after approximately 25 s, after which the peak had similar kinetics of decay when compared to the other peaks.

Data was compared to establish if there were any differences in the peaks generated by samples from patients with positive or negative pregnancy outcomes. When peaks were aligned there was no significant difference noted between responses. All had similar maximum peak heights (*IVF^{Neg} 10% (v/v)* : 20.1 ± 4.2%; *$ICSI^{Pos}$ 10% (v/v) 1^{st} application*: 19.4 ± 1.4%; *$ICSI^{Neg}$ 10% (v/v)*: 19.3 ± 2.4%; *IVF^{Pos} 10% (v/v) 2^{nd} application: 20.4 ± 2.7%*) and peak durations (*IVF^{Neg} 10% (v/v)*: 37 s; *$ICSI^{Pos}$ 10% (v/v) 1^{st} application*: 36 s; *$ICSI^{Neg}$ 10% (v/v)*: 40 s; *IVF^{Pos} 10% (v/v) 2^{nd} application: 37 s)* and intensity levels returned to pre-stimulation baseline values (figure 2.17).

In collaboration with Dr. Angela Taylor and Dr. Wiebke Arlt (University of Birmingham), we were able to quantify the concentration of progesterone from a number of human follicular fluid samples (table 2.11). This allowed direct comparison of responses generated by follicular fluid samples to those from 3.2 µM progesterone. Spermatozoa exposed to progesterone and follicular fluid had a similar peak duration (35 s), however the maximum peak height of follicular fluid samples containing 0.4 µM (IVF^{Pos} 10% (v/v) 1^{st} application) and 2.2 µM (IVF^{Pos} 50% (v/v)) was significantly larger when compared to that of 3.2 µM progesterone (max height 8.7 ± 2.0%). The progesterone-induced peak also exhibited a much shallower decent (figure 2.18).

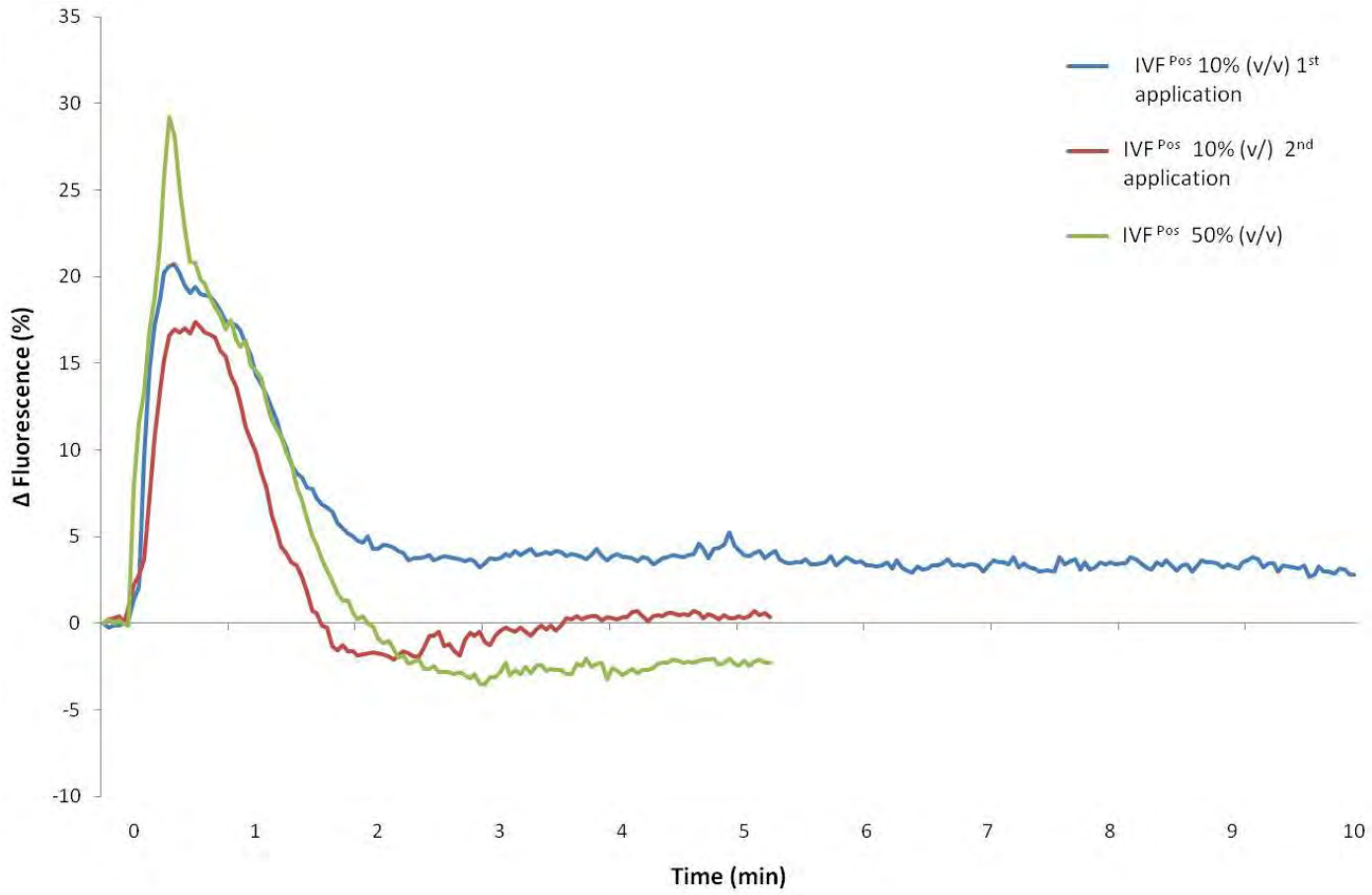

Figure 2.16: Peak alignment of mean response (R_{tot}) trace of normalised Δ fluorescence (%) from spermatozoa exposed to multiple applications of human follicular fluid from an IVF patient with a positive pregnancy outcome.

Peaks aligned are IVF^{Pos} 10% (v/v) 1st application, IVF^{Pos} 10% (v/v) 2nd application and IVF^{Pos} 50% (v/v) and are aligned from time 0, the initiation of the peak. Cells were exposed to follicular fluid samples for 50 s, followed by either a 5 or 10 min control perfusion of sEBSS + 0.3% (w/v) BSA. R_{tot} were analysed from 206 cells over 3 replicate experiments.

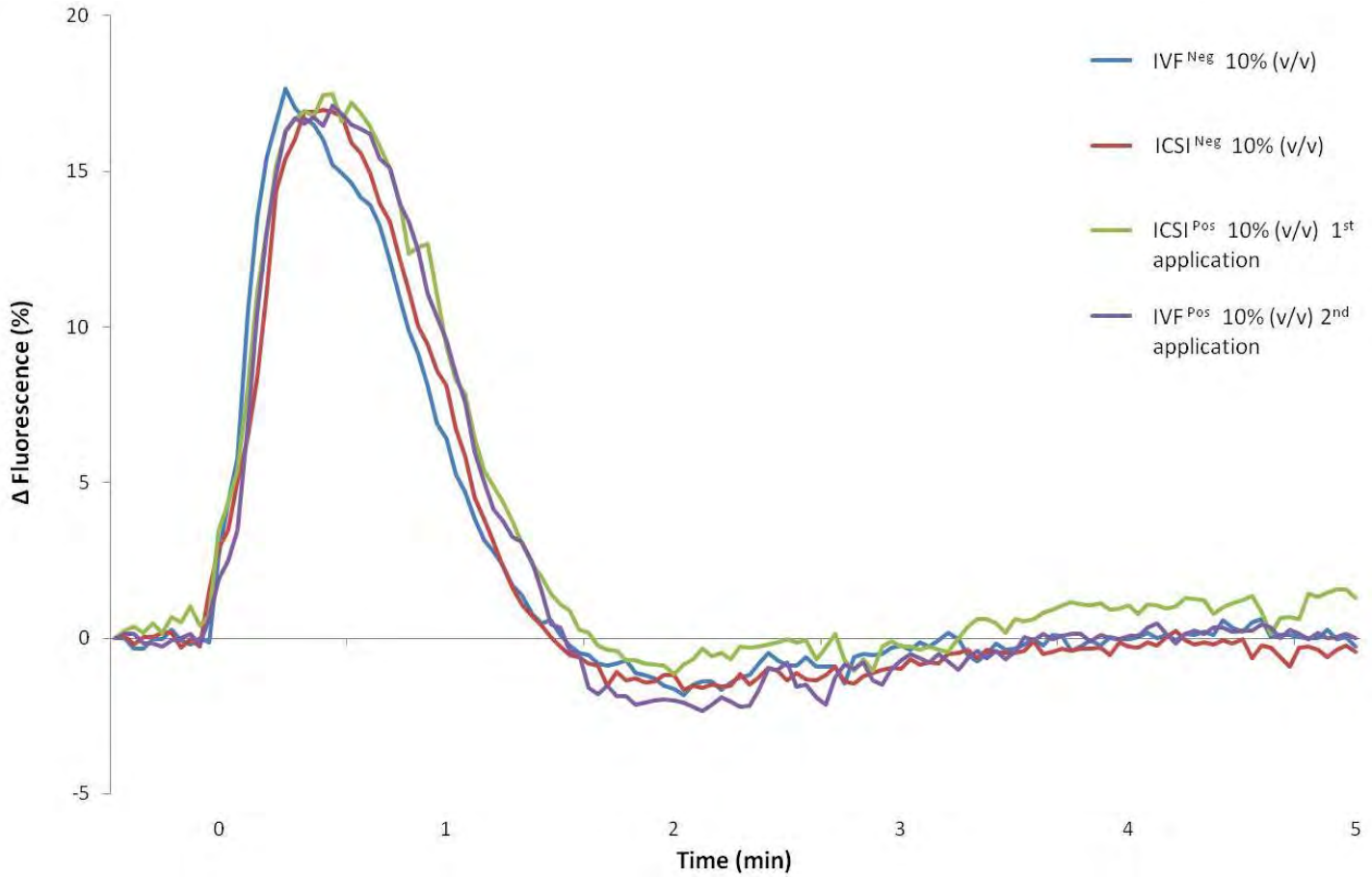

Figure 2.17: Peak alignment of mean response (R_{tot}) trace of normalised Δ fluorescence (%) from spermatozoa exposed to human follicular fluid from IVF and ICSI patients with positive and negative pregnancy outcomes.

Peaks aligned are IVF^{Neg} 10% (v/v), $ICSI^{Neg}$ 10% (v/v), $ICSI^{Pos}$ 10% (v/v)1st application and IVF^{Pos} 10% (v/v) 2nd application. Peaks are aligned from the initiation of the peak (time 0). Cells were exposed to follicular fluid treatments for 50 s, followed by either a 5 min control perfusion of sEBSS + 0.3% (w/v) BSA. R_{tot} were analysed from 206 cells over 3 replicate experiments.

Donor number	Dilution (v/v)	Final progesterone concentration (µM)
119ECF04	10%	0.4
119ECF08	10%	1.7
119ECF21	10%	1.7
119ECF25	10%	1.4
119ECF04	50%	2.2
119ECF25	50%	6.9

Table 2.11: Progesterone concentrations of human follicular fluid samples used in experiments.

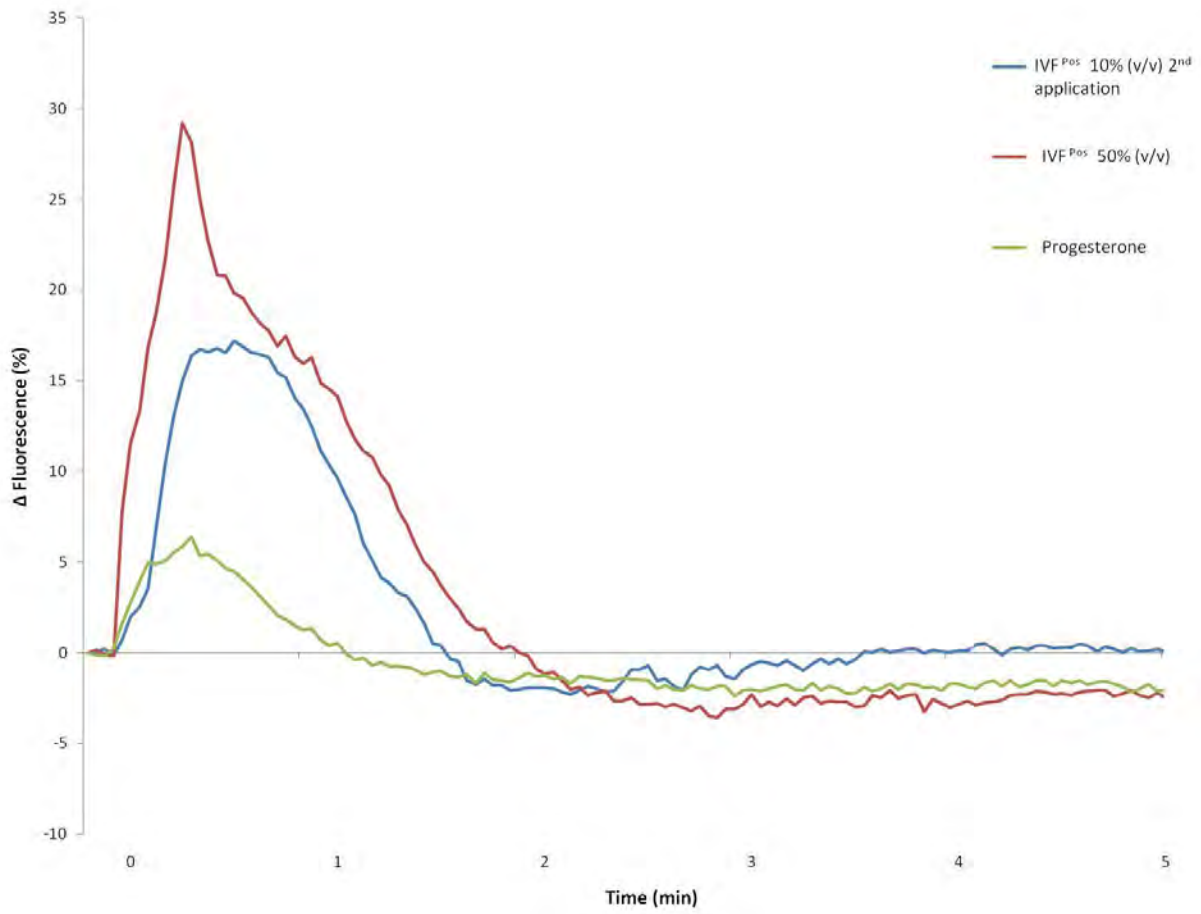

Figure 2.18: Peak alignment of mean response (R_{tot}) trace of normalised Δ fluorescence (%) from spermatozoa exposed to human follicular fluid from IVF^{Pos} and a positive responsive control 3.2 µM Progesterone.

Peaks aligned are IVF^{Pos} 50% (v/v), IVF^{Pos} 10% (v/v) 2nd application and Progesterone (3.2 µM). Peaks are aligned from the initiation of the peak (time 0). Cells were exposed to follicular fluid treatments for 50 s, followed by either a 5 min control perfusion of sEBSS + 0.3% (w/v) BSA. R_{tot} were analysed from 206 cells over 3 replicate experiments.

2.6 Discussion

When investigating the interactions between spermatozoa and cumulus cells it is important to select the 'correct' population containing the fertilising spermatozoon. As mentioned previously, traditional sperm preparations select based on either normal morphology (density centrifugation) or motility through an aqueous environment (direct swim-up); neither method represents the physiological barriers spermatozoa meet *in vivo* (Henkel and Schill. 2003). *In vivo* spermatozoa are selected by their ability to penetrate through the viscous barriers of the female reproductive tract: the cervix (Karni et al. 1971;Wolf et al. 1977); oviductal fluid (Jansen. 1980) and the cumulus cell and hyaluronic acid matrix that surrounds the oocyte (Dandekar et al. 1992).

Ivic et al demonstrated that the viscosity of 1% methylcellulose 4000 was comparable to that of human cervical mucus (Ivic et al. 2002) and our laboratory's assessment of its viscosity was approximately 140 centipoise, a measurement of dynamic viscosity. Although the viscosity measurements of 1% methylcellulose 4000 is lower than the values of Wolf et al measurement of human cervical mucus (approximately 180-520 cp dependent on time in menstrual cycle) (Wolf et al. 1977), methylcellulose does provides a more accurate physiological selection than an aqueous medium. Data showed (figure 2.5) that the percentage of motile and progressive spermatozoa effectively selected from seminal plasma by the methylcellulose swim-up technique was comparable to the two traditional preparation techniques. Notably both the direct swim-up and modified swim-up sperm preparation methods, which select spermatozoa based on progressive motility, do not recover a population that is completely motile which could be due to recovery of the lower

layer of immotile spermatozoa. Seminal plasma must be removed effectively as it contains factors that inhibit the fertilisation ability of spermatozoa in addition to inhibiting capacitation (Rogers et al. 1983;Mortimer. 2000a).

The modified methylcellulose method was used to assess the interaction between sperm and cumulus cells recovered from patients undergoing ART treatment (figure 2.3). Analyses indicated that there was no effect on sperm motility parameters regardless of whether spermatozoa were exposed to cumulus cells stripped from the oocytes of ICSI patients prior to fertilisation or post-fertilisation cumulus cells from IVF patients (figures 2.6-2.10 a). However there were different effects on the three sperm velocity values VSL, VAP and VCL in addition to BCF, when spermatozoa were exposed to pregnancy-positive and pregnancy-negative cumulus cells (figures 2.6-2.10 b). This may imply altered cumulus cell-receptor expression or factor secretion in women who have a successful pregnancy outcome. One can only hypothesise about the physiological role of increases in sperm velocity caused by pregnancy-positive cumulus but it could facilitate COC or ZP penetration.

Cumulus cells have previously been shown to elicit effects on motility parameters of spermatozoa, potentially initiating sperm hyperactivation. Increases in curvilinear velocity and amplitude of lateral head displacement and decreases in beat cross frequency of spermatozoa have been shown when exposed to both cumulus cell conditioned medium and cumulus cells. The effects were not as great in comparison to this study, even with a longer interaction time of 24 h, however whether this was related to their use of a different sperm preparation method (direct swim-up) not selecting the same spermatozoa population would require further investigation (Fetterolf et al. 1994). There is evidence however to suggest

that *in vivo* hyperactivation is induced much earlier in sperm migration through the female reproductive tract and before interaction with the COC (Cooper. 1979;Overstreet and Cooper. 1979;Suarez and Osman. 1987). However after decades of investigation since the first report the physiological triggers of hyperactivation are still not identified, reviewed in (Suarez. 2008).

This study offers interesting results that warrant further investigation. Although CASA is useful for assessing sperm motility it is not without limitations. Curvature values can being skewed by spermatozoa sticking to the glass slides (Suarez. 2008) and if BCF is faster than the rate of image acquisition results can be underestimated (Mortimer and Swan. 1999). Chamber depth has also been known to affect the assessment of sperm motility (Le et al. 1992), and future experiments could use 50 µm chambers which would provide a better assessment of spermatozoa with wide ALH and non-progressive trajectories (Kay and Robertson. 1998). As previously mentioned a viscous medium has been shown to alter flagellum bending (Smith et al. 2009) so further investigations should focus on high speed acquisition experiments, analysing sperm motility in a viscous medium.

Mural granulosa cells dislodged during the aspiration process of oocyte collection exhibited expression of the cytochrome P450 enzyme, CYP17 unlike cumulus cells (figure 2.11). This enzyme is essential in the synthesis of dehydroepiandrosterone (DHEA) a precursor molecule of testosterone and oestradiol (figure 2.1). This correlates with a previous report, that although CYP17 expression is nil in cumulus and granulosa cells, it is highly expressed in the theca cells of the follicle suggesting that the aspiration process may have disrupted not only the mural granulosa cells, but also the underlying theca cells (Patel et al. 2010).

The expression profile of cumulus cells was negative for CYP17, limiting steroidogenic synthesis to the progesterone side of the pathway (figure 2.19). This is in line with studies that show that after ovulation cumulus cells continue to synthesise and secrete progesterone (Baltes et al. 1998). Lower activities of the conversion enzymes, HSD11β1 and 2, which interconvert 'active' cortisol to 'inert' cortisone, have been associated with positive pregnancy outcomes for patients undergoing ART (Michael et al. 1995). Expression of steroidogenic enzymes in cumulus cells may be predictive of pregnancy outcome as an IVF patient, who had a positive pregnancy outcome, was missing expression of the isoform HSD11β2 (figure 2.19), whereas this enzyme was present in cumulus cell samples from pregnancy-negative patients. The expression profiles from cumulus cells seem to correlate with the findings of Michael et al (1995). Due to limited sample availability, further investigation involving larger sample sizes, quantification of genetic expression and activity of the additional isoform, HSD11β1, would be needed to identify a true relationship between steroidogenic enzyme expression patterns and pregnancy outcome and whether this could be useful in the process of choosing which embryos to transfer.

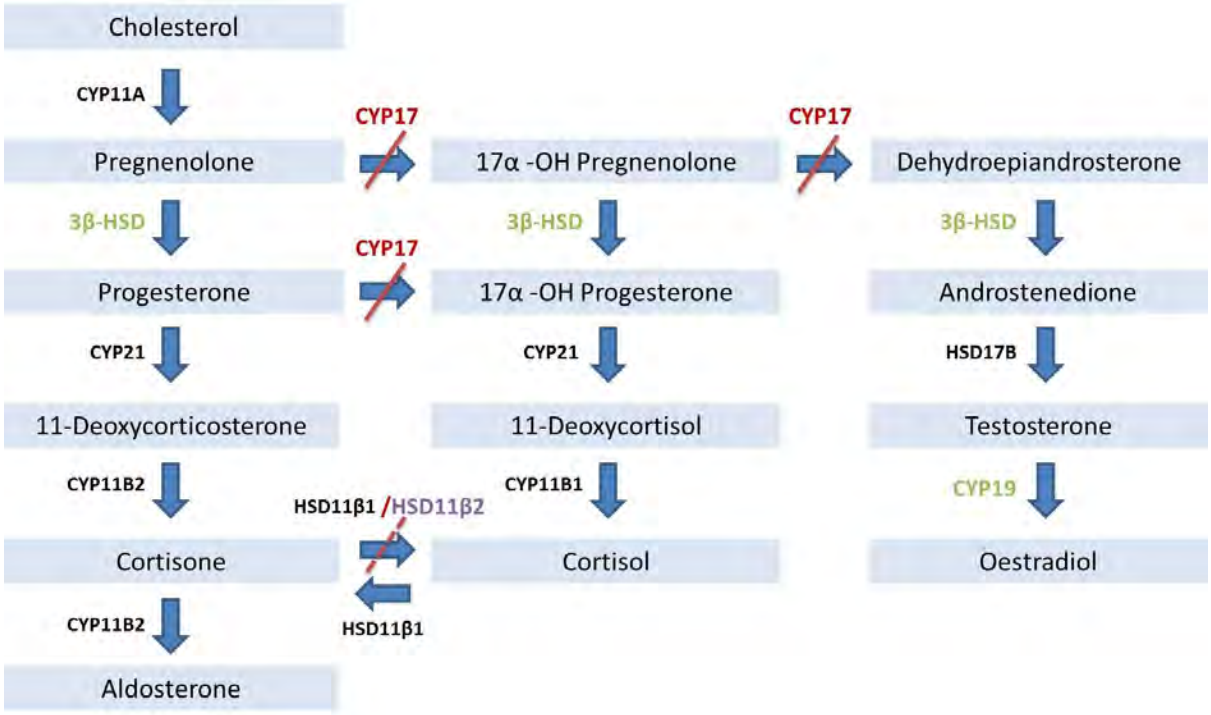

Figure 2.19: A schematic representation of steroidogenic pathway in human cumulus relating to possible pregnancy outcome.

Preliminary findings of steroidogenic enzyme gene expression in cumulus cells from patients undergoing ART. Genes expressed in human cumulus cells are indicated by green text, genes not expressed are indicated by red text. Steroid synthesis in human cumulus cells seems to be limited to left hand branch of steroidogenic pathway. HSD11β2 was the only gene that showed differential expression between cumulus from donors who had either a positive or negative pregnancy outcome, Potential lower activity levels of HSD11β2 would lead to lower levels of cortisone to cortisol conversion, which has been implicated in increased pregnancy outcome (Michael et al. 1995).Genes indicated in black were not investigated in this study, but would be interesting to investigate for in future research. Diagram modified from (Holt & Hanley. 2007).

In addition to the effect of cumulus cells on spermatozoa it has also been shown that human follicular fluid modulates sperm function (figure 2.14). $[Ca^{2+}]_i$ signalling has been previously shown to be critical in sperm function (Jimenez-Gonzalez et al. 2006). The elevation of $[Ca^{2+}]_i$ levels by follicular fluid, is perhaps unsurprising given that a component of follicular fluid is the well-known $[Ca^{2+}]_i$ elevator, progesterone (Bar-Ami et al. 1994;Harper et al. 2004;).

The full steroid and proteomic profile of follicular fluid is still unclear, with a few studies using follicular fluid from ART patients, suggesting the progesterone concentration being 19 – 32 µM (Tarlatzis et al. 1993;de Resende et al. 2010). However progesterone concentration measured from samples in this study ranged from 1 – 27.8 µM (Appendix I.viii).

Exposure to all human follicular fluid samples elicited a similar $[Ca^{2+}]_i$ response, regardless of the differing progesterone concentrations (figure 2.17) and initiated a greater response, with a lower concentration of progesterone, when compared to that of 3.2 µM progesterone control (figure 2.18). Progesterone was not the only steroid identified and quantified in this study. Steroids such as oestradiol, androstenedione and a selection of glucocorticoids were found (full list Appendix I.viii). It is plausible that spermatozoa may respond not only to progesterone but also to a number of other steroids or some other unidentified modulators found in follicular fluid. Recent data has demonstrated that the CatSper channels are at least one progesterone receptor on spermatozoa (Strunker et al. 2011) and these may be affected by an array of the other steroids in follicular fluid.

Significantly different $[Ca^{2+}]_i$ kinetics were observed when spermatozoa were exposed to 50% (v/v) follicular fluid in comparison to 10% (v/v) dilutions, which is a novel finding. The differing, much sharper, kinetics of the initial spike may underlie physiological responses that we have not yet characterised. Only further experiments examining possible calcium channel or other specific antagonists of this response, flagellar movement and acrosome reaction will reveal what is occurring. It could be that this higher elevation is analogous to the 'T-Channel' spike seen when mouse spermatozoa are stimulated to acrosome react by ZP (Bhandari et al. 2010).

Currently it is not known how much follicular fluid spermatozoa are exposed to within the oviduct. Some data from porcine studies have suggested it might be as little as <0.01% of the initiation volume of the follicle (Hansen et al. 1991). Micromolar concentrations of progesterone have been shown to initiate a rapid $[Ca^{2+}]_i$ elevation, with a proportion of the sperm population undergoing the acrosome reaction (AR) (Baldi et al. 1999). Spermatozoa have been known to present a different $[Ca^{2+}]_i$ response when exposed gradually to progesterone gradient, which may be more representative of the exposure that spermatozoa experience *in vivo*. They exhibit a slower rise in $[Ca^{2+}]_i$ with no apparent AR induction, but there is modulation of flagellar activity (Harper et al. 2004;Harper and Publicover 2005). In my experiments the exposure was as a follicular fluid bolus (comparable to single cell experiments in Kirkman-Brown et al. 2000 and those of Baldi et al. 1999 in cell populations). It may be that future presentation as a gradient would have differing effects. This may explain the differing $[Ca^{2+}]_i$ response at a 10% (v/v) dilution. It could be that the $[Ca^{2+}]_i$ spike in the 50% (v/v) follicular fluid is due to very high abundance of a certain compound such as progesterone with a low-affinity receptor, or a trace of a very scarce, as yet unidentified, compound with a high-affinity receptor that is found at very low concentration in follicular fluid. Presenting sperm with fractionated human follicular fluid or preparing steroid solutions to create 'synthetic' follicular fluid may be useful to identify the important components of follicular fluid and the potential channels in involved $[Ca^{2+}]_i$.

It is important to point out that the spermatozoa contributing to a successful pregnancy outcome were not the sperm population used for these studies, and to gauge a true reflection on pregnancy outcome the spermatozoa used for fertilisation must be used. However this provides practical challenges in itself. In addition it has to be considered that

pregnancy outcome may be affected by the single embryo transfer and blastocyst culture system employed and the patient diversity, ethnic background or other factors. However even so, this study has identified interesting avenues for further research which could lead to improved ART techniques.

CHAPTER 3

In vitro oocyte development

3.1 Introduction

The practical and ethical problems associated with collecting sufficient material to thoroughly investigate the interactions between human spermatozoa and oocytes, has forced scientists to rely heavily on animal models for human fertilisation. Researchers have primarily used murine models, however with the fundamental differences between the two species, especially within the protein composition of the zona matrix , there is an requirement for a new model to study human fertilisation (Lefievre et al. 2004).

There have been a number of reports in the literature promoting the ability of embryonic stem (ES) cells (derived from the inner cell mass of the blastocyst prior to epiblast formation) to generate all cell lineages of the embryo *in vitro* and recent studies have shown embryonic stem cells are capable of differentiating into female and male germ cells (Hubner et al. 2003;Toyooka et al. 2003;Clark et al. 2004a;Lacham-Kaplan et al. 2006;Qing et al. 2007;). If a human embryonic stem cell (hESC) line could be induced to produce oocytes this would clearly give a substantial, and genetically manipulatable, source of material for research.

Studies in mouse embryonic stem cells (mESCs) demonstrated that oocyte-like structures could be produced from ES cells. Hubner *et al*., first reported the derivation of oocyte-like structures by enrichment of the germ cell population using the pluripotent and germline specific marker, *Oct4* in a green fluorescent protein (GFP) reporter system. Progression of differentiation was assessed by analysis of germ cell-specific markers such as *Scp3*, *Gdf3* and *Vasa* in addition to morphological evaluation (Hubner et al. 2003).

More recently, Lacham-Kaplan *et al*., directed differentiation of mESCs into ovarian structures containing oocytes that although lacking a zona pellucida, expressed the zona transcription factor, Fig-α and zona pellucida protein 3 (ZP3). Differentiation of mESCs was directed by culturing differentiating stem cell colonies, termed embryoid bodies, in testicular cell-conditioned medium. It was hypothesised that this could be as a result of large amount of growth factors within the media, such as bone morphogenetic protein 4 (BMP4) (Pellegrini et al. 2003;Lacham-Kaplan et al. 2006).

A co-culture technique with murine ovarian granulosa cells used by Qing *et al*., induced the differentiation of mESCs into oocyte-like structures. After 14 days of culture, expression of germ cell markers: mouse vasa homologue (*Mvh*) and synaptonemal complex protein 3 (*SCP3*) in addition to other female germ cell-specific genes, *Fig-α* and ZP genes, 1-3 were observed. It was suggested that the cellular interactions between developing EBs and granulosa cells help to propagate germ cell differentiation (Qing et al. 2007).

Investigators have striven to replicate the results from mESCs in hESCs. Clark *et al*., detected spontaneously differentiated germ cells precursors from hESCs, with some cells in EBs identified as being positive for the expression of germ cell specific markers such as *DAZL, VASA, SCP3* and *GDF9* (Clark et al. 2004a).

More recently human primordial germ cells (PGCs) were differentiated from hESCs by enriching the population using a VASA-GFP fluorescent reporter system, which was further enhanced by co-culture with BMPs (BMP4, BMP7 and BMP8b). Although only showing *SCP3* expression characteristic of later germ cell expression there was positive expression of *DAZL, STELLAR*, *VASA* and *OCT4* characteristic of PGCs differentiation (Kee et al. 2009).

Male germ cells have also been produced from mESCs. Embryoid bodies were found to contain expression patterns of post-migratory primordial germ cells (PGCs) using an *Mvh*-GFP reporter system. Expression was enhanced by EB co-culture with somatic cells secreting BMP4. The PGC population was enriched, and then co-cultured with gonadal cells before transplantation into host testis where they developed into morphologically normal spermatozoa (Toyooka et al. 2003). Male haploid PGCs were also spontaneously derived from mESCs by Geijsen *et al*. who noted that when these cells were isolated and injected into oocytes, blastocyst-like structures were formed (Geijsen et al. 2004). Only one study has reported the production of live offspring as a result of ICSI fertilisation with an in vitro developed male gamete (Nayernia et al. 2006). Sperm development was followed using *Stra8*-GFP and *Prml*-DsRed fluorescent reporter systems, utilising genes specific to spermatogenesis, and although offspring died only a few months after birth, it showed the potential of *in vitro* generated gametes (Nayernia et al. 2006).

The work in this chapter investigates the development of a novel research model for human fertilisation, by directing hESC differentiation into the female germ cell lineage. Follicular fluid and an immortalised granulosa cell line were used to mimic the physiological environment of the ovarian follicle, with development being assessed by pluripotent ES cell and germ line specific markers. Successful generation of limitless human oocytes *in vitro* would overcome the shortage of human oocytes for research and therefore have potential to revolutionise the understanding of oocyte-spermatozoa interaction and fertilisation and provide a source of patient-specific oocytes for ART patients.

3.2 Aims

- To develop a novel model system for *in vitro* oogenesis using hESC differentiation, by mimicking the follicular environment, using:
    - Human follicular fluid
    - An immortalised human granulosa cell line (COV434)

3.3 Materials

3.3.1 Cells

Product Name	Company	Product Number
Human Foreskin Fibroblasts CCD-11125K	LCG Promochem, Middlesex, UK	CRL-2429

3.3.2 Cell Culture reagents

Product Name	Company	Product Number
0.25% (w/v) Trypsin-0.53mM EDTA	Invitrogen, Paisley, UK.	25200-056
Dimethyl sulfoxide (DMSO)	Sigma, Dorset, UK.	D4540
Dulbecco's Modified Eagle/F-12 Medium (DMEM/F-12)	Invitrogen, Paisley, UK.	21041-033
Fetal Bovine Serum (FBS) ES Cell Qualified	Invitrogen, Paisley, UK	10439-024
Gelatine	Sigma, Dorset, UK.	271616
Iscove's Modified Dulbecco's Medium (IMDM)	Invitrogen, Paisley, UK	21980-032
KnockOut™ Dulbecco's Modified Eagle Medium	Invitrogen, Paisley, UK	10829-018
KnockOut™ Serum Replacement	Invitrogen, Paisley, UK	10828-028
L-Glutamine	Invitrogen, Paisley, UK	25030
Non Essential Amino Acids (NEAA)	Invitrogen, Paisley, UK	11140-035
Phosphate buffered saline (PBS)	Invitrogen, Paisley, UK	14040083
Penicillin/Streptomycin	Invitrogen, Paisley, UK.	15140-122
Recombinant human FGF-basic	Peprotech EC Ltd, London, UK	100-18B
β- mercaptoethanol	Invitrogen, Paisley, UK	21985-023

3.3.3 Chemicals

Product Name	Company	Product Number
Agarose	Bioline, London, UK.	41025

Product Name	Company	Product Number
Deoxynucleoside triphosphates (dNTPs)	Promega, Southampton, UK	C1141
Ethidium bromide	Sigma, Dorset, UK.	160539
Ethylenediaminetetraacetic acid disodium salt dehydrate (EDTA)	Sigma, Dorset, UK	E5134
Glacial acetic acid	Fisher Scientific, Loughborough, UK	A/0400/PB17
Tris(hydroxymethyl)aminomethane	Sigma, Dorset, UK	25285-9

3.3.4 Commercial Kits

Product Name	Company	Product Number
Sensiscript Reverse Transcriptase (RT) kit	Qiagen, Crawley, UK.	205211
Total RNA purification kit	Norgen Bioteck Corp	17200

3.3.5 DNA and Protein ladders

Product Name	Company	Product Number
25bp DNA Step Ladder	Promega, Southampton, UK.	G4511
HyperLadder V	Bioline, London, UK	Bio-33031

3.3.6 Dyes

Product Name	Company	Product Number
6X Blue/Orange loading dye	Promega, Southampton, UK.	G1881

3.3.7 Enzymes

Product Name	Company	Product Number
RNase Inhibitor	Bioline, London, UK.	65027
Red Taq DNA Polymerase	Bioline, London, UK	21038

3.4 Methods

3.4.1 Human foreskin fibroblast (hff) cell culture

A commercially available human foreskin fibroblast (hff) cell line was used as a cell feeder layer for hESCs. The cells were cultured in Iscove's Modified Dulbecco's medium (IMDM) supplemented with 10% (v/v) ES cell qualified FBS and 100 IU/ml (each) Penicillin/Streptomycin and incubated at 37°C, 6% CO_2. Culture medium was changed every 3-4 days.

Once hff cells were fully 100% confluent, cells were subcultured. Cells were trypsinised with 0.25% (w/v) trypsin-0.53mM EDTA and incubated at 37°C for approximately 5 min until cell detachment occurred. Cells were recovered in complete growth media and centrifuged for 5 min at 500 x *g.* Cells were resuspended in an appropriate volume of growth medium at a typical subcultivation ratio 1:3. Cells were either used for further hff culture or treated with irradiation (35 Gy) before being used as substrate cells for hESCs.

For long-term storage, frozen aliquots of hffs in cryoprotectant medium (IMDM, 10% (v/v) ES cell qualified FBS, 100 IU/ml (each) Penicillin/Streptomycin and 5% (v/v) DMSO) were stored in liquid nitrogen. If necessary frozen aliquots of hff cells were thawed in a 37°C water-bath and slowly rehydrated with complete growth medium in order to avoid osmotic shock. Cells were then centrifuged for 5 min at 500 x *g,* and then seeded in an appropriate volume of culture medium.

3.4.2 Human embryonic stem cell (hESC) culture

A hESC cell line (HS181),derived by Hovatta *et al*., (Hovatta et al. 2003) was gifted by Dr Outi Hovatta, Karolinska Institute, Sweden. Irradiated hff cells were seeded onto a 1% (w/v) gelatine coated 6-well dish, in 2 ml of hff culture medium (section 3.4.1), cells were left to adhere for approximately 24 h before hESC addition.

Embryonic stem cell colony morphology was assessed microscopically on a daily basis, when colonies were deemed large enough and morphologically 'normal', cells were sub-cultivated. Plated fibroblast cells were washed with culture sterile PBS to remove traces of hff media before the addition of hESC. Colonies were sub-cultivated via mechanical micro-dissection with a 19 gauge needle and colony fragments were transferred to freshly prepared feeder cells.

Cells were cultured in Knockout DMEM supplemented with 20% (v/v) serum replacement, 2 mM L-glutamine, 1% (v/v) non-essential amino acid (NEAA), 100 IU/ml (each) Penicillin/Streptomycin, 0.1 mM β-mercaptoethanol, 4 ng/ml bFGF at 37°C, 6% CO_2. Media was exchanged every 24 h.

When required for storage hESC colonies could be frozen in aliquots of cryoprotectant medium (20% (v/v) DMSO diluted in complete hESC growth medium) at a 1:1 ratio with complete hESC growth medium, and stored in liquid nitrogen. If necessary frozen hESC colonies could be thawed in a 37°C water-bath bath and slowly rehydrated with complete growth medium in order to avoid osmotic shock. Cells were then centrifuged for 5 min at 500 x *g,* and then seeded in an appropriate volume of culture medium.

3.4.3 Immortalised Human Granulosa cell line (COV434) cell culture

See section 2.4.4

3.4.4 Human follicular fluid preparation

See section 2.4.3. Prior to use in EB culture, three samples of human follicular fluid were pooled (table 3.1) and mixed before being added to cell culture medium.

Donor number	Pregnancy outcome	Procedure
119ECF11	Positive	IVF
119ECF22	Negative	ICSI
119ECF25	Positive	ICSI

Table 3.1: Human follicular fluid samples, pooled for EB cell culture.

3.4.5 Embryoid body (EB) formation

Hanging drop method

Stem cell colonies that were visually deemed morphologically 'normal' were microdissected with a 19 gauge needle, and colony fragments were resuspended in 50 µl drops of EB medium (Knockout DMEM supplemented with 20% (v/v) serum replacement, 2 mM L-glutamine, 1% (v/v) non-essential amino acid (NEAA), 100 IU/ml (each) Penicillin/Streptomycin and 0.1 mM β-mercaptoethanol). EB medium was 'conditioned' by incubation with 100% confluent hff cells at 37°C, 6% CO_2, for 24 h prior to use in EB culture. Drops containing hESC colonies were inverted on a Petri dish lid and cultured at 37°C, 6% CO_2 (figure 3.1 a).

Suspension method

EBs were also cultured in suspension. Morphologically 'normal' stem cell fragments were transferred to non-treated tissue culture dishes and resuspended in EB medium. For some experiments EB medium was supplemented with 10% (v/v) human follicular fluid, pooled from three donors (table 3.1). EBs were cultured at 37°C, 6% CO_2 for as long as desired until harvesting. Culture media was exchanged every 2-3 days (figure 3.1 b).

Immortalised Human Granulosa cell line (COV434) co-culture method

EBs were also co-cultured with COV434 cells. Morphologically 'normal' stem cell fragments were transferred to individual wells of a V bottomed 96 well plates with COV434 cells. Cells were cultured with EB medium incubated at 37°C, 6% CO_2 for as long as desired until harvesting. Culture media was exchanged every 24 h (figure 3.1.c).

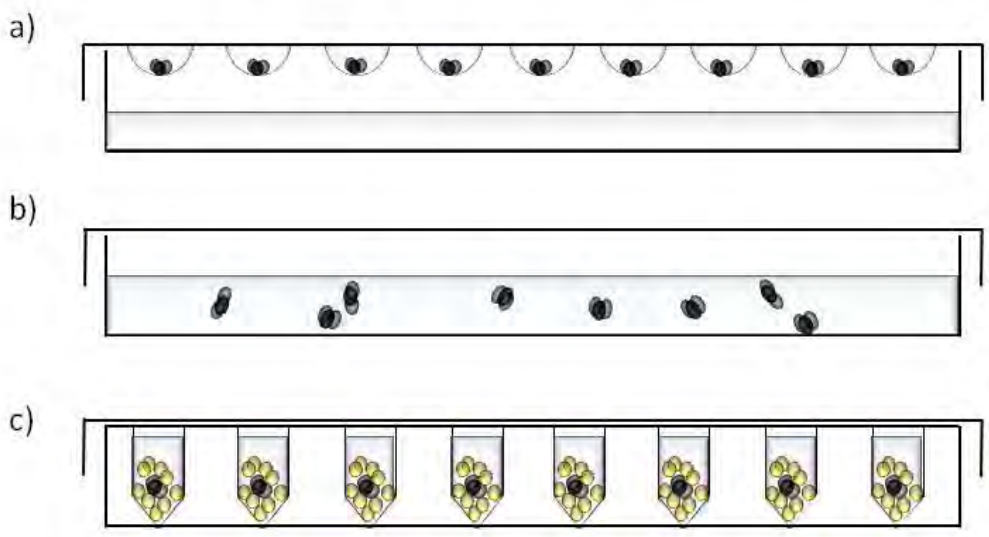

Figure 3.1: Methods for embryoid body formation.

Morphologically "normal" hESC colonies were mechanically dissected and transferred and cultured using one of the following EB culturing methods. (**a**) Hanging drop, (**b**) Suspension or (**c**) Co-culture with an immortalised granulosa cell line, COV434.

3.4.6 Embryonic stem cell and oocyte gene expression

Total RNA was extracted from hESC, COV434 and EB samples using the Total RNA purification kit in accordance with manufacturers' protocol, once extracted RNA was stored at -80°C.

Reverse transcription was carried out with Sensiscript Reverse Transcriptase (RT) kit according to manufacturers' protocol. Briefly reactions contained; 1 µM Oligo-dT primer, 1 X Buffer, 0.5 mM (each) dNTPs , 10 U RNAase inhibitor, 1 µl Sensiscript Reverse Transcriptase enzyme and 50 ng of RNA template. Reactions were incubated at 37°C for 1 h, and then stored at -20°C until PCR reaction.

Primers were designed to screen for pluripotent hESC and germ cell specific genes at various stages of development. Primers used in PCR amplifications were obtained from Eurogentec, Southampton, UK. Oligonucleotide sequences with expected product size are indicated in table 3.2.

PCR reactions contained 1 U Taq DNA polymerase, 0.5 µM (each) appropriate reverse and forward primers, 1 X Buffer, 0.5 mM (each) dNTPs, 2 mM $MgCl_2$ and 2 µl of RT Sensiscript reaction. Each PCR reaction had a corresponding negative water control to ensure no contamination. Reactions were performed under the following conditions: 95°C, 2 min; 35 cycles of 95°C, 30 s; 51°C, 30 s; 72°C, 45 s and one cycle of 72°C, 5 min. PCR products were then run on a 2% (w/v) agarose gel (section 2.4.7).

Primer	Oligonucleotide sequence(5'-3')	PCR amplicon size (bp)
GAPDH - Forward	CAATGACCCCTTCATTGACC	159
GAPDH - Reverse	TTGATTTTGGAGGGATCTCG	
OCT4 – Forward[a]	ACATCAAAGCTCTGCAGAAAGAAC	127
OCT4 – Reverse[a]	CTGAATACCTTCCCAAATAGAACC	
OCT4 – Forward[b]	CTCACCCTGGGGGTTCTATT	234
OCT4 – Reverse[b]	CTCCAGGTTGCCTCTCACTC	
STELLAR – Forward[a]	GTTACTGGGCGGAGTTCGTA	168
STELLAR – Reverse[a]	TGAAGTGGCTTGGTGTCTTG	
STELLAR – Forward[b]	CTCTCAAATCTCCTCCGAGACG	240
STELLAR – Reverse[b]	GTACGAACTCCGCCCAGTAA	
C-KIT - Forward	CCACACCCTGTTCACTCCTT	206
C-KIT - Reverse	TTCTGGGAAACTCCCATTTG	
BOULE - Forward	TATAAGGATAAGAAGCTGAACATTGGT	171
BOULE - Reverse	CGAAGTTACCTCTGGAGTATGAAAATA	
VASA - Forward	AGAAAGTAGTGATACTCAAGGACCAA	189
VASA - Reverse	TGACAGAGATTAGCTTCTTCAAAAGT	
DAZL - Forward	ATGTTAGGATGGATGAAACTGAGATTA	172
DAZL - Reverse	CCATGGAAATTTATCTGTGATTCTACT	
SCP3 - Forward	AAATCTGGGAAGCCGTCTGT	150
SCP3 - Reverse	TGCAGAAGACCTTTTCTTCCT	
GDF3 - Forward	AGACTTATGCTACGTAAAGGAGCT	149
GDF3 - Reverse	CTTTGATGGCAGACAGGTTAAAGTA	
FIGLA - Forward	AATCTCAACCGTGGTTTTGC	212
FIGLA - Reverse	CTTGCCGAGGATGTATGTGA	

Table 3.2: hESC and germ cell specific gene oligonucleotide sequences and expected product size.

3.5 Results

3.5.1 Embryoid body formation

Initially EBs were cultured using the hanging drop method (see section 3.4.5, figure 3.1 a). This method is commonly used to form EBs from single ES cells, sub-cultured via trypsinisation. However trypsinisation was not a suitable subculture method for the HS181 hESC line. Through both anecdotal advice and experimentation, I found that trypsinsation had a negative impact on the sub-cultivation process, so manual micro-dissection of hESCs was employed. This inability to split the hESCs into single cells unfortunately meant that the hanging drop method was inappropriate as colonies were too heavy to be supported for prolonged periods of time within the hanging drop, frequent and full media exchange was also difficult.

The suspension method (see section 3.4.5, figure 3.1.b) was deemed a more appropriate EB culture method due to the cell line constraints described above. Media exchange was more convenient, and multiple EBs could be cultured within the same culture vessel. A disadvantage of the suspension method is that structural uniformity of the EBs was difficult to control and appeared random, irrespective of growth culture medium (figure 3.2). Another issue associated with growing EBs via the suspension method was EB adhesion to the culture vessel (figure 3.3). Multiple culture dishes were tested, but cellular adhesion even occurred with non-treated culture plastics. Daily agitation was required to minimise EB adhesion.

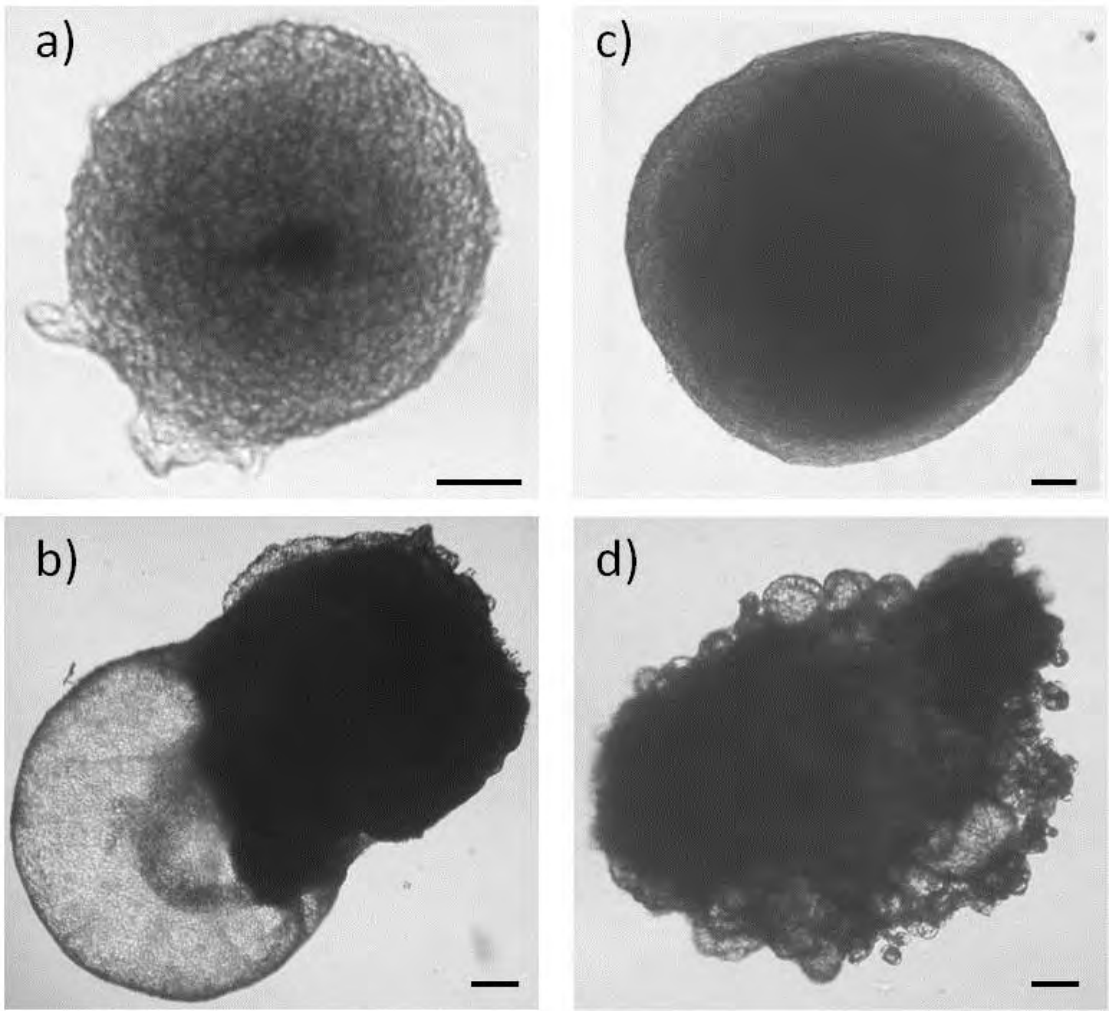

Figure 3.2: Suspension culture embryoid body formation.

Bright field images of differentiating EB cultures via suspension method. Uniformity of EBs could not be guaranteed regardless of culture conditions. (**a**) and (**b**) were cultured in complete EB growth medium for 38 days. (**c**) and (**d**) were cultured in EB growth medium supplemented with 10% (v/v) follicular fluid for 55 days. Both conditions showed ideal spherical development as well as irregular EB formation. Scale bars = approximately 100 µm.

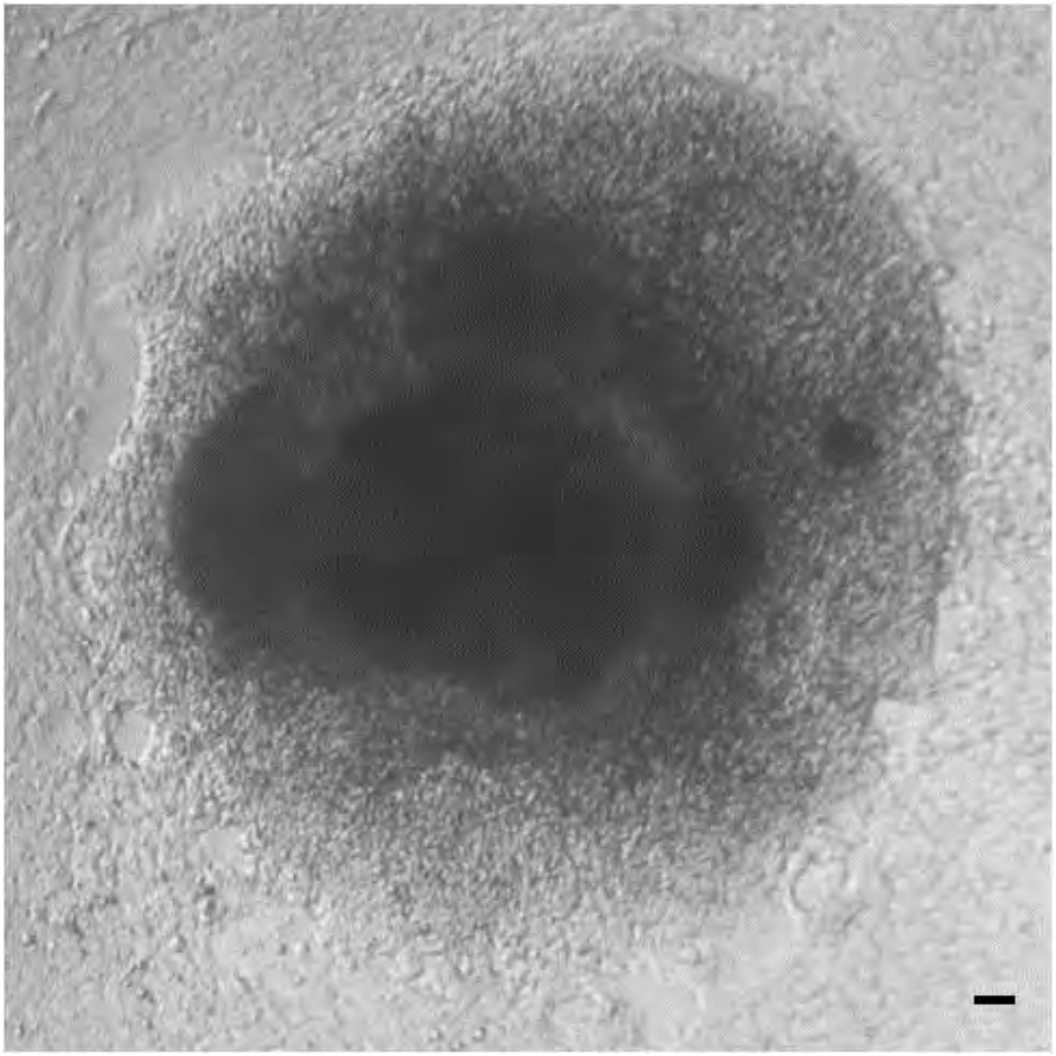

Figure 3.3: Embryoid body culture vessel adhesion.

Bright field image of a differentiating EB, cultured via the suspension method. EB was cultured in EB medium and image was taken at 10 days of culture. Image demonstrated the problematic issue of EB adhesion to the culture vessel, even in non-treated cell culture plastics. Scale bar = approximately 100 µm.

3.5.2 Embryoid body spontaneous differentiation

To assess the developmental progression of differentiated EBs, a profile of various key markers, previously used by Clark et al., (2004a) was employed in this study. These markers were either germ cell-specific or highly expressed in the germ cell lineage and allowed differentiating EBs to be assessed from pluripotent hESC to differentiated oocyte (figure 3.4).

Initial investigations confirmed the presence of pluripotent genes within our starting hESC population. In addition to the positive expression of RT-PCR positive control, *GAPDH*, the undifferentiated hESC line, HS181 (*passage 66*), showed positive expression of pluripotent genes *OCT4, STELLAR* and *GDF3*. There was also positive expression for *DAZL* a gene encoding for proteins containing RNA binding motifs, which are thought to be important for PGC formation (Kee et al. 2009) (figure 3.5).

To investigate the possible spontaneous germ cell differentiation in hESCs, hESC colonies were cultured in suspension (section 3.4.5). Culture duration varied between different experiments (from 0 to 100 days). EBs were closely observed for any morphological changes relating to the development of oocyte-like structures. Some populations perished with EBs shrinking in volume and starting to fragment. Other populations contained both regular and irregular shaped EBs. However no observation indicated the development of oocyte-like structures.

After analysis with RT-PCR spontaneously differentiated EBs retained expression of *GAPDH*, *OCT4* and *STELLAR*, no other germ cell marker was identified (figure 3.6).

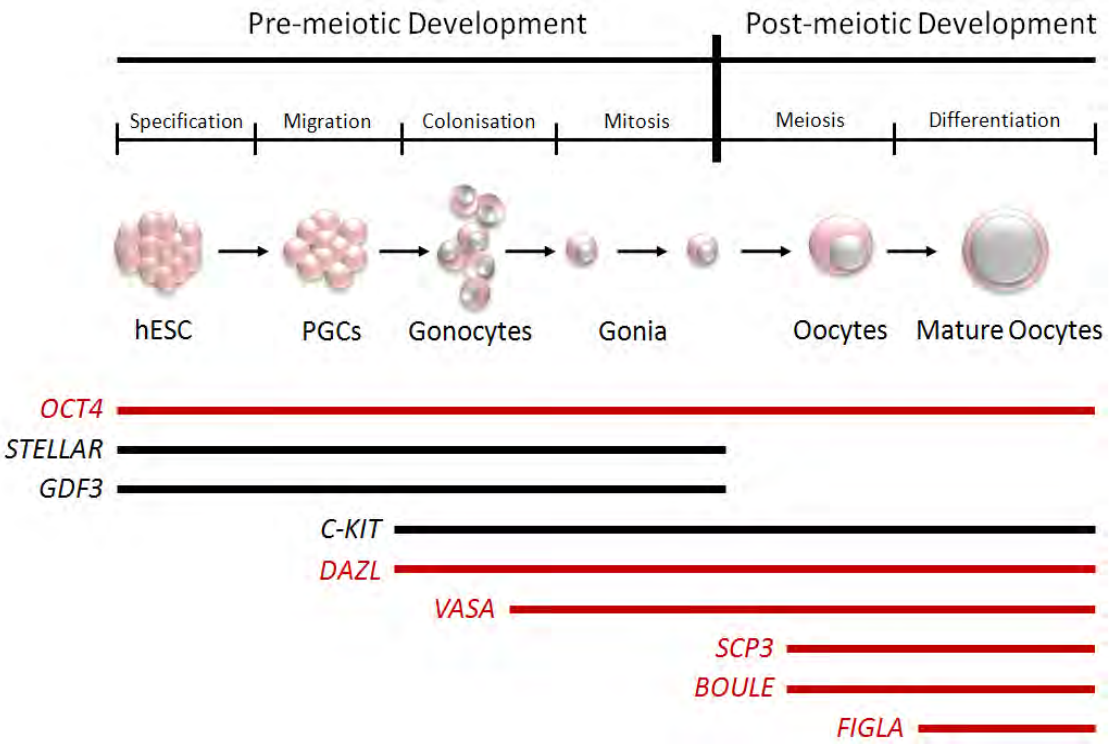

Figure 3.4: Gene expression in oocyte differentiation.

Expected expression patterns of chosen germ cell genes at different stages of fetal and adult development. All genes are enriched in germ cells relative to somatic cells however germ cell-specific expression is highlighted in red. *OCT4*, *STELLAR* and *GDF3* are known to be expressed in pluripotent embryonic stem cells. Genes expressed in PGC include *DAZL*, *C-KIT*. Genes expressed in gonocyte formation include *VASA*. Genes expressed during meiosis include *SCP3* and *BOULE*. Adult germ cell specific markers include *FIGLA*. Modified from Clark et al. 2004a.

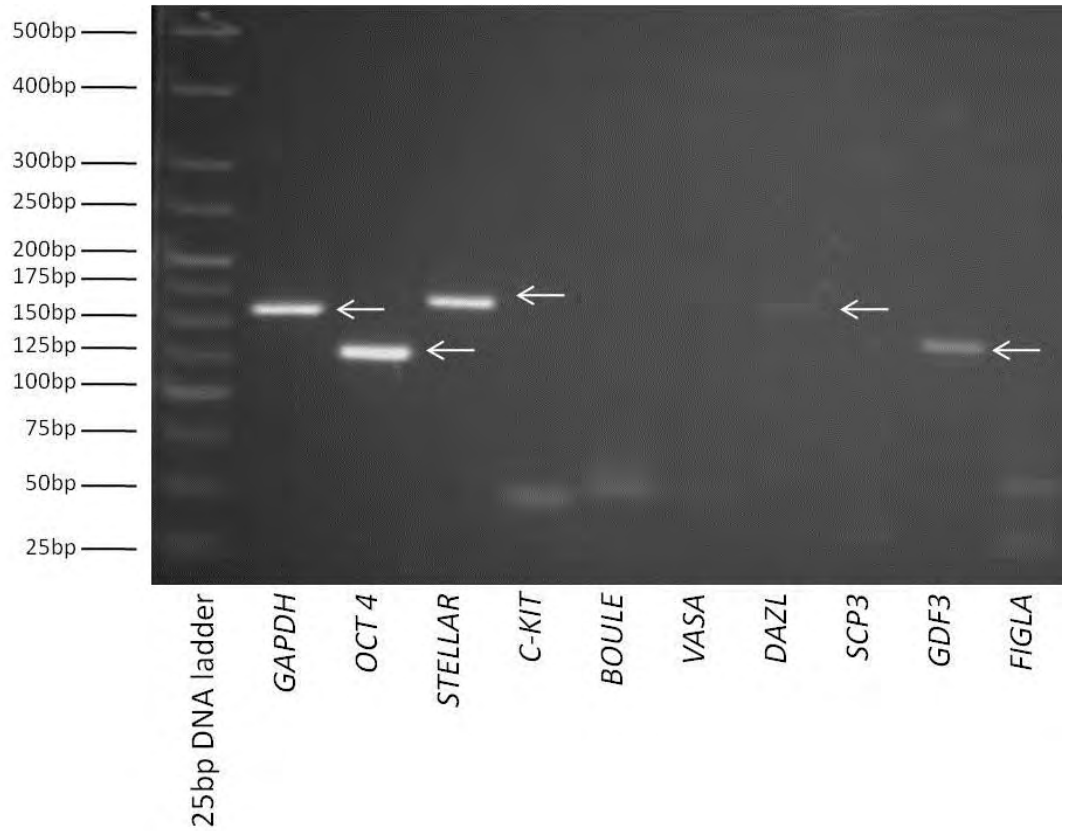

Figure 3.5: Stem and germ cell marker expression in human embryonic stem cells.

Reverse transcription-polymerase chain reaction for the identification of pluripotent stem cell and germ cell specific genetic markers in human embryonic stem cells (HS181 hESC line, *passage 66*). White arrow denotes positive expression. Shown are PCR products separated by gel electrophoresis performed on the following genes: *GAPDH*; *OCT4*[a]*; STELLAR*[a]*; C-KIT; BOULE; VASA; DAZL; SCP3; GDF3* and *FIGLA.*[a] denotes primer sequence used (see table 3.2).

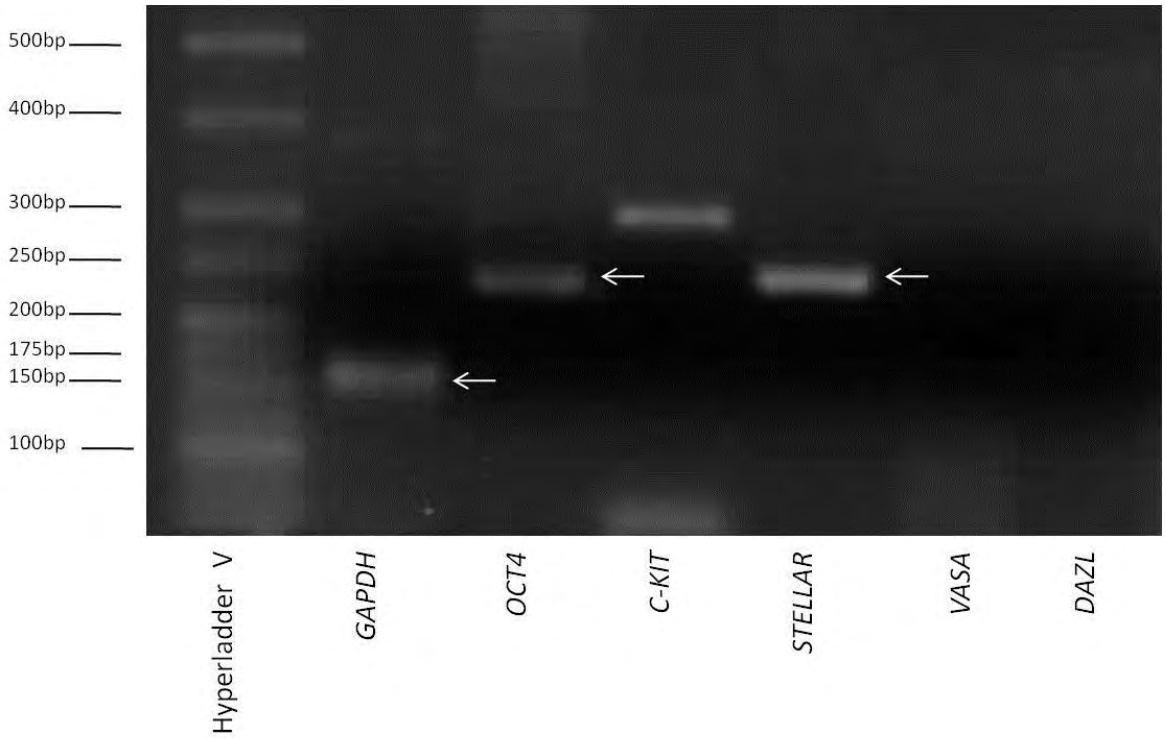

Figure 4.6: Stem and germ cell marker expression in spontaneous embryoid body differentiation.

Representative reverse transcription-polymerase chain reaction for the identification of pluripotent stem cell and germ cell specific genetic markers that spontaneously differentiate in EB population (cultured for 39 days). White arrow denotes positive expression. Shown are PCR products separated by gel electrophoresis performed on the following genes: *GAPDH*; *OCT4*[b]*; STELLAR*[b]*; C-KIT; BOULE; VASA; DAZL; SCP3; GDF3* and *FIGLA*. [b] denotes primer sequence used (see table 3.2).

3.5.3 Embryoid body culture with human follicular fluid

In order to direct differentiation of EBs into the germ cell lineage, EBs cultured in suspension had their complete growth medium supplemented with human follicular fluid in order to expose EBs to potential differentiating promoting growth factors (section 3.4.4 and section 3.4.5).

EBs cultured with human follicular fluid exhibited positive expression for *GAPDH, OCT4* and *STELLAR*, with no other germ cell-specific genes identified (figure 3.7).

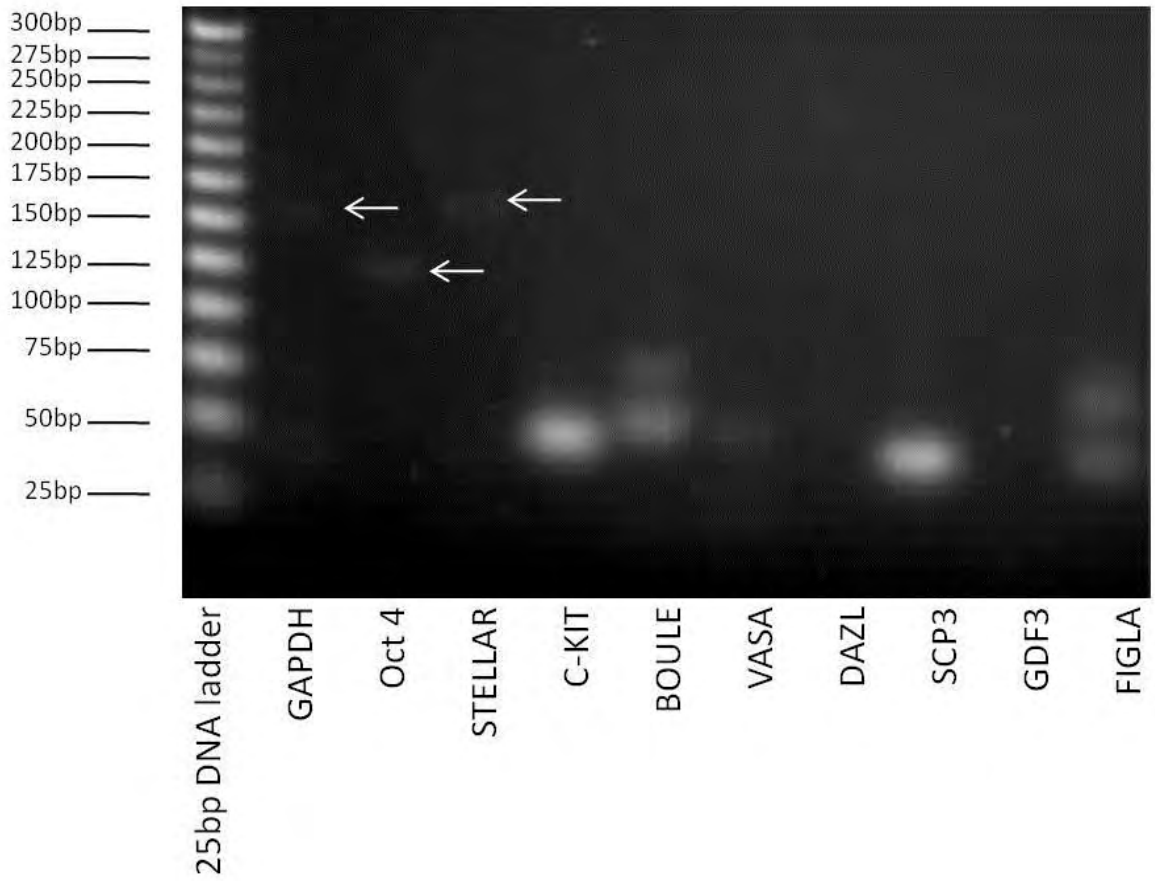

Figure 3.7: Stem and germ cell marker expression in embryoid bodies cultured with human follicular fluid.

Reverse transcription-polymerase chain reaction for the identification of pluripotent stem cell and germ cell specific genetic markers in embryoid bodies cultured with human follicular fluid (cultured for 35 days). White arrow denotes positive expression. Shown are PCR products separated by gel electrophoresis performed on the following genes: *GAPDH*; *OCT4*[a]*; STELLAR*[a]*; C-KIT; BOULE; VASA; DAZL; SCP3; GDF3* and *FIGLA.* [a] denotes primer sequence used (see table 3.2).

3.5.4 Embryoid body co-culture with an immortalised granulosa cell line (COV434)

To further encourage germ cell differentiation, EBs were co-cultured with an immortalised human granulosa cell line (COV434) whose cellular characteristics may be useful in directing germ cell development (Zhang et al. 2000). As culturing EBs via the suspension method was ineffective in order to promote direct cellular contact and aggregation, a different culture method had to be used. Effective EB-COV434 co-culture was achieved by using V-bottomed 96 well dishes (section 3.4.5, figure 3.1 c).

The EBs that were co-cultured with COV434 cells showed positive expression for the previously seen bands *GAPDH*, *OCT4* and *STELLAR* with no other germ cell markers identified (figure 3.8). There were however difficulties separating the EBs from the COV434 cells after co-culturing making the risk of cellular contamination difficult to rule out. So it seemed prudent to establish the germ cell marker expression profile of the COV434 cells themselves. Surprisingly the COV434 cells expressed the same pattern of expression of the EBs they were co-cultured with, having positive expression of *GAPDH*, *OCT4* and *STELLAR* (figure 3.9).

To establish if this pattern of expression was exclusive to the COV434 cell line, and not a true representation of native cumulus cells, the expression of germ cell markers in native human cumulus was examined. Cumulus cells stripped from an unfertilised oocyte (ICSI patient, donor number 119ECF08) showed the same pattern of expression with positive bands for *GAPDH*, *OCT4* and *STELLAR*, when compared to the immortalised granulosa cell line (figure 3.10).

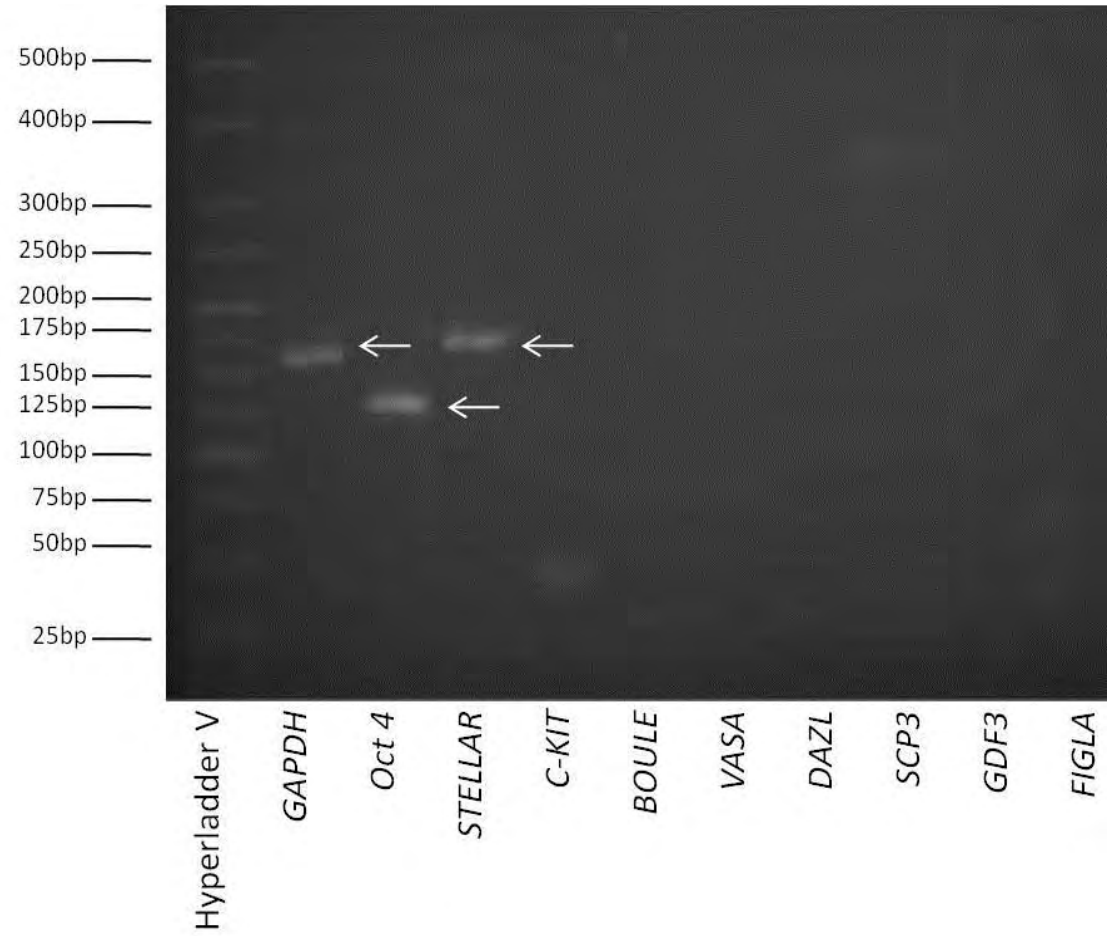

Figure 3.8: Stem and germ cell marker expression in embryoid bodies co-cultured with COV434 cells.

Reverse transcription-polymerase chain reaction for the identification of pluripotent stem cell and germ cell specific genetic markers in embryoid bodies co-cultured with an immortalised granulosa cell line, COV434 (cultured for 40 days, COV434 *passage 19*). White arrow denotes positive expression. Shown are PCR products separated by gel electrophoresis performed on the following genes: *GAPDH*; *OCT4*[a]*; STELLAR*[a]*; C-KIT; BOULE; VASA; DAZL; SCP3; GDF3* and *FIGLA.* [a] denotes primer sequence used (see table 3.2).

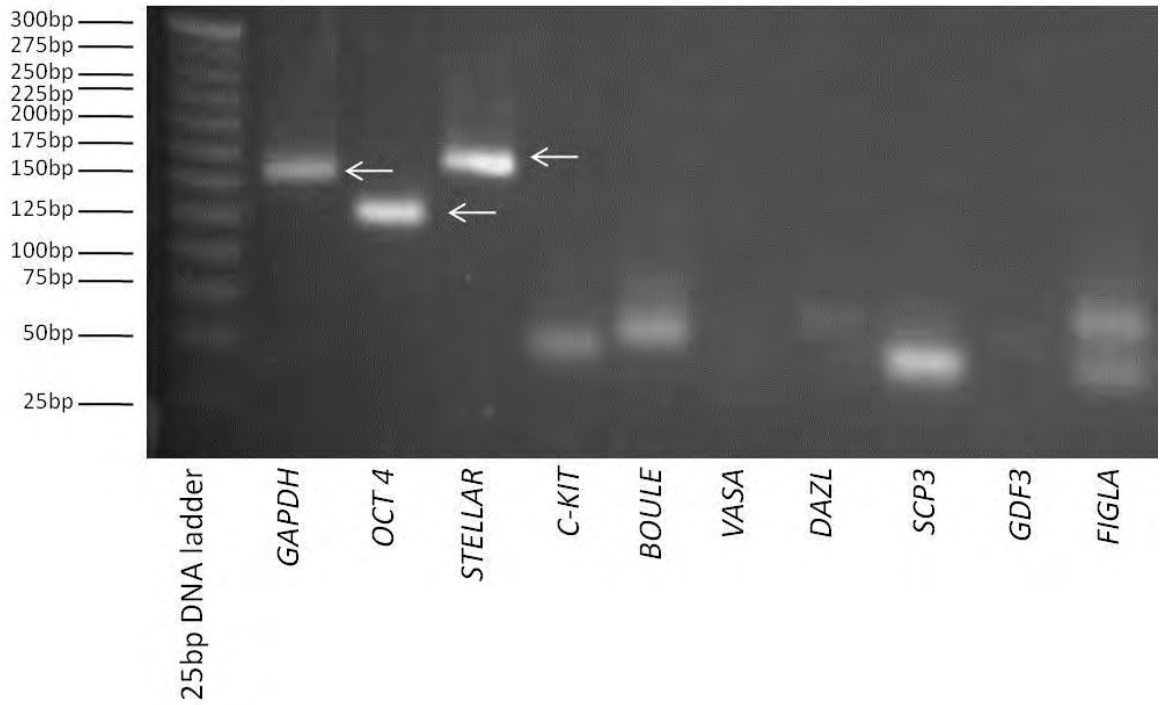

Figure 3.9: Stem and germ cell marker expression by COV434 cells.

Reverse transcription-polymerase chain reaction for the identification of pluripotent stem cell and germ cell specific markers in an immortalised granulosa cell line, COV434 (*passage 19*). White arrow denotes positive expression. Shown are PCR products separated by gel electrophoresis performed on the following genes: *GAPDH*; *OCT4*[a]*; STELLAR*[a]*; C-KIT; BOULE; VASA; DAZL; SCP3; GDF3* and *FIGLA*. [a] denotes primer sequence used (see table 3.2).

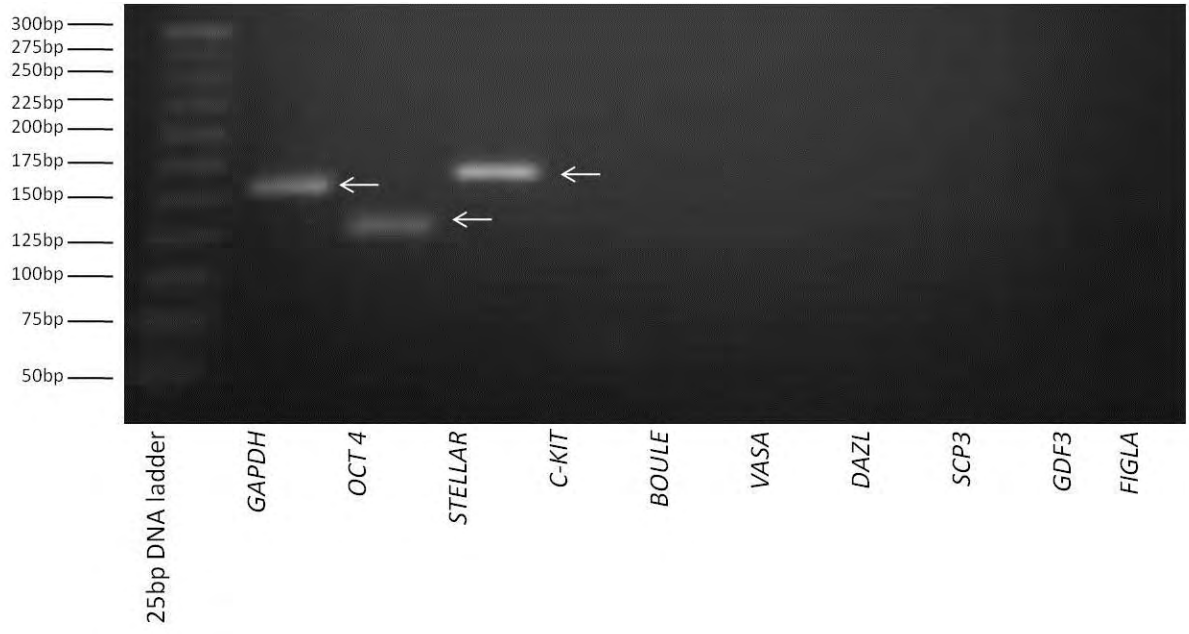

Figure 3.10: Stem and germ cell marker expression by native human cumulus.

Reverse transcription-polymerase chain reaction for the identification of pluripotent stem cell and germ cell specific markers in native human cumulus (ICSI recovered cumulus, donor number 119ECF08). White arrow denotes positive expression. Shown are PCR products separated by gel electrophoresis performed on the following genes: *GAPDH*; *OCT4*[a]*; STELLAR*[a]*; C-KIT; BOULE; VASA; DAZL; SCP3; GDF3* and *FIGLA.* [a] denotes primer sequence used (see table 3.2).

3.6 Discussion

Over the last decade ES cells have become an extremely valuable model in many research fields such as neurology and cardiology (Wobus et al. 2002;Kato et al. 2004). The prospects of creating an *in vitro* model producing human oocytes for research would lead to a much greater understanding of gametogenesis and the possible development of novel treatments for infertility.

Initial examination of the genetic expression in the HS181 hESC line showed positive expression of a gene which is restricted to pluripotent ES and germ cell lines (Scholer et al. 1990;Pesce et al. 1998) *OCT4,* in addition to pluripotency genes *GDF3* and *STELLAR.* All genes have been previously reported to be expressed in hESCs (Thomson et al. 1998;Clark et al. 2004b). Clark *et al*., (2004a) also reported the expression of a germ cell-specific gene *DAZL* in hESC populations, expression of which was also present in HS181 hESCs. However presence of *CKIT*, a marker of pre-meiotic germ cells which had been identified in hESC populations in the Clark *et al*., (2004a) paper was found to be absent in HS181 hESC line. To our knowledge there have been no reports of testing for *CKIT* expression in the HS181 hESC line, however genetic expression has been shown to vary greatly between hESC populations which may account for the absence of *CKIT* from our hESC population (Stahlberg et al. 2009) (figure 3.5).

Clark *et al*., (2004) identified that the pre-meiotic germ cell gene, DAZL was not expressed in the inner cell mass (ICM) of the human embryo, from which hESCs are derived. The process of removing the ICM from the outer trophectoderm may result *in vitro* cultures exhibiting a change in genetic expression. *DAZL* expression in hESCs may be a result of unregulated gene expression, spontaneous germ cell differentiation, or it may be due to germ cells being the

closest *in vivo* equivalent to hESCs, explaining why they have similar genetic expression patterns, reviewed (Zwaka and Thomson. 2005).

Germ cell differentiation appears to occur faster in EB culture systems, however EB formation in this study was fraught with a number of difficulties. The HS181 hESC line has been shown sensitive to different subculture methods, inducing karyotypic instability (Catalina et al. 2008). The inability to subculture the HS181 hESC line into single cells, created a lack of control over the number of cells seeded to form each EB, which has been showed to affect differentiation pathways (Park et al. 2007;Bauwens et al. 2008;Messana et al. 2008). The lack of single cell subculture also had an impact on the uniformity of the EBs (figure 3.2). The subculture method unfortunately ruled out the use of the hanging drop method which is commonly used for EB formation and is useful in controlling EB size (Keller. 1995;Yamada et al. 2002). This lead to a requirement to use the suspension method for EB formation, which is known to give a wide array of EB sizes (Dang et al. 2002). The lack of uniformity of EBs was further exacerbated by the additional problem of EB adhesion to culture vessels (figure 3.3), however future studies could both address both the problems with uniformity and cellular adhesion by using a rotation suspension method (Cameron et al. 2006).

Regardless whether EBs were left to spontaneously differentiate or directed differentiation was attempted through culture with human follicular fluid and/or immortalised granulosa cell line (COV434), neither oocyte-specific morphological changes nor later germ cell genetic markers were identified in EBs (figures 3.6, 3.7 and 3.8). All cultures appeared to retain the expression of the pluripotency markers *OCT4* and *STELLAR,* that were observed in hESCs

cultures. However they did lose expression of *GDF3* and *DAZL*. The expression of *OCT4* and *STELLAR* in human EBs has been shown to fall after three days of culture (Clark et al. 2004a) and no other reports of long term *OCT4* and *STELLAR* retention was found, this makes the expression in EB cell cultures difficult to explain. However as only RT-PCR was used it would be useful to repeat experiments using real-time PCR which would allow quantification of *OCT4* and *STELLAR* expression in such cultures. This observation may be HS181 hESC cell line-specific, however it could be due to the EB culture medium being hff 'conditioned' prior to EB culture. 'Conditioning' the medium supported EB growth, however factors secreted by the hff cells into the growth medium could have potentially supported the continued expression of the pluripotency genes *OCT4* and *STELLAR.* The use of a different hESC cell line in future experiments may help answer this question.

Surprisingly *OCT4* and *STELLAR* were also found to be expressed by COV434 cells themselves (figure 3.9). There are however studies identifying *OCT4* and *STELLAR* expression in breast cell carcinomas and colon cancer cells and it has been hypothesised that *OCT4* and *STELLAR* may play a large role in cancer cell self-renewal. (Ezeh et al. 2005;Chen et al. 2011;Kim and Nam. 2011). COV434 cells are an immortalised human granulosa cell line derived from a primary human granulosa cell tumour (van den Berg-Bakker et al. 1993), so this may explain the expression of *OCT4* and *STELLAR*. This result however calls into question the expression profile of EBs co-cultured with COV434 cells, as it is not possible to exclude COV434 cellular contamination (figure 3.8).

To compare the expression profile of COV434 cells to that of native human cumulus, the expression profile of donated cumulus cells from a patient undergoing ICSI fertility

treatment was examined. Surprisingly they exhibited the exact profile of that of COV434 cells (figure 3.10). This could imply that OCT4 and STELLAR are important to the developing oocyte. To further investigate more cumulus samples would need to be investigated, in conjunction with real-time PCR in order to quantify expression levels.

It also has to be noted that positive controls for germ cell-specific genes were not available. Most of the primer sequences were taken from published studies and annealing temperatures were set deliberately low to ensure no positive expression was missed. This explains why there is a certain level of unspecific binding.

Although early PGC markers have been shown in both male and female karyotypes in hESCs, there have been differences in the level of expression (Clark et al. 2004a; Kee et al. 2009). The female karyotype (XX) of the HS181 hESC cell line could have a negative effect on germ cell differentiation, due to the instability of the X chromosomes (Zvetkova et al. 2005) and the complex requirements for X chromosomes inactivation and reactivation in developing XX germ cells (Chuva de Sousa Lopes et al. 2008). In mice, many studies showing female germ cell differentiation are from mESCs with an XY karyotype (Hubner et al. 2003;Lacham-Kaplan et al. 2006;Qing et al. 2007). Female development is known to be the default gamete developmental pathway, regardless of karyotype, in the absence of certain factors. Although oocyte-like structures have been shown to differentiate from XY ES karyotypes, to achieve the ultimate goal of an *in vitro* developed oocyte which can fertilise and producing live offspring, one needs differentiation of XX ES cells, which would be able to support the post fertilisation development (Amleh and Taketo. 1998;Villemure et al. 2007).

Due to the heterogeneous nature of hESC population it may not be possible to direct the differentiation of the population in its entirety. Many successful studies have enriched their hESC populations with germ cell specific markers, such as *OCT4* and *VASA* reporter systems, prior to EB formation (Hubner et al. 2003;Toyooka et al. 2003;Kee et al. 2009). *In vivo* both follicular fluid and cumulus cells are vital in the later stages of development of the oocyte. It would be interesting to see if an enriched hESCs population would be more receptive to culture with human follicular fluid and COV434 cells. As the full proteomics profile of human follicular fluid and cumulus cells is unknown it is hard to hypothesise which factors might be beneficial in germ cell hESC differentiation. As mentioned previously, collaborative work provided the identification and quantification of steroids in the human follicular fluid used in EB culture (Appendix I.viii). EBs are known to secrete a measurable level of both estradiol and dihydrotestosterone (Aflatoonian et al. 2009) and testosterone. In conjunction with retinoic acid these secreted steroids can promote mES germ cell differentiation (Bowles et al. 2006;Koubova et al. 2006;Silva et al. 2009). So the hormonal niche provided by follicular fluid may be beneficial for hESC germ cell differentiation, however this needs further investigation.

Ultimately the prospect of developing a novel *in vitro* oocyte development model using hESC differentiation is an exciting prospect in the field of reproductive biology. However since the initial reports of female germ cell differentiation from ES cells there is currently no reliable model for oocyte differentiation *in vitro*.

CHAPTER 4

Investigation of the role of the zona pellucida in spermatozoa binding

4.1 Introduction

A critical stage for natural fertility, prior to fertilisation, is the successful binding to and penetration of the zona pellucida (ZP) matrix by spermatozoa. The ZP is a glycoprotein layer comprised of a number of individual ZP proteins, that surrounds all mammalian oocytes and early embryos (Wassarman. 1990).

The traditional dogma for the composition of the ZP matrix and sperm-zona binding (SZB) in mammalian fertilisation has been primarily based on a murine model. Investigations, many of which were led by Bleil and Wassarman (Bleil and Wassarman 1980a;Bleil and Wassarman 1980b;Bleil and Wassarman. 1983;Vazquez et al. 1989), established that the murine zona matrix consists of three individual glycoproteins. Murine zona pellucida protein 3 (mZP3), was established as the primary spermatozoa binding ligand and inducer of the acrosome reaction. Murine zona pellucida protein 2 (mZP2) was found to subsequently bind to acrosome-reacted spermatozoa and is thought to be involved in events preventing polyspermy. The final murine protein, zona pellucida protein 1 (mZP1), appeared to have no functional role in sperm binding, and instead was proposed to have a role creating structural integrity in the zona matrix.

However the number and combination of ZP proteins that form the zona matrix in fact varies, ranging from three to six ZP proteins (ZP1, ZP2, ZP3, ZP4, ZPD, ZPAX), across higher vertebrates (table 4.1) (reviewed in Goudet et al. 2008). Along with many other species of primate, human zona matrices have been identified as containing an additional fourth zona protein compared to mice, human zona pellucida protein 4 (ZP4). A mZP4 orthologue has been identified, however it appears to be a non-functioning pseudogene due to a number of

sequence deletions (Lefievre et al. 2004). Questions therefore exist over the relevance of the murine model for human fertilisation.

	ZP1	ZP2	ZP3	ZP4	ZPD	ZPAX
Human (*Homo sapiens*)	•	•	•	•		§
Chimpanzee (*Pan troglodytes*)	•	•	•	•		§
Rhesus macaque (*Macaca mulata*)	•	•	•	•		§
Crab-eating macaque (*Macaca fascicularis*)		•	•	•		
White-tufted-ear marmoset (*Callithrix jacchus*)		•		•		
Yellow baboon (*Papio cynocephalus*)				•		
Bonnet monkey (*Macaca radiate*)	•	•	•	•		
Pig (*Sus scrofa*)		•	•	•		
Cow (*Bos taurus*)	§	•	•	•		§
Cat (*Felis catus*)		•	•	•		
Dog (*Canis familiaris*)	§	•	•	•		
Rabbit (*Oryctolagus cuniculus*)		•	•	•		
Mouse (*Mus musculus*)	•	•	•	§		
Hamster (*Mesocricetus auratus*)	•	•	•	•		
Rat (*Rattus norvegicus*)	•	•	•	•		
Possum (*Trichosurus vulpecula*)		•	•	•		
Chicken (*Gallus gallus*)	•	•	•	•	•	•
Quail (*Coturnix japonica*)	•	•	•	•	•	
African clawed frog (*Xenopus laevis*)		•	•	•	•	•
Western clawed frog (*Xenopus tropicalis*)		•	•	•	•	•

Table 4.1: The presence of ZP genes in higher vertebrates.

Table modified from (Conner et al. 2005;Goudet et al. 2008) with additional information (Izquierdo-Rico et al. 2009;Sato et al. 2009;Kinoshita et al. 2010;Serizawa et al. 2011). § denotes the presence of a pseudogene. Gaps denote that the presence/absence of the gene has not yet been investigated.

The identity of the zona receptor on spermatozoa still remains elusive, even after decades of research. Early *in vitro* studies identified a number of candidate receptors such as β-1,4-galactosyltransferase 1 (B4galt1) and acrosin (Acr) as being involved in spermatozoa-zona binding (Lopez et al. 1985;Urch and Patel. 1991). However in subsequent gene knockout experiments, *B4galt1* and *Acr* null male mice remained fertile (Baba et al. 1994;Adham et al. 1997;Asano et al. 1997;Lu and Shur. 1997).

Some mouse knockouts have exhibited defective SZB: *Clgn* $^{-/-}$ (Ikawa et al. 1997); *Ace*$^{-/-}$ (Hagaman et al. 1998); *Adam1a*$^{-/-}$ (Nishimura et al. 2004); *Adam2*$^{-/-}$ (Cho et al. 1998) and *Adam3*$^{-/-}$ (Shamsadin et al. 1999) null mice have defective SZB and are infertile. However Clgn is not expressed in mature spermatozoa and is a testis-specific endoplasmic reticulum (ER) molecular chaperone, leading to speculation that it is involved in the correct maturation of spermatozoa. The Adam family, in particular Adam3 seems to be one of the most important factors involved in SZB in mice, but as the human homologue of Adam3 has been identified as a pseudogene, other proteins must be involved in human fertilisation (Hall and Frayne. 1999;Grzmil et al. 2001).

There is also debate over the role of protein glycosylation in SZB. Experiments using chimeric zona matrices replacing mZP2 and mZP3 with human zona proteins in genetically modified mice saw no binding by human spermatozoa. However mouse spermatozoa did bind to the humanised ZPs and were able to fertilise the oocyte (Rankin et al. 2003). Binding is also abolished between spermatozoa and zona by the removal of terminal galactose (Gal) or N-acetylglucosamine (GlcNac) (Shur and Hall. 1982;Florman and Wassarman. 1985;Bleil and Wassarman. 1988) which are key enzymes in glycosylation of ZP proteins. Recent

investigations have identified the potential importance of a well know selectin ligand sequence, sialyl-Lewis-X sequence, found on N and O glycans of human ZP proteins. The inhibition of this sequence caused a significant reduction in human SZB (Pang et al. 2011). However the disruption of vital glycosylation enzymes, mannoside acetylglucosaminyltransferase1 (Mgat1) and T-synthase (C1galt1) in oocytes, did not affect SZB or fertilisation (Shi et al. 2004;Williams et al. 2007).

Questions also remain over the interaction between the zona proteins themselves and how they interact to form the ZP matrix. The current model, based on mice, is composed of filaments of either ZP1/ZP3 or ZP2/ZP3 heterodimers (Dean. 2004). However the question remains of how relevant this can be to human zona, with its additional fourth ZP protein (Lefievre et al. 2004) (figure 4.1).

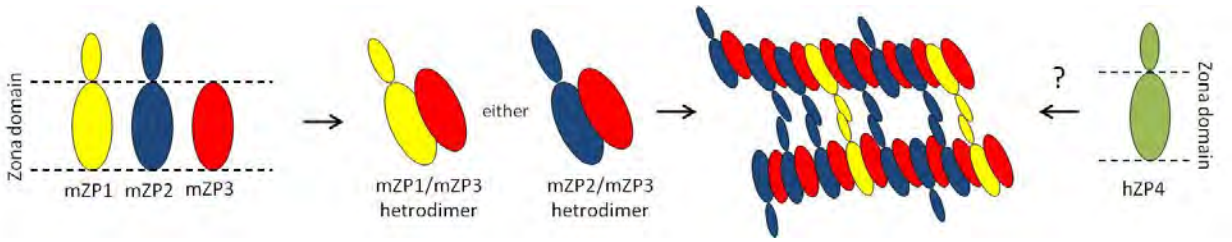

Figure 4.1: Structural zona matrix model in mouse.

Proposed model of the mZP matrix structure. From mouse knockout experiments it is hypothesised that the zona matrix is composed of mZP1/mZP3 and mZP2/mZP3 heterodimers, forming bonds between their zona domains. Arranged in a filamentous structure, cross linkages are formed between mZP1 and mZP2, with only mZP1 forming disulfide bonds. With the additional fourth hZP protein (hZP4), there are questions if this model can be translated into humans. Figure adapted from Dean. 2004.

As studies are limited by the availability of human zona, and the inability to use knockout experiments, recombinant ZP protein expression has been widely used. Groups have expressed ZP proteins in both prokaryotic (*E. coli*) and eukaryotic (insect cells and mammalian cells) protein expression systems (van et al. 1994;Chakravarty et al. 2005). Studies employing recombinant ZP proteins have shown they are functionally active on spermatozoa (van et al. 1994;Chapman et al. 1998;Tsubamoto et al. 1999;Chakravarty et al. 2005;Chakravarty et al. 2008).

Many of the studies in the field of SZB research have focused on individual molecules, rather than offering an unbiased approach which screens for all molecules that might be involved in SZB. The work in this chapter focuses on taking an unbiased approach to identifying potential key molecules in SZB by using surface plasmon resonance (SPR) technology. SPR enables real time detection of biomolecular events, providing a wealth of quantitative information about protein binding; in addition it can be used in association with mass spectrometry, offering the opportunity to identify protein binding partners (figure 4.2). This study explores the potential of using SPR technology with both recombinant human zona proteins and native zona material to screen human spermatozoa for potential zona receptors.

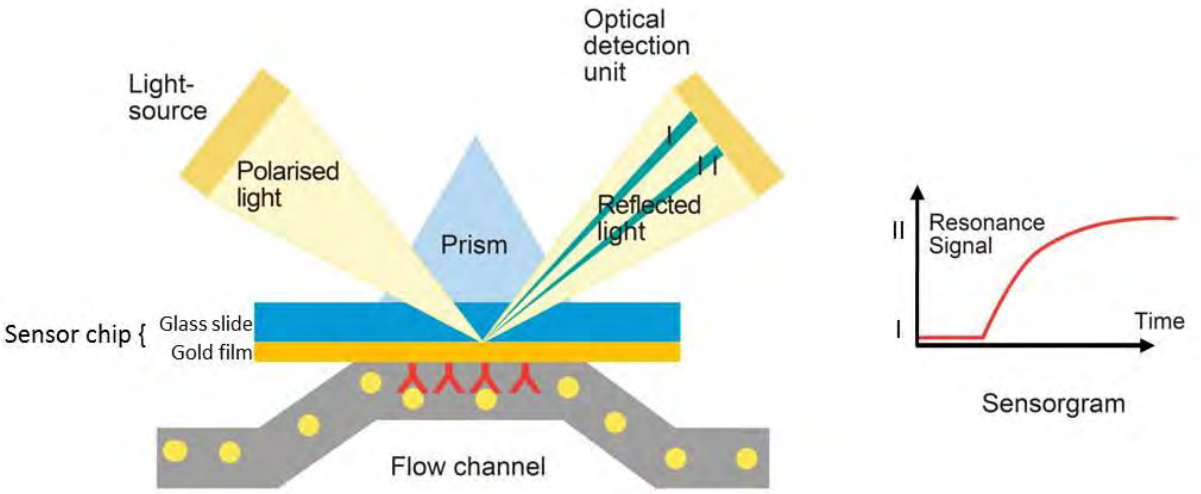

Figure 4.2: Surface plasmon resonance.

Surface plasmon resonance (SPR) occurs when a polarised light source is reflected from a gold conducting film at the interface between two different mediums (the sample and a glass slide) which have a different refractive index. An optical detection unit detects the reflected light and expresses it as resonance units (RU). As protein binding occurs on the sensor chip it causes a reduction in the intensity of light reflected which causes changes in the refraction index, which is exhibited as an increase of RU. Image modified from (The University of Jerusalem. 2011).

4.2 Aims

- Utilising both recombinant and native zona proteins with SPR technology to elucidate:
    - The roles of the individual zona proteins in spermatozoa binding.
    - The roles of the individual zona proteins in zona matrix formation.
    - Potential zona receptor candidates on spermatozoa.

4.3 Materials.

4.3.1 Antibodies

Product Name	Company	Product Number
Penta-His antibody	Qiagen, Crawley, UK.	34660
Goat anti-mouse IgG HRP antibody	Jackson ImmunoResearch Laboratories, Pennsylvania, USA.	115035003

4.3.2 Cells

Product Name	Company	Product Number
Alpha-select gold efficiency *E.Coli*	Bioline, London, UK.	BIO-85027

4.3.3 Cell Culture reagents

Product Name	Company	Product Number
Bovine Serum Albumin (BSA)	Millipore, Watford, UK.	82-002-4
Dimethyl sulfoxide (DMSO)	Sigma, Dorset, UK.	D4540
Dulbecco's Modified Eagle/F-12 Medium (DMEM/F-12)	Invitrogen, Paisley, UK.	21041-033
Fetal Bovine Serum (FBS)	Biosera, Ringmer, UK.	S181X
L-Glutamine	Invitrogen, Paisley, UK	25030
Non-Essential Amino Acids (NEAA)	Invitrogen, Paisley, UK	11140-035
Opti-MEM I reduced serum medium	Invitrogen, Paisley, UK	11058021
Supplemented Earle's balanced salt solution	Geneflow, Fradley, UK	06-2010-03-18
Penicillin/Streptomycin	Invitrogen, Paisley, UK.	15140-122
Zeocin	InvivoGen, San Diego, USA,	ant-2n-1
0.25% (w/v) Trypsin-0.53mM EDTA	Invitrogen, Paisley, UK.	25200-056

4.3.4 Chemicals

Product Name	Company	Product Number
1-ethyl-3-(3-dimethylaminopropyl)-carbodiimide hydrochloride (EDC),	Sigma, Dorset, UK.	03449
AB-NTA free acid	NBS Biologicals Ltd	A459-10
Agarose	Bioline, London, UK.	41025
Ammonium persulphate	Sigma, Dorset, UK.	A3678
Ampicillin sodium salt	Sigma, Dorset, UK.	A9518
Bicinchoninic acid	Sigma, Dorset, UK.	B9643
Bovine serum albumin (BSA)	Millipore, Watford, UK	82-002-4
Calcium Ionophore A23187	Sigma, Dorset, UK.	C5149
Complete, Mini, EDTA free protease inhibitor cocktail	Roche Diagnostics, Burgess Hill, UK.	04693159001
Copper(II) sulphate	Sigma, Dorset, UK.	C2284
Deoxynucleoside triphosphates (dNTPs)	Promega, Southampton, UK	C1141
Dithiothreitol (DTT)	Sigma, Dorset, UK.	D9163
ECL Western blotting substrate	Thermo Fisher Scientific, Rockford, USA.	32109
Ethanol	Fisher Scientific, Loughborough,	E/0650DF/17
Ethanolamine	Sigma, Dorset, UK.	110167
Ethidium bromide	Sigma, Dorset, UK.	160539
Ethylenediaminetetraacetic acid (EDTA)	Sigma, Dorset, UK.	E5134
Ferrous sulphate	Sigma, Dorset, UK.	F8048
Glacial acetic acid	Fisher Scientific, Loughborough, UK	A/0400/PB17
Glycerol	Sigma, Dorset, UK.	G5516
Glycine	Sigma, Dorset, UK.	G8898
Glycine pH 2	GE Healthcare, Buckinghamshire, UK.	BR100355

Product Name	Company	Product Number
HBS-EP	GE Healthcare, Bucks, UK.	BR100188
HBS-P	GE Healthcare, Bucks, UK.	BR100368
Hydrochloric acid (HCl)	Sigma, Dorset, UK.	H1758
Hydromount	Geneflow, Fradley, UK.	HS-106
Imidazole	Sigma, Dorset, UK.	I2399
Isopropanol	Sigma, Dorset, UK.	I9516
Lipofectamine 2000 Transfection Reagent	Invitrogen, Paisley, UK.	11668-027
Luria-Bertani (LB) agar powder	Sigma, Dorset, UK.	L2897
Luria-Bertani (LB) broth powder	Sigma, Dorset, UK.	L3022
Methanol	Fisher Scientific, Loughborough, UK.	M/3950/17
N hydroxysuccinimide (NHS),	Sigma, Dorset, UK.	130672
Nickel acetate tetrahydrate	Sigma, Dorset, UK.	244066
Nickel chloride	Sigma, Dorset, UK.	451193
Phosphate buffered saline (PBS)	Sigma, Dorset, UK	P4417
Poly D lysine solution	Sigma, Dorset, UK.	P8920
Propidium iodide	Invitrogen, Paisley, UK	P1304MP
ProtoBlock	Geneflow, Fradley, UK.	CL-252
ProtoGel (30%)	Geneflow, Fradley, UK.	A20072
Silver nitrate	Sigma, Dorset, UK.	209139
Sodium acetate	Sigma, Dorset, UK.	S8750
Sodium chloride	Sigma, Dorset, UK.	S9888
Sodium citrate	Sigma, Dorset, UK.	S1804
Sodium dodecyl sulphate(SDS)	Sigma, Dorset, UK.	L6026
Tetramethylethylenediamine (TEMED)	Sigma, Dorset, UK.	T9281
Tris(hydroxymethyl)aminomethane	Sigma, Dorset, UK	25285-9
Triton X-100	Sigma, Dorset, UK.	T8532

Product Name	Company	Product Number
TWEEN-20	Sigma, Dorset, UK.	P1379

4.3.5 Commercial kits

Product Name	Company	Product Number
Endo Free Plasmid Maxi kit	Qiagen, Crawley, UK.	12362
QIAprep Spin Miniprep kit	Qiagen, Crawley, UK.	27104
QIAquick Gel Extraction Kit	Qiagen, Crawley, UK.	28704

4.3.6 DNA and Protein ladders

Product Name	Company	Product Number
1Kb DNA Step Ladder	Promega, Southampton, UK.	G6941
25bp DNA Step Ladder	Promega, Southampton, UK.	G4511
6 X His Protein Ladder	Qiagen, Crawley, UK.	34705
HyperLadder I	Bioline, London, UK	BIO-33025

4.3.7 Dyes

Product Name	Company	Product Number
6 X Blue/Orange loading dye	Promega, Southampton, UK.	G1881
Bromophenol blue	Sigma, Dorset, UK.	B5525
Lectin from *Pisum sativum* (pea) (FITC-PSA)	Sigma, Dorset, UK.	L0770

4.3.8 Enzymes

Product Name	Company	Product Number
EcoRV	New England BioLabs, Hitchin, UK	R0195T
HindIII	New England BioLabs, Hitchin, UK	R0104S

Product Name	Company	Product Number
Pfu DNA polymerase	Promega, Southampton, UK.	M7741
PshAI	New England BioLabs, Hitchin, UK	R0593S
RNase Inhibitor	Bioline, London, UK.	65027
T4 DNA ligase	Promega, Southampton, UK.	M1801

4.3.9 Equipment

Product Name	Company	Product Number
5 ml Polypropylene round-bottom tube	Becton Dickinson Labware, New Jersey, USA.	352063
96 Well flat bottom plate	Corning Incorporated, New York, USA.	3595
AcroSep IMAC HyperCell column	PALL Life Sciences, Farlington, UK.	20093-C001
Centrifugal filter column Micron YM-10 10KDa	Millipore , Watford, UK.	42406
Hybond ECL nitrocellulose membrane	GE Healthcare, Buckinghamshire, UK.	RPN3032D
Hyper film	GE Healthcare, Buckinghamshire, UK.	RPN1675K
Micro Cell- HAC slides	Conception Technologies, San Diego, USA.	MC-20-4
Microlance needle 19G	SLS, Nottingham, UK.	SYR6102
Pierce Concentrators 20K MWCO	Thermo Fisher Scientific, Rockford, USA.	87750
Polyacrylamide spin desalting columns 7K MWCO	Thermo Fisher Scientific, Rockford, USA.	89849
Sensor chip CM5	GE Healthcare, Buckinghamshire, UK.	BR100012
T75 cm^2 Tissue culture flask	SLS, Yorkshire, UK.	354638

4.3.10 Protein expression vectors

Product Name	Company	Product Number
pcDNA4 HisMax B	Invitrogen, Paisley, UK.	V86420

4.4 Methods

4.4.1 Recombinant protein preparation

Baculovirus-expressed recombinant human zona pellucida protein 2, 3 and 4 (Bac-rhZP2, Bac-rhZP3 and Bac-rhZP4) (gifted by Dr. Satish Gupta, National Institute of Immunology, New Delhi, India) and a control His-tagged recombinant protein (CΔ105) (gifted by Dr. Eva Hyde, University of Birmingham) were prepared for surface plasmon resonance (SPR) analysis.

Buffer exchange

The buffer for all recombinant proteins was exchanged using centrifugal filter columns. Briefly, 500 µl of PBS was added to the column and centrifuged at 14000 *x g* for 10 min, to remove potential contamination from the column filter. Recombinant protein solution was then added to the column along with an additional 200 µl of PBS, which were then centrifuged at 14000 *x g* for 10 min, this step was repeated a further two times. Finally the filter column was inverted and placed into a collection tube which was then centrifuged at 1000 *x g* for 3 min. The eluate was then stored at -20°C.

BCA protein assay

In a flat bottomed 96 well plate, 200 µl of working solution (bicinchoninic acid and copper(II) sulphate, 50:1 respectively) was added to 25 µl of diluted recombinant protein samples (diluted at a concentration range 1:5, 1:10 and 1:20), and to a bovine serum albumin (BSA) standard (ranging from 0 µg/ml to 1000 µg/ml). The working reagent was left to incubate for 30 min at 37°C. The optical density (OD) values were measured using a plate spectrophotometer at a 540 nm wavelength. The protein concentrations were determined

through OD comparison to BSA standards, and then diluted to 100 µg/ml with an appropriate volume of PBS.

4.4.2 Surface plasmon resonance (SPR) analysis with Bac-rhZPs

All experiments were performed using a BIAcore ™ 3000 instrument with research-grade CM5 sensor chips (BIAcore, Uppsala, Sweden).

Amine coupling

Initially the CM5 chip was exposed to HBS-EP buffer (0.01 M HEPES pH 7.4, 0.15 M NaCl, 0.005% Surfactant P20 and 3 mM EDTA) at a flow rate of 30 µl/min. The chip was activated with a mixture of 0.2 M 1-ethyl-3-(3'-dimethylamino-propyl) carbodiimide hydrochloride and 0.05 M N-hydroxysuccinimide (EDC:NHS) (35 µl, at a flow rate of 10 µl/min). Recombinant proteins were diluted to a concentration of 10 µg/ml in 10 mM sodium acetate pH 5. To immobilise proteins to the CM5 chip, via amine coupling, 35 µl of protein was injected at a flow rate of 5 µl/min, then the chip surface was blocked with 50 µl of 1 M ethanolamine pH 8.5 (flow rate: 5 µl/ml). To ensure responses were not due to non-specific background binding, a control cell on the CM5 chip was activated with a 1:1 solution of 1-ethyl-3-(3-dimethylaminopropyl) carbodiimide (EDC) and *N*-Hydroxysuccinimide (NHS) solution (35 µl, at a flow rate of 10 µl/min), then immediately blocked with 50 µl of 1 M ethanolamine pH 8.5 (flow rate: 5 µl/min), without recombinant protein exposure (figure 4.3 a).

His tag coupling

To immobilise His-tagged recombinant proteins, the surface of the BIAcore CM5 chip had to be modified with nitrilotriacetic acid, to allow binding of poly-histidine when in complex with nickel. One hundred microlitres of a 1:1 EDC:NHS solution was applied to the gold concave surface of a BIAcore CM5 sensor chip. The chip was incubated at room temperature for 20 min and then rinsed with deionised H_2O and dried using compressed air. The chip was then covered with 100 µl of (S)-N-(5-Amino-1-Carboxypentyl)iminodiacetic acid (NTA-NH2),pH 8.0 and incubated for 30 min at room temperature. The chip was then rinsed with deionised H_2O and dried using compressed air.

Initially the modified CM5 chip was exposed to a 1:60 dilution of HBS-EP (0.01 M HEPES pH7.4, 0.15 M NaCl, 0.005% Surfactant P20, 3.4 mM EDTA) and HBS-P buffer (0.01 M HEPES pH 7.4, 0.15 M NaCl, 0.005% Surfactant P20) giving rise to a modified HBS-EP buffer with a final concentration of: 0.01 M HEPES pH 7.4, 0.15 M NaCl, 0.005% Surfactant P20 and 50 µM EDTA at a flow rate of 30 µl/min. The chip was activated with 300 µM nickel chloride (10 µl, at a flow rate of 10 µl/min) and recombinant proteins were diluted to a concentration of 10 µg/ml in 10 mM sodium acetate pH 5. To immobilise proteins to the CM5 chip, via his-tag coupling, 30 µl of protein was injected at a flow rate of 10 µl/min. Proteins were routinely stripped from the chip using 0.35 M EDTA pH 8 (30 µl, at a flow rate of 10 µl/min), however in cases where proteins could not be removed 10 mM glycine pH 2.2 (15 µl, at multiple flow rates of either 10 µl/min or 30 µl/min) was used (figure 4.3 b).

Data was analysed using BIA evaluation 4.1 software (BIAcore, Uppsala, Sweden).

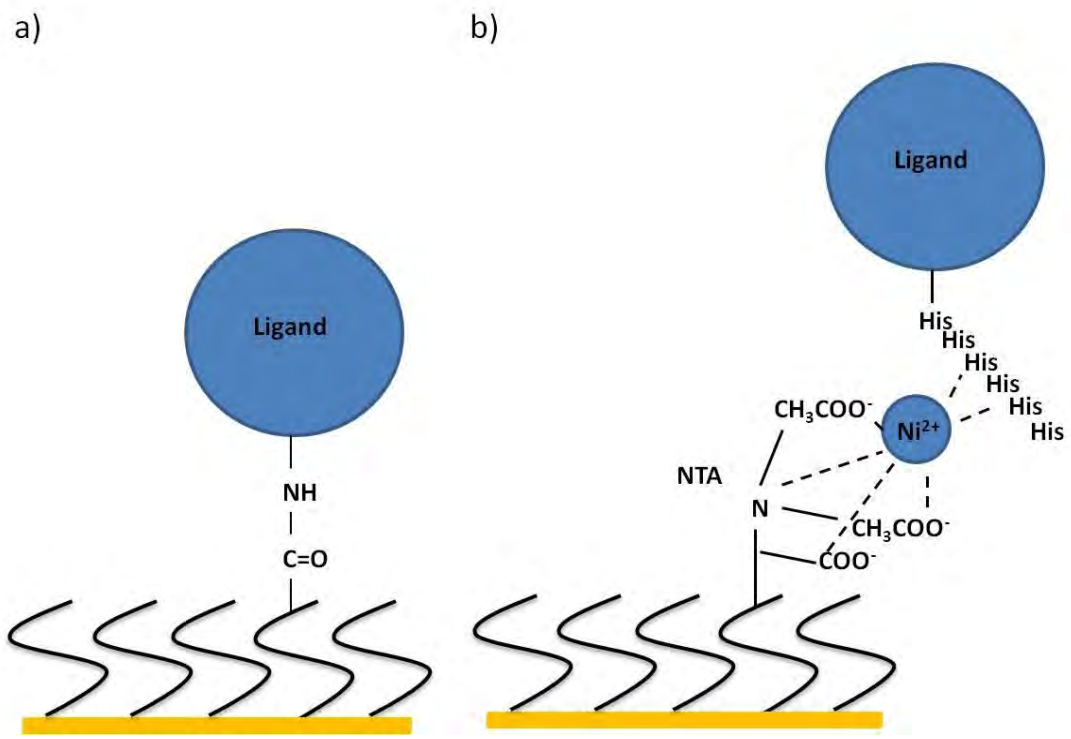

Figure 4.3: BIAcore immobilisation chemistries.

BIAcore CM5 sensor chips have a carboxymethylated dextran matrix covalently attached to a gold surface. Ligands can be attached by various different chemistries such as (**a**) Amine coupling, where ligands are immobilised through a covalent chemical bond. (**b**) His-tag coupling, where NTA chelates with nickel ions to immobilise ligands that are attached to a poly-histidine tag. Image modified from (BIAcore. 2003).

4.4.3 Construction of CHO-rhZP3 protein expression vector

ZP3 polymerase chain reaction amplification

To clone human ZP3 (hZP3) into the mammalian protein expression vectors pcDNA4/HisMax B, a pBluescript clone containing the complete coding sequence of hZP3 (clones ZP3-PB) was used as a template for PCR amplification. Primers used in PCR amplifications were obtained from Eurogentec, Southampton, UK. Oligonucleotide sequences are indicated in table 4.2.

PCR amplification reactions contained: 2 U of high fidelity *Pfu* DNA polymerase, 1 X Reaction Buffer, 0.5 µM (each) reverse and forward primers, 200 µM (each) of the four dNTPs and 1 µl ZP3-PB DNA template. PCR reaction had a negative water control to ensure no contamination. Reactions were performed under the following conditions: 95°C, 2 min; 35 cycles of 95°C, 30 s; 51°C, 30 s; 72°C, 2 min 30 s and one cycle of 72°C, 5 min.

PCR amplicons were run on 1% (w/v) agarose gel (section 2.4.7) and then purified using a QIAquick gel extraction kit, .according to the manufacturers' protocol.

Primer	Oligonucleotide sequence(5'-3')	PCR amplicon size (bp)
ZP3pcDNA4 HisMax-Forward	CAACCCCTCTGGCTCTTG	
ZP3pcDNA4 HisMax-Reverse	TTATTCGGAAGCAGACACAG	1209

Table 4.2: Primer oligonucleotide sequence ZP3 amplification.

Protein expression vector pcDNA4 HisMax preparation

Prior to ligation, the mammalian protein expression vector pcDNA4 HisMax B was linearised with *EcoRV*. Digestion reactions contained 2 U *EcoRV,* 1 X NEBuffer 3, 100 µg/ml BSA, and 20 µl of pcDNA4 HisMax B and reactions were incubated at 37°C for 4 h. Linearised protein expression vector was run on 1% (w/v) agarose gel (section 2.4.7) and products were purified according to manufacturers' protocol using QIAquick gel extraction kit.

Ligation

For blunt end ligation reactions insert and vector DNA was mixed at a ratio of 3:1. All DNA concentrations were quantified by spectrophotometer analysis. Reactions also contained 3 U of T4 DNA ligase, 1 X Buffer and 10 U *EcoRV,* to minimise re-ligation of the vector to itself.

Ligations were incubated at 22°C for 1 h, followed by enzyme inactivation step for 10 min at 65°C.

E.Coli Transformation

Fifty microlitre aliquots of Alpha-select gold efficiency *E.Coli* cells were taken from storage at -80°C and thawed on wet ice. Five microlitres of ligation reactions were added to individual aliquots and incubated on ice for 30 min. Cells were heat shocked at 42°C for 45 s, and then plunged into ice for a further 2 min. The *E.Coli*-DNA mixture was added to 945 µl of sterile Luria-Bertani (LB) broth with tubes then being incubated for 1 h at 37°C, shaking at 180 rpm. Fifty microlitres of cell transformation mixture was spread across sterile LB agar plates containing 50 ug/ml ampicillin and plates were incubated overnight at 37°C.

DNA preparation

To confirm correct vector:insert ligation, DNA digests were performed (section ***DNA digests***). Initially DNA was prepared using a small scale method. Five millilitres of sterile LB broth supplemented with 50 µg/ml ampicillin was inoculated with individual colonies cultured from the incubated overnight transformation spread plates. Cultures were incubated for 12-16 h at 37°C, shaking at 180 rpm. DNA was then prepared using a QIAprep Spin miniprep kit, according to the manufacturers' protocol. DNA was then stored at -20°C.

In preparation for mammalian cell transfection (section 4.4.5), DNA was prepared on a larger scale. Two hundred millilitres of sterile LB broth supplemented 50 µg/ml ampicillin, was inoculated with an individual colony from the incubated overnight transformation spread plates. Cultures were incubated for 12-16 h at 37°C, shaking at 180 rpm. DNA was then

prepared using an Endo-free plasmid maxi kit, according to the manufacturers' protocol. Spectrophotometric DNA quantification, was completed before samples were stored at -20°C.

DNA digests

To confirm vector:insert ligation, putative CHO-rhZP3 pcDNA4 HisMax DNA was linearised with *HindIII*. Reactions contained 2 U *HindIII*, 1 X Reaction buffer and 3 µl of DNA from mini DNA preparations. Digests were then incubated at 37°C for 1 h. Linearised DNA was run on 1% (w/v) agarose gel (section 2.4.7).

Vector DNA was also double digested with *HindIII* and *PshAI* to confirm the correct orientation of the ZP3 in the pcDNA4 HisMax protein expression vector. Reactions contained 1 U *HindIII*, 1 U *PshAI*, 1 X Reaction buffer and 3 µl of DNA from mini DNA preparations. Digests were then incubated at 37°C for 1 h. Double digested DNA was run on 1% (w/v) agarose gel (section 2.4.7).

Sequencing

DNA sequencing was performed by the Functional Genomics and Proteomics Laboratory, University of Birmingham. Reactions contained 500 ng of CHO-rhZP3 pcDNA4 HisMax DNA, and 3.2 pmol of individual primers. Primers were obtained from Eurogentec, Southampton, UK. Oligonucleotide sequences are indicated in table 4.3. Results were analysed using Chromas Lite 2.01 and Mega 4.1.

Primer	Oligonucleotide sequence(5'-3')
ZP3pcDNA4 HisMax-Forward	CAACCCCTCTGGCTCTTG
ZP3pcDNA4 HisMax-Reverse	TTATTCGGAAGCAGACACAG
ZP3_int_rev1	GGCCACGCAGTGGTCCACAA
ZP3_int_rev2	TGCATGCTGTTGCCACACTGG

Table 4.3: Primer oligonucleotide sequence CHO-rhZP3 pcDNA4 HisMax sequencing.

4.4.4 Chinese hamster ovary (CHO) cell culture

A Chinese hamster ovary (CHO) cell line (gifted from Beata Grygielska, University of Birmingham) was cultured in Dulbecco's Modified Eagle's Medium F-12 (DMEM/F-12) supplemented with 10% (v/v) FBS, 1% (v/v) NEAA, 100 IU/ml (each) penicillin and streptomycin and 4 mM L-glutamine at 37°C, 6% CO_2. Culture media was exchanged every 3-4 days.

CHO cells were subcultured when fully confluent. Cells were trypsinised with 0.25% (w/v) trypsin-0.53 mM EDTA and incubated at 37°C for approximately 5 min until cell detachment. Cells were recovered in complete growth medium and centrifuged for 5 min at 500 x *g*. Cells were resuspended in an appropriate volume of growth medium at a typical subcultivation ratio 1:5.

For storage, frozen aliquots of CHO cells in cryoprotectant medium (90% (v/v) FBS, 10% (v/v) DMSO) were stored in liquid nitrogen. If required frozen aliquots of cells were thawed in a 37°C water-bath and slowly resuspended in complete growth medium in order to avoid osmotic shock. Cells were then centrifuged for 5 min at 500 x *g,* and seeded in an appropriate volume of culture medium.

4.4.5 Transfection

CHO cells were cultured in 15 ml of growth medium minus antibiotics in T75 cm^2 culture flasks until cells reached 90-95% confluency. At the time of transfection for each individual T75 cm^2 culture flask, 24 µg of plasmid DNA and 60 µl Lipofectamine 2000 were each diluted into 1.5 ml of Opti-MEM I Reduced serum media and incubated for 5 min at room temperature. The DNA and Lipofectamine solutions were mixed and incubated for a further 30 min at room temperature before adding to CHO cells. Growth medium was then exchanged 24 h after transfection.

4.4.6 Selection of CHO-rhZP3 pcDNA4 HisMax transfected CHO cell line

Approximately 3 days after transfection, rhZP3 pcDNA4 HisMax transfected CHO cells were subcultured using the normal CHO subcultivation procedures (section 4.4.4). Complete growth medium was supplemented with 250 µg/ml of the selection agent, Zeocin. Lethal levels of Zeocin were determined by culture with non-transfected CHO cells. CHO cells were cultured in Zeocin supplemented growth medium for 3 weeks to select for a population containing CHO-rhZP3 pcDNA4 HisMax protein expression vector.

4.4.7 Mammalian rhZP3 protein expression

rhZP3 protein recovery

Cell culture medium from CHO-rhZP3 pcDNA4 HisMax transfected and non-transfected control CHO cells were analysed for CHO-rhZP3 protein expression. Medium was recovered after cell culture and was supplemented with 10% (v/v) EDTA free protease inhibitor media.

Medium was concentrated using a protein concentrator for easier protein purification. Samples were stored at -20°C.

Cell lysates from CHO-rhZP3 pcDNA4 HisMax transfected and non-transfected control CHO cells were also analysed for CHO-rhZP3 protein expression. Cells were incubated with 0.25% (w/v) trypsin-0.53 mM EDTA at 37°C, until cell detachment. Cells were recovered with complete CHO growth medium then cells were centrifuged at 500 *x g* for 5 min. Cells were then lysed in 500 µl of lysis buffer (50 mM Tris-HCl ph 8, 150 mM NaCl and 1% (v/v) Triton X-100) supplemented with 10% (v/v) EDTA-free protease inhibitor. Samples were vortexed for 20 s and then incubated on ice for 15 min. Cell lysates were then centrifuged at 14000 *x g* for 10 min, at 4°C. The supernatant was recovered and stored at -20°C.

His-tag protein purification

Media and cell lysates collected from (5 and 2 T75 cm^2 culture flasks respectively) of successfully transfected CHO cells were purified via AcroSep IMAC HyperCell column. Briefly, columns were washed with 10 column volumes (CV) of ddH_2O, then loaded sequentially with 6 CV of 100 mM nickel acetate, 3 CV of 1 M sodium chloride and then further rinsed with 20 CV of ddH_2O. Prior to sample loading the column was prepared with 10 CV of loading buffer (50 mM tris-HCL pH 8.0, 400 mM NaCl, 15 mM imidazole). Either cell lysate preparations or collected culture medium were then loaded onto the column. Ten CV of loading buffer was further added to remove any unbound proteins from the column. To exclude non-specific proteins that were weakly bound to the column, 3 CV of 30 mM imidazole was applied prior to elution. To elute the His_6 tagged recombinant zona protein from the column, 7 CV of

elution buffer (200 mM imidazole, 0.5 M NaCl) were passed through the column, and eluate was recovered and saved.

SDS-PAGE and Western Blotting.

Purified protein samples, controls and 6 X His protein ladder were heated at 98°C for 10 min in 5 X SDS-PAGE sample buffer (0.225 M Tris-Cl, pH 6.8, 5% (w/v) SDS, 50% (v/v) glycerol, 0.05% (w/v) bromophenol blue and 0.25 M DTT). Proteins were resolved by electrophoresis on 12% SDS-PAGE gel in tris-glycine buffer (250 mM tris, 1.92 M glycine) supplemented with 10% (w/v) SDS at a voltage of 200V. Proteins were electrophoretically transferred onto 0.20 µm nitrocellulose membrane at a constant voltage of 100V for 1 h in tris-glycine buffer supplemented with 20% (v/v) methanol. Nonspecific binding sites on membranes were blocked with ProtoBlock according to manufacturers' protocol for 30 min at room temperature with gentle agitation. The membranes were then incubated with an anti-his antibody at a concentration of 1:2000 either for 1 h at room temperature or overnight at 4°C. Membranes were extensively washed with agitation in Tris-buffered saline (20 mM Tris, pH 7.5, 500 mM NaCl) supplemented with 0.1% (v/v) Tween-20) (TTBS) for 30 min, changing buffer three times at 10 min intervals. Membranes were then incubated with a 1:10000 concentration of corresponding goat anti-mouse IgG-HRP secondary antibody for 1 h at room temperature with gentle agitation, followed by extensive washing with TTBS. Positive bands were detected by chemiluminescence with ECL Western blotting substrate, according to manufactures' instructions.

Nitrocellulose membrane silver staining

To detect total protein in purified protein samples nitrocellulose membranes were silver stained. Membranes were washed in ddH_2O to remove residual ECL Western blotting substrate, then a silver stain was added (0.7 M sodium citrate, 0.3 M ferrous sulphate and 0.1 M silver nitrate) and left to stain for approximately 5 min, with gentle agitation. To enhance protein bands, membranes were further stained with Farmers solution (2 mM potassium ferricyanide, 2 mM sodium carbonate and 6 mM sodium thiosulphate) for approximately 1 min. Membranes were further washed in ddH_2O then air dried.

4.4.8 Human sperm preparation

Human spermatozoa were prepared via the direct swim up method (section 2.4.1). Capacitated spermatozoa were then diluted to 6 x 10^6 spermatozoa ml^{-1} with sEBSS + 0.3% (w/v) BSA.

4.4.9 Acrosome reaction assay

Human spermatozoa in 100 µl aliquots were incubated with either: 25 µl of crude purified medium from CHO-rhZP3 pcDNA4 HisMax transfected or non-transfected CHO cells; a negative control of sEBBS + 0.3% (w/v) BSA and a positive control containing 10 µM calcium ionophore. 0.2 µg/ml propidium iodide was added to each tube and then samples were incubated at 37°C, 6% CO_2 for 15 min. Once the desired incubation period was completed, cells were centrifuged at 300 *x g* for 5 min and smeared on to pre-coated poly-D-lysine (20 µg/ml) microscope slides. Slides were air dried and cells were then permeabilised with 100% methanol for 1 min. Slides were left to air dry, then cells were stained with 50 µg/ml FITC-

PSA and incubated in a humidified chamber for 45 min at 37°C. Slides were rinsed with ddH_2O, air-dried and coverslips mounted using Hydromount.

Acrosome status was assessed using a fluorescent microscope. Cells were visualised using a 60 X oil immersion lens. Only viable cells assessed by propidium iodide exclusion were scored with 500 cells being scored per slide. Duplicates of each treatment provided mean acrosome status for each treatment.

The percentage of AR induction for both treatments (CHO-rhZP3 pcDNA4 HisMax transfected CHO medium and non-transfected CHO medium) were normalised to both the positive control (10 µM calcium ionophore) and spontaneous AR levels (sEBBS + 0.3% (w/v) BSA) and expressed as percentage (%) stimulation of acrosome reaction (see formula below). Statistical significance between the two treatments was assessed by a student's independent t-test, which was completed using SPSS 14.0.

$$\%\ \boldsymbol{Stimulation\ of\ acrosome\ reaction} = \left[\frac{\boldsymbol{Treatment\ AR}\ \% - \boldsymbol{Spontaneous\ AR}\ \%}{\boldsymbol{Positive\ \ AR}\% - \boldsymbol{Spontaneous\ AR}\ \%}\right] \mathbf{x\ 100}$$

4.4.10 Native sheep zona preparation

Zona intact oocytes were collected from frozen thawed sheep ovaries by aspirating palpable antral follicles with a 19 gauge needle. Oocytes with a visible ZP were located with the aid of a microdissection microscope and collected and stored at -20°C until heat solubilisation.

Prior to use, 150 sheep oocytes were thawed and resuspended in 500 µl of 1 X PBS. The ZP matrices were removed from the oocytes by vigorous pipetting through a small bore glass pipette. The suspension was centrifuged for 15 min at 2000 *x g*, then resuspended in 100 µl of 1 X PBS. Sheep ZP was then heat solubilised at 70°C for 90 min.

Before SPR experimentation, heat solubilised sheep zona underwent a buffer exchange using a polyacrylamide spin desalting column, according to manufactures' protocol. Briefly, the column was placed into a microcentrifuge collection tube and centrifuged at 1500 *x g* for 1 min to remove excess column liquid. Four hundred microlitres of 10 mM sodium acetate pH5 was added to the column, which was then centrifuged at 1500 *x g* for 1 min. This step was repeated three times, discarding buffer recovered in the collection tube. Eighty microlitres of heat solubilised sheep zona was added to the column with an additional 30 µl of 10 mM sodium acetate pH 5 added on top of the column resin. The column was centrifuged at 1500 *x g* for 2 min to recover heat solubilised sheep zona.

4.4.11 Ram sperm lysate preparation

Ram spermatozoa were collected from three ram testicles. The outer covering of the testes were removed and ram spermatozoa was aspirated from the cauda of the epididymis using a 19 gauge needle.

Ram spermatozoa were diluted to 100 x 10^6 sperm/ml with 1 X PBS supplemented with 1% (v/v) triton and 10% (v/v) protease inhibitor. Samples were then sonicated for 10 s, followed by an incubation period of 30 min at room temperature with gentle agitation. After incubation 1 mM dithiothreitol (DTT) was added to the samples which were then left for a further 30 min at room temperature with gentle agitation. Samples were then sonicated for 10 s, and centrifuged at 14000 *x g* for 10 min. The supernatant was removed and stored at -20°C until use.

4.4.12 Surface plasmon resonance (SPR) analysis with heat solubilised sheep zona

All experiments were performed with a BIAcore ™ 3000 instrument with research-grade CM5 sensor chips (BIAcore, Uppsala, Sweden).

Heat solubilised sheep zona protein immobilisation

Initially the CM5 chip was exposed to HBS-EP buffer (0.01 M HEPES pH 7.4, 0.15 M NaCl, 0.005% Surfactant P20 and 3 mM EDTA) at a flow rate of 30 µl/min. The chip was activated with a mixture of 0.2 M 1-ethyl-3-(3'-dimethylamino-propyl) carbodiimide hydrochloride and 0.05 M N-hydroxysuccinimide (EDC:NHS) (50 µl, at a flow rate of 5 µl/min). To immobilise heat solubilised sheep zona proteins to the CM5 chip, via amine coupling, 90 µl of protein was injected at a flow rate of 10 µl/min, then the chip surface was blocked with 50 µl of 1 M ethanolamine pH 8.5 (flow rate: 10 µl/min). To ensure reposes were not due to non-specific background binding, a control cell on the CM5 chip was activated with the EDC:NHS solution (50 µl, at a flow rate of 5 µl/min), then immediately blocked with 50 µl of 1 M ethanolamine pH 8.5 (flow rate: 5 µl/min).

Ram sperm binding and elution

The ram sperm lysate solution was diluted in buffer HBS-EP (1:1 solution). Fifty microlitres of diluted ram sperm lysate was injected at a flow rate of 10 µl/min any binding proteins were recovered by injecting 15 µl of glycine pH 2 at a flow rate of 30 µl/min and collected. Ram sperm binding and elution cycles were repeated five times to collect maximum material for mass spectrometry analysis (section 4.1.13).

4.4.13 Mass spectrometry analysis

The product from the ram sperm binding and elution cycles (section 4.4.12) in addition to a sample of the heat solubilised sheep zona pellucida protein (section 4.4.10) were sent for mass spectrometry analysis. This work was completed in by Dr. Ashley Martin, University of Birmingham.

Briefly the samples were reduced with 10 mM dithiothreitol (DTT) in 50 mM ammonium bicarbonate for 1 h at 60^{o}C and then alkylated using 20 mM iodoacetamide at room temperature in the dark. The proteins were then digested using porcine trypsin overnight at 37^{o}C. The tryptic peptides generated were separated using a gradient of 2-36% acetonitrilein and 0.1% formic acid over 60 min at 350 nl/min using a Dionex Ultimate 3000 High-performance liquid chromatography (HPLC) system. The HPLC column was an Acclaim PepMap100 (75 μM I.D. x 25 cm C18 3 uM particle size) connected to a Bruker ETD Amazon ion trap mass spectrometer with an online nanospray source fitted with a metal needle with a 10 μM tip. 1600 V was applied to the end plate and the drying gas set to 6.5 l/min at 180^{o}C. An MS survey scan from 350 to 1600 m/z was performed and the 5 most intense ions in each survey scan were selected for collision induced dissociation (CID) fragmentation. After ions were fragmented twice they were placed on an exclusion list for 30 s.

The raw data was processed using the Bruker DatAnalysis peak detection program to select peaks which were then searched using the Mascot search engine (version 2.1) using the SwissProt protein database for “all mammals”. The minimum mass accuracy for both the MS and MS/MS scans were set to 0.5 Da and trypsin protease selection used. The peptides were

filtered using a minimum Mascot score of 30. The data output was via the Bruker ProteinScape software package.

This process alkylates the cysteine residues, preventing mixed disulphide generation during the subsequent analysis. The mass change caused by the modification was included in the database search.

4.5 Results

4.5.1 Bac-rhZP protein immobilisation

Baculovirus-expressed recombinant human zona pellucida protein 2, 3 and 4 (Bac-rhZP2, Bac-rhZP3 and Bac-rhZP4) were donated by Dr. Satish Gupta, of the National Institute of Immunology, New Delhi, India (Chakravarty et al. 2005). To immobilise the Bac-rhZP proteins amine coupling was initially used (section 4.4.2, figure 4.3 a). There was no increase in Resonance Units (RU) after protein injection (figure 4.4) indicating that none of the Bac-rhZP proteins bound to the chip. One possible explanation could be binding interference caused by the glycosylation patterning of the rhZP proteins so alternate immobilisation chemistries were used.

As the Bac-rhZP proteins have a poly-histidine tag, this feature was also utilised as a method to immobilise the proteins to the chip. To accommodate this different immobilisation chemistry, the existing CM5 chips had to be modified, by permanently attaching nitrilotriacetic acid (NTA) to the carboxymethylated dextran matrix. This surface could then be activated with nickel to bind with the Bac-rhZPs poly-histidine tags (section 4.4.2, figure 4.3 b) (BIAcore. 2003).

In order to validate the modified CM5 chip, a control poly-histidine tagged recombinant protein was immobilised. The control poly-histidine protein had previously shown to be immobilised via his-tag coupling. Upon injection there was identifiable binding of the control protein, with an increase of 2876 RU. When Bac-rhZP3 and Bac-rhZP4 were injected there

was no significant binding observed, however there was an increase in RU after two injections with Bac-rhZP2 (increase of 353 RU) (figure 4.5).

Unlike the control protein, the Bac-rhZP2 could not be removed from the chip after protein injection. The RU units remained at 197 RU, after three successive rounds of 0.35 M EDTA (figure 4.6). Glycine (10 mM) was also used to attempt to remove the Bac-rhZP2 (Appendix II.i), however the RU still remained above the pre-injection baseline level.

The inability of immobilising rhZP3 and 4 to the chip, along with the irregularities in rhZP2 protein removal, lead to uncertainties about the structural integrity of the rhZP proteins. This doubt made them inappropriate for these studies, which lead to a rethink in experimental strategy.

All work in this study was in collaboration with Dr. Stephen Young, University of Birmingham.

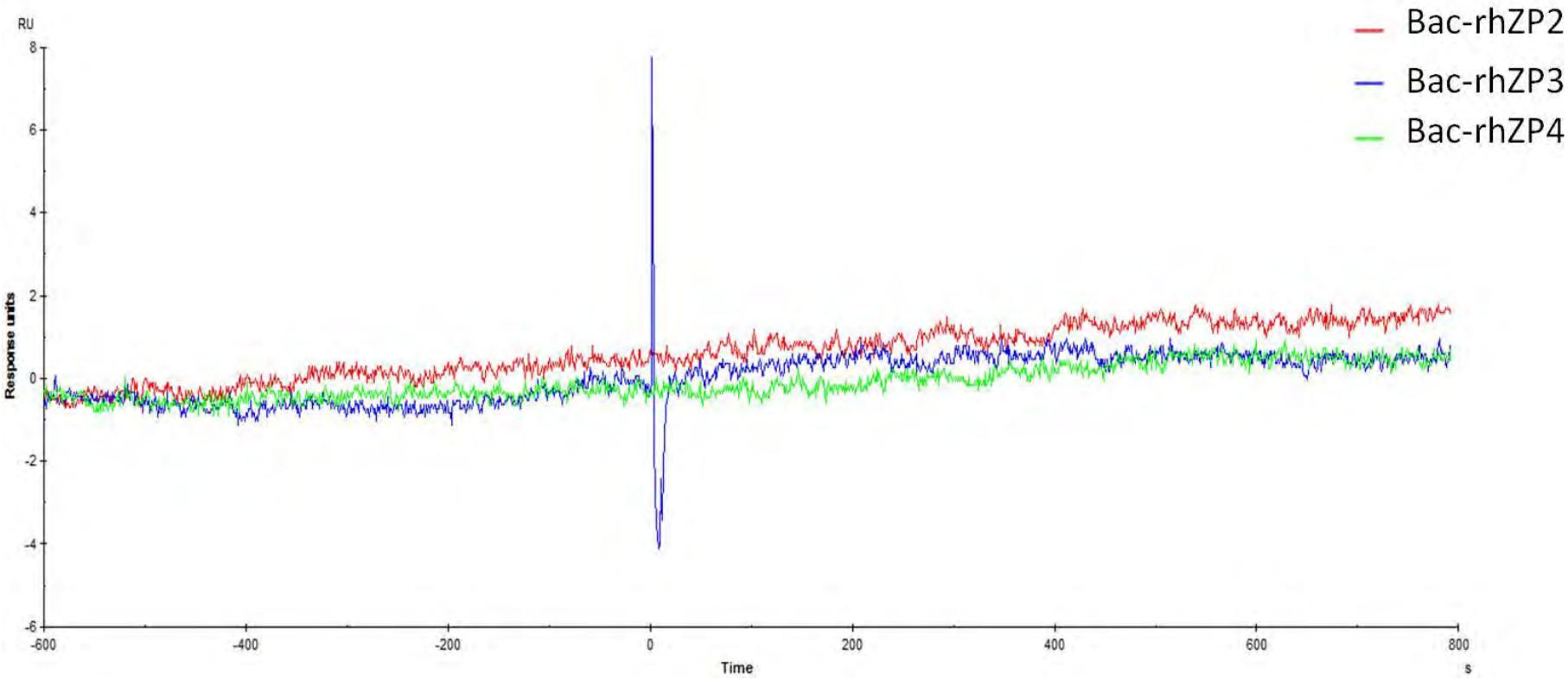

Figure 4.4: Bac-rhZP amine coupling immobilisation.

BIAcore sensogram showing attempted amine coupling immobilisation of Bac-rhZP2, Bac-rhZP3 and Bac-rhZP4 (35 µl, at a flow rate of 5 µl/min). To BIAcore CM5 sensor chips. After injection there was no increase in resonance units (RU), consistent with no protein immobilisation.

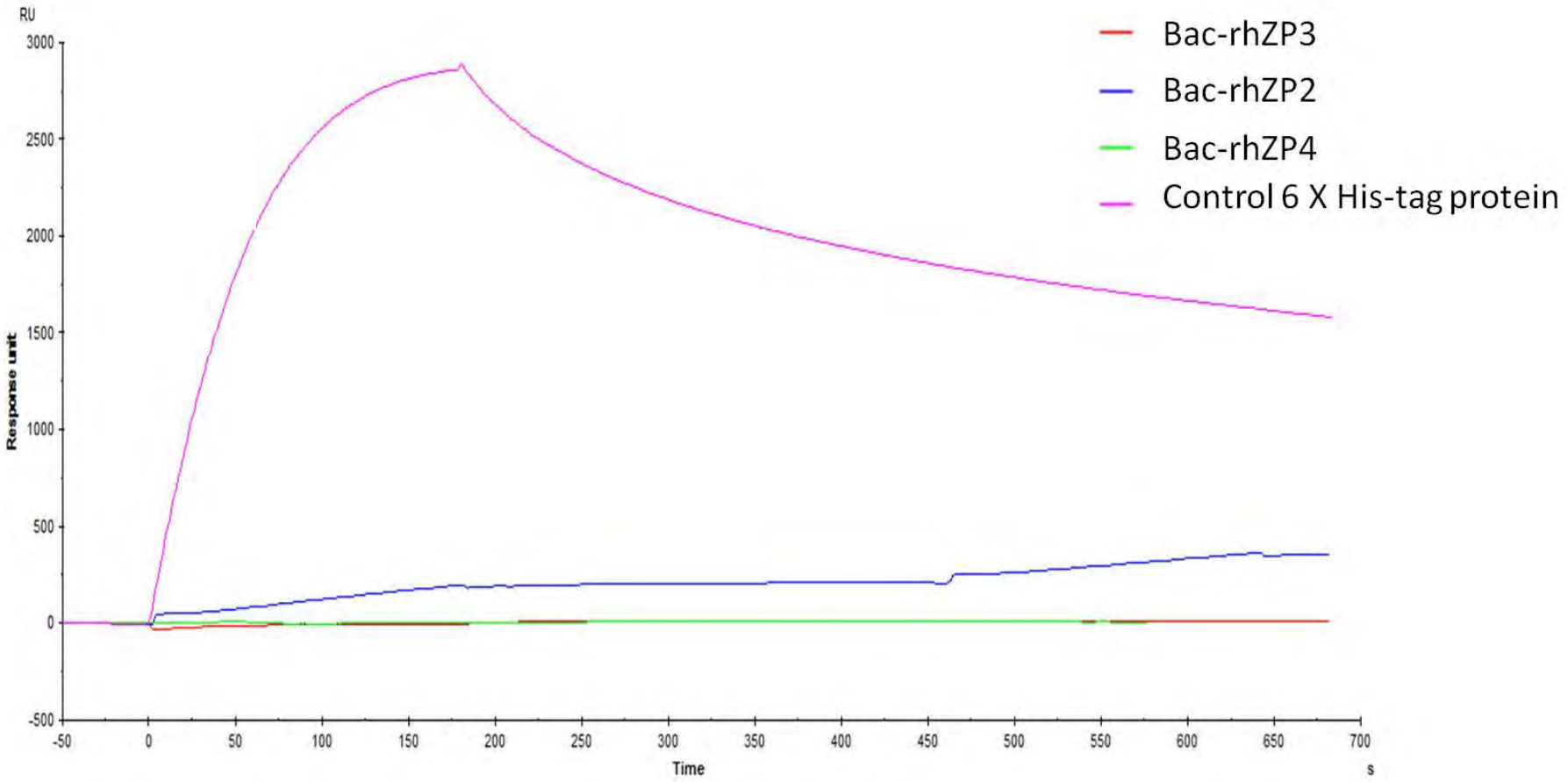

Figure 4.5: Bac-rhZP his-tag coupling immobilisation.

BIAcore sensogram showing attempted his-tag coupling immobilisation of Bac-rhZP2, Bac-rhZP3, Bac-rhZP4 and a control 6 X his-tag protein. A modified BIAcore CM5 sensor chips was used (section 4.4.2). To validate the CM5 chip, a control recombinant 6 X his-tagged protein, that had be immobilised via his-tag coupling previously, was used. For all proteins, 30 µl of protein was injected at a flow rate of 10 µl/min.

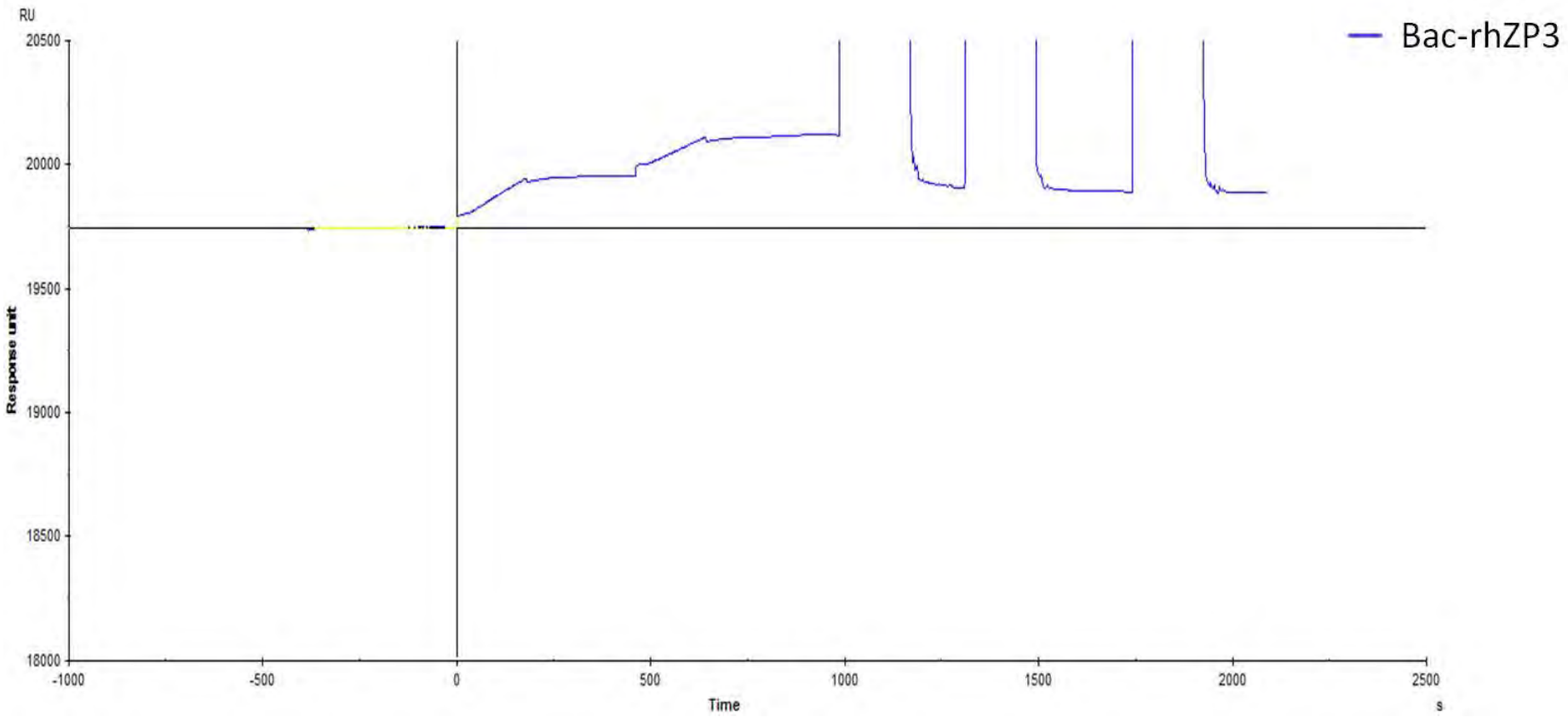

Figure 4.6: Removal of immobilised Bac-rhZP2, from modified CM5 chip.

BIAcore sensogram showing attempted removal of his-tag immobilised Bac-rhZP2 from a modified BIAcore CM5 sensor chip (section 4.4.2). After two injections with Bac-rhZP2 (30 µl, at a flow rate of 10 µl/min), there showed an overall increase in 353 RU, however after three rounds of 0.35 M EDTA pH 8 (30 µl, at a flow rate of 10 µl/min), the RU did not fall to pre-injection RU, and remained at 197 RU above baseline levels.

4.5.2 CHO-rhZP3 pcDNA4 HisMax protein expression construct

To pursue the SPR protein binding studies further, it was deemed prudent to begin expressing rhZP proteins. Initial work focused on the expression of CHO-rhZP3.

A mammalian protein expression system was chosen, with the hope of providing a glycosylation pattern similar to native ZP glycosylation. A commercially available protein expression vector, pcDNA4 HisMax was used. The particular protein expression vector was chosen as it contained an N-terminal poly-histidine tag, which could be utilised in protein immobilisation. It also contained an enterokinase recognition cleavage site that could lead to his-tag removal if required (pcDNA4 HisMax B vector information, Appendix II.ii, iii, iv).

The complete coding hZP3 DNA sequence was PCR amplified using a high fidelity *Pfu* DNA polymerase, from a pBluescript hZP3 containing vector (ZP3-PB), cloned by Dr. Sarah Conner, University of Birmingham. Primers were designed to amplify the CHO-hZP3 sequence devoid of the signal peptide, due to concerns of premature cleavage of the N-terminal poly-histidine tag (figure 4.7).

CHO-hZP3 PCR amplicons were ligated to the *EcoRV* linearised pcDNA4 HisMax protein expression vector via blunt end ligation (figure 4.8 a, b). The complete CHO-rhZP3 pcDNA4 HisMax construct was confirmed by *HindIII* and *HindIII*/*PshAI* digests, each providing the expected product sizes resulting from correct ligation (6468 bp and 5284 bp/1184 bp respectively) (figure 4.8 c, d).

DNA sequence confirmation was also established by DNA sequencing (figure 4.9) and the complete CHO-rhZP3 pcDNA4 HisMax vector map is shown in figure 4.10.

Figure 4.7: CHO-rhZP3 pcDNA4 HisMax primer design.

Primers were designed to amplify CHO-hZP3 sequence from a hZP3-pBluescript clone. Annealing sites for forward and reverse primers to hZP3 DNA sequence are illustrated by the red arrows. The forward primer (denoted by left to right arrow) was designed to avoid the signal peptide (denoted in green text), this was to ensure no premature cleavage of the N terminal His-tag, when ligated to the pcDNA4 HisMax B vector. (GeneBank sequence: M60504.1).

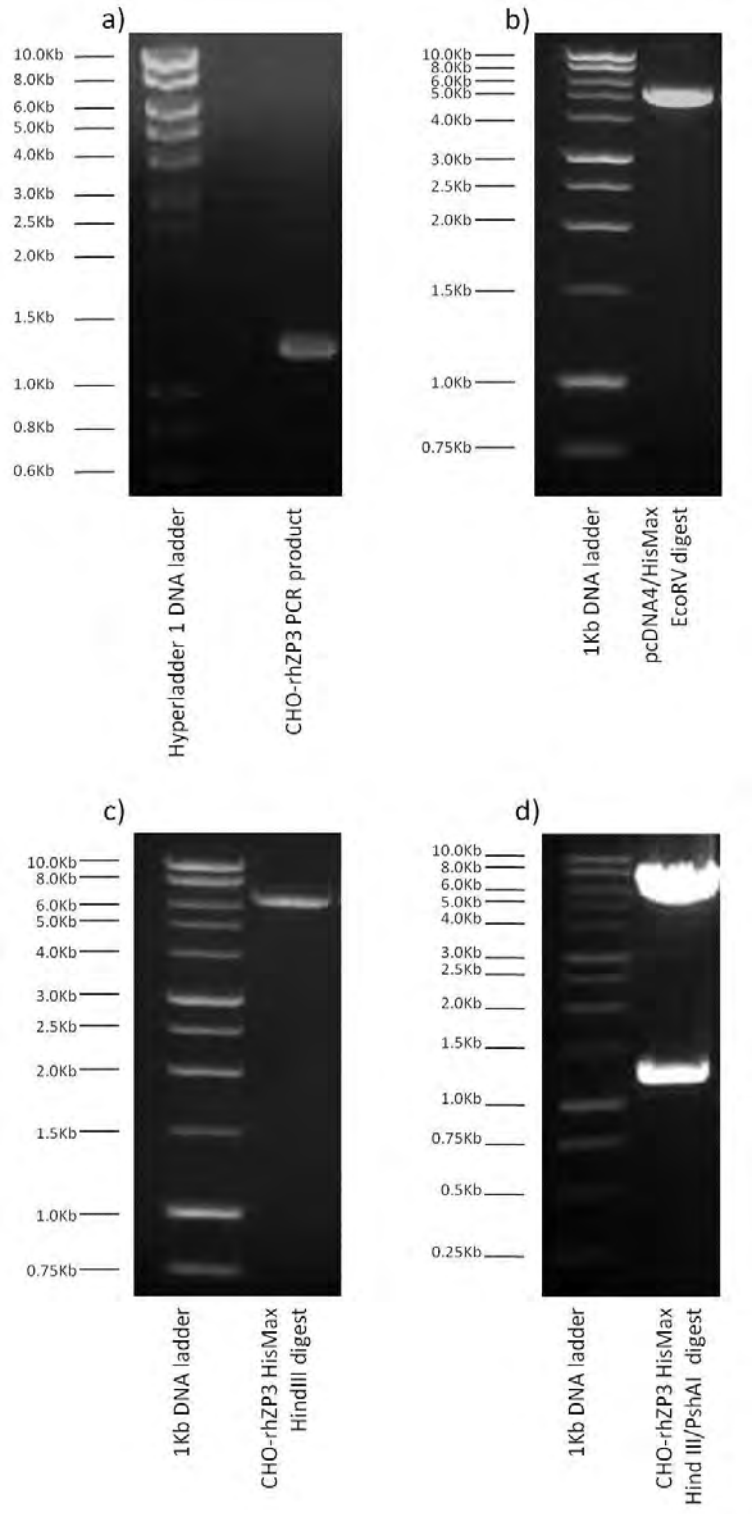

Figure 4.8: Cloning CHO-rhZP3 pcDNA4 HisMax protein expression vector.

Agarose gel electrophoresis showing (**a**) CHO-rhZP3 PCR amplification (1209 bp), (**b**) linearised pcDNA4 HisMax B protein expression vector with *EcoRV* (5259 bp), (**c**) complete CHO-rhZP3 pcDNA4 HisMax protein expression vector, linearised with *HindIII* (6468 bp) and (**d**) complete CHO-rhZP3 pcDNA4 HisMax protein expression vector, digested with *HindIII* and *PshAI* (5285 bp/1184 bp).

```
Expected        GCAGATCAACCCCTCTGGCTCTTGCAGGGTGGAGCCAGCCATCCTGAGACGTCCGTACAG
Actual          GCAGATCAACCCCTCTGGCTCTTGCAGGGTGGAGCCAGCCATCCTGAGACGTCCGTACAG
                ************************************************************

Expected        CCCGTACTGGTGGAGTGTCAGGAGGCCACTCTGATGGTCATGGTCAGCAAAGACCTTTTT
Actual          CCCGTACTGGTGGAGTGTCAGGAGGCCACTCTGATGGTCATGGTCAGCAAAGACCTTTTT
                ************************************************************

Expected        GGCACCGGGAAGCTCATCAGGGCTGCTGACCTCACCTTGGGCCCAGAGGCCTGTGAGCCT
Actual          GGCACCGGGAAGCTCATCAGGGCTGCTGACCTCACCTTGGGCCCAGAGGCCTGTGAGCCT
                ************************************************************

Expected        CTGGTCTCCATGGACACAGAAGATGTGGTCAGGTTTGAGGTTGGACTCCACGAGTGTGGC
Actual          CTGGTCTCCATGGACACAGAAGATGTGGTCAGGTTTGAGGTTGGACTCCACGAGTGTGGC
                ************************************************************

Expected        AACAGCATGCAGGTAACTGACGATGCCCTGGTGTACAGCACCTTCCTGCTCCATGACCCC
Actual          AACAGCATGCAGGTAACTGACGATGCCCTGGTGTACAGCACCTTCCTGCTCCATGACCCC
                ************************************************************

Expected        CGCCCCGTGGGAAACCTGTCCATCGTGAGGACTAACCGCGCAGAGATTCCCATCGAGTGC
Actual          CGCCCCGTGGGAAACCTGTCCATCGTGAGGACTAACCGCGCAGAGATTCCCATCGAGTGC
                ************************************************************

Expected        CGCTACCCCAGGCAGGGCAATGTGAGCAGCCAGGCCATCCTGCCCACCTGGTTGCCCTTC
Actual          CGCTACCCCAGGCAGGGCAATGTGAGCAGCCAGGCCATCCTGCCCACCTGGTTGCCCTTC
                ************************************************************

Expected        AGGACCACGGTGTTCTCAGAGGAGAAGCTGACTTTCTCTCTGCGTCTGATGGAGGAGAAC
Actual          AGGACCACGGTGTTCTCAGAGGAGAAGCTGACTTTCTCTCTGCGTCTGATGGAGGAGAAC
                ************************************************************

Expected        TGGAACGCTGAGAAGAGGTCCCCCACCTTCCACCTGGGAGATGCAGCCCACCTCCAGGCA
Actual          TGGAACGCTGAGAAGAGGTCCCCCACCTTCCACCTGGGAGATGCAGCCCACCTCCAGGCA
                ************************************************************

Expected        GAAATCCACACTGGCAGCCACGTGCCACTGCGGTTGTTTGTGGACCACTGCGTGGCCACA
Actual          GAAATCCACACTGGCAGCCACGTGCCACTGCGGTTGTTTGTGGACCACTGCGTGGCCACA
                ************************************************************

Expected        CCGACACCAGACCAGAATGCCTCCCCTTATCACACCATCGTGGACTTCCATGGCTGTCTT
Actual          CCGACACCAGACCAGAATGCCTCCCCTTATCACACCATCGTGGACTTCCATGGCTGTCTT
                ************************************************************

Expected        GTCGACGGTCTCACTGATGCCTCTTCTGCATTCAAAGTTCCTCGACCCGGGCCAGATACA
Actual          GTCGACGGTCTCACTGATGCCTCTTCTGCATTCAAAGTTCCTCGACCCGGGCCAGATACA
                ************************************************************

Expected        CTCCAGTTCACAGTGGATGTCTTCCACTTTGCTAATGACTCCAGAAACATGATATACATC
Actual          CTCCAGTTCACAGTGGATGTCTTCCACTTTGCTAATGACTCCAGAAACATGATATACATC
                ************************************************************

Expected        ACCTGCCACCTGAAGGTCACCCTAGCTGAGCAGGACCCAGATGAACTCAACAAGGCCTGT
Actual          ACCTGCCACCTGAAGGTCACCCTAGCTGAGCAGGACCCAGATGAACTCAACAAGGCCTGT
                ************************************************************

Expected        TCCTTCAGCAAGCCTTCCAACAGCTGGTTCCCAGTGGAAGGCCCGGCTGACATCTGTCAA
Actual          TCCTTCAGCAAGCCTTCCAACAGCTGGTTCCCAGTGGAAGGCCCGGCTGACATCTGTCAA
                ************************************************************
```

```
Expected        TGCTGTAACAAAGGTGACTGTGGCACTCCAAGCCATTCCAGGAGGCAGCCTCATGTCATG
Actual          TGCTGTAACAAAGGTGACTGTGGCACTCCAAGCCATTCCAGGAGGCAGCCTCATGTCATG
                ************************************************************

Expected        AGCCAGTGGTCCAGGTCTGCTTCCCGTAACCGCAGGCATGTGACAGAAGAAGCAGATGTC
Actual          AGCCAGTGGTCCAGGTCTGCTTCCCGTAACCGCAGGCATGTGACAGAAGAAGCAGATGTC
                ************************************************************

Expected        ACCGTGGGGCCACTGATCTTCCTGGACAGGAGGGGTGACCATGAAGTAGAGCAGTGGGCT
Actual          ACCGTGGGGCCACTGATCTTCCTGGACAGGAGGGGTGACCATGAAGTAGAGCAGTGGGCT
                ************************************************************

Expected        TTGCCTTCTGACACCTCAGTGGTGCTGCTGGGCGTAGGCCTGGCTGTGGTGGTGTCCCTG
Actual          TTGCCTTCTGACACCTCAGTGGTGCTGCTGGGCGTAGGCCTGGCTGTGGTGGTGTCCCTG
                ************************************************************

Expected        ACTCTGACTGCTGTTATCCTGGTTCTCACCAGGAGGTGTCGCACTGCCTCCCACCCTGTG
Actual          ACTCTGACTGCTGTTATCCTGGTTCTCACCAGGAGGTGTCGCACTGCCTCCCACCCTGTG
                ************************************************************

Expected        TCTGCTTCCGAATAAATCCAG
Actual          TCTGCTTCCGAATAAATCCAG
                ********************
```

Figure 4.9: Sequencing results for CHO-rhZP3 pcDNA4 HisMax protein expression vector.

Sequence confirmation of CHO-rhZP3 pcDNA4 HisMax protein expression vector. The results from the vector sequencing (Actual), was compared to the expected DNA sequence (Expected). Nucleotides highlighted in blue correspond to sequence from protein expression (pcDNA4 HisMax B) with black nucleotides correspond to human ZP3 protein sequence. Asterisks denote sequencing matching.

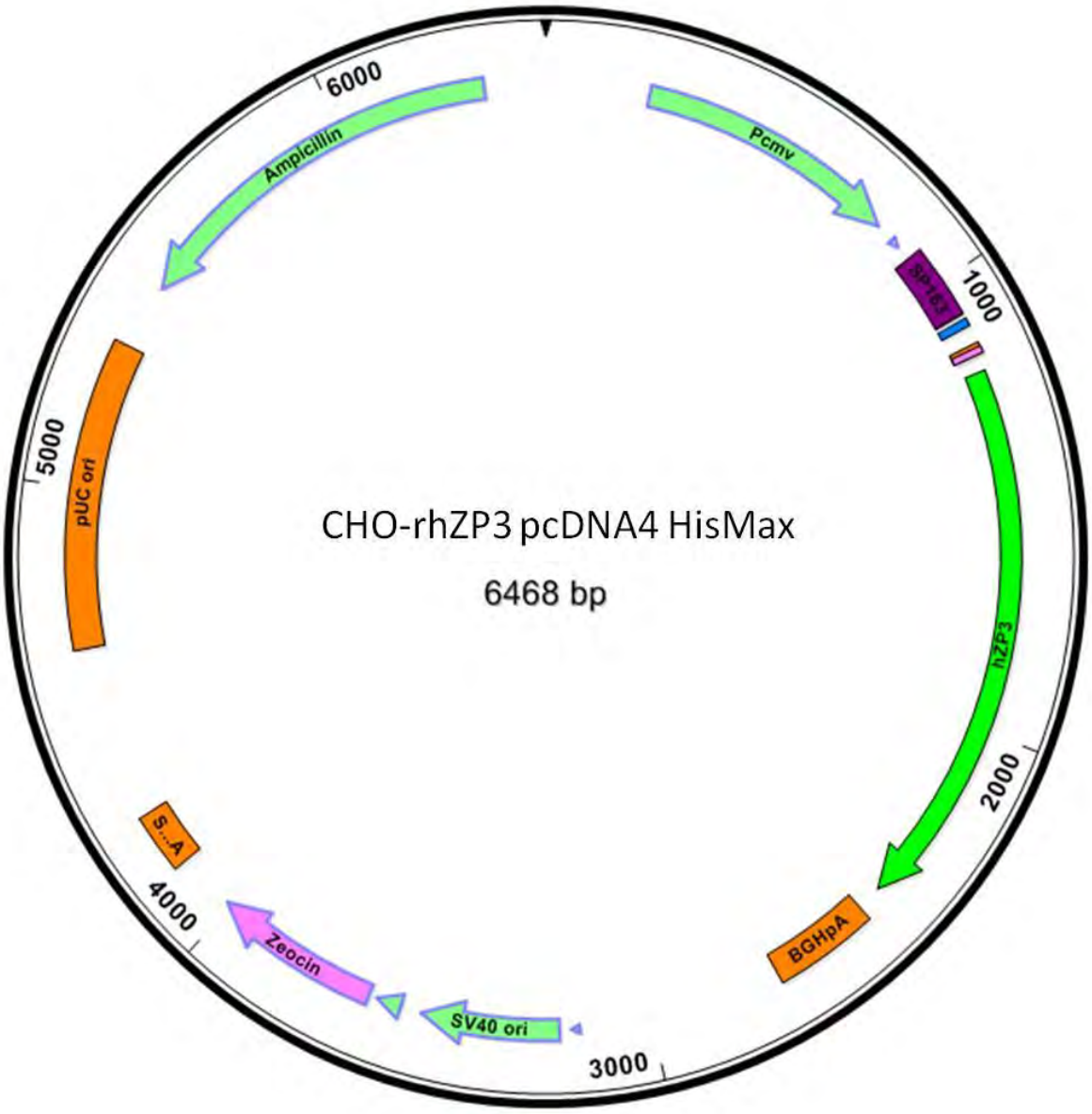

Figure 4.10: CHO-rhZP3 pcDNA4 HisMax vector map.

Vector map, showing key features of CHO-rhZP3 pcDNA4 HisMax protein expression construct. The CHO-hZP3 DNA sequence (labelled green arrow) is preceded by a poly-histidine tag (blue box) as well as an enterokinase recognition cleavage site (pink box).The completed vector DNA sequence is 6468 bp. (Further information regarding pcDNA4 HisMax B vector features can be found in Appendix II.ii).

4.5.3 Transfection

Initial attempts were made to transfect the rhZP3 pcDNA4 HisMax protein expression vector into an immortalised human granulosa cell line, COV434, with no success. Sequential attempts with a GFP-vector and a variety of transfection methods revealed this cell line was particularly resistant to transfection. However successful transfection and creation of a stable rhZP3 pcDNA4 HisMax cell line was achieved by transfecting into a Chinese hamster ovary cell line (*passage 11)* (section 4.4.5). A Zeocin resistance cassette on the pcDNA4 HisMax expression vector was utilised and Zeocin was used as a selection agent to enhance the population containing the CHO-rhZP3 pcDNA4 HisMax protein expression vector (section 4.4.6) (figure 4.11).

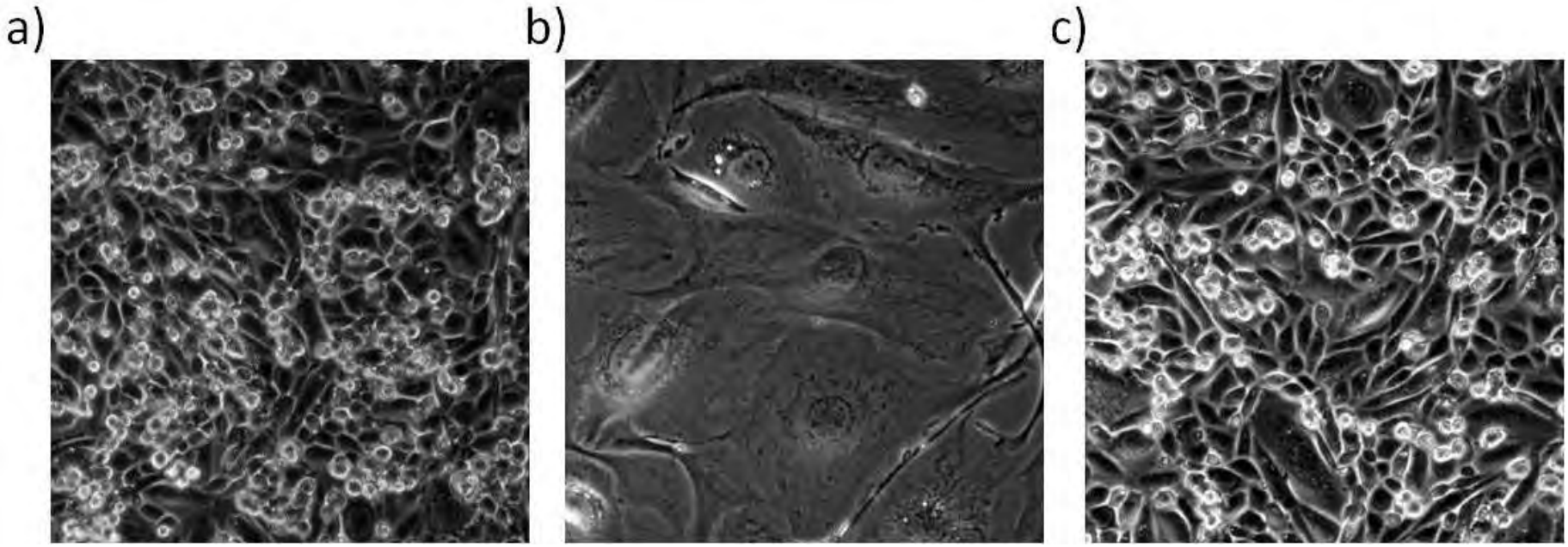

Figure 4.11: Selection of CHO-rhZP3 pcDNA4 HisMax containing CHO cells.

Bright field images of (**a**) non transfected CHO cells cultured in complete medium (*passage 11*), (**b**) non transfected CHO cells cultured in complete growth medium supplemented with 250 µg/ml of Zeocin (*passage 11*) and (**c**) CHO-rhZP3 pcDNA4 HisMax transfected CHO cells cultured in complete growth medium supplemented with 250 µg/ml of Zeocin (*passage 11*). All images were taken at x40 magnification.

4.5.4 CHO-rhZP3 protein expression

To assess rhZP3 protein expression by CHO cells, both cell lysates and cell medium were collected and purified via poly-histidine tag on AcroSep IMAC HyperCell columns. Due to the unknown glycosylation patterning of the expressed rhZP3 the molecular weight can only be estimated. Based on information from sequence based molecular weight calculators, the protein backbone of CHO-rhZP3 can be predicted to be at least 50kDa. Western blot analysis, using an anti-his antibody of both samples showed no identifiable bands from cell lysate samples (data not shown), however samples of cell medium from transfected CHO-rhZP3 pcDNA4 HisMax CHO cells exhibited two bands at approximately 50kDa. Samples from purified non-transfected CHO cell medium did exhibit one band in a similar position, implying a certain amount of non-specific binding (figure 4.12).

Silver stain analysis of nitrocellulose membranes show that, even with the purification, cell medium from both CHO-rhZP3 pcDNA4 HisMax and non-transfected CHO cells remained heavily contaminated with other proteins (figure 4.13), leaving it difficult to quantify the CHO-rhZP3 present.

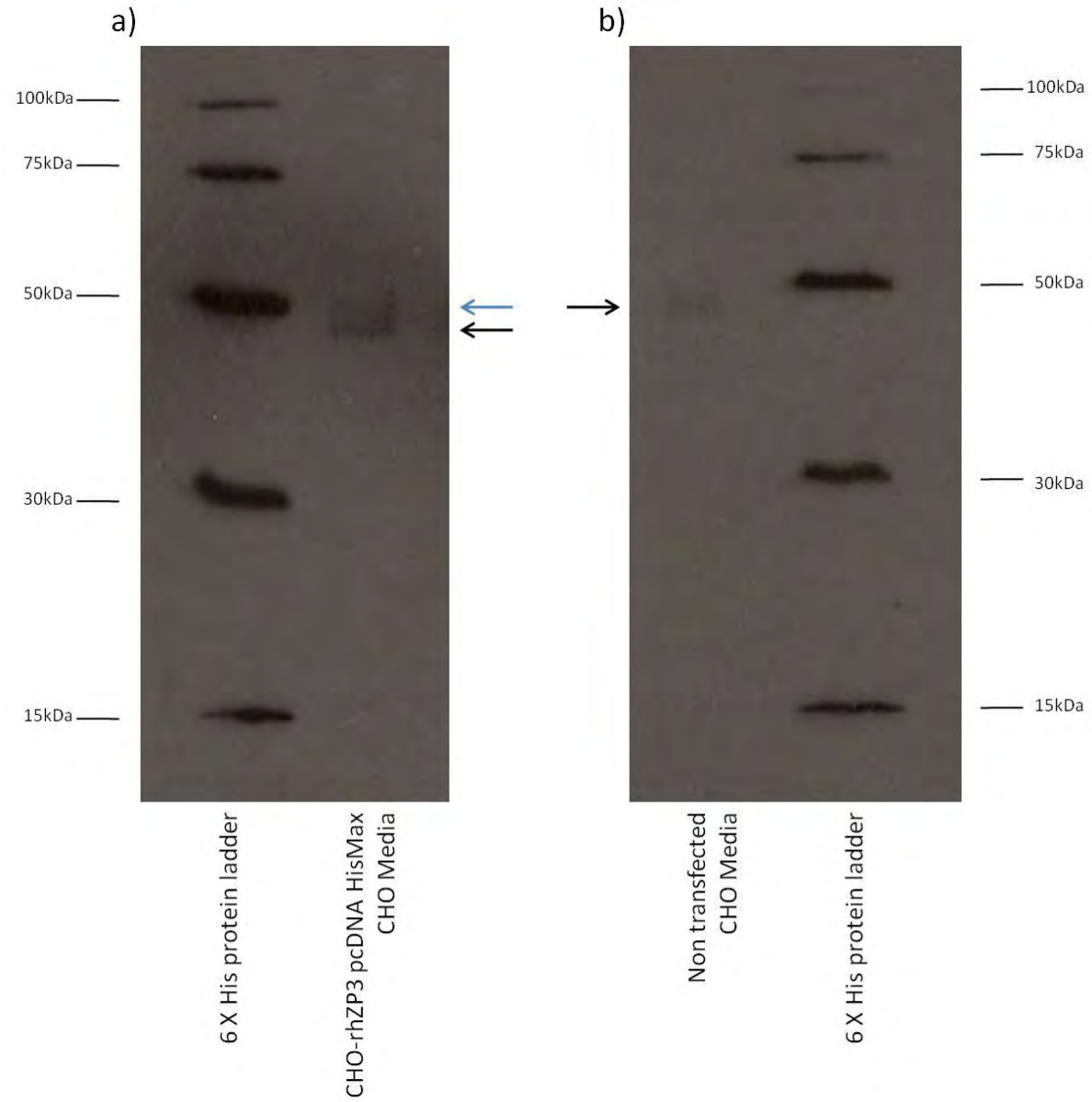

Figure 4.12: CHO-rhZP3 Western blotting.

Western blot analysis, using an anti-his antibody to identify expression of his-tagged CHO-rhZP3, (**a**) from media collected and purified from CHO cells transfected with CHO-rhZP3 pcDNA4 HisMax protein expression vector. A doublet was identified at approximately 50kDa. (**b**) Media collected and purified form non-transfected CHO cells showed only one band, indicating that bands indicated by black arrows may be a result of unspecific binding, and the band indicated by the blue arrow may be that of CHO-rhZP3.

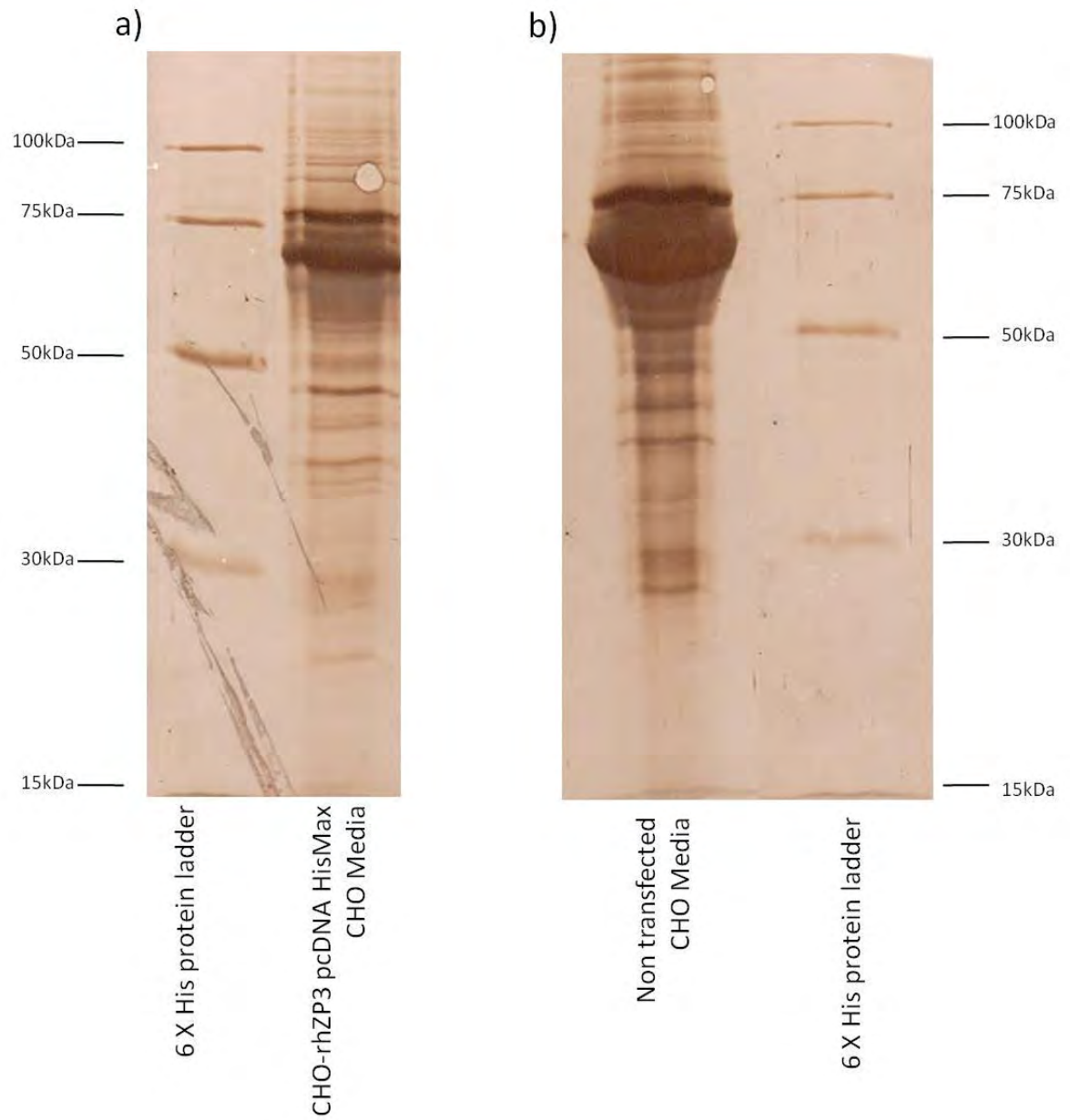

Figure 4.13: Nitrocellulose membrane protein silver stain.

Silver staining of nitrocellulose membrane of (**a**) media collected and purified from CHO cells transfected with CHO-rhZP3 pcDNA4 HisMax protein expression vector and (**b**) media collected and purified from non-transfected CHO cells Multiple protein bands were identified in both samples, even after purification using the His-tag.

4.5.5 Acrosome reaction induction

To establish if the crude medium purification from CHO-rhZP3 pcDNA4 HisMax transfected CHO cells had any functional effect on spermatozoa, purified mediums from both transfected and non-transfected CHO cells were incubated with human spermatozoa, then analysed for their ability to induce acrosome reaction (AR) in the spermatozoa.

Induction of spermatozoa AR was assessed by a characteristic loss of the bright FITC-PSA staining of the anterior portion of the spermatozoa head, often leaving a prominent band around the equatorial region (figure 4.14).

Data showed there was an increase of AR induction in spermatozoa that were incubated with purified medium from CHO-rhZP3 pcDNA4 HisMax transfected CHO cells (58.5 ± 14.4) compared to that of spermatozoa incubated with purified medium from non-transfected CHO cells (35.5 ± 3.6). However the increase was not found to be statistically significant ($P = 0.166$) (figure 4.15).

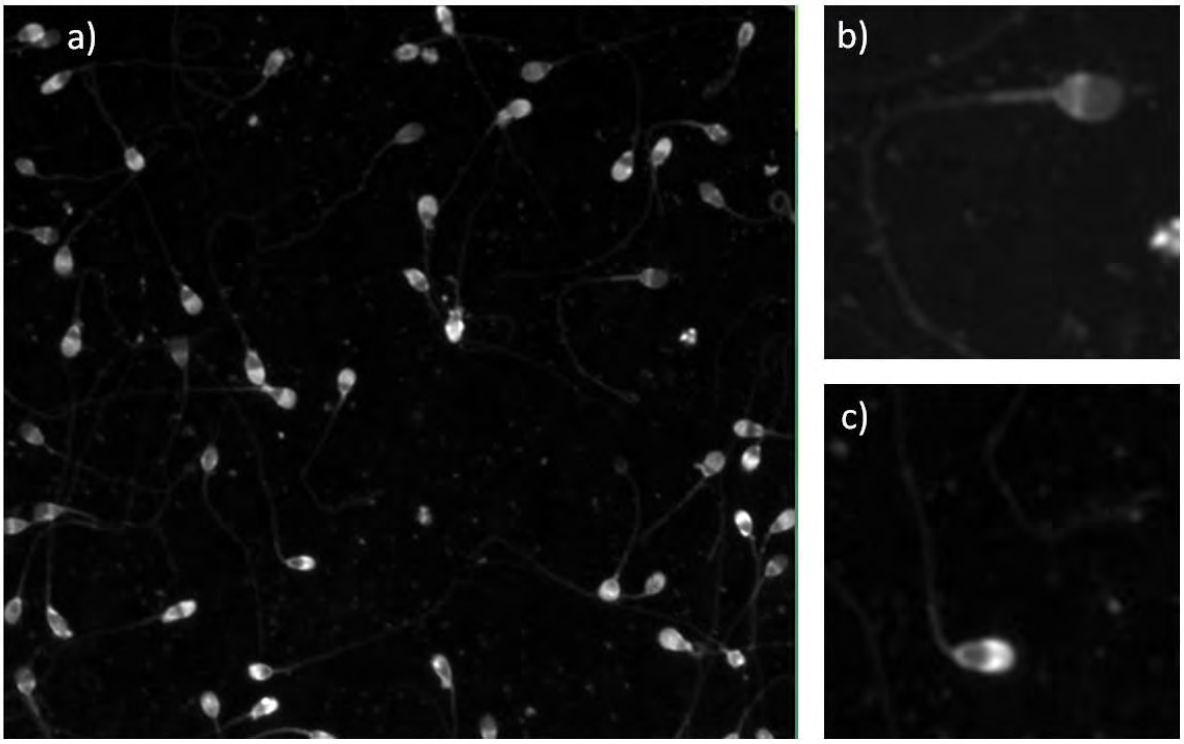

Figure 4.14: Acrosome reaction image scoring.

Multiple fluorescent images were taken from AR slides, cells were visualised using a 60 X oil immersion lens (**a**), spermatozoa that had undergone the AR were characterised by loss of bright anterior region of the head and a characteristic brighter equatorial region (**b**) Spermatozoa with intact acrosomes were characterised by bright anterior region of the head (**c**).

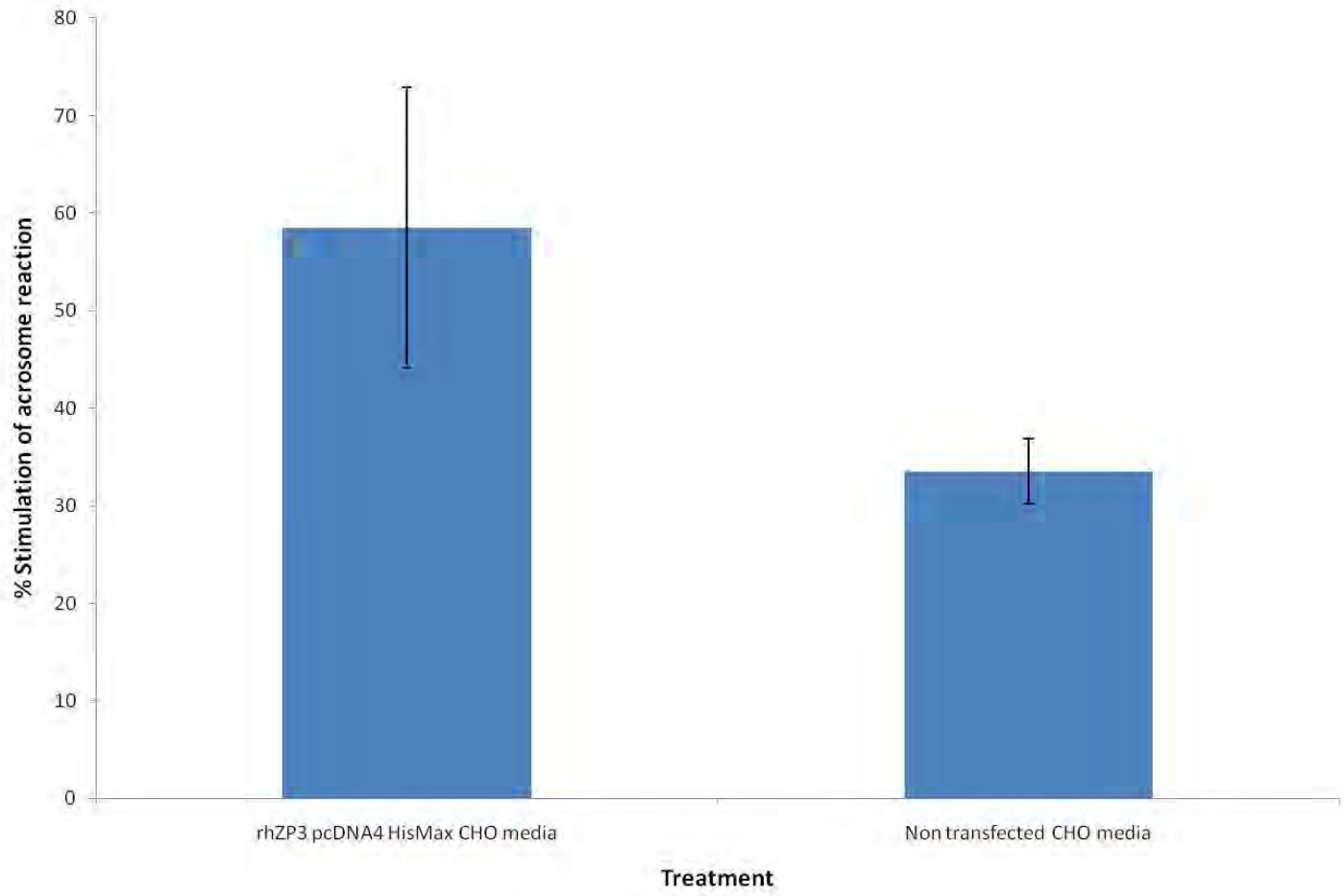

Figure 4.15: CHO-rhZP3 pcDNA4 HisMax transfected CHO media acrosome induction.

Mean percentage of AR stimulation, after incubation for 15 min with purified medium from both CHO-rhZP3 pcDNA4 HisMax transfected and non-transfected CHO cells. Data is normalised to both maximum AR induction levels after incubation with 10 µM calcium ionophore A23187 and spontaneous AR induction levels after incubation with sEBSS + 0.3% (w/v) Bars represent mean (%) ± SEM and n = 3.

4.5.6 *Ovis aries* sperm-zona interaction

There was also an investigation to assess the feasibility of using native ZP material from oocytes in SPR experiments, in order to identify spermatozoa-zona binding partners. Initial SPR experiments used heat solubilised sheep zona proteins and ram spermatozoa lysates.

There was a small amount of binding detected when heat solubilised sheep zona was injected onto the chip (an increase of 90 RU) (figure 4.16). After zona immobilisation, there were multiple cycles of ram spermatozoa lysate injections followed by an elution phase, which was collected. However alignment of the sequential cycles shows that after the injection phase the actual binding of spermatozoa proteins to the immobilised zona was very low, with only a couple of cycles showing increases in the resonance unit levels (cycle B: 11RU, cycle C: 8RU). It was noted that after every elution cycle resonance levels fell below initial baseline levels (figure 4.17).

The composition of sheep zona matrix has currently not been reported, so both native sheep zona and recovered SPR eluate were sent for mass spectrometry analysis. Due to the lack of sequence information in relation to *Ovis aries* species, the results had to be compared to a general mammalian database, which generated a large number of results. 323 and 330 proteins were identified in sheep zona and SPR eluate samples, respectively. Within the peptides identified bovine ZP3 and ZP4 were identified in sheep zona sample and the spermatozoa eluate identified members of the ADAM family (Appendix II.v, vi).

This work was in collaboration with Dr. Stephen Young and Dr. Ashley Martin, University of Birmingham.

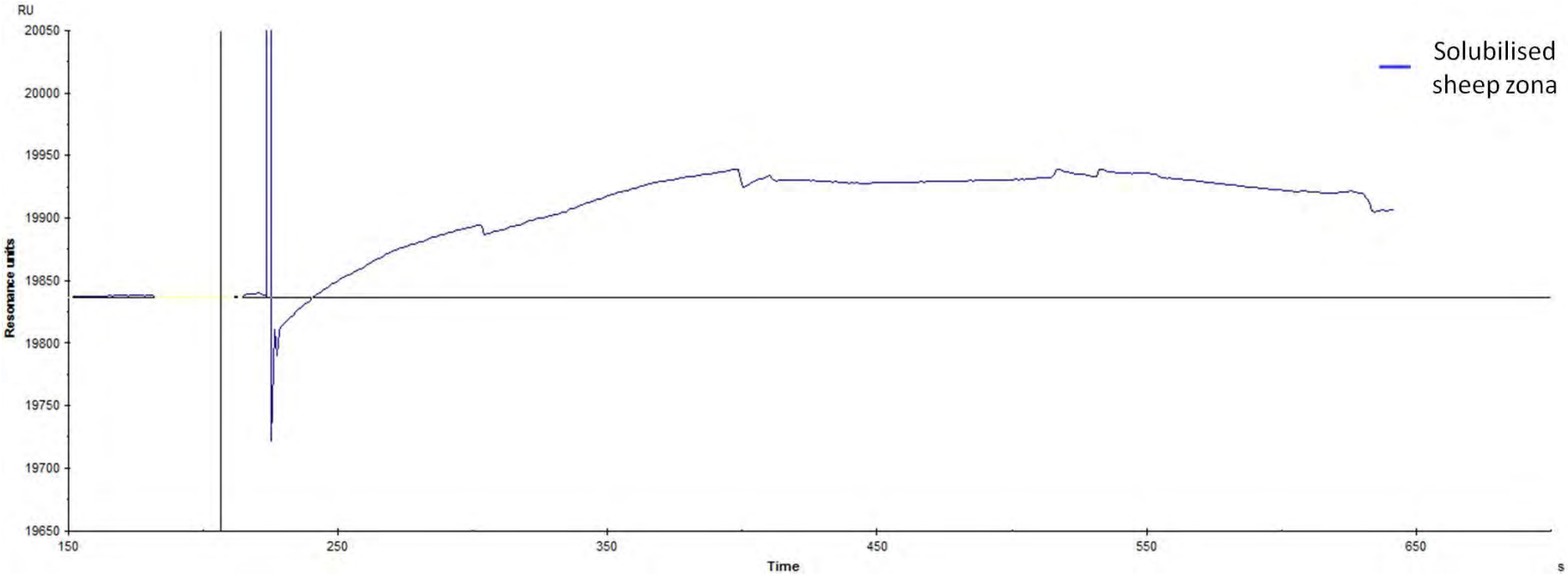

Figure 4.16: Native heat solubilised sheep zona immobilisation.

BIAcore sensogram showing the amine-coupling immobilisation of native heat solubilised sheep zona. After sample injection there was an increase of 90 resonance units (RU) (90 µl of protein was injected at a flow rate of 10 µl/min).

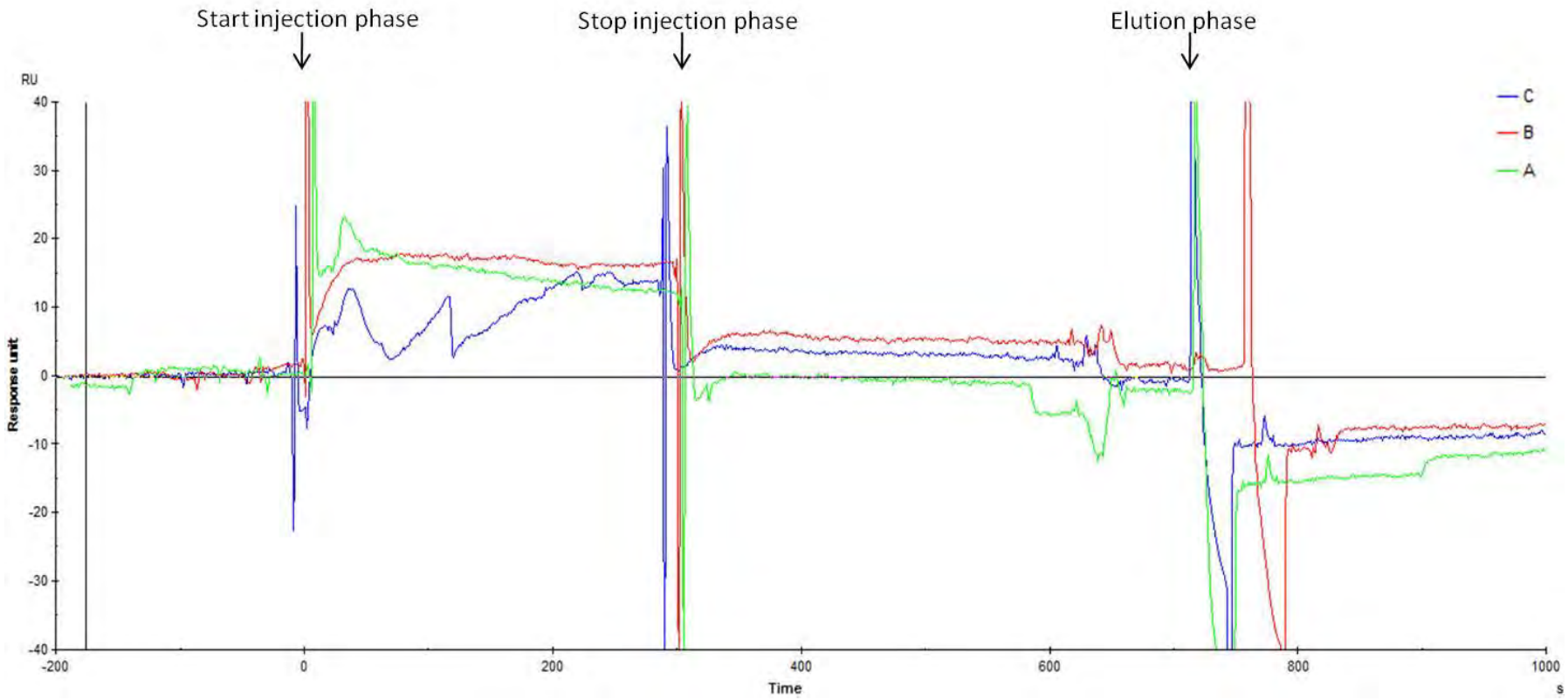

Figure 4.17: Alignments of sequential cycles of ram spermatozoa binding and elution.

BIAcore sensogram showing three sequential cycles of attempted ram sperm binding and elution. Labelled arrows indicate the start and stop of ram sperm lysate solution injections (50 µl, at a flow rate of 10 µl/min). True assessment of ram sperm binding could only be made after injection had stopped. Elution with Glycine pH 2 (15 µl, at a flow rate of 30 µl/min) was then performed and elute was then collected.

4.6 Discussion

Extracellular protein interactions are notoriously difficult to study. Often their hydrophobic residues leave proteins unable to solubilise, unless resorting to harsh denaturing conditions (Wright. 2009). Extracellular protein interactions also exhibit low affinity binding, often having half-lives of just seconds (van der Merwe and Barclay. 1994). The potential development of using SPR technology and other protein interaction techniques such as avidity-based extracellular interaction screening (AVEXIS) which is a novel technique for identifying low affinity extracellular interactions (Bushell et al. 2008) offers the opportunity for unbiased large scale protein screening. It is believed to be more likely that extracellular protein interaction events involve an array of receptors, which together increase the avidity enough to induce a significant signalling event (Wright. 2009). This may have contributed to the inability of identifying only one definitive zona receptor on spermatozoa, which could mean that SZB could be a result of a cohort of receptors that rely on low-affinity bonds, taking form as a multimeric zona recognition complex (Castle. 2002;Nixon et al. 2005).

The inability to immobilise Bac-rhZP3 and 4 to the chip, along with the irregularities in Bac-rhZP2 protein removal, lead to uncertainties about the structural integrity of the Bac-rhZP proteins. Bac-rhZP proteins could be quantified using a BCA protein assay; however, additional AR studies in our laboratory using the Bac-rhZP proteins showed no functional effect on spermatozoa (data not shown). Ultimately the Bac-rhZP proteins from collaborators in India were not suitable for use in these SPR studies, which led to a rethink in experimental strategy and led me to express my own zona proteins.

Purified medium from rhZP3 pcDNA4 HisMax transfected CHO cells did exhibit a band of the correct size for rhZP3 on a Western blot (figure 4.12 a) although rhZP3 protein recovery appeared low which could be due for numerous reasons. It could be as a result of low CHO-rhZP3 protein expression or potential protein degradation. There is also the possibility that CHO-rhZP3 created small aggregates that may have masked the His- tag, leading to poor recovery after purification (Lichty et al. 2011).

After His-tag purification, samples from CHO medium remained highly "dirty" with other protein contaminants that had a high affinity for positively charged nickel ions (figure 4.13 a).The aim was to use the same His-tag chemistry to immobilise CHO-rhZP3 to the BIAcore sensor chip; however this level of protein contamination meant that the sole immobilisation of CHO-rhZP3 could not be guaranteed, making the CHO-rhZP3 purifications unsuitable for SPR studies. To solve this problem, dialysis of the medium or fractionation by High Performance Liquid Chromatography (HPLC) before purification could be useful in removing protein contamination in future preparations. To obtain the protein purity desired for SPR experiments using a different affinity tag such as FLAG or HPC might be more appropriate. Although purification using these tags produces a purer protein sample, it does result in a lower protein yield when compared to His-tag purification (Lichty at al. 2011).

As samples were heavily contaminated it was not possible to isolate or quantify CHO-rhZP3, although purified CHO-rhZP3 pcDNA HisMax transfected CHO cell medium did appear to have an induction effect on spermatozoa AR. There was, however, still background AR induction caused by purified medium from non-transfected CHO cell medium (figure 4.15).

The possibility of immobilising native ZP in SPR studies was also investigated. Due to the limited availability of human ZP it was deemed appropriate to experiment and optimise using a more readily available source of mammalian ZP, in this case *Ovis aries* (sheep). As there is little research regarding sheep ZP, the protein content of sheep ZP had to be estimated based on the other mammals. Mammals such as pigs and mice contain approximately 4 ng and 6 ng, respectively in their zona matrices (Lowenstein and Cohen. 1964;Noda et al. 1983). So it was estimated with 150 sheep oocytes amount of total ZP protein could be approximately 600-900 ng, however with only limited ZP protein we were not able to confirm this directly.

Little binding of sheep zona occurred when immobilising to the SPR sensor chip, which could have been potentially due to low protein concentration or possible binding interference from native glycosylation (figure 4.16). Ram sperm lysate showed further poor binding, which may be due to zona denaturation by heat solubilisation during preparation; however there is evidence to show that ZP prepared by this method causes a functional response in spermatozoa (Bailey and Storey. 1994;Chiu et al. 2008a). The RU level after the elution phase did continuously fall below pre-spermatozoa lysate injection levels; however it cannot be ruled out that the elution phase was not removing the existing pre-bound sheep zona from the chip (figure 4.17).

The eluate that was recovered and a sample of sheep ZP itself were sent to mass spectrometry analysis. Due to the lack of information regarding the sheep genome the peptides recovered had to be compared to a general mammalian database. This produced a large number of hits for both samples (Appendix II.v, vi). The identification of bovine ZP3 and

ZP4 in sheep zona sample and identified members of the ADAM family in the spermatozoa eluate suggests that binding of the ZP material to the chip and subsequently of the spermatozoa lysate did occur, albeit at low levels. ADAM proteins have previously been shown to have a role in SZB (Cho et al. 1998;Shamsadin et al. 1999;Nishimura et al. 2004). However without comparison to a sheep database no solid conclusions can be made. Future experiments need further optimisation to gain optimal binding. 150 sheep oocytes were used for this study; unless SPR interaction studies can be optimised using less zona material, this technique might not be feasible using the limited number of human oocytes available. Using either porcine or bovine oocytes would allow better information to be derived as mass spectrometry protein databases are available for these species. Using species such as rat or hamster would provide a physiological comparison to human SZB, due to their zona matrices comprising of four ZP proteins (table 4.1).

SPR technology not only has the potential to assess protein interactions between spermatozoa and zona but it could also provide information of the assembly and interaction between the four hZP proteins themselves. As previously mentioned, whether SZB is a result of the peptide sequence or in fact regulated by the peptide's carbohydrate moieties has been widely debated. Identification of potential binding partners through protein screening techniques could lead to further experiments comparing binding kinetics of glycosylated and deglycosylated proteins, analysing the importance of glycosylation patterning in SZB.

This type of investigation has the potential not only to investigate the interactions between human spermatozoa and the zona matrix, but could also be used to elucidate other molecular interaction events important for fertilisation, such as interactions between

spermatozoa and the female reproductive tract, cumulus oophorus and oocyte plasma membrane.

CHAPTER 5

General Discussion

5.1 General Discussion

Many of the key interactions around the time of human fertilisation have not been fully characterised. By utilising a multi-pronged experimental approach, this study aimed to investigate the interactions between human spermatozoa and the released ovulatory components (the COC and follicular fluid), and their relationship to pregnancy outcome.

Physiological selection

When investigating the physiological interactions of spermatozoa and the ovulatory components it is important to ensure the 'correct' sperm population is used. *In vivo* the *s*perm population is selected by their ability to penetrate the viscous barriers of the cervical mucus (Karni et al. 1971;Wolf et al. 1977), oviduct (Jansen. 1980) and the cumulus cell matrix (Dandekar et al. 1992), this study aimed to develop a better selection method which replicated the physiological environment better than existing sperm preparation techniques. Data showed that motile and progressive spermatozoa were selected from raw semen effectively, comparable to that of the existing techniques. Preliminary unpublished data from within our laboratory suggests that spermatozoa penetrating through a viscous medium may possess lower levels of DNA damage, however this would need further investigation.

The cumulus matrix and follicular fluid

The cumulus matrix and follicular fluid are the first ovulatory components that spermatozoa 'see' when they are on their final approach towards the waiting oocyte, creating a complex modulating environment.

Experiments identified higher velocity values in spermatozoa that had interacted with cumulus cells from ART patients who had a pregnancy-positive outcome. This suggests that surface receptors and/or secretory products from the cumulus cells modulate sperm motility. This correlates with studies showing that the cumulus oophorus produces modulators of sperm motility such as progesterone (Bar-Ami. 1994;Harper et al. 2004) and NO (Lewis et al. 1996;Machado-Oliveira et al. 2008). This is the first time to our knowledge that cumulus cell modulation of spermatozoa function has been reported to be indicative of pregnancy outcome. The mechanisms behind this interaction have not been fully elucidated nor has the functional role of increased sperm velocity, but it has been suggested that it may facilitate the penetrability of spermatozoa through the cumulus cell matrix and the ZP (Suarez. 2008).

Whether the increase in velocity is a universal effect caused by cumulus cells from fertile patients or the effects on sperm motility are follicle-specific, would require further investigation to determine. Differences in sperm modulation between the cumulus cells from different follicles could be a marker for good oocyte quality and therefore an increased chance of successful ART treatment. There is evidence to suggest that cumulus cell-derived markers can be used to predict pregnancy outcome and our results concur with previous studies that expression of 11 beta-hydroxysteroid dehydrogenase, an enzyme that regulates the conversion of glucocorticoids, can be predicative of pregnancy outcome (Michael et al. 1995).

Cumulus cells may have other selective and functional effects on spermatozoa. There is evidence that cumulus cells select spermatozoa based on ‘normal morphology’ (Hong et al.

2004), and levels of DNA damage (Franken and Bastiaan. 2009); this would be interesting to investigate further as high levels of DNA damage in spermatozoa have previously been associated with poor pregnancy outcome (Simon and Lewis. 2011). It has also been suggested that the COC matrix and its products are responsible for inducing the AR in spermatozoa, challenging the traditional dogma that the ZP matrix induces the AR (Siiteri et al. 1988;Bedford et al. 2004;Jin et al. 2011;Watanabe and Kondoh. 2011). There may also chemotactic effects created by products secreted by cumulus cells, aiding spermatozoa migration to the oocyte (Sun et al. 2005).

Using the modified swim-up method with cumulus or COV434 cells better replicates the physiological environment of the female reproductive tract. Such methods could prove beneficial for sperm selection for ART particularly for ICSI where current methods of spermatozoa selection are based on morphological characteristics and viability, which do not always reflect gamete quality.

The observed increase in $[Ca^{2+}]_i$ initiated by follicular fluid was not surprising given that progesterone is a known component of follicular fluid (Wen et al. 2010), and is a recognised initiator of Ca^{2+} signalling in spermatozoa (Blackmore et al. 1990;Harper et al. 2004). However the responses seen were larger than the progesterone controls, implying that other components of the follicular fluid could be causing additional $[Ca^{2+}]_i$ responses. In particular, at higher concentrations, follicular fluid elicited a novel $[Ca^{2+}]_i$ response, which has not previously been reported in response to progesterone. The differing kinetics of the initial spike may underlie physiological responses that are not yet characterised. It could be that this elevated response is analogous to the 'T-Channel' spike seen when mouse

spermatozoa are stimulated to acrosome react by ZP (Bhandari et al. 2010). Further investigation is required to assess the possible mechanisms and the functional effects on spermatozoa, examining possible calcium channel or other specific antagonists of this response, flagellar movement and AR induction.

The zona pellucida

Once spermatozoa have traversed the cumulus matrix barrier, they must bind and penetrate the ZP in order to fuse with the oocyte plasma membrane. The molecular mechanisms behind this spermatozoa-zona binding (SZB) remain elusive despite decades of investigation. Much research in this area has relied on using a mouse model; however studies have highlighted intrinsic differences between mouse and human zona matrices (Lefievre et al. 2004), calling into question the relevance of using the mouse for human fertilisation.

Unlike cumulus cells and follicular fluid, ZP is not a surplus by-product of fertility treatment and obtaining sufficient human oocytes to provide ZP material for research is difficult. The lack of human oocytes for research, and also as donor gametes for ART treatment, has led to attempts to develop *in vitro* models of oogenesis (Hubner et al. 2003;Clark et al. 2004a;Qing et al. 2007). Such a model would also have the advantage of being amenable to genetic manipulation. Although over recent years several groups have reported hESC differentiation into oocyte-like structures that express some oocyte-specific markers, we are still far off achieving the goal of a reliable and replicable method for producing human oocytes. There is recent evidence that adult stem cells can be obtained from the ovarian surface epithelium which differentiate into of oocyte-like structures (Parte et al. 2011), and germ line markers have also been identified in bone marrow of mice (Johnson et al. 2005). Whether these adult

stem cells are more useful than hESC in developing an *in vitro* oogenesis model is yet to be determined.

Many studies have used human recombinant ZP proteins as an alternative to native material and, although a useful tool, it has to be noted that there are limitations. There is still debate over the importance of native ZP glycosylation in SZB (Rankin et al. 2003;Shi et al. 2004;Williams et al. 2007;Pang et al. 2011). Caution must be taken when using rhZP proteins that, dependent upon the heterologous system used, might not necessarily replicate the native glycosylation pattern. Also questions remain over how individual rhZP proteins can accurately reflect the three dimensional structure of the ZP matrix and how they can replicate the effects that the native ZP matrix elicits in spermatozoa.

Many researchers have chased after the elusive sole zona receptor on spermatozoa; often using a biased approach focusing on a single protein for *in vitro* studies (Lopez et al. 1985;Urch and Patel. 1991), but often *in vivo* fertility remained (Baba et al. 1994;Adham et al. 1997;Asano et al. 1997; Lu and Shur. 1997). To identify new candidate receptors and to address the possibility that the ZP receptor on spermatozoa is a multimeric complex, involving several proteins with multiple low-affinity bonds (Castle. 2002;Nixon et al. 2005), and an unbiased protein screening approach is vital to establishing the proteins that may play a role in SZB.

Other animals such as the chimpanzee, Rhesus macaque, hamster and rat have all been identified as having four ZP proteins within their ZP matrices (table 4.1). These offer the opportunity of animal models more relevant for human fertilisation.

Elucidation of the interactions between human spermatozoa, the oocyte vestments and follicular fluid is a challenging field of research due to ethical and practical restrictions on using human subjects and it requires novel approaches. Elucidation of the molecular mechanisms could be of clinical relevance, leading to better treatment and diagnosis for ART patients. Improved sperm selection could be particularly useful in patients undergoing ICSI, where spermatozoa are currently selected based on morphology and viability. Markers predictive of fertilisation success expressed in cumulus cells could also aid oocyte/embryo selection. New clinical pathologies could be discovered which could provide a diagnosis for some of the 23.9% of patients with unexplained infertility (HFEA. 2008). Sequence variations in human ZP genes have already been shown to have a direct correlation with ART fertilisation success (Männikkö et al. 2005). In addition to promoting fertilisation, elucidation of key interactions critical to fertilisation success could provide targets for novel non-hormonal contraceptives.

Although further investigation is needed within this field it does appear that the ovulatory components, the COC and follicular fluid are not mere bystanders in the process of fertilisation and are critical to fertilisation success.

APPENDIX

Appendix I: Chapter 2

Appendix I. i

Supplemented Earle's Balanced Salt Solution (sEBSS)

1 mM Sodium Dihyd. Phosphate

5.4 mM Potassium Chloride

0.81 mM Magnesium Sulphate.7H2O

5.6 mM Dextrose Anhydrous

2.7 mM Sodium Pyruvate

41.8 mM DL-Lactic Acid, Sodium

5 mM Calcium Chloride.2H2O

26.2 mM Sodium Bicarbonate

85.6 mM Sodium Chloride

10 mM HEPES

sEBSS had an osmolarity of 285-295 mOsm, with pH 7.3-7.4, produced by Geneflow, Fradley, UK.

Appendix I.ii

Straight line velocity (VSL) P values

	IVF	ICSI	COV434
IVF		0.850	0.834
ICSI	0.850		0.886
COV434	0.834	0.886	

	Positive pregnancy outcome	Negative pregnancy outcome
Positive pregnancy outcome		0.086
Negative pregnancy outcome	0.086	

P values from students independent t-test relating to figure 2.6 a, b.

Appendix I.iii

Average path velocity (VAP) P values

	IVF	ICSI	COV434
IVF		0.961	0.874
ICSI	0.961		0.741
COV434	0.874	0.741	

	Positive pregnancy outcome	Negative pregnancy outcome
Positive pregnancy outcome		0.054
Negative pregnancy outcome	0.054	

P values from students independent t-test relating to figure 2.7 a, b

Appendix I.iv

Curvilinear velocity (VCL) P values

	IVF	ICSI	COV434
IVF		0.720	0.782
ICSI	0.720		0.944
COV434	0.782	0.944	

	Positive pregnancy outcome	Negative pregnancy outcome
Positive pregnancy outcome		0.211
Negative pregnancy outcome	0.211	

P values from students independent t-test relating to figure 2.8 a, b

Appendix I. v

Lateral head displacement (ALH) P values

	IVF	ICSI	COV434
IVF		0.635	0.789
ICSI	0.635		0.708
COV434	0.789	0.708	

	Positive pregnancy outcome	Negative pregnancy outcome
Positive pregnancy outcome		0.950
Negative pregnancy outcome	0.950	

P values from students independent t-test relating to figure 2.9 a, b.

Appendix I.vi

Beat cross frequency (BCF) P values

	IVF	ICSI	COV434
IVF		0.810	0.611
ICSI	0.810		0.335
COV434	0.611	0.335	

	Positive pregnancy outcome	Negative pregnancy outcome
Positive pregnancy outcome		0.06
Negative pregnancy outcome	0.06	

P values from students independent t-test relating to figure 2.10 a, b. Green boxes highlighting statistical significance, $P<0.05$.

Appendix I.vii

Sperm population responses

	IVF^{Pos} 10% (v/v)	**IVF^{Neg} 10% (v/v)**	**ICSI^{Pos} 10% (v/v)**	**ICSI^{Neg} 10% (v/v)**	**IVF^{Pos} 10% (v/v) 2nd app**	**IVF^{Pos} 50% (v/v)**	**ICSI^{Pos} 10% (v/v) 2nd app**	**ICSI^{Pos} 50% (v/v)**	**Prog (3.2 µM)**
IVF^{Pos} 10% (v/v)		0.405	0.270	0.526	0.899	0.825	0.352	1.000	0.039
IVF^{Neg} 10% (v/v)	0.405		0.491	0.522	0.415	0.386	0.949	0.405	0.691
ICSI^{Pos} 10% (v/v)	0.270	0.491		0.861	0.332	0.283	0.431	0.270	0.058
ICSI^{Neg} 10% (v/v)	0.526	0.522	0.861		0.562	0.478	0.456	0.526	0.123
IVF^{Pos} 10% (v/v) 2nd app	0.899	0.415	0.332	0.562		0.749	0.309	0.899	0.042
IVF^{Pos} 50% (v/v)	0.825	0.386	0.283	0.478	0.749		0.334	0.825	0.039
ICSI^{Pos} 10% (v/v) 2nd app	0.352	0.949	0.431	0.456	0.309	0.334		0.352	0.739
ICSI^{Pos} 50% (v/v)	1.000	0.405	0.270	0.526	0.899	0.825	0.352		0.039
Prog (3.2 µM)	0.039	0.691	0.058	0.123	0.042	0.039	0.739	0.039	

P values from students paired t-test relating to figure 2.15. Green boxes highlighting statistical significance, P<0.05.

Appendix I.viii

Quantification of human follicular fluid components

	#119ECF01	#119ECF04	#119ECF05	#119ECF06	#119ECF07	#119ECF08	#119ECF10	#119ECF11
Oestrone	118.5926	396.7556	170.637	163.7778	171.3037	143.4259	297.5778	124.8074
Oestradiol	512.989	817.3676	947.8456	846.8824	912.0956	612.4743	1705.857	554.5809
Progesterone	978.7383	4409.552	2360.979	7279.966	6776.985	16716.87	10834.14	15140.27
17-hydroxyprogesterone	2610.246	6504.997	5260.637	7444.616	6808.218	6868.412	8981.477	5567.998
Pregnenolone	453.6076	234.1456	418.7658	1092.848	557.9747	302.4367	694.9367	718.3861
17-Hydroxypregnenolone	4.98494	9.86747	20.1747	24.4006	10.54819	20.16566	24.00904	9.490964
Glucocorticoid S	0.893064	3.375723	1.765896	4.306358	1.430636	2.219653	6.927746	3.520231
Glucocorticoid E	4.476732	11.12721	6.463621	23.16123	11.03599	15.84141	28.73242	9.338035
Glucocorticoid F	28.24461	42.49506	30.45082	83.25166	46.73122	57.64213	82.63942	43.26655
Glucocorticoid B	N/A	N/A	N/A	N/A	N/A	N/A	0.305063	1.950535
Dehydroepiandrosterone	N/A	N/A	N/A	N/A	N/A	N/A	N/A	N/A
Androstenedione	336.0979	140.2448	165.2098	101.5175	54.44755	147.8776	672.3811	168.3636
Testosterone	0.854167	N/A	0.607639	N/A	N/A	N/A	5.864583	0.107639
Dihydrotestosterone	1.927586	0.786207	1.489655	N/A	1.017241	1.913793	5.075862	0.834483

Values represent nM concentrations. This work was in collaboration with Dr. Angela Taylor and Dr. Wiebke Arlt, University of Birmingham

	#119ECF16	#119ECF18	#119ECF19	#119ECF20	#119ECF21	#119ECF22	#119ECF23	#119ECF25
Oestrone	107.7333	88.69259	275.9519	112.2667	341.1444	107.6704	77.28889	290.6296
Oestradiol	558.6875	597.5735	1375.158	432.8309	1260.195	601.0772	887.1324	576.8493
Progesterone	10913.77	27863.76	19796.74	18607.8	8051.036	38077.9	14965.77	13701.41
17-hydroxyprogesterone	3270.886	4016.742	8815.08	1994.037	5877.967	7405.614	4566.279	3289.448
Pregnenolone	473.2595	1424.494	1249.146	450.981	700.1899	1655.38	922.3734	308.1646
17-Hydroxypregnenolone	25.15663	5.942771	22.25	17.62952	28.75602	8.927711	0.674699	10.23494
Glucocorticoid S	2.141618	0.867052	6.569364	0.794798	4.482659	2.578035	2.442197	1.855491
Glucocorticoid E	18.94589	15.21609	18.43746	6.604525	12.88567	16.6207	-3.1459	15.59509
Glucocorticoid F	58.50188	43.68508	39.15042	24.28032	62.38185	47.94864	N/A	40.453
Glucocorticoid B	N/A	N/A	N/A	N/A	N/A	N/A	N/A	N/A
Dehydroepiandrosterone	13.55556	N/A	N/A	N/A	9.510417	N/A	N/A	N/A
Androstenedione	1313.448	47.77622	154.3042	74.53497	2003.748	45.48252	477.601	95.42657
Testosterone	4.052083	N/A	0.006944	N/A	17.94444	N/A	0.934028	N/A
Dihydrotestosterone	1.568966	3.786207	1.924138	0.424138	2.155172	2.941379	3.086207	1.7

Values represent nM concentrations. This work was in collaboration with Dr. Angela Taylor and Dr. Wiebke Arlt, University of Birmingham.

Appendix II: Chapter 4

Appendix II.i

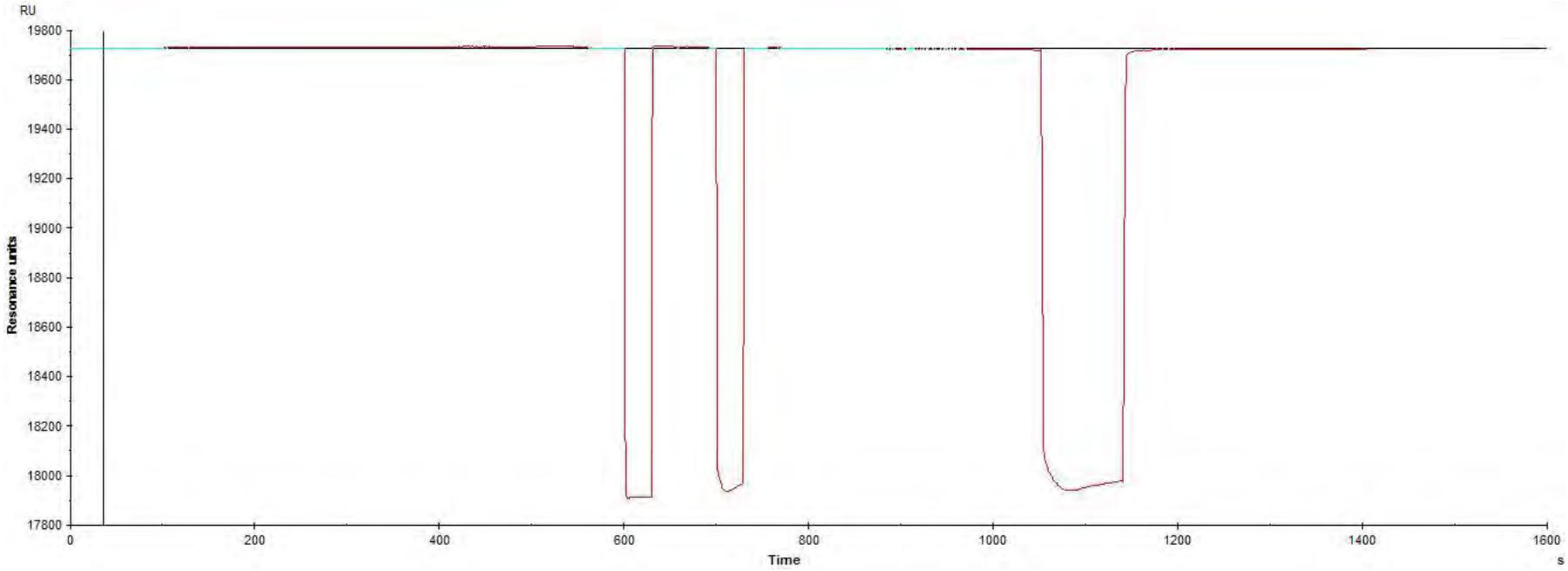

BIAcore sensogram showing attempted removal of Bac-rhZP2, with three rounds of 10mM Glycine pH 2.2, two successive rounds of 15 µl at a flow rate of 30 µl/min, followed by one round of 15 µl at a flow rate of 10 µl/min. RU levels stayed at 19727.8, above pre-bound Bac-rhZP2 RU levels.

Appendix II.ii

pcDNA4 HisMax B vector map

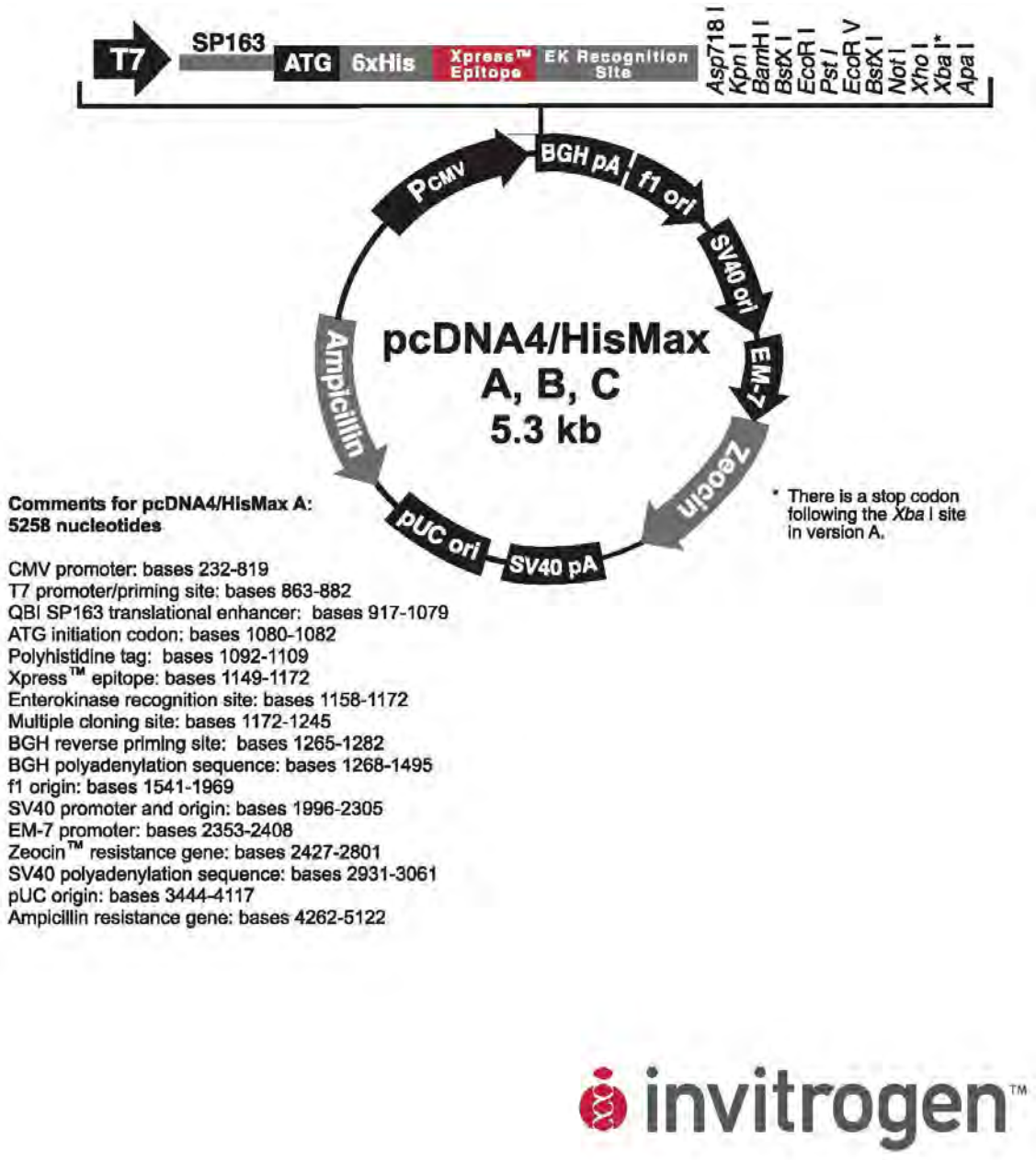

(Invitrogen. 2011c)

Appendix II.iii

pcDNA4 HisMax B polylinker

Invitrogen™
life technologies

pcDNA4/HisMax© B

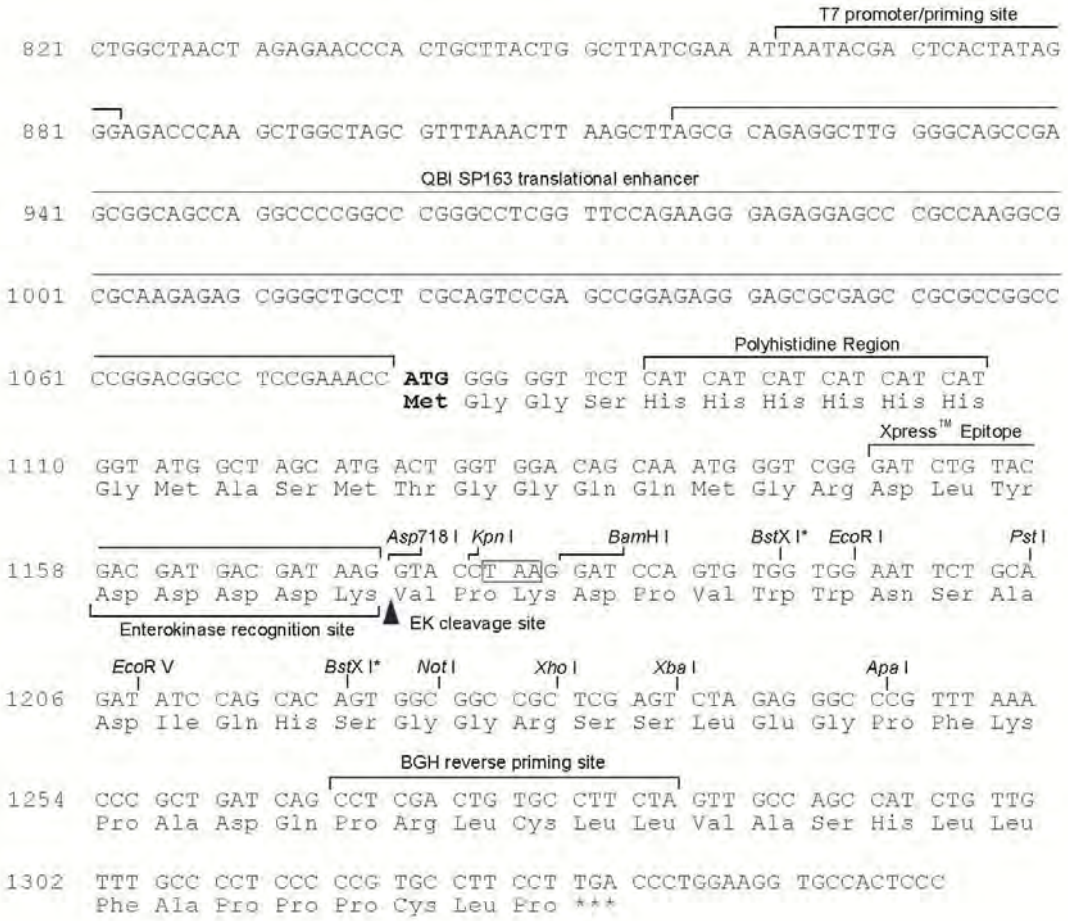

(Invitrogen. 2011a)

Appendix II.iv

rhZP3 pcDNA4 HisMax B sequence

GACGGATCGGGAGATCTCCCGATCCCCTATGGTCGACTCTCAGTACAATCTGCTCTGATGCCGCATAGTT
AAGCCAGTATCTGCTCCCTGCTTGTGTGTTGGAGGTCGCTGAGTAGTGCGCGAGCAAAATTTAAGCTACA
ACAAGGCAAGGCTTGACCGACAATTGCATGAAGAATCTGCTTAGGGTTAGGCGTTTTGCGCTGCTTCGCG
ATGTACGGGCCAGATATACGCGTTGACATTGATTATTGACTAGTTATTAATAGTAATCAATTACGGGGTC
ATTAGTTCATAGCCCATATATGGAGTTCCGCGTTACATAACTTACGGTAAATGGCCCGCCTGGCTGACCG
CCCAACGACCCCCGCCCATTGACGTCAATAATGACGTATGTTCCCATAGTAACGCCAATAGGGACTTTCC
ATTGACGTCAATGGGTGGACTATTTACGGTAAACTGCCCACTTGGCAGTACATCAAGTGTATCATATGCC
AAGTACGCCCCCTATTGACGTCAATGACGGTAAATGGCCCGCCTGGCATTATGCCCAGTACATGACCTTA
TGGGACTTTCCTACTTGGCAGTACATCTACGTATTAGTCATCGCTATTACCATGGTGATGCGGTTTTGGC
AGTACATCAATGGGCGTGGATAGCGGTTTGACTCACGGGGATTTCCAAGTCTCCACCCCATTGACGTCAA
TGGGAGTTTGTTTTGGCACCAAAATCAACGGGACTTTCCAAAATGTCGTAACAACTCCGCCCCATTGACG
CAAATGGGCGGTAGGCGTGTACGGTGGGAGGTCTATATAAGCAGAGCTCTCTGGCTAACTAGAGAACCCA
CTGCTTACTGGCTTATCGAAATTAATACGACTCACTATAGGGAGACCCAAGCTGGCTAGCGTTTAAACTT
AAGCTTAGCGCAGAGGCTTGGGGCAGCCGAGCGGCAGCCAGGCCCCGGCCCGGGCCTCGGTTCCAGAAGG
GAGAGGAGCCCGCCAAGGCGCGCAAGAGAGCGGGCTGCCTCGCAGTCCGAGCCGGAGAGGGAGCGCGAGC
CGCGCCGGCCCCGGACGGCCTCCGAAACCATGGGGGGTTCTCATCATCATCATCATCATGGTATGGCTAG
CATGACTGGTGGACAGCAAATGGGTCGGGATCTGTACGACGATGACGATAAGGTACCTAAGGATCCAGTG
TGGTGGAATTCTGCAGATCAACCCCTCTGGCTCTTGCAGGGTGGAGCCAGCCATCCTGAGACGTCCGTAC
AGCCCGTACTGGTGGAGTGTCAGGAGGCCACTCTGATGGTCATGGTCAGCAAAGACCTTTTTGGCACCGG
GAAGCTCATCAGGGCTGCTGACCTCACCTTGGGCCCAGAGGCCTGTGAGCCTCTGGTCTCCATGGACACA
GAAGATGTGGTCAGGTTTGAGGTTGGACTCCACGAGTGTGGCAACAGCATGCAGGTAACTGACGATGCCC
TGGTGTACAGCACCTTCCTGCTCCATGACCCCCGCCCCGTGGGAAACCTGTCCATCGTGAGGACTAACCG
CGCAGAGATTCCCATCGAGTGCCGCTACCCCAGGCAGGGCAATGTGAGCAGCCAGGCCATCCTGCCCACC
TGGTTGCCCTTCAGGACCACGGTGTTCTCAGAGGAGAAGCTGACTTTCTCTCTGCGTCTGATGGAGGAGA
ACTGGAACGCTGAGAAGAGGTCCCCCACCTTCCACCTGGGAGATGCAGCCCACCTCCAGGCAGAAATCCA
CACTGGCAGCCACGTGCCACTGCGGTTGTTTGTGGACCACTGCGTGGCCACACCGACACCAGACCAGAAT
GCCTCCCCTTATCACACCATCGTGGACTTCCATGGCTGTCTTGTCGACGGTCTCACTGATGCCTCTTCTG
CATTCAAAGTTCCTCGACCCGGGCCAGATACACTCCAGTTCACAGTGGATGTCTTCCACTTTGCTAATGA
CTCCAGAAACATGATATACATCACCTGCCACCTGAAGGTCACCCTAGCTGAGCAGGACCCAGATGAACTC
AACAAGGCCTGTTCCTTCAGCAAGCCTTCCAACAGCTGGTTCCCAGTGGAAGGCCCGGCTGACATCTGTC
AATGCTGTAACAAAGGTGACTGTGGCACTCCAAGCCATTCCAGGAGGCAGCCTCATGTCATGAGCCAGTG
GTCCAGGTCTGCTTCCCGTAACCGCAGGCATGTGACAGAAGAAGCAGATGTCACCGTGGGGCCACTGATC
TTCCTGGACAGGAGGGGTGACCATGAAGTAGAGCAGTGGGCTTTGCCTTCTGACACCTCAGTGGTGCTGC
TGGGCGTAGGCCTGGCTGTGGTGGTGTCCCTGACTCTGACTGCTGTTATCCTGGTTCTCACCAGGAGGTG
TCGCACTGCCTCCCACCCTGTGTCTGCTTCCGAATAAATCCAGCACAGTGGCGGCCGCTCGAGTCTAGAG
GGCCCGTTTAAACCCGCTGATCAGCCTCGACTGTGCCTTCTAGTTGCCAGCCATCTGTTGTTTGCCCCTC
CCCCGTGCCTTCCTTGACCCTGGAAGGTGCCACTCCCACTGTCCTTTCCTAATAAAATGAGGAAATTGCA
TCGCATTGTCTGAGTAGGTGTCATTCTATTCTGGGGGGTGGGGTGGGGCAGGACAGCAAGGGGGAGGATT
GGGAAGACAATAGCAGGCATGCTGGGGATGCGGTGGGCTCTATGGCTTCTGAGGCGGAAAGAACCAGCTG
GGGCTCTAGGGGGTATCCCCACGCGCCCTGTAGCGGCGCATTAAGCGCGGCGGGTGTGGTGGTTACGCGC
AGCGTGACCGCTACACTTGCCAGCGCCCTAGCGCCCGCTCCTTTCGCTTTCTTCCCTTCCTTTCTCGCCA
CGTTCGCCGGCTTTCCCCGTCAAGCTCTAAATCGGGGCATCCCTTTAGGGTTCCGATTTAGTGCTTTACG
GCACCTCGACCCCAAAAAACTTGATTAGGGTGATGGTTCACGTAGTGGGCCATCGCCCTGATAGACGGTT
TTTCGCCCTTTGACGTTGGAGTCCACGTTCTTTAATAGTGGACTCTTGTTCCAAACTGGAACAACACTCA
ACCCTATCTCGGTCTATTCTTTTGATTTATAAGGGATTTTGGGGATTTCGGCCTATTGGTTAAAAAATGA
GCTGATTTAACAAAAATTTAACGCGAATTAATTCTGTGGAATGTGTGTCAGTTAGGGTGTGGAAAGTCCC
CAGGCTCCCCAGGCAGGCAGAAGTATGCAAAGCATGCATCTCAATTAGTCAGCAACCAGGTGTGGAAAGT
CCCCAGGCTCCCCAGCAGGCAGAAGTATGCAAAGCATGCATCTCAATTAGTCAGCAACCATAGTCCCGCC
CCTAACTCCGCCCATCCCGCCCCTAACTCCGCCCAGTTCCGCCCATTCTCCGCCCCATGGCTGACTAATT
TTTTTTATTTATGCAGAGGCCGAGGCCGCCTCTGCCTCTGAGCTATTCCAGAAGTAGTGAGGAGGCTTTT
TTGGAGGCCTAGGCTTTTGCAAAAAGCTCCCGGGAGCTTGTATATCCATTTTCGGATCTGATCAGCACGT
GTTGACAATTAATCATCGGCATAGTATATCGGCATAGTATAATACGACAAGGTGAGGAACTAAACCATGG
CCAAGTTGACCAGTGCCGTTCCGGTGCTCACCGCGCGCGACGTCGCCGGAGCGGTCGAGTTCTGGACCGA

CCGGCTCGGGTTCTCCCGGGACTTCGTGGAGGACGACTTCGCCGGTGTGGTCCGGGACGACGTGACCCTG
TTCATCAGCGCGGTCCAGGACCAGGTGGTGCCGGACAACACCCTGGCCTGGGTGTGGGTGCGCGGCCTGG
ACGAGCTGTACGCCGAGTGGTCGGAGGTCGTGTCCACGAACTTCCGGGACGCCTCCGGGCCGGCCATGAC
CGAGATCGGCGAGCAGCCGTGGGGGCGGGAGTTCGCCCTGCGCGACCCGGCCGGCAACTGCGTGCACTTC
GTGGCCGAGGAGCAGGACTGACACGTGCTACGAGATTTCGATTCCACCGCCGCCTTCTATGAAAGGTTGG
GCTTCGGAATCGTTTTCCGGGACGCCGGCTGGATGATCCTCCAGCGCGGGGATCTCATGCTGGAGTTCTT
CGCCCACCCCAACTTGTTTATTGCAGCTTATAATGGTTACAAATAAAGCAATAGCATCACAAATTTCACA
AATAAAGCATTTTTTTCACTGCATTCTAGTTGTGGTTTGTCCAAACTCATCAATGTATCTTATCATGTCT
GTATACCGTCGACCTCTAGCTAGAGCTTGGCGTAATCATGGTCATAGCTGTTTCCTGTGTGAAATTGTTA
TCCGCTCACAATTCCACACAACATACGAGCCGGAAGCATAAAGTGTAAAGCCTGGGGTGCCTAATGAGTG
AGCTAACTCACATTAATTGCGTTGCGCTCACTGCCCGCTTTCCAGTCGGGAAACCTGTCGTGCCAGCTGC
ATTAATGAATCGGCCAACGCGCGGGGAGAGGCGGTTTGCGTATTGGGCGCTCTTCCGCTTCCTCGCTCAC
TGACTCGCTGCGCTCGGTCGTTCGGCTGCGGCGAGCGGTATCAGCTCACTCAAAGGCGGTAATACGGTTA
TCCACAGAATCAGGGGATAACGCAGGAAAGAACATGTGAGCAAAAGGCCAGCAAAAGGCCAGGAACCGTA
AAAAGGCCGCGTTGCTGGCGTTTTTCCATAGGCTCCGCCCCCCTGACGAGCATCACAAAAATCGACGCTC
AAGTCAGAGGTGGCGAAACCCGACAGGACTATAAAGATACCAGGCGTTTCCCCCTGGAAGCTCCCTCGTG
CGCTCTCCTGTTCCGACCCTGCCGCTTACCGGATACCTGTCCGCCTTTCTCCCTTCGGGAAGCGTGGCGC
TTTCTCAATGCTCACGCTGTAGGTATCTCAGTTCGGTGTAGGTCGTTCGCTCCAAGCTGGGCTGTGTGCA
CGAACCCCCCGTTCAGCCCGACCGCTGCGCCTTATCCGGTAACTATCGTCTTGAGTCCAACCCGGTAAGA
CACGACTTATCGCCACTGGCAGCAGCCACTGGTAACAGGATTAGCAGAGCGAGGTATGTAGGCGGTGCTA
CAGAGTTCTTGAAGTGGTGGCCTAACTACGGCTACACTAGAAGGACAGTATTTGGTATCTGCGCTCTGCT
GAAGCCAGTTACCTTCGGAAAAAGAGTTGGTAGCTCTTGATCCGGCAAACAAACCACCGCTGGTAGCGGT
GGTTTTTTTGTTTGCAAGCAGCAGATTACGCGCAGAAAAAAAGGATCTCAAGAAGATCCTTTGATCTTTT
CTACGGGGTCTGACGCTCAGTGGAACGAAAACTCACGTTAAGGGATTTTGGTCATGAGATTATCAAAAAG
GATCTTCACCTAGATCCTTTTAAATTAAAAATGAAGTTTTAAATCAATCTAAAGTATATATGAGTAAACT
TGGTCTGACAGTTACCAATGCTTAATCAGTGAGGCACCTATCTCAGCGATCTGTCTATTTCGTTCATCCA
TAGTTGCCTGACTCCCCGTCGTGTAGATAACTACGATACGGGAGGGCTTACCATCTGGCCCCAGTGCTGC
AATGATACCGCGAGACCCACGCTCACCGGCTCCAGATTTATCAGCAATAAACCAGCCAGCCGGAAGGGCC
GAGCGCAGAAGTGGTCCTGCAACTTTATCCGCCTCCATCCAGTCTATTAATTGTTGCCGGGAAGCTAGAG
TAAGTAGTTCGCCAGTTAATAGTTTGCGCAACGTTGTTGCCATTGCTACAGGCATCGTGGTGTCACGCTC
GTCGTTTGGTATGGCTTCATTCAGCTCCGGTTCCCAACGATCAAGGCGAGTTACATGATCCCCCATGTTG
TGCAAAAAAGCGGTTAGCTCCTTCGGTCCTCCGATCGTTGTCAGAAGTAAGTTGGCCGCAGTGTTATCAC
TCATGGTTATGGCAGCACTGCATAATTCTCTTACTGTCATGCCATCCGTAAGATGCTTTTCTGTGACTGG
TGAGTACTCAACCAAGTCATTCTGAGAATAGTGTATGCGGCGACCGAGTTGCTCTTGCCCGGCGTCAATA
CGGGATAATACCGCGCCACATAGCAGAACTTTAAAAGTGCTCATCATTGGAAAACGTTCTTCGGGGCGAA
AACTCTCAAGGATCTTACCGCTGTTGAGATCCAGTTCGATGTAACCCACTCGTGCACCCAACTGATCTTC
AGCATCTTTTACTTTCACCAGCGTTTCTGGGTGAGCAAAAACAGGAAGGCAAAATGCCGCAAAAAAGGGA
ATAAGGGCGACACGGAAATGTTGAATACTCATACTCTTCCTTTTTCAATATTATTGAAGCATTTATCAGG
GTTATTGTCTCATGAGCGGATACATATTTGAATGTATTTAGAAAAATAAACAAATAGGGGTTCCGCGCAC
ATTTCCCCGAAAAGTGCCACCTGACGTC

Black text denotes pcDNA4 His Max B DNA sequence from (Invitrogen. 2011b), red text denotes human ZP3 sequence.

Appendix II.v

Sheep zona

Protein	Peptides	Score	Protein	Peptides	Score	Protein	Peptides	Score	Protein	Peptides	Score
H4_MOUSE	6	45.6	**LONF1_HUMAN**	2	1.4	**HBB_SUNMU**	1	15.1	**TRIMM_HUMAN**	2	5.2
DCD_HUMAN	5	28.2	**DYH1_HUMAN**	1	0.5	**LASP1_MOUSE**	2	7.6	**TET1_HUMAN**	1	1.4
CASA1_BOVIN	4	17.8	**UBP54_MOUSE**	1	1.8	**NAP1_RAT**	2	5.1	**DLG5_HUMAN**	1	1.1
H33_PONAB	4	24.3	**PK3CA_HUMAN**	3	2.2	**PSMD9_RAT**	2	9.9	**MRRP1_RAT**	2	5.8
H2AJ_HUMAN	3	20.9	**CH10_HUMAN**	1	23.5	**KLH26_MOUSE**	1	2.3	**BIRC6_HUMAN**	1	0.4
GFAP_BOVIN	3	6.8	**CCD52_PONAB**	2	2.7	**K1C9_RAT**	1	3.6	**YD026_HUMAN**	1	2.7
ZP3_BOVIN	3	9.7	**NUMA1_HUMAN**	2	1.5	**PAF_RAT**	1	16.4	**SPA2L_HUMAN**	1	3.5
CTRO_MOUSE	3	2.5	**MCM6_MOUSE**	2	2.1	**METH_HUMAN**	1	1.3	**NSUN6_HUMAN**	1	6.4
H2AV_MOUSE	3	23.4	**SPTN5_HUMAN**	2	0.4	**CCD71_MOUSE**	2	3.7	**SAMD7_MOUSE**	1	11.1
H2B2E_PONAB	3	18.3	**ITPR3_HUMAN**	2	0.4	**ZKSC4_HUMAN**	1	6.1	**PHF20_HUMAN**	1	1.4
TITIN_HUMAN	2	0.2	**CKAP5_HUMAN**	1	1.3	**CELR2_RAT**	1	1.3	**TMPS7_HUMAN**	1	2.2
NSD2_MOUSE	3	2.1	**ARFG3_MOUSE**	1	2.9	**BANK1_MOUSE**	2	2.3	**RPA34_HUMAN**	1	1.6
ASPM_SHEEP	2	1.6	**CSTFT_MOUSE**	2	4.3	**LMO7_HUMAN**	1	1.4	**MMP20_PIG**	1	5.4
BPAEA_HUMAN	3	1.2	**POL2_MOUSE**	2	1.2	**LPHN3_RAT**	2	1.2	**CE152_HUMAN**	1	1.4
ZP4_BOVIN	1	2.2	**HMCN1_HUMAN**	1	0.9	**LCMT2_HUMAN**	1	2.3	**E41L1_HUMAN**	1	3.2
TITIN_MOUSE	3	0.1	**DEN5B_HUMAN**	1	2.8	**LAMB2_MOUSE**	2	1.4	**PLD1_RAT**	1	2.0
DYH17_MOUSE	2	1.3	**CJ079_HUMAN**	1	1.6	**MYOM3_MOUSE**	2	1.4	**CROCC_HUMAN**	1	1.0
ARI2_MOUSE	2	6.5	**CP250_HUMAN**	1	0.8	**PTHB1_HUMAN**	1	3.6	**ADAD1_HUMAN**	1	1.6
SRRM2_MOUSE	2	1.8	**FSIP2_HUMAN**	1	1.2	**ADCYA_RAT**	2	0.7	**CO039_MOUSE**	1	2.2
H11_BOVIN	2	23.1	**CAC1A_RAT**	2	0.5	**NLRC3_HUMAN**	1	2.2	**Z518A_RAT**	1	0.9
DYH11_HUMAN	1	0.8	**NR1D1_MOUSE**	1	5.7	**ARHGB_RAT**	1	1.0	**SODE_HUMAN**	1	12.5
APOA1_BOVIN	1	8.3	**IGS10_MOUSE**	1	1.3	**EIF3C_BOVIN**	2	2.0	**WDR33_HUMAN**	1	2.0
RHG05_MOUSE	3	1.4	**DYSF_MOUSE**	1	1.2	**GEMI5_MOUSE**	1	1.8	**IFIX_HUMAN**	1	5.9
SYNE1_HUMAN	2	0.4	**SLIT1_MOUSE**	2	1.8	**ZN407_HUMAN**	1	1.5	**CD244_MOUSE**	1	6.3
SYNC_HUMAN	2	6.2	**TRFL_HUMAN**	1	2.4	**RS30_HUMAN**	1	10.2	**BAI1_HUMAN**	1	1.3
SYRC_CRILO	2	3.6	**CM038_MOUSE**	2	8.4	**H90B4_HUMAN**	1	6.1	**IF4G3_MOUSE**	1	1.7
GNN_RAT	1	1.8	**APC1_MOUSE**	2	1.2	**MDR3_MOUSE**	1	2.2	**MN1_HUMAN**	1	1.7
KDM3A_MOUSE	2	1.1	**AP4M1_HUMAN**	2	4.9	**ROR2_HUMAN**	1	3.1	**RNF14_MOUSE**	1	3.9

Protein	Peptides	Score	Protein	Peptides	Score	Protein	Peptides	Score	Protein	Peptides	Score
NRX1A_MOUSE	1	2.0	**CFAH_HUMAN**	1	0.8	**C2TA_HUMAN**	1	2.1	**APBA2_PONAB**	1	1.1
ACE_RAT	1	2.3	**ZFHX3_HUMAN**	1	0.3	**ZBT38_RAT**	1	0.9	**CMYA5_HUMAN**	1	0.5
NKTR_MOUSE	1	0.8	**CE164_HUMAN**	1	0.7	**TRI13_MOUSE**	1	3.2	**PLMN_MACEU**	1	2.2
EIF3D_MOUSE	1	3.8	**PER1_RAT**	1	0.8	**LCN10_MOUSE**	1	3.8	**TLR8_HUMAN**	1	1.2
S10A8_HUMAN	1	11.8	**SCN4A_MOUSE**	1	0.7	**HOT_MOUSE**	1	4.1	**ANO9_MOUSE**	1	1.3
TNR17_HUMAN	1	8.7	**NWD1_MOUSE**	1	0.6	**PDE11_MOUSE**	1	1.3	**KCNB2_HUMAN**	1	1.2
ASXL3_MOUSE	1	1.2	**TMM9B_HUMAN**	1	3.0	**K1C23_HUMAN**	1	2.8	**GRAB_MOUSE**	1	4.0
SIA4B_RAT	1	1.7	**AA2AR_HORSE**	1	4.6	**UBN1_MOUSE**	1	0.7	**TBCD1_BOVIN**	1	2.7
ZN512_MOUSE	1	2.1	**ADA19_MOUSE**	1	1.4	**ATL1_MOUSE**	1	2.9	**TRAF3_HUMAN**	1	2.6
FETUA_BOVIN	1	2.8	**FA18B_MOUSE**	1	4.4	**NOTC1_RAT**	1	0.6	**AGRIN_MOUSE**	1	0.6
PCGF1_RAT	1	5.3	**RBM5_MOUSE**	1	1.2	**TRM2_MOUSE**	1	2.6	**CNDH2_BOVIN**	1	1.6
RN19B_HUMAN	1	1.1	**CENPS_BOVIN**	1	5.1	**SECR_BOVIN**	1	22.2	**HSP74_RAT**	1	1.1
IPO5_MOUSE	1	2.1	**GP176_RAT**	1	2.5	**INHBA_MOUSE**	1	4.2	**ZN391_HUMAN**	1	4.5
CE192_HUMAN	1	0.5	**MYO1G_MOUSE**	1	1.2	**ESX1_HUMAN**	1	3.7	**AT1A1_PIG**	1	0.8
KBTB8_MOUSE	1	2.5	**TLR13_MOUSE**	1	1.5	**LACB2_RAT**	1	4.2	**DDHD1_MOUSE**	1	1.8
M3K12_MOUSE	1	0.7	**WNT1_HUMAN**	1	2.2	**NCOA6_RAT**	1	3.3	**CP048_BOVIN**	1	4.3
NPA1P_HUMAN	1	0.4	**IMPA3_MOUSE**	1	2.2	**VIP_CANFA**	1	21.4	**URP2_MOUSE**	1	1.2
CASA2_BOVIN	1	5.0	**FUT10_BOVIN**	1	2.3	**PEX5_HUMAN**	1	2.8	**RNAS1_NIVCR**	1	14.8
ZFP57_HUMAN	1	3.1	**MX2_SHEEP**	1	2.0	**CP21A_MOUSE**	1	3.5	**ZNRF2_HUMAN**	1	4.1
CCND1_CANFA	1	4.7	**NKD2_HUMAN**	1	4.0	**XPOT_MOUSE**	1	1.7	**CI068_RAT**	1	2.0
ANKR6_MOUSE	1	2.2	**MS3L2_HUMAN**	1	2.5	**OSBL8_HUMAN**	1	1.3	**PHTNS_PIG**	1	1.3
SPX3_BOVIN	1	1.6	**GDF8_TAUDE**	1	2.7	**GP152_HUMAN**	1	1.3	**CB088_HUMAN**	1	20.0
MESD_MOUSE	1	2.2	**YETS4_HUMAN**	1	4.4	**ABCA3_MOUSE**	1	0.9	**UBP43_MOUSE**	1	0.8
QRSL1_MACFA	1	2.7	**RBBP5_MOUSE**	1	2.0	**ERF3B_PONAB**	1	1.6	**DEF2_RABIT**	1	23.5
ID1_HUMAN	1	7.1	**CP042_MOUSE**	1	5.3	**TF2LX_PAPHA**	1	5.5	**ZN467_HUMAN**	1	2.7
ATP4B_HUMAN	1	6.5	**SUNC1_BOVIN**	1	3.1	**P2RY2_HUMAN**	1	3.4	**COQ4_BOVIN**	1	7.9
HECAM_BOVIN	1	1.7	**UHRF2_HUMAN**	1	1.0	**OSBL6_HUMAN**	1	0.9	**GSCR2_HUMAN**	1	1.5
ES8L2_MOUSE	1	1.1	**FR1L5_HUMAN**	1	0.4	**SPKAP_RAT**	1	0.5	**SCRN3_HUMAN**	1	3.5
SPY1_HUMAN	1	4.4	**INAR1_BOVIN**	1	2.9	**RN219_HUMAN**	1	1.9	**REST_HUMAN**	1	0.7

Protein	Peptides	Score	Protein	Peptides	Score	Protein	Peptides	Score
GALT8_HUMAN	1	3.3	**MYD88_HUMAN**	1	3.7	**SBNO1_RAT**	1	0.7
HXD1_MOUSE	1	4.6	**AP2A_SHEEP**	1	2.6	**TFB2M_MOUSE**	1	3.8
CAH4_RABIT	1	2.9	**ELFN1_MOUSE**	1	2.1	**ZN251_HUMAN**	1	1.1
RENBP_MOUSE	1	1.4	**TFP11_RABIT**	1	1.0	**LPIN2_HUMAN**	1	1.8
GP158_HUMAN	1	0.7	**F161A_MOUSE**	1	1.8	**UBE2C_BOVIN**	1	7.8
CP2E1_BOVIN	1	2.4	**EFR3A_MOUSE**	1	1.8	**ZN414_RAT**	1	3.0
ZCHC8_PONAB	1	2.1	**NDRG4_HUMAN**	1	3.7	**FOG1_HUMAN**	1	2.1
RBL2_MOUSE	1	0.6	**T2AG_MOUSE**	1	10.1	**ROMO1_PIG**	1	30.4
BIRC5_BOVIN	1	12.7	**P4R3A_MOUSE**	1	1.2	**EHBP1_HUMAN**	1	0.7
TVB5_MOUSE	1	14.8	**TAF9_BOVIN**	1	5.3	**CC075_MOUSE**	1	8.6
DIP2B_MOUSE	1	0.6	**EID3_BOVIN**	1	4.0	**LRP2_RAT**	1	0.3
S46A3_HUMAN	1	4.6	**GASP2_MOUSE**	1	1.0	**VTDB_MOUSE**	1	4.2
GPN1_MOUSE	1	4.6	**RHG07_MOUSE**	1	1.3	**ARRD3_BOVIN**	1	4.8
EMAL5_RAT	1	0.5	**VPS35_HUMAN**	1	1.3	**PELO_MOUSE**	1	6.2
ACTBL_HUMAN	1	4.8	**TLR2_HORSE**	1	1.4	**ENPP2_RAT**	1	1.5
PCSK5_MOUSE	1	1.1	**BMCC1_HUMAN**	1	0.5	**PAPOA_MOUSE**	1	1.9
ABCA2_HUMAN	1	0.6	**S41A1_HUMAN**	1	3.5	**MPRB_MOUSE**	1	2.0
GTPB3_MOUSE	1	4.7	**GP124_HUMAN**	1	0.8	**THTPA_MACFA**	1	10.0
ANR40_HUMAN	1	2.2	**ZDBF2_HUMAN**	1	0.5	**TDRD5_MOUSE**	2	2.3
SIN1_MOUSE	1	1.0	**ASPP2_MOUSE**	1	1.1	**WDR44_RAT**	1	2.3
RCBT1_HUMAN	1	2.4	**KDM6A_MOUSE**	1	0.9	**TLR9_PIG**	1	1.3
PTN6_MOUSE	1	2.7	**CC110_MOUSE**	1	1.7	**VWA3A_RAT**	1	4.6
ESRP1_HUMAN	1	2.1	**CHERP_HUMAN**	1	0.5			
SCEL_HUMAN	1	2.2	**YK006_HUMAN**	1	3.5			
HBAZ_HORSE	1	7.0	**TRI45_MOUSE**	1	1.6			
CC129_HUMAN	1	1.9	**PKHA5_HUMAN**	1	1.3			
LMTK3_MOUSE	1	0.8	**YD002_HUMAN**	1	2.5			
EFR3B_MOUSE	1	1.5	**MTND_RAT**	1	8.9			
BMP3B_BOVIN	1	2.3	**GFPT1_RAT**	1	3.4			

Appendix II.vi

Sperm elute

Protein	Peptides	Score	Protein	Peptides	Score	Protein	Peptides	Score	Protein	Peptides	Score
BPAEA_HUMAN	2	1.3	**TRY3_RAT**	2	11.3	**F132B_HUMAN**	1	3.1	**KIFC3_MOUSE**	1	2.5
RBP2_HUMAN	2	1.3	**NEBU_HUMAN**	2	0.4	**PKN3_HUMAN**	2	3.5	**CPZIP_MOUSE**	1	3.4
ASPM_MACFA	2	1.1	**NUMA1_HUMAN**	2	1.0	**GG6L6_HUMAN**	2	2.4	**PTN11_HUMAN**	1	2.5
SYNE1_HUMAN	1	0.6	**CENPF_HUMAN**	1	1.6	**TBX18_MOUSE**	2	2.9	**MIDA_BOVIN**	1	4.8
S10A8_HUMAN	1	11.8	**APOB_RAT**	1	0.5	**MRCKB_HUMAN**	1	1.5	**NASP_HUMAN**	1	2.7
SYNE2_HUMAN	1	0.8	**NPT2A_SHEEP**	2	3.4	**ZN252_CANFA**	1	1.7	**PININ_BOVIN**	1	3.4
TARA_HUMAN	2	1.6	**LTBP4_HUMAN**	1	1.8	**FEN1_MOUSE**	1	5.3	**PYC_MOUSE**	1	1.5
UBP38_MOUSE	2	2.4	**MYH1_HUMAN**	1	1.6	**PCDG7_PANTR**	1	2.3	**IGEB_MOUSE**	1	3.2
FBN2_HUMAN	2	2.7	**EP400_HUMAN**	2	1.1	**XIRP2_RAT**	2	0.6	**SMC1B_HUMAN**	1	1.6
DYH1_RAT	1	0.6	**SLN13_HUMAN**	1	3.0	**PK3CA_HUMAN**	2	1.2	**ZN296_HUMAN**	1	3.6
ABCF1_MOUSE	1	1.3	**PRGR_ATEPA**	1	2.5	**HORN_HUMAN**	1	1.3	**DIDO1_HUMAN**	1	1.4
MACF1_HUMAN	2	0.7	**SPTCS_HUMAN**	2	1.5	**ATS15_MOUSE**	1	2.5	**SAC1_MOUSE**	1	2.7
SYNJ1_BOVIN	2	2.3	**ASPM_MOUSE**	1	0.9	**PLAK_MOUSE**	1	3.1	**SRBD1_PONAB**	1	2.0
PDE1A_HUMAN	2	4.3	**ANKF1_HUMAN**	2	4.2	**TIM_MOUSE**	1	2.1	**CR058_HUMAN**	1	4.3
OPTN_PONAB	3	3.6	**CASA2_BOVIN**	2	8.1	**MASTL_MOUSE**	1	1.3	**BIG1_BOVIN**	1	1.5
XAF1_BOVIN	1	2.7	**TIAM2_MOUSE**	1	0.6	**PCLO_MOUSE**	1	0.6	**IRF3_PIG**	1	3.8
MTL5_RAT	3	4.2	**RPP38_BOVIN**	3	13.5	**CP4B1_RAT**	2	4.7	**DOP2_HUMAN**	1	0.6
CHD2_HUMAN	3	1.0	**MYH9_RAT**	2	1.2	**FA5_PIG**	2	1.0	**OAS3_HUMAN**	1	1.7
KIF11_HUMAN	1	2.5	**ASAP2_MOUSE**	2	1.4	**EWS_MOUSE**	1	2.9	**BRI3_BOVIN**	1	7.3
AGRIN_MOUSE	3	1.4	**ZN567_HUMAN**	2	2.2	**TRIMM_HUMAN**	1	3.4	**LIN9_MACFA**	1	4.1
THAP4_RAT	1	4.0	**ZN492_HUMAN**	1	4.3	**ATS12_MOUSE**	1	0.8	**F75A6_HUMAN**	1	2.0
DNJC2_RAT	2	3.5	**ANR50_HUMAN**	1	1.2	**ASPM_CANFA**	1	0.8	**HAUS5_MOUSE**	1	1.9
TTLL5_CERAE	1	0.8	**PPIP1_MOUSE**	1	6.3	**MYOME_HUMAN**	2	1.4	**ASPM_BOVIN**	1	0.4
SLX4_HUMAN	2	2.0	**LRRN1_MOUSE**	2	2.2	**ATS19_HUMAN**	1	1.3	**CI117_RAT**	1	1.3
CALL5_HUMAN	2	6.2	**MT3_MACFA**	1	29.4	**HRT7A_BOVIN**	1	1.0	**FURIN_BOVIN**	1	4.9
RBM44_MOUSE	2	3.1	**CBPC2_MOUSE**	1	2.8	**CA189_HUMAN**	1	27.7	**SPT5H_MOUSE**	1	2.8
SCFD1_RAT	2	4.4	**CKAP4_HUMAN**	2	5.3	**GPSM3_HUMAN**	1	18.1	**MK06_RAT**	1	2.6
CKP2L_BOVIN	2	5.1	**CCD33_MOUSE**	1	1.3	**SVEP1_HUMAN**	1	0.6	**DSCL1_HUMAN**	1	0.9

Protein	Peptides	Score	Protein	Peptides	Score	Protein	Peptides	Score	Protein	Peptides	Score
PKHG5_MOUSE	1	2.4	KRI1_HUMAN	1	2.1	TM2D2_RAT	1	3.3	SOSSC_MOUSE	1	12.5
DYH6_HUMAN	1	0.5	CT177_HUMAN	1	2.9	KANK4_HUMAN	1	1.2	K1C40_HUMAN	1	2.8
GOGB1_HUMAN	1	0.6	CELR1_HUMAN	1	0.3	OCAD2_MOUSE	1	6.5	NOL3_MOUSE	1	3.2
SETX_HUMAN	1	0.7	TULP3_MOUSE	1	2.0	RL18_MOUSE	1	10.1	FBX18_HUMAN	1	1.6
LBXCO_HUMAN	1	3.0	LRC41_MOUSE	1	2.6	SRRM2_MOUSE	1	0.3	ASIP_HUMAN	1	17.4
CC114_RAT	1	2.3	RGPA2_RAT	1	0.6	STABP_RAT	1	1.4	CP11A_RAT	1	2.5
CAN11_RAT	1	4.6	EPN2_HUMAN	1	4.4	PRPS2_HUMAN	1	4.1	AT1B2_MOUSE	1	5.2
TR10A_HUMAN	1	4.7	SSPO_HUMAN	1	0.2	K1143_HUMAN	1	9.1	PR2B1_MOUSE	1	5.3
CCD39_MOUSE	1	1.0	ATS17_HUMAN	1	1.1	ADAM2_CAVPO	1	1.6	U633B_HUMAN	1	18.1
ZN287_MOUSE	1	2.2	IKBZ_HUMAN	1	1.4	TEC_MOUSE	1	1.9	CB053_HUMAN	1	1.9
TBCK_MOUSE	1	2.2	RMTL1_MOUSE	1	5.3	GNTK_HUMAN	1	7.0	BAZ2A_MOUSE	1	1.2
EPHB3_MOUSE	1	3.0	NF1_RAT	1	0.7	GDE1_MOUSE	1	3.9	PGRP1_BOSIN	1	5.8
CHD9_MOUSE	1	1.2	ARL6_MOUSE	1	3.8	SYCP1_MOUSE	1	1.4	K1462_MOUSE	1	0.6
NRAP_MOUSE	1	1.2	STAB1_HUMAN	1	0.5	CRY1_RAT	1	2.4	TFG_HUMAN	1	4.2
TES_OTOGA	1	5.0	SAFB2_HUMAN	1	0.9	SYT2_HUMAN	1	2.1	DCTN4_MOUSE	1	4.3
CBX4_MOUSE	1	4.9	SEP13_HUMAN	1	4.2	PREX1_MOUSE	1	1.3	CCNT2_HUMAN	1	2.3
SH3G2_RAT	1	3.1	TP53B_MOUSE	1	0.8	ENOF1_PONAB	1	2.7	ZMYM4_MOUSE	1	0.5
LSP1_MOUSE	1	2.7	KLDC4_PONAB	1	1.7	FAH2A_HUMAN	1	5.4	SPB6_BOVIN	1	2.4
ZFY19_HUMAN	1	3.2	ILEUB_MOUSE	1	4.2	GGTA1_CEBAP	1	2.7	MMP8_HUMAN	1	3.2
KIN17_MOUSE	1	4.1	RAB4B_HUMAN	1	6.1	KCNA6_MOUSE	1	1.9	GUAD_MOUSE	1	3.3
USP9X_HUMAN	1	0.4	CJ052_HUMAN	1	11.6	MLF1_BOVIN	1	4.4	IF44L_HUMAN	1	1.5
MKRN2_MOUSE	1	1.9	DDX41_MOUSE	1	3.1	MTMR6_HUMAN	1	2.7	MDHC_FELCA	1	4.8
SBK1_RAT	1	2.2	DUS2L_MOUSE	1	2.6	CP2CV_CAPAE	1	4.2	COR2A_MOUSE	1	1.3
B3A4_RABIT	1	1.0	NCOA1_HUMAN	1	1.8	RUVB1_MOUSE	1	2.2	T10IP_BOVIN	1	1.6
SPAS2_MOUSE	1	2.8	RHPN2_MOUSE	1	2.9	CC142_HUMAN	1	0.9	MYC_BOVIN	1	2.1
ESPNL_MOUSE	1	0.9	LONM_BOVIN	1	1.2	WDR49_HUMAN	1	3.0	ZEP2_MOUSE	1	0.7
ZN841_HUMAN	1	2.0	NUD13_MOUSE	1	1.7	RL9_PONAB	1	8.3	GSDMC_MOUSE	1	1.3
MYO7B_HUMAN	1	0.9	CSPG2_MOUSE	1	0.3	RIN1_HUMAN	1	2.0	KR192_HUMAN	1	48.1
ADA2B_ELEMA	1	2.1	AMRP_RAT	1	2.8	GCDH_PIG	1	4.7	PRD10_PONAB	1	0.7

Protein	Peptides	Score	Protein	Peptides	Score	Protein	Peptides	Score	Protein	Peptides	Score
CP110_HUMAN	1	1.0	**DYHC2_RAT**	1	0.3	**PLXB1_HUMAN**	1	0.4	**DIP2A_MOUSE**	3	1.2
IAC1_BOVIN	1	19.0	**OGR1_HUMAN**	1	5.5	**PO5F1_MOUSE**	1	3.7	**AKA12_MOUSE**	1	1.0
VIGLN_PONAB	1	0.6	**ARSH_HUMAN**	1	2.7	**CELR1_MOUSE**	1	0.5	**DBF4A_MOUSE**	1	2.6
SCML1_PYGBI	1	4.3	**PR3D1_MOUSE**	1	4.0	**REBL1_BOVIN**	1	8.8	**ACTBM_HUMAN**	1	2.9
RM09_PAPAN	1	3.4	**CELA1_MACFA**	1	1.9	**LPP_HUMAN**	1	2.3	**GPC3_MOUSE**	1	1.4
TTC36_HUMAN	1	6.9	**DJB14_MOUSE**	1	2.9	**DDX47_MOUSE**	1	2.4	**ZBT41_HUMAN**	2	2.4
ABRA_PIG	1	3.4	**1B58_HUMAN**	1	3.0	**CD97_HUMAN**	1	1.2			
CAH15_MOUSE	1	2.5	**SMKX_MOUSE**	1	1.4	**ACINU_MOUSE**	1	1.0			
ASPX_MOUSE	1	11.5	**ADCY4_RAT**	1	1.7	**FBXL8_MOUSE**	1	2.4			
BBS12_MOUSE	1	1.0	**SIVA_HUMAN**	1	16.0	**NAP1_HUMAN**	1	1.1			
DSG4_MOUSE	1	0.9	**IQCG_MOUSE**	1	1.7	**NPT2B_MOUSE**	1	2.2			
HBB_MYOVE	1	8.2	**RTTN_MOUSE**	1	1.1	**POTE1_MOUSE**	1	1.7			
CTTB2_HORSE	1	1.3	**BACH_HUMAN**	1	4.2	**SUIS_RABIT**	1	0.5			
P2Y13_MOUSE	1	5.0	**STF1_PIG**	1	2.8	**AGT2_RAT**	1	2.9			
GGLO_BOVIN	1	1.8	**TTLL5_HUMAN**	1	1.5	**PI3R6_HUMAN**	1	2.3			
CLSPN_MOUSE	1	1.1	**PECR_MOUSE**	1	4.0	**IFFO2_RAT**	1	5.9			
LHPP_HUMAN	1	1.9	**ALKB3_BOVIN**	1	4.2	**MYO7A_HUMAN**	1	0.6			
ADCY8_RAT	1	0.8	**CYB_PLAIN**	1	2.6	**SO1B3_HUMAN**	1	2.7			
SUSD3_MOUSE	1	4.1	**CS2LB_RAT**	1	10.1	**CABP1_HUMAN**	1	2.4			
KAIN_HUMAN	1	1.9	**TGS1_HUMAN**	1	0.8	**M3K14_MOUSE**	1	2.0			
COOA1_MOUSE	1	1.2	**GSX1_MOUSE**	1	6.1	**FJX1_HUMAN**	1	4.3			
MCP62_HUMAN	1	2.9	**JERKY_MOUSE**	1	2.7	**INO80_MOUSE**	1	0.4			
B3GT4_CANFA	1	3.7	**ENPP6_HUMAN**	1	2.0	**PHF2_MOUSE**	1	0.9			
TRPM2_HUMAN	1	1.5	**HMOX1_PONAB**	1	5.2	**JPH3_MOUSE**	1	1.3			
DY12L_HUMAN	1	1.7	**STX8_BOVIN**	1	4.7	**RECK_HUMAN**	1	0.8			
ACOXL_HUMAN	1	2.7	**PI2R_HUMAN**	1	2.6	**ATL4_RAT**	1	0.9			
VPS39_MOUSE	1	1.7	**PKD2_HUMAN**	1	1.7	**SYLC_MOUSE**	1	0.6			
ROBO1_HUMAN	1	0.7	**ABC3G_ERYPA**	1	0.0	**KCMA1_RABIT**	1	2.2			

Appendix III: Poster and abstracts

Maternal interaction with Gametes and Embryo 2nd General Meeting (COST-GEMINI), Italy (2009). *Modulation of human sperm by the cumulus oophorus*. R.L. Frettsome, J.C. Kirkman-Brown and S.J. Conner.

College of Medicine and Dental Sciences Research Day, University of Birmingham (2008). *Structural and Functional Studies of the human zona pellucida*. R.L. Frettsome and S. J. Conner.

REFERENCES

Abbott, A.L. & Ducibella, T. 2001. Calcium and the control of mammalian cortical granule exocytosis. *Front Biosc*., 6, D792-D806.

Abel, M.H., Wootton, A.N., Wilkins, V., Huhtaniemi, I., Knight, P.G., & Charlton, H.M. 2000. The effect of a null mutation in the follicle-stimulating hormone receptor gene on mouse reproduction. *Endocrinology.*, 141, (5) 1795-1803.

Abou-Haila, A. & Tulsiani, D.R. 2000. Mammalian sperm acrosome: formation, contents, and function. *Arch.Biochem.Biophys*., 379, (2) 173-182.

Acosta, T.J. 2007. Studies of follicular vascularity associated with follicle selection and ovulation in cattle. *J.Reprod.Dev*., 53, (1) 39-44.

Adham, I.M., Nayernia, K., & Engel, W. 1997. Spermatozoa lacking acrosin protein show delayed fertilization. *Mol.Reprod.Dev*., 46, (3) 370-376.

Adhikari, D., Zheng, W., Shen, Y., Gorre, N., Hamalainen, T., Cooney, A.J., Huhtaniemi, I., Lan, Z.J., & Liu, K. 2010. Tsc/mTORC1 signaling in oocytes governs the quiescence and activation of primordial follicles. *Hum.Mol.Genet*., 19, (3) 397-410.

Aflatoonian, B., Ruban, L., Jones, M., Aflatoonian, R., Fazeli, A., & Moore, H.D. 2009. In vitro post-meiotic germ cell development from human embryonic stem cells. *Hum.Reprod*., 24, (12) 3150-3159.

Aitken, R.J., Buckingham, D.W., & Irvine, D.S. 1996. The extragenomic action of progesterone on human spermatozoa: evidence for a ubiquitous response that is rapidly down-regulated. *Endocrinology,*, 137, (9) 3999-4009.

Aitken, R.J., Harkiss, D., Knox, W., Paterson, M., & Irvine, D.S. 1998. A novel signal transduction cascade in capacitating human spermatozoa characterised by a redox-regulated, cAMP-mediated induction of tyrosine phosphorylation. *J.Cell Sci*., 111 (Pt 5), 645-656.

Aitken, R.J., Nixon, B., Lin, M., Koppers, A.J., Lee, Y.H., & Baker, M.A. 2007. Proteomic changes in mammalian spermatozoa during epididymal maturation. *Asian J.Androl.*, 9, (4) 554-564.

Amleh, A. & Taketo, T. 1998. Live-borns from XX but not XY oocytes in the chimeric mouse ovary composed of B6.Y(TIR) and XX cells. *Biol.Reprod*., 58, (2) 574-582.

Andersen, C.Y. 1993. Characteristics of human follicular fluid associated with successful conception after in vitro fertilization. *J.Clin.Endocrinol.Metab*, 77, (5) 1227-1234.

Asano, M., Furukawa, K., Kido, M., Matsumoto, S., Umesaki, Y., Kochibe, N., & Iwakura, Y. 1997. Growth retardation and early death of beta-1,4-galactosyltransferase knockout mice with augmented proliferation and abnormal differentiation of epithelial cells. *EMBO J*., 16, (8) 1850-1857.

Austin, C. 1951. Observations on the penetration of the sperm in the mammalian egg. *Aust.J.Sci.R*es *B*., 4, (4) 581-596.

Austin, C. 1952. The capacitation of the mammalian sperm. *Nature.,* 170, (4321) 326.

Baba, D., Kashiwabara, S., Honda, A., Yamagata, K., Wu, Q., Ikawa, M., Okabe, M., & Baba, T. 2002. Mouse sperm lacking cell surface hyaluronidase PH-20 can pass through the layer of cumulus cells and fertilize the egg. *J.Biol.Chem*., 277, (33) 30310-30314.

Baba, T., Azuma, S., Kashiwabara, S., & Toyoda, Y. 1994. Sperm from mice carrying a targeted mutation of the acrosin gene can penetrate the oocyte zona pellucida and effect fertilization. *J.Biol.Chem*., 269, (50) 31845-31849.

Baibakov, B., Gauthier, L., Talbot, P., Rankin, T.L., & Dean, J. 2007. Sperm binding to the zona pellucida is not sufficient to induce acrosome exocytosis. *Development.*, 134, (5) 933-943.

Bailey, J.L. & Storey, B.T. 1994. Calcium influx into mouse spermatozoa activated by solubilized mouse zona pellucida, monitored with the calcium fluorescent indicator, fluo-3. Inhibition of the influx by three inhibitors of the zona pellucida induced acrosome reaction: tyrphostin A48, pertussis toxin, and 3-quinuclidinyl benzilate. *Mol.Reprod.Dev*., 39, (3) 297-308.

Baker, T.G. 1963. A quantitative and cytological study of germ cells in human ovaries. *Proc.R.Soc.Lond B Biol.Sci*., 158, 417-433.

Baldi, E., Luconi, M., Bonaccorsi, L., Maggi, M., Francavilla, S., Gabriele, A., Properzi, G., & Forti, G. 1999. Nongenomic progesterone receptor on human spermatozoa: biochemical aspects and clinical implications. *Steroids.*, 64, (1-2) 143-148.

Baldi, E., Luconi, M., Bonaccorsi, L., Muratori, M., & Forti, G. 2000. Intracellular events and signaling pathways involved in sperm acquisition of fertilizing capacity and acrosome reaction. *Front Biosci*., 5, E110-E123.

Baltes, P., Sanchez, R., Pena, P., Villegas, J., Turley, H., & Miska, W. 1998. Evidence for the synthesis and secretion of a CBG-like serpin by human cumulus oophorus and fallopian tubes. *Andrologia.*, 30, (4-5) 249-253.

Baltus, A.E., Menke, D.B., Hu, Y.C., Goodheart, M.L., Carpenter, A.E., de Rooij, D.G., & Page, D.C. 2006. In germ cells of mouse embryonic ovaries, the decision to enter meiosis precedes premeiotic DNA replication. *Nat.Genet*., 38, (12) 1430-1434.

Bar-Ami, S. 1994. Increasing progesterone secretion and 3 beta-hydroxysteroid dehydrogenase activity of human cumulus cells and granulosa-lutein cells concurrent with successful fertilization of the corresponding oocyte. *J.Steroid Biochem.Mol.Biol*., 51, (5-6) 299-305.

Bauersachs, S., Blum, H., Mallok, S., Wenigerkind, H., Rief, S., Prelle, K. & Wolf, E. 2003. Regulation of ipsilateral and contralateral bovine oviduct epithelial cell function in the postovulation period: a transcriptomics approach. *Biol.Reprod.*, 68, (4) 1170-1177.

Bauwens, C.L., Peerani, R., Niebruegge, S., Woodhouse, K.A., Kumacheva, E., Husain, M., & Zandstra, P.W. 2008. Control of human embryonic stem cell colony and aggregate size heterogeneity influences differentiation trajectories. *Stem Cells*, 26., (9) 2300-2310.

Bedford, J. 1963. Morphological changes in rabbit spermatozoa during passage through the epididymis. *J.Reprod.Fertil*., 5, 169-177.

Bedford, J. 1965. Changes in fine structure of the rabbit sperm head during passage through the epididymis. *J.Anat*., 99, (Pt 4) 891-906.

Bedford, J., Mock, O.B., & Goodman, S.M. 2004. Novelties of conception in insectivorous mammals (Lipotyphla), particularly shrews. *Biol.Rev.Camb.Philos.Soc*., 79, (4) 891-909.

Bedford, J.M. 1968. Ultrastructural changes in the sperm head during fertilization in the rabbit. *Am.J.Anat*., 123, (2) 329-358.

Bedu-Addo, K., Costello, S., Harper, C., Machado-Oliveira, G., Lefievre, L., Ford, C., Barratt, C., & Publicover, S. 2008. Mobilisation of stored calcium in the neck region of human sperm--a mechanism for regulation of flagellar activity. *Int.J.Dev.Biol*., 52, (5-6) 615-626.

Berisha, B. & Schams, D. 2005. Ovarian function in ruminants. *Domest.Anim Endocrinol*., 29, (2) 305-317.

Berridge, M.J., Bootman, M.D., & Roderick, H.L. 2003. Calcium signalling: dynamics, homeostasis and remodelling. *Nat.Rev.Mol.Cell Biol*., 4, (7) 517-529.

Bhandari, B., Bansal, P., Talwar, P., & Gupta, S.K. 2010. Delineation of downstream signalling components during acrosome reaction mediated by heat solubilized human zona pellucida. *Reprod.Biol.Endocrinol*., 8, 7.

BIAcore. BIAcore Sensor Surface Handbook. Version AA. 2003.

Björndahl, L., Kirkman-Brown, J., Hart, G., Rattle, S. & Barratt, C.L.R. 2006. Development of a novel sperm test. *Human Reprodction.,* 21, (1)145-149.

Blackmore, P.F., Beebe, S.J., Danforth, D.R., & Alexander, N. 1990. Progesterone and 17 alpha-hydroxyprogesterone. Novel stimulators of calcium influx in human sperm. *J.Biol.Chem*., 265, (3) 1376-1380.

Bleil, J.D. & Wassarman, P.M. 1980a. Mammalian sperm-egg interaction: identification of a glycoprotein in mouse egg zonae pellucidae possessing receptor activity for sperm. *Cell*., 20, (3) 873-882.

Bleil, J.D. & Wassarman, P.M. 1980b. Structure and function of the zona pellucida: identification and characterization of the proteins of the mouse oocyte's zona pellucida. *Dev.Biol*., 76, (1) 185-202.

Bleil, J.D. & Wassarman, P.M. 1983. Sperm-egg interactions in the mouse: sequence of events and induction of the acrosome reaction by a zona pellucida glycoprotein. *Dev.Biol*., 95, (2) 317-324.

Bleil, J.D. & Wassarman, P.M. 1988. Galactose at the nonreducing terminus of O-linked oligosaccharides of mouse egg zona pellucida glycoprotein ZP3 is essential for the glycoprotein's sperm receptor activity. *Proc.Natl.Acad.Sci.U.S.A*., 85, (18) 6778-6782.

Bork, P. & Sander, C. 1992. A large domain common to sperm receptors (Zp2 and Zp3) and TGF-beta type III receptor. *FEBS Lett*., 300, (3) 237-240.

Bowles, J., Knight, D., Smith, C., Wilhelm, D., Richman, J., Mamiya, S., Yashiro, K., Chawengsaksophak, K., Wilson, M.J., Rossant, J., Hamada, H., & Koopman, P. 2006. Retinoid signaling determines germ cell fate in mice. *Science.*, 312, (5773) 596-600.

Braun, B.C., Ringleb, J., Waurich, R., Viertel, D., & Jewgenow, K. 2009. Functional role of feline zona pellucida protein 4 trefoil domain: a sperm receptor or structural component of the domestic cat zona pellucida? *Reprod.Domest.Anim.*, 44 Suppl 2, 234-238.

Brewer, L., Corzett, M., & Balhorn, R. 2002. Condensation of DNA by spermatid basic nuclear proteins. *J.Biol.Chem*., 277, (41) 38895-38900.

Britt, K.L., Drummond, A.E., Cox, V.A., Dyson, M., Wreford, N.G., Jones, M.E., Simpson, E.R., & Findlay, J.K. 2000. An age-related ovarian phenotype in mice with targeted disruption of the Cyp 19 (aromatase) gene. *Endocrinology.*, 141, (7) 2614-2623.

Brokaw, C.J. 1991. Calcium sensors in sea urchin sperm flagella. *Cell Motil.Cytoskeleton.*, 18, (2) 123-130.

Brunelli, R., Papi, M., Arcovito, G., Bompiani, A., Castagnola, M., Parasassi, T., Sampaolese, B., Vincenzoni, F., & De, S.M. 2007. Globular structure of human ovulatory cervical mucus. *FASEB J.*, 21, (14) 3872-3876.

Brunet, S. & Verlhac, M.H. 2011. Positioning to get out of meiosis: the asymmetry of division. *Hum.Reprod.Update*., 17, (1) 68-75.

Bushell, K.M., Sollner, C., Schuster-Boeckler, B., Bateman, A., & Wright, G.J. 2008. Large-scale screening for novel low-affinity extracellular protein interactions. *Genome Res*., 18, (4) 622-630.

Callebaut, I., Mornon, J.P., & Monget, P. 2007. Isolated ZP-N domains constitute the N-terminal extensions of Zona Pellucida proteins. *Bioinformatics*., 23, (15) 1871-1874.

Camaioni, A., Salustri, A., Yanagishita, M., & Hascall, V.C. 1996. Proteoglycans and proteins in the extracellular matrix of mouse cumulus cell-oocyte complexes. *Arch.Biochem.Biophys*., 325, (2) 190-198.

Cameron, C.M., Hu, W.S., & Kaufman, D.S. 2006. Improved development of human embryonic stem cell-derived embryoid bodies by stirred vessel cultivation. *Biotechnol.Bioeng*., 94, (5) 938-948.

Carabatsos, M.J., Elvin, J., Matzuk, M.M., & Albertini, D.F. 1998. Characterization of oocyte and follicle development in growth differentiation factor-9-deficient mice. *Dev.Biol*., 204, (2) 373-384.

Carlson, A.E., Hille, B., & Babcock, D.F. 2007. External Ca2+ acts upstream of adenylyl cyclase SACY in the bicarbonate signaled activation of sperm motility. *Dev.Biol*., 312, (1) 183-192.

Carlstedt, I. & Sheehan, J.K. 1984. Is the macromolecular architecture of cervical, respiratory and gastric mucins the same? *Biochem.Soc.Trans*., 12, (4) 615-617.

Castle, P.E. 2002. Could multiple low-affinity bonds mediate primary sperm-zona pellucida binding? *Reproduction.*, 124, (1) 29-32

Castrillon, D.H., Miao, L., Kollipara, R., Horner, J.W., & DePinho, R.A. 2003. Suppression of ovarian follicle activation in mice by the transcription factor Foxo3a. *Science.*, 301, (5630) 215-218.

Catalina, P., Montes, R., Ligero, G., Sanchez, L., de la Cueva, T., Bueno, C., Leone, P.E., & Menendez, P. 2008. Human ESCs predisposition to karyotypic instability: Is a matter of culture adaptation or differential vulnerability among hESC lines due to inherent properties? *Mol.Cancer.*, 7, 76.

Chakravarty, S., Kadunganattil, S., Bansal, P., Sharma, R.K., & Gupta, S.K. 2008. Relevance of glycosylation of human zona pellucida glycoproteins for their binding to capacitated human spermatozoa and subsequent induction of acrosomal exocytosis. *Mol.Reprod.Dev*., 75, (1) 75-88.

Chakravarty, S., Suraj, K., & Gupta, S.K. 2005. Baculovirus-expressed recombinant human zona pellucida glycoprotein-B induces acrosomal exocytosis in capacitated spermatozoa in addition to zona pellucida glycoprotein-C. *Mol.Hum.Reprod*., 11, (5) 365-372.

Chang, H. & Matzuk, M.M. 2001. Smad5 is required for mouse primordial germ cell development. *Mech.Dev*., 104, (1-2) 61-67.

Chang, M. 1951. Fertilizing capacity of spermatozoa deposited into the fallopian tubes. *Nature.*, 168, (4277) 697-698.

Chapman, N., Kessopoulou, E., Andrews, P., Hornby, D., & Barratt, C.R. 1998. The polypeptide backbone of recombinant human zona pellucida glycoprotein-3 initiates acrosomal exocytosis in human spermatozoa in vitro. Biochem.J., 330 (Pt 2), 839-845.

Chen, L., Zhang, H., Powers, R.W., Russell, P.T., & Larsen, W.J. 1996. Covalent linkage between proteins of the inter-alpha-inhibitor family and hyaluronic acid is mediated by a factor produced by granulosa cells. *J.Biol.Chem*., 271, (32) 19409-19414.

Chen, W.S., Ma, L., Hu, X.Y., Liu, X.Y., Jin, C., Li, Z.B., & Li, W.D. 2011. [Expressions of OCT4 and CD133 and their correlation in colonic cancer]. *Nan.Fang Yi.Ke.Da.Xue.Xue.Bao*., 31, (8) 1434-1436.

Cheng, C.Y. & Mruk, D.D. 2002. Cell junction dynamics in the testis: Sertoli-germ cell interactions and male contraceptive development. *Physiol Rev*., 82, (4) 825-874.

Cherr, G.N., Lambert, H., Meizel, S., & Katz, D.F. 1986. In vitro studies of the golden hamster sperm acrosome reaction: completion on the zona pellucida and induction by homologous soluble zonae pellucidae. *Dev.Biol*., 114, (1) 119-131.

Chevrier, C. & Dacheux, J.L. 1987. Analysis of the flagellar bending waves of ejaculated ram sperm. *Cell Motil.Cytoskeleton.*, 8, (3) 261-273.

Chirinos, M., Carino, C., Gonzalez-Gonzalez, M.E., Arreola, E., Reveles, R., & Larrea, F. 2011. Characterization of human sperm binding to homologous recombinant zona pellucida proteins. *Reprod.Sci*., 18, (9) 876-885.

Chiu, P.C., Chung, M.K., Koistinen, R., Koistinen, H., Seppala, M., Ho, P.C., Ng, E.H., Lee, K.F., & Yeung, W.S. 2007. Cumulus oophorus-associated glycodelin-C displaces sperm-bound glycodelin-A and -F and stimulates spermatozoa-zona pellucida binding. *J.Biol.Chem*., 282, (8) 5378-5388.

Chiu, P.C., Chung, M.K., Tsang, H.Y., Koistinen, R., Koistinen, H., Seppala, M., Lee, K.F., & Yeung, W.S. 2005. Glycodelin-S in human seminal plasma reduces cholesterol efflux and inhibits capacitation of spermatozoa. *J.Biol.Chem*., 280, (27) 25580-25589.

Chiu, P.C., Koistinen, R., Koistinen, H., Seppala, M., Lee, K.F., & Yeung, W.S. 2003a. Binding of zona binding inhibitory factor-1 (ZIF-1) from human follicular fluid on spermatozoa. *J.Biol.Chem*., 278, (15) 13570-13577.

Chiu, P.C., Koistinen, R., Koistinen, H., Seppala, M., Lee, K.F., & Yeung, W.S. 2003b. Zona-binding inhibitory factor-1 from human follicular fluid is an isoform of glycodelin. *Biol.Reprod*., 69, (1) 365-372.

Chiu, P.C., Wong, B.S., Chung, M.K., Lam, K.K., Pang, R.T., Lee, K.F., Sumitro, S.B., Gupta, S.K., & Yeung, W.S. 2008a. Effects of native human zona pellucida glycoproteins 3 and 4 on acrosome reaction and zona pellucida binding of human spermatozoa. *Biol.Reprod*., 79, (5) 869-877.

Chiu, P.C., Wong, B.S., Lee, C.L., Pang, R.T., Lee, K.F., Sumitro, S.B., Gupta, S.K., & Yeung, W.S. 2008b. Native human zona pellucida glycoproteins: purification and binding properties. *Hum.Reprod*., 23, (6) 1385-1393.

Cho, C., Bunch, D.O., Faure, J.E., Goulding, E.H., Eddy, E.M., Primakoff, P., & Myles, D.G. 1998. Fertilization defects in sperm from mice lacking fertilin beta. *Science.*, 281, (5384) 1857-1859.

Chu, G.C., Dunn, N.R., Anderson, D.C., Oxburgh, L., & Robertson, E.J. 2004. Differential requirements for Smad4 in TGFbeta-dependent patterning of the early mouse embryo. *Development.*, 131, (15) 3501-3512.

Chuva de Sousa Lopes SM, Hayashi, K., Shovlin, T.C., Mifsud, W., Surani, M.A., & McLaren, A. 2008. X chromosome activity in mouse XX primordial germ cells. *PLoS.Genet*., 4, (2).

Clark, A.T., Bodnar, M.S., Fox, M., Rodriquez, R.T., Abeyta, M.J., Firpo, M.T., & Pera, R.A. 2004a. Spontaneous differentiation of germ cells from human embryonic stem cells in vitro. *Hum.Mol.Genet*., 13, (7) 727-739.

Clark, A.T., Rodriguez, R.T., Bodnar, M.S., Abeyta, M.J., Cedars, M.I., Turek, P.J., Firpo, M.T., & Reijo Pera, R.A. 2004b. Human STELLAR, NANOG, and GDF3 genes are expressed in pluripotent cells and map to chromosome 12p13, a hotspot for teratocarcinoma. *Stem Cells.*, 22, (2) 169-179.

Clarke, H.G., Hope, S.A., Byers, S., & Rodgers, R.J. 2006. Formation of ovarian follicular fluid may be due to the osmotic potential of large glycosaminoglycans and proteoglycans. *Reproduction*., 132, (1) 119-131.

Clermont, Y., Oko, R., & Hermo, L. 1990. Immunocytochemical localization of proteins utilized in the formation of outer dense fibers and fibrous sheath in rat spermatids: an electron microscope study. *Anat.Rec*., 227, (4) 447-457.

Cohen-Dayag, A., Tur-Kaspa, I., Dor, J., Mashiach, S., & Eisenbach, M. 1995. Sperm capacitation in humans is transient and correlates with chemotactic responsiveness to follicular factors. *Proc.Natl.Acad.Sci.U.S.A.*, 92, (24) 11039-11043.

Conner, S.J., Lefievre, L., Hughes, D.C., & Barratt, C.L. 2005. Cracking the egg: increased complexity in the zona pellucida. *Hum.Reprod*., 20, (5) 1148-1152.

Connolly, T.J. 2011. Calcium signalling during human sperm interaction with cells of the female reproductive tract. Doctor of Philosophy University of Birmingham.

Conti, M., Andersen, C.B., Richard, F., Mehats, C., Chun, S.Y., Horner, K., Jin, C., & Tsafriri, A. 2002. Role of cyclic nucleotide signaling in oocyte maturation. *Mol.Cell Endocrinol*., 187, (1-2) 153-159.

Cooper GW. 1979. The motility of rabbit spermatozoa recovered from the female reproductive tract. *Gamete Res.*, 2, 35-42.

Cooper, T.G., Noonan, E., von, E.S., Auger, J., Baker, H.W., Behre, H.M., Haugen, T.B., Kruger, T., Wang, C., Mbizvo, M.T., & Vogelsong, K.M. 2010. World Health Organization reference values for human semen characteristics. *Hum.Reprod.Update*., 16, (3) 231-245.

Cornwall, G.A. 2009. New insights into epididymal biology and function. *Hum.Reprod.Update*., 15, (2) 213-227.

Cross, P.C. & Brinster, R.L. 1970. In vitro development of mouse oocytes. *Biol.Reprod*., 3, (3) 298-307.

Dadoune, J.P. 2003. Expression of mammalian spermatozoal nucleoproteins. *Microsc.Res Tech*., 61, (1) 56-75.

Dandekar, P., Aggeler, J., & Talbot, P. 1992. Structure, distribution and composition of the extracellular matrix of human oocytes and cumulus masses. *Hum.Reprod*., 7, (3) 391-398.

Dang, S.M., Kyba, M., Perlingeiro, R., Daley, G.Q., & Zandstra, P.W. 2002. Efficiency of embryoid body formation and hematopoietic development from embryonic stem cells in different culture systems. *Biotechnol.Bioeng*., 78, (4) 442-453.

Darszon, A., Acevedo, J.J., Galindo, B.E., Hernandez-Gonzalez, E.O., Nishigaki, T., Trevino, C.L., Wood, C., & Beltran, C. 2006. Sperm channel diversity and functional multiplicity. *Reproduction*., 131, (6) 977-988.

Davis, B.K. 1981. Timing of fertilization in mammals: sperm cholesterol/phospholipid ratio as a determinant of the capacitation interval. *Proc.Natl.Acad.Sci.U.S.A.*, 78, (12) 7560-7564.

de Resende, L.O., dos Reis, R.M., Ferriani, R.A., Vireque, A.A., Santana, L.F., de Sa Rosa e Silva AC, & Martins, W.P. 2010. Concentration of steroid hormones in the follicular fluid of mature and immature ovarian follicles of patients with polycystic ovary syndrome submitted to in vitro fertilization. *Rev.Bras.Ginecol.Obstet*., 32, (9) 447-453.

de Sousa Lopes, S.M., Hayashi, K., & Surani, M.A. 2007. Proximal visceral endoderm and extraembryonic ectoderm regulate the formation of primordial germ cell precursors. *BMC.Dev.Biol*., 7, 140.

Dean, J. 2004. Reassessing the molecular biology of sperm-egg recognition with mouse genetics. *Bioessays*., 26, (1) 29-38.

Dean, J., Cohen, G., Kemp, J., Robson, L., Tembe, V., Hasselaar, J., Webster, B., Lammi, A., & Smith, A. 1997. Karyotype 69,XXX/47,XX,+15 in a 2 1/2 year old child. *J.Med.Genet*., 34, (3) 246-249.

Demott, R.P. & Suarez, S.S. 1992. Hyperactivated sperm progress in the mouse oviduct. *Biol.Reprod*., 46, (5) 779-785.

Dobrinski, I., Smith, T.T., Suarez, S.S., & Ball, B.A. 1997. Membrane contact with oviductal epithelium modulates the intracellular calcium concentration of equine spermatozoa in vitro. *Biol.Reprod*., 56, (4) 861-869.

Dong, J., Albertini, D.F., Nishimori, K., Kumar, T.R., Lu, N., & Matzuk, M.M. 1996. Growth differentiation factor-9 is required during early ovarian folliculogenesis. *Nature.*, 383, (6600) 531-535.

Durlinger, A.L., Gruijters, M.J., Kramer, P., Karels, B., Ingraham, H.A., Nachtigal, M.W., Uilenbroek, J.T., Grootegoed, J.A., & Themmen, A.P. 2002. Anti-Mullerian hormone inhibits initiation of primordial follicle growth in the mouse ovary. *Endocrinology.*, 143, (3) 1076-1084.

Durlinger, A.L., Kramer, P., Karels, B., de Jong, F.H., Uilenbroek, J.T., Grootegoed, J.A., & Themmen, A.P. 1999. Control of primordial follicle recruitment by anti-Mullerian hormone in the mouse ovary. *Endocrinology.*, 140, (12) 5789-5796.

Ellington, J.E., Ignotz, G.G., Ball, B.A., Meyers-Wallen, V.N. & Currie, W.B. 1993. De novo protein synthesis by bovine uterine tube (oviduct) epithelial cells changes during co-culture with bull spermatozoa. *Biol.Reprod.*, 48, (4) 851-856.

El-Taieb, M.A., Herwig, R., Nada, E.A., Greilberger, J., & Marberger, M. 2009. Oxidative stress and epididymal sperm transport, motility and morphological defects. *Eur.J.Obstet.Gynecol.Reprod.Biol*., 144 Suppl 1, S199-S203.

Eyestone, W.H., Leibfried-Rutledge, M.L., Northey, D.L., Gilligan, B.G., & First, N.L. 1987. Culture of one- and two-cell bovine embryos to the blastocyst stage in the ovine oviduct. *Theriogenology.*, 28, (1) 1-7.

Ezeh, U.I., Turek, P.J., Reijo, R.A., & Clark, A.T. 2005. Human embryonic stem cell genes OCT4, NANOG, STELLAR, and GDF3 are expressed in both seminoma and breast carcinoma. *Cancer.*, 104, (10) 2255-2265.

Fabritius, A.S., Ellefson, M.L., & McNally, F.J. 2011. Nuclear and spindle positioning during oocyte meiosis. *Curr.Opin.Cell Biol*., 23, (1) 78-84.

Falin, L.I. 1969. The development of genital glands and the origin of germ cells in human embryogenesis. *Acta Anat.(Basel).*, 72, (2) 195-232.

Familiari, G., Heyn, R., Relucenti, M., & Sathananthan, H. 2008. Structural changes of the zona pellucida during fertilization and embryo development. *Front Biosci*., 13, 6730-6751.

Fawcett, D.W. 1965. The anatomy of the mammalian spermatozoon with particular reference to the guinea pig. *Z.Zellforsch.Mikrosk.Anat*., 67, (3) 279-296.

Fawcett, D.W. 1975a. The anatomy of the spermatozoon after 300 years. *Kaibogaku Zasshi.*, 50, (6) 326-327.

Fawcett, D.W. 1975b. The mammalian spermatozoon. *Dev.Biol*., 44, (2) 394-436.

Fazeli, A., Affara, N.A., Hubank, M. & Holt, W.V. 2004. Sperm-induced modification of the oviductal gene expression profile after natural insemination in mice. *Biol.Reprod.*, 71, (1) 60-65.

Feki, N.C., Therond, P., Couturier, M., Limea, G., Legrand, A., Jouannet, P., & Auger, J. 2004. Human sperm lipid content is modified after migration into human cervical mucus. *Mol.Hum.Reprod*., 10, (2) 137-142.

Fetterolf, P.M., Jurisicova, A., Tyson, J.E., & Casper, R.F. 1994. Conditioned medium from human cumulus oophorus cells stimulates human sperm velocity. *Biol.Reprod*., 51, (2) 184-192.

Florman, H.M. & Storey, B.T. 1982. Mouse gamete interactions: the zona pellucida is the site of the acrosome reaction leading to fertilization in vitro. *Dev.Biol*., 91, (1) 121-130.

Florman, H.M. & Wassarman, P.M. 1985. O-linked oligosaccharides of mouse egg ZP3 account for its sperm receptor activity. *Cell*., 41, (1) 313-324.

Florman, H.M. 1994. Sequential focal and global elevations of sperm intracellular Ca2+ are initiated by the zona pellucida during acrosomal exocytosis. *Dev.Biol*., 165, (1) 152-164.

Ford, W.C. 2006. Glycolysis and sperm motility: does a spoonful of sugar help the flagellum go round? *Hum.Reprod.Update*., 12, (3) 269-274.

Foresta, C., Rossato, M., & Di, V.F. 1993. Ion fluxes through the progesterone-activated channel of the sperm plasma membrane. *Biochem.J*., 294 (Pt 1), 279-283.

Fortune, J.E. 1994. Ovarian follicular growth and development in mammals. *Biol.Reprod*., 50, (2) 225-232.

Franken, D.R. & Bastiaan, H.S. 2009. Can a cumulus cell complex be used to select spermatozoa for assisted reproduction? *Andrologia.*, 41, (6) 369-376.

Fraser, L.R. 1984. Mouse sperm capacitation in vitro involves loss of a surface-associated inhibitory component. *J.Reprod.Fertil*., 72, (2) 373-384.

Fraser, L.R. 1998. Interactions between a decapacitation factor and mouse spermatozoa appear to involve fucose residues and a GPI-anchored receptor. *Mol.Reprod.Dev*., 51, (2) 193-202.

Fraser, L.R. 2010. The "switching on" of mammalian spermatozoa: molecular events involved in promotion and regulation of capacitation. *Mol.Reprod.Dev*., 77, (3) 197-208.

Gadella, B.M. & Harrison, R.A. 2000. The capacitating agent bicarbonate induces protein kinase A-dependent changes in phospholipid transbilayer behavior in the sperm plasma membrane. *Development.*, 127, (11) 2407-2420.

Ganguly, A., Bukovsky, A., Sharma, R.K., Bansal, P., Bhandari, B., & Gupta, S.K. 2010. In humans, zona pellucida glycoprotein-1 binds to spermatozoa and induces acrosomal exocytosis. *Hum.Reprod*.

Garcia, M.A. & Meizel, S. 1999. Progesterone-mediated calcium influx and acrosome reaction of human spermatozoa: pharmacological investigation of T-type calcium channels. *Biol.Reprod*., 60, (1) 102-109.

Geijsen, N., Horoschak, M., Kim, K., Gribnau, J., Eggan, K., & Daley, G.Q. 2004. Derivation of embryonic germ cells and male gametes from embryonic stem cells. *Nature.*, 427, (6970) 148-154.

Georgiou, A.S., Snijders, A.P., Sostaric, E., Aflatoonian, R., Vazquez, J.L., Vazquez, J.M., Roca, J., Martinez, E.A., Wright, P.C. & Fazeli, A. 2007. Modulation of the oviductal environment by gametes. *J.Proteome.Res.*, 6, (12) 4656-4666.

Georgiou, A.S., Sostaric, E., Wong, C.H., Snijders, A.P., Wright, P.C., Moore, H.D. & Fazeli, A. 2005. Gametes alter the oviductal secretory proteome. *Mol.Cell Proteomics.*, 4, (11) 1785-1796.

Gibbons, R., Adeoya-Osiguwa, S.A., & Fraser, L.R. 2005. A mouse sperm decapacitation factor receptor is phosphatidylethanolamine-binding protein 1. *Reproduction*., 130, (4) 497-508.

Gilchrist, R.B., Ritter, L.J., & Armstrong, D.T. 2004. Oocyte-somatic cell interactions during follicle development in mammals. *Anim Reprod.Sci*., 82-83, 431-446.

Ginsburg, M., Snow, M.H., & McLaren, A. 1990. Primordial germ cells in the mouse embryo during gastrulation. *Development.*, 110, (2) 521-528.

Giretti, M.S. & Simoncini, T. 2008. Rapid regulatory actions of sex steroids on cell movement through the actin cytoskeleton. *Steroids.*, 73, (9-10) 895-900.

Giwercman, A., Richthoff, J., Hjollund, H., Bonde, J.P., Jepson, K., Frohm, B., & Spano, M. 2003. Correlation between sperm motility and sperm chromatin structure assay parameters. *Fertil.Steril*., 80, (6) 1404-1412.

Goldenberg, R.L., Powell, R.D., Rosen, S.W., Marshall, J.R., & Ross, G.T. 1976. Ovarian morphology in women with anosmia and hypogonadotropic hypogonadism. *Am.J.Obstet.Gynecol*., 126, (1) 91-94.

Goodwin, L.O., Karabinus, D.S., Pergolizzi, R.G., & Benoff, S. 2000. L-type voltage-dependent calcium channel alpha-1C subunit mRNA is present in ejaculated human spermatozoa. *Mol.Hum.Reprod*., 6, (2) 127-136.

Goto, K., Kajihara, Y., Kosaka, S., Koba, M., Nakanishi, Y., & Ogawa, K. 1988. Pregnancies after co-culture of cumulus cells with bovine embryos derived from in-vitro fertilization of in-vitro matured follicular oocytes. *J.Reprod.Fertil*., 83, (2) 753-758.

Goudet, G., Mugnier, S., Callebaut, I., & Monget, P. 2008. Phylogenetic analysis and identification of pseudogenes reveal a progressive loss of zona pellucida genes during evolution of vertebrates. *Biol.Reprod*., 78, (5) 796-806.

Gregory, L., Booth, A.D., Wells, C., & Walker, S.M. 1994. A study of the cumulus-corona cell complex in in-vitro fertilization and embryo transfer; a prognostic indicator of the failure of implantation. *Hum.Reprod*., 9, (7) 1308-1317.

Grzmil, P., Kim, Y., Shamsadin, R., Neesen, J., Adham, I.M., Heinlein, U.A., Schwarzer, U.J., & Engel, W. 2001. Human cyritestin genes (CYRN1 and CYRN2) are non-functional. *Biochem.J*., 357, (Pt 2) 551-556.

Gupta, S.K. & Bhandari, B. 2011. Acrosome reaction: relevance of zona pellucida glycoproteins. *Asian J.Androl.*, 13, (1) 97-105.

Gur, Y. & Breitbart, H. 2008. Protein synthesis in sperm: dialog between mitochondria and cytoplasm. *Mol.Cell Endocrinol*., 282, (1-2) 45-55.

Guraya, S.S. 1995. The comparative cell biology of accessory somatic (or Sertoli) cells in the animal testis. *Int.Rev.Cytol*., 160, 163-220.

Hagaman, J.R., Moyer, J.S., Bachman, E.S., Sibony, M., Magyar, P.L., Welch, J.E., Smithies, O., Krege, J.H., & O'Brien, D.A. 1998. Angiotensin-converting enzyme and male fertility. *Proc.Natl.Acad.Sci.U.S.A.,* 95, (5) 2552-2557.

Haidl, G. & Opper, C. 1997. Changes in lipids and membrane anisotropy in human spermatozoa during epididymal maturation. *Hum.Reprod*., 12, (12) 2720-2723.

Halaby, D.M., Poupon, A., & Mornon, J. 1999. The immunoglobulin fold family: sequence analysis and 3D structure comparisons. *Protein Eng.*, 12, (7) 563-571.

Hall, L. & Frayne, J. 1999. Non-functional fertility genes in humans: contributory factors in reduced male fertility? *Hum.Fertil.(Camb).*, 2, (1) 36-41.

Hammack's universe of ideas. Spermatogenesis. http://www.hammiverse.com/lectures/46/images2/Spermatogenesis%20copy.jpg . 2011. Accessed 1-7-2011.

Han, L., Monne, M., Okumura, H., Schwend, T., Cherry, A.L., Flot, D., Matsuda, T., & Jovine, L. 2010. Insights into egg coat assembly and egg-sperm interaction from the X-ray structure of full-length ZP3. *Cell.*, 143, (3) 404-415.

Hanrieder, J., Nyakas, A., Naessen, T., & Bergquist, J. 2008. Proteomic analysis of human follicular fluid using an alternative bottom-up approach. *J.Proteome.Res*., 7, (1) 443-449.

Hansen, C., Srikandakumar, A., & Downey, B.R. 1991. Presence of follicular fluid in the porcine oviduct and its contribution to the acrosome reaction. *Mol.Reprod.Dev*., 30, (2) 148-153.

Hanson, F.W. & Overstreet, J.W. 1981. The interaction of human spermatozoa with cervical mucus in vivo. *Am.J.Obstet.Gynecol*., 140, (2) 173-178.

Harper JK. 1994, "Gamete and zygote transport," *In The Physiology of Reproduction*, 2nd ed. Knobil E & Neill JD, eds., New York: Raven Press, pp. 123-185.

Harper, C.V. & Publicover, S.J. 2005. Reassessing the role of progesterone in fertilization--compartmentalized calcium signalling in human spermatozoa? *Hum.Reprod*., 20, (10) 2675-2680.

Harper, C.V., Barratt, C.L., & Publicover, S.J. 2004. Stimulation of human spermatozoa with progesterone gradients to simulate approach to the oocyte. Induction of [Ca(2+)](i) oscillations and cyclical transitions in flagellar beating. *J.Biol.Chem*., 279, (44) 46315-46325.

Harper, C.V., Barratt, C.L., Publicover, S.J., & Kirkman-Brown, J.C. 2006. Kinetics of the progesterone-induced acrosome reaction and its relation to intracellular calcium responses in individual human spermatozoa. *Biol.Reprod*., 75, (6) 933-939.

Harrison, R.A. & Gadella, B.M. 2005. Bicarbonate-induced membrane processing in sperm capacitation. *Theriogenology.*, 63, (2) 342-351.

Hasegawa, T., Harada, N., Ikeda, K., Ishii, T., Hokuto, I., Kasai, K., Tanaka, M., Fukuzawa, R., Niikawa, N., & Matsuo, N. 1999. Digynic triploid infant surviving for 46 days. *Am.J.Med.Genet*., 87, (4) 306-310.

Hassold, T. & Hunt, P. 2001. To err (meiotically) is human: the genesis of human aneuploidy. *Nat.Rev.Genet*., 2, (4) 280-291.

Hayashi, K., Kobayashi, T., Umino, T., Goitsuka, R., Matsui, Y., & Kitamura, D. 2002. SMAD1 signaling is critical for initial commitment of germ cell lineage from mouse epiblast. *Mech.Dev*., 118, (1-2) 99-109.

Henkel, R.R. & Schill, W.B. 2003. Sperm preparation for ART. *Reprod.Biol.Endocrinol*., 1, 108.

Hermo, L., Pelletier, R.M., Cyr, D.G., & Smith, C.E. 2010a. Surfing the wave, cycle, life history, and genes/proteins expressed by testicular germ cells. Part 1: background to spermatogenesis, spermatogonia, and spermatocytes. *Microsc.Res Tech*., 73, (4) 241-278.

Hermo, L., Pelletier, R.M., Cyr, D.G., & Smith, C.E. 2010b. Surfing the wave, cycle, life history, and genes/proteins expressed by testicular germ cells. Part 2: changes in spermatid organelles associated with development of spermatozoa. *Microsc.Res Tech*., 73, (4) 279-319.

Hermo, L., Pelletier, R.M., Cyr, D.G., & Smith, C.E. 2010c. Surfing the wave, cycle, life history, and genes/proteins expressed by testicular germ cells. Part 3: developmental changes in spermatid flagellum and cytoplasmic droplet and interaction of sperm with the zona pellucida and egg plasma membrane. *Microsc.Res Tech*., 73, (4) 320-363.

Hermo, L., Pelletier, R.M., Cyr, D.G., & Smith, C.E. 2010d. Surfing the wave, cycle, life history, and genes/proteins expressed by testicular germ cells. Part 4: intercellular bridges, mitochondria, nuclear envelope, apoptosis, ubiquitination, membrane/voltage-gated channels, methylation/acetylation, and transcription factors. *Microsc.Res Tech*., 73, (4) 364-408.

Hermo, L., Pelletier, R.M., Cyr, D.G., & Smith, C.E. 2010e. Surfing the wave, cycle, life history, and genes/proteins expressed by testicular germ cells. Part 5: intercellular junctions and contacts between germs cells and Sertoli cells and their regulatory interactions, testicular cholesterol, and genes/proteins associated with more than one germ cell generation. *Microsc.Res Tech*., 73, (4) 409-494.

Herrero, M.B., de, L.E., & Gagnon, C. 1999. Nitric oxide regulates human sperm capacitation and protein-tyrosine phosphorylation in vitro. *Biol.Reprod*., 61, (3) 575-581.

Herrmann, G. & Spanel-Borowski, K. 1998. A sparsely vascularised zone in the cortex of the bovine ovary. *Anat.Histol.Embryol*., 27, (3) 143-146.

HFEA. Code of Practice
http://www.hfea.gov.uk/docs/8th_Code_of_Practice.pdf [8th]. 2011. Accessed 5-4-2008.

HFEA. HFEA Quick facts about fertility
http://www.hfea.gov.uk/infertility-facts.html#1253 . 2008. Accessed 21-11-2010.

Ho, H.C. & Suarez, S.S. 2001. Hyperactivation of mammalian spermatozoa: function and regulation. *Reproduction*., 122, (4) 519-526.

Ho, H.C. & Suarez, S.S. 2003. Characterization of the intracellular calcium store at the base of the sperm flagellum that regulates hyperactivated motility. *Biol.Reprod*., 68, (5) 1590-1596.

Ho, H.C., Granish, K.A., & Suarez, S.S. 2002. Hyperactivated motility of bull sperm is triggered at the axoneme by Ca2+ and not cAMP. *Dev.Biol*., 250, (1) 208-217.

Holt, R. I. G. & Hanley, N. A. 2007, "The biological principles of endocrinology," Fifth edition.

Holt, W.V. & Fazeli, A. 2010. The oviduct as a complex mediator of mammalian sperm function and selection. *Mol.Reprod.Dev.*, 77, (11) 934-943.

Hong, S.J., Chiu, P.C., Lee, K.F., Tse, J.M., Ho, P.C., & Yeung, W.S. 2004. Establishment of a capillary-cumulus model to study the selection of sperm for fertilization by the cumulus oophorus. *Hum.Reprod*., 19, (7) 1562-1569.

Horan, A.H. & Bedford, J.M. 1972. Development of the fertilizing ability of spermatozoa in the epididymis of the Syrian hamster. *J.Reprod.Fertil*., 30, (3) 417-423.

Hovatta, O., Mikkola, M., Gertow, K., Stromberg, A.M., Inzunza, J., Hreinsson, J., Rozell, B., Blennow, E., Andang, M., & Ahrlund-Richter, L. 2003. A culture system using human foreskin fibroblasts as feeder cells allows production of human embryonic stem cells. *Hum.Reprod*., 18, (7) 1404-1409.

Hubner, K., Fuhrmann, G., Christenson, L.K., Kehler, J., Reinbold, R., De La Fuente, R., Wood, J., Strauss, J.F., III, Boiani, M., & Scholer, H.R. 2003. Derivation of oocytes from mouse embryonic stem cells. *Science.*, 300, (5623) 1251-1256.

Huckins, C. & Clermont, Y. 1968. Evolution of gonocytes in the rat testis during late embryonic and early post-natal life. *Arch.Anat.Histol.Embryol*., 51, (1) 341-354.

Huey, S., Abuhamad, A., Barroso, G., Hsu, M.I., Kolm, P., Mayer, J., & Oehninger, S. 1999. Perifollicular blood flow Doppler indices, but not follicular pO2, pCO2, or pH, predict oocyte developmental competence in in vitro fertilization. *Fertil.Steril*., 72, (4) 707-712.

Hung, P.H. & Suarez, S.S. 2010. Regulation of sperm storage and movement in the ruminant oviduct. *Soc.Reprod.Fertil.Suppl.*, 67, 257-266.

Ignotz, G.G., Lo, M.C., Perez, C.L., Gwathmey, T.M., & Suarez, S.S. 2001. Characterization of a fucose-binding protein from bull sperm and seminal plasma that may be responsible for formation of the oviductal sperm reservoir. *Biol.Reprod*., 64, (6) 1806-1811.

Ikawa, M., Nakanishi, T., Yamada, S., Wada, I., Kominami, K., Tanaka, H., Nozaki, M., Nishimune, Y., & Okabe, M. 2001. Calmegin is required for fertilin alpha/beta heterodimerization and sperm fertility. *Dev.Biol*., 240, (1) 254-261.

Ikawa, M., Wada, I., Kominami, K., Watanabe, D., Toshimori, K., Nishimune, Y., & Okabe, M. 1997. The putative chaperone calmegin is required for sperm fertility. *Nature*., 387, (6633) 607-611.

Ikenishi, K. 1998. Germ plasm in Caenorhabditis elegans, Drosophila and Xenopus. *Dev.Growth Differ*., 40, (1) 1-10.

Inoue, N., Ikawa, M., Isotani, A., & Okabe, M. 2005. The immunoglobulin superfamily protein Izumo is required for sperm to fuse with eggs. *Nature*., 434, (7030) 234-238.

Invitrogen. pcDNA4 His Max B polyliner. http://tools.invitrogen.com/content/sfs/vectors/pcdna4hismaxb_mcs.pdf . 2011a. Accessed 1-1-2011.

Invitrogen. pcDNA4 His Max DNA sequence. http://tools.invitrogen.com/content/sfs/vectors/pcdna4hismaxb_seq.txt . 2011b. Accessed 1-1-2011.

Invitrogen. pcDNA4 HisMax vector map. http://tools.invitrogen.com/content/sfs/vectors/pcdna4hismax_map.pdf . 2011c. Accessed 1-1-2011.

Ivic, A., Onyeaka, H., Girling, A., Brewis, I.A., Ola, B., Hammadieh, N., Papaioannou, S., & Barratt, C.L. 2002. Critical evaluation of methylcellulose as an alternative medium in sperm migration tests. *Hum.Reprod*., 17, (1) 143-149.

Izquierdo-Rico, M.J., Jimenez-Movilla, M., Llop, E., Perez-Oliva, A.B., Ballesta, J., Gutierrez-Gallego, R., Jimenez-Cervantes, C., & Aviles, M. 2009. Hamster zona pellucida is formed by four glycoproteins: ZP1, ZP2, ZP3, and ZP4. J.Proteome.Res., 8, (2) 926-941.

Jagannathan, S., Publicover, S.J., & Barratt, C.L. 2002. Voltage-operated calcium channels in male germ cells. *Reproduction*., 123, (2) 203-215.

Jaiswal, B.S., Tur-Kaspa, I., Dor, J., Mashiach, S., & Eisenbach, M. 1999. Human sperm chemotaxis: is progesterone a chemoattractant? *Biol.Reprod*., 60, (6) 1314-1319.

Jansen, R.P. 1980. Cyclic changes in the human fallopian tube isthmus and their functional importance. *Am.J.Obstet.Gynecol*., 136, (3) 292-308.

Jarkovska, K., Martinkova, J., Liskova, L., Halada, P., Moos, J., Rezabek, K., Gadher, S.J., & Kovarova, H. 2010. Proteome mining of human follicular fluid reveals a crucial role of complement cascade and key biological pathways in women undergoing in vitro fertilization. *J.Proteome.Res*., 9, (3) 1289-1301.

Jiang, J.Y., Macchiarelli, G., Miyabayashi, K., & Sato, E. 2002. Follicular microvasculature in the porcine ovary. *Cell Tissue Res.*, 310, (1) 93-101.

Jimenez-Gonzalez, C., Michelangeli, F., Harper, C.V., Barratt, C.L., & Publicover, S.J. 2006. Calcium signalling in human spermatozoa: a specialized 'toolkit' of channels, transporters and stores. *Hum.Reprod.Update*., 12, (3) 253-267.

Jin, M., Fujiwara, E., Kakiuchi, Y., Okabe, M., Satouh, Y., Baba, S.A., Chiba, K., & Hirohashi, N. 2011. Most fertilizing mouse spermatozoa begin their acrosome reaction before contact with the zona pellucida during in vitro fertilization. *Proc.Natl.Acad.Sci.U.S.A.*, 108, (12) 4892-4896.

Johnson, J., Bagley, J., Skaznik-Wikiel, M., Lee, H.J., Adams, G.B., Niikura, Y., Tschudy, K.S., Tilly, J.C., Cortes, M.L., Forkert, R., Spitzer, T., Iacomini, J., Scadden, D.T., & Tilly, J.L. 2005. Oocyte generation in adult mammalian ovaries by putative germ cells in bone marrow and peripheral blood. *Cell.*, 122, (2) 303-315.

Johnson, M. H. 2007a, "Ovarian Function in the Adult," *In Essential Reproduction*, 6th ed. pp. 80-101.

Johnson, M. H. 2007b, "Testicular function in the adult," *In Essential Reproduction*, 6th Edition ed. Blackwell Publishing, pp. 61-79.

Jones, R., Howes, E., Dunne, P.D., James, P., Bruckbauer, A., & Klenerman, D. 2010. Tracking diffusion of GM1 gangliosides and zona pellucida binding molecules in sperm plasma membranes following cholesterol efflux. *Dev.Biol*., 339, (2) 398-406.

Jones, R., James, P.S., Howes, L., Bruckbauer, A., & Klenerman, D. 2007. Supramolecular organization of the sperm plasma membrane during maturation and capacitation. *Asian J.Androl.*, 9, (4) 438-444.

Jovine, L., Darie, C.C., Litscher, E.S., & Wassarman, P.M. 2005. Zona pellucida domain proteins. *Annu.Rev.Biochem*., 74, 83-114.

Jovine, L., Qi, H., Williams, Z., Litscher, E.S., & Wassarman, P.M. 2004. A duplicated motif controls assembly of zona pellucida domain proteins. *Proc.Natl.Acad.Sci.U.S.A.*, 101, (16) 5922-5927.

Kaji, K., Oda, S., Shikano, T., Ohnuki, T., Uematsu, Y., Sakagami, J., Tada, N., Miyazaki, S., & Kudo, A. 2000. The gamete fusion process is defective in eggs of Cd9-deficient mice. *Nat.Genet*., 24, (3) 279-282.

Kanai, S., Kitayama, T., Yonezawa, N., Sawano, Y., Tanokura, M., & Nakano, M. 2008. Disulfide linkage patterns of pig zona pellucida glycoproteins ZP3 and ZP4. *Mol.Reprod.Dev*., 75, (5) 847-856.

Kang, W., Zhou, C., Koga, Y., & Baba, T. 2010. Hyaluronan-degrading activity of mouse sperm hyaluronidase is not required for fertilization? *J.Reprod.Dev*., 56, (1) 140-144.

Kapelnikov, A., Zelinger, E., Gottlieb, Y., Rhrissorrakrai, K., Gunsalus, K.C. & Heifetz, Y. 2008. Mating induces an immune response and developmental switch in the Drosophila oviduct. *Proc.Natl.Acad.Sci.U.S.A*., 105, (37) 13912-13917.

Karni, Z., Polishuk, W.Z., Adoni, A., & Diamant, Y. 1971. Newtonian viscosity of the human cervical mucus during the menstrual cycle. *Int.J.Fertil*., 16, (4) 185-188.

Kato, M., Yoshimura, S., Kokuzawa, J., Kitajima, H., Kaku, Y., Iwama, T., Shinoda, J., Kunisada, T., & Sakai, N. 2004. Hepatocyte growth factor promotes neuronal differentiation of neural stem cells derived from embryonic stem cells. *Neuroreport.*, 15, (1) 5-8.

Katz, D.F. & Vanagimachi, R. 1980. Movement characteristics of hamster spermatozoa within the oviduct. *Biol.Reprod*., 22, (4) 759-764.

Katz, D.F., Slade, D.A., & Nakajima, S.T. 1997. Analysis of pre-ovulatory changes in cervical mucus hydration and sperm penetrability. *Adv.Contracept*., 13, (2-3) 143-151.

Kawano, N., Kang, W., Yamashita, M., Koga, Y., Yamazaki, T., Hata, T., Miyado, K., & Baba, T. 2010. Mice lacking two sperm serine proteases, ACR and PRSS21, are subfertile, but the mutant sperm are infertile in vitro. *Biol.Reprod*., 83, (3) 359-369.

Kay, V.J. & Robertson, L. 1998. Hyperactivated motility of human spermatozoa: a review of physiological function and application in assisted reproduction. *Hum.Reprod.Update*., 4, (6) 776-786.

Kee, K., Angeles, V.T., Flores, M., Nguyen, H.N., & Reijo Pera, R.A. 2009. Human DAZL, DAZ and BOULE genes modulate primordial germ-cell and haploid gamete formation. *Nature.*, 462, (7270) 222-225.

Keller, G.M. 1995. In vitro differentiation of embryonic stem cells. *Curr.Opin.Cell Biol*., 7, (6) 862-869.

Kim, E., Baba, D., Kimura, M., Yamashita, M., Kashiwabara, S., & Baba, T. 2005. Identification of a hyaluronidase, Hyal5, involved in penetration of mouse sperm through cumulus mass. *Proc.Natl.Acad.Sci.U.S.A.*, 102, (50) 18028-18033.

Kim, E., Yamashita, M., Kimura, M., Honda, A., Kashiwabara, S., & Baba, T. 2008. Sperm penetration through cumulus mass and zona pellucida. *Int.J.Dev.Biol*., 52, (5-6) 677-682.

Kim, R.J. & Nam, J.S. 2011. OCT4 Expression Enhances Features of Cancer Stem Cells in a Mouse Model of Breast Cancer. *Lab Anim Res.*, 27, (2) 147-152.

Kimura, M., Kim, E., Kang, W., Yamashita, M., Saigo, M., Yamazaki, T., Nakanishi, T., Kashiwabara, S., & Baba, T. 2009. Functional roles of mouse sperm hyaluronidases, HYAL5 and SPAM1, in fertilization. *Biol.Reprod*., 81, (5) 939-947.

Kinoshita, M., Rodler, D., Sugiura, K., Matsushima, K., Kansaku, N., Tahara, K., Tsukada, A., Ono, H., Yoshimura, T., Yoshizaki, N., Tanaka, R., Kohsaka, T., & Sasanami, T. 2010. Zona pellucida protein ZP2 is expressed in the oocyte of Japanese quail (Coturnix japonica). *Reproduction*., 139, (2) 359-371.

Kirkman-Brown, J.C., Bray, C., Stewart, P.M., Barratt, C.L., & Publicover, S.J. 2000. Biphasic elevation of [Ca(2+)](i) in individual human spermatozoa exposed to progesterone. *Dev.Biol*., 222, (2) 326-335.

Kirkman-Brown, J.C., Punt, E.L., Barratt, C.L., & Publicover, S.J. 2002. Zona pellucida and progesterone-induced Ca2+ signalling and acrosome reaction in human spermatozoa. *J.Androl.*, 23, (3) 306-315.

Kohn, M.J., Sztein, J., Yagi, R., DePamphilis, M.L., & Kaneko, K.J. 2010. The acrosomal protein Dickkopf-like 1 (DKKL1) facilitates sperm penetration of the zona pellucida. *Fertil.Steril*., 93, (5) 1533-1537.

Kolle, S., Reese, S. & Kummer, W. 2010. New aspects of gamete transport, fertilization, and embryonic development in the oviduct gained by means of live cell imaging. *Theriogenology.*, 73, (6) 786-795.

Koubova, J., Menke, D.B., Zhou, Q., Capel, B., Griswold, M.D., & Page, D.C. 2006. Retinoic acid regulates sex-specific timing of meiotic initiation in mice. *Proc.Natl.Acad.Sci.U.S.A.*, 103, (8) 2474-2479.

Kumar, T.R., Wang, Y., Lu, N., & Matzuk, M.M. 1997. Follicle stimulating hormone is required for ovarian follicle maturation but not male fertility. *Nat.Genet*., 15, (2) 201-204.

Lacham-Kaplan, O., Chy, H., & Trounson, A. 2006. Testicular cell conditioned medium supports differentiation of embryonic stem cells into ovarian structures containing oocytes. *Stem Cells.*, 24, (2) 266-273.

Lamb, J.D., Zamah, A.M., Shen, S., McCulloch, C., Cedars, M.I., & Rosen, M.P. 2010. Follicular fluid steroid hormone levels are associated with fertilization outcome after intracytoplasmic sperm injection. *Fertil.Steril*., 94, (3) 952-957.

Lancaster, J.R. 1997. A tutorial on the diffusibility and reactivity of free nitric oxide. *Nitric.Oxide*., 1, (1) 18-30.

Langlais, J., Kan, F.W., Granger, L., Raymond, L., Bleau, G., & Roberts, K.D. 1988. Identification of sterol acceptors that stimulate cholesterol efflux from human spermatozoa during in vitro capacitation. *Gamete Res.*, 20, (2) 185-201.

Laurent, T.C. & Fraser, J.R. 1992. Hyaluronan. *FASEB J.,* 6, (7) 2397-2404.

Lawson, K.A., Dunn, N.R., Roelen, B.A., Zeinstra, L.M., Davis, A.M., Wright, C.V., Korving, J.P., & Hogan, B.L. 1999. Bmp4 is required for the generation of primordial germ cells in the mouse embryo. *Genes Dev*., 13, (4) 424-436.

Le, L.D., Griveau, J.F., Le Pichon, J.P., & Quero, J.C. 1992. Effects of chamber depth on the motion pattern of human spermatozoa in semen or in capacitating medium. *Hum.Reprod*., 7, (10) 1417-1421.

Le, N.F., Rubinstein, E., Jasmin, C., Prenant, M., & Boucheix, C. 2000. Severely reduced female fertility in CD9-deficient mice. *Science.*, 287, (5451) 319-321.

Lee, K.F., Yao, Y.Q., Kwok, K.L., Xu, J.S. & Yeung, W.S. 2002. Early developing embryos affect the gene expression patterns in the mouse oviduct. *Biochem.Biophys.Res.Commun.*, 292, (2) 564-570.

Lee, W.S., Yoon, S.J., Yoon, T.K., Cha, K.Y., Lee, S.H., Shimasaki, S., Lee, S., & Lee, K.A. 2004. Effects of bone morphogenetic protein-7 (BMP-7) on primordial follicular growth in the mouse ovary. *Mol.Reprod.Dev*., 69, (2) 159-163.

Lefievre, L., Chen, Y., Conner, S.J., Scott, J.L., Publicover, S.J., Ford, W.C., & Barratt, C.L. 2007. Human spermatozoa contain multiple targets for protein S-nitrosylation: an alternative mechanism of the modulation of sperm function by nitric oxide? *Proteomics*., 7, (17) 3066-3084.

Lefievre, L., Conner, S.J., Salpekar, A., Olufowobi, O., Ashton, P., Pavlovic, B., Lenton, W., Afnan, M., Brewis, I.A., Monk, M., Hughes, D.C., & Barratt, C.L. 2004. Four zona pellucida glycoproteins are expressed in the human. *Hum.Reprod*., 19, (7) 1580-1586.

Lefievre, L., Machado-Oliveira, G., Ford, C., Kirkman-Brown, J., Barratt, C., & Publicover, S. 2009. Communication between female tract and sperm: Saying NO* when you mean yes. *Commun.Integr.Biol*., 2, (2) 82-85.

Lei, Z.M., Mishra, S., Zou, W., Xu, B., Foltz, M., Li, X., & Rao, C.V. 2001. Targeted disruption of luteinizing hormone/human chorionic gonadotropin receptor gene. *Mol.Endocrinol*., 15, (1) 184-200.

Lewis, S.E., Donnelly, E.T., Sterling, E.S., Kennedy, M.S., Thompson, W., & Chakravarthy, U. 1996. Nitric oxide synthase and nitrite production in human spermatozoa: evidence that endogenous nitric oxide is beneficial to sperm motility. *Mol.Hum.Reprod*., 2, (11) 873-878.

Lichty, J.J., Malecki, J.L., Agnew, H.D., Michelson-Horowitz, D.J., & Tan, S. 2011. Reprint of: Comparison of affinity tags for protein purification. *Protein Expr.Purif*.

Lin, Y., Mahan, K., Lathrop, W.F., Myles, D.G., & Primakoff, P. 1994. A hyaluronidase activity of the sperm plasma membrane protein PH-20 enables sperm to penetrate the cumulus cell layer surrounding the egg. *J.Cell Biol*., 125, (5) 1157-1163.

Long, E.L., Sonstegard, T.S., Long, J.A., Van Tassell, C.P. & Zuelke, K.A. 2003. Serial analysis of gene expression in turkey sperm storage tubules in the presence and absence of resident sperm. *Biol.Reprod.*, 69, (2) 469-474.

Longo, F.J. 1985. Fine structure of the mammalian egg cortex. *Am.J.Anat*., 174, (3) 303-315.

Lopez, L.C., Bayna, E.M., Litoff, D., Shaper, N.L., Shaper, J.H., & Shur, B.D. 1985. Receptor function of mouse sperm surface galactosyltransferase during fertilization. *J.Cell Biol*., 101, (4) 1501-1510.

Lowenstein, J.E. & Cohen, A.I. 1964. Dry mass, lipid content and protein content of the intact and zona-free mouse ovum. *J.Embryol.Exp.Morphol*., 12, 113-121.

Lu, Q. & Shur, B.D. 1997. Sperm from beta 1,4-galactosyltransferase-null mice are refractory to ZP3-induced acrosome reactions and penetrate the zona pellucida poorly. *Development.*, 124, (20) 4121-4131.

Lubahn, D.B., Moyer, J.S., Golding, T.S., Couse, J.F., Korach, K.S., & Smithies, O. 1993. Alteration of reproductive function but not prenatal sexual development after insertional disruption of the mouse estrogen receptor gene. *Proc.Natl.Acad.Sci.U.S.A.*, 90, (23) 11162-11166.

MacGregor, G.R., Zambrowicz, B.P., & Soriano, P. 1995. Tissue non-specific alkaline phosphatase is expressed in both embryonic and extraembryonic lineages during mouse embryogenesis but is not required for migration of primordial germ cells. *Development.*, 121, (5) 1487-1496.

Machaca, K. 2010. Ca(2+) signaling, genes and the cell cycle. *Cell Calcium.*, 48, (5) 243-250.

Machado-Oliveira, G., Lefievre, L., Ford, C., Herrero, M.B., Barratt, C., Connolly, T.J., Nash, K., Morales-Garcia, A., Kirkman-Brown, J., & Publicover, S. 2008. Mobilisation of Ca2+ stores and flagellar regulation in human sperm by S-nitrosylation: a role for NO synthesised in the female reproductive tract. *Development.*, 135, (22) 3677-3686.

Maheshwari, A. & Fowler, P.A. 2008. Primordial follicular assembly in humans--revisited. *Zygote*., 16, (4) 285-296.

Maniatis, T. Fritsch, E, F. & Sambroot, J. 1982. *Molecular Cloning, a laboratory manual*.

Männikkö M., Törmälä R.M., Tuuri T., Haltia A., Martikainen H., Ala-Kokko L., Tapanainen J.S. & Lakkakorpi J.T. 2005. Association between sequence variations in genes encoding human zona pellucida glycoproteins and fertilization failure in IVF. *Hum Reprod.*, 20, (6) 1578-1585.

Marchant, J.S. & Parker, I. 2000. Functional interactions in Ca(2+) signalling over different time and distance scales. *J.Gen.Physiol.*, 116, (5) 691-696.

Marks, A.R. 1997. Intracellular calcium-release channels: regulators of cell life and death. *Am.J.Physiol.*, 272, (2 Pt 2) H597-H605.

Marquez, B. & Suarez, S.S. 2004. Different signalling pathways in bovine sperm regulate capacitation and hyperactivation. *Biol.Reprod*., 70, (6) 1626-1633.

Marquez, B. & Suarez, S.S. 2007. Bovine sperm hyperactivation is promoted by alkaline-stimulated Ca2+ influx. *Biol.Reprod*., 76, (4) 660-665.

Martinez, P. & Morros, A. 1996. Membrane lipid dynamics during human sperm capacitation. *Front Biosci*., 1, d103-d117.

Mattioli, M., Galeati, G., Bacci, M.L., & Seren, E. 1988. Follicular factors influence oocyte fertilizability by modulating the intercellular cooperation between cumulus cells and oocyte. *Gamete Res*., 21, (3) 223-232.

McGee, E., Spears, N., Minami, S., Hsu, S.Y., Chun, S.Y., Billig, H., & Hsueh, A.J. 1997. Preantral ovarian follicles in serum-free culture: suppression of apoptosis after activation of the cyclic guanosine 3',5'-monophosphate pathway and stimulation of growth and differentiation by follicle-stimulating hormone. *Endocrinology*, 138, (6) 2417-2424.

McGee, E.A. & Hsueh, A.J. 2000. Initial and cyclic recruitment of ovarian follicles. *Endocr.Rev*., 21, (2) 200-214.

Memili, E., Peddinti, D., Shack, L.A., Nanduri, B., McCarthy, F., Sagirkaya, H., & Burgess, S.C. 2007. Bovine germinal vesicle oocyte and cumulus cell proteomics. *Reproduction*., 133, (6) 1107-1120.

Mendoza, C., Cremades, N., Ruiz-Requena, E., Martinez, F., Ortega, E., Bernabeu, S., & Tesarik, J. 1999. Relationship between fertilization results after intracytoplasmic sperm injection, and intrafollicular steroid, pituitary hormone and cytokine concentrations. *Hum.Reprod*., 14, (3) 628-635.

Messana, J.M., Hwang, N.S., Coburn, J., Elisseeff, J.H., & Zhang, Z. 2008. Size of the embryoid body influences chondrogenesis of mouse embryonic stem cells. *J.Tissue Eng Regen.Med*., 2, (8) 499-506.

Michael, A.E. & Papageorghiou, A.T. 2008. Potential significance of physiological and pharmacological glucocorticoids in early pregnancy. *Hum.Reprod.Update*., 14, (5) 497-517.

Michael, A.E., Gregory, L., Piercy, E.C., Walker, S.M., Shaw, R.W., & Cooke, B.A. 1995. Ovarian 11 beta-hydroxysteroid dehydrogenase activity is inversely related to the outcome of in vitro fertilization-embryo transfer treatment cycles. *Fertil.Steril*., 64, (3) 590-598.

Michael, A.E., Gregory, L., Walker, S.M., Antoniw, J.W., Shaw, R.W., Edwards, C.R., & Cooke, B.A. 1993. Ovarian 11 beta-hydroxysteroid dehydrogenase: potential predictor of conception by in-vitro fertilisation and embryo transfer. *Lancet.*, 342, (8873) 711-712.

Miyado, K., Yamada, G., Yamada, S., Hasuwa, H., Nakamura, Y., Ryu, F., Suzuki, K., Kosai, K., Inoue, K., Ogura, A., Okabe, M., & Mekada, E. 2000. Requirement of CD9 on the egg plasma membrane for fertilization. *Science.*, 287, (5451) 321-324.

Miyazaki, S. 1995. Calcium signalling during mammalian fertilization. *Ciba Found.Symp*., 188, 235-247.

Moller, C.C. & Wassarman, P.M. 1989. Characterization of a proteinase that cleaves zona pellucida glycoprotein ZP2 following activation of mouse eggs. *Dev.Biol*., 132, (1) 103-112.

Monne, M. & Jovine, L. 2011. A Structural View of Egg-Coat Architecture and Function in Fertilization. *Biol.Reprod*.

Mortimer, D. & Templeton, A.A. 1982. Sperm transport in the human female reproductive tract in relation to semen analysis characteristics and time of ovulation. *J.Reprod.Fertil*., 64, (2) 401-408.

Mortimer, D. 1994. *Pratical Laboratory Andrology*. New York, Oxford University Press.

Mortimer, D. 2000a. Sperm preparation methods. *J.Androl*, 21, (3) 357-366.

Mortimer, S.T. & Swan, M.A. 1999. Effect of image sampling frequency on established and smoothing-independent kinematic values of capacitating human spermatozoa. *Hum.Reprod*., 14, (4) 997-1004.

Mortimer, S.T. 1997. A critical review of the physiological importance and analysis of sperm movement in mammals. *Hum.Reprod.Update*., 3, (5) 403-439.

Mortimer, S.T. 2000b. CASA – practical aspects. *J Androl*., 21, (4) 515-524.

Motta, P.M., Makabe, S., Naguro, T., & Correr, S. 1994. Oocyte follicle cells association during development of human ovarian follicle. A study by high resolution scanning and transmission electron microscopy. *Arch.Histol.Cytol*., 57, (4) 369-394.

Motta, P.M., Nottola, S.A., Pereda, J., Croxatto, H.B., & Familiari, G. 1995. Ultrastructure of human cumulus oophorus: a transmission electron microscopic study on oviductal oocytes and fertilized eggs. *Hum.Reprod*., 10, (9) 2361-2367.

Mruk, D.D. & Cheng, C.Y. 2004. Cell-cell interactions at the ectoplasmic specialization in the testis. *Trends Endocrinol.Metab.*, 15, (9) 439-447.

Murray, S.C. & Smith, T.T. 1997. Sperm interaction with fallopian tube apical membrane enhances sperm motility and delays capacitation. *Fertil.Steril*., 68, (2) 351-357.

Myles, D.G. & Primakoff, P. 1997. Why did the sperm cross the cumulus? To get to the oocyte. Functions of the sperm surface proteins PH-20 and fertilin in arriving at, and fusing with, the egg. *Biol.Reprod*., 56, (2) 320-327.

Nagyova, E., Camaioni, A., Prochazka, R., & Salustri, A. 2004. Covalent transfer of heavy chains of inter-alpha-trypsin inhibitor family proteins to hyaluronan in in vivo and in vitro expanded porcine oocyte-cumulus complexes. *Biol.Reprod*., 71, (6) 1838-1843.

Nakanishi, T., Ikawa, M., Yamada, S., Parvinen, M., Baba, T., Nishimune, Y., & Okabe, M. 1999. Real-time observation of acrosomal dispersal from mouse sperm using GFP as a marker protein. *FEBS Lett*., 449, (2-3) 277-283.

Nakanishi, T., Ikawa, M., Yamada, S., Toshimori, K., & Okabe, M. 2001. Alkalinization of acrosome measured by GFP as a pH indicator and its relation to sperm capacitation. *Dev.Biol*., 237, (1) 222-231.

Nayernia, K., Nolte, J., Michelmann, H.W., Lee, J.H., Rathsack, K., Drusenheimer, N., Dev, A., Wulf, G., Ehrmann, I.E., Elliott, D.J., Okpanyi, V., Zechner, U., Haaf, T., Meinhardt, A., & Engel, W. 2006. In vitro-differentiated embryonic stem cells give rise to male gametes that can generate offspring mice. *Dev.Cell.*, 11, (1) 125-132.

Nayudu, P.L., Lopata, A., Jones, G.M., Gook, D.A., Bourne, H.M., Sheather, S.J., Brown, T.C., & Johnston, W.I. 1989. An analysis of human oocytes and follicles from stimulated cycles: oocyte morphology and associated follicular fluid characteristics. *Hum.Reprod*., 4, (5) 558-567.

Neal, P. & Baker, T.G. 1975. Response of mouse graafian follicles in organ culture to varying doses of follicle-stimulating hormone and luteinizing hormone. *J.Endocrinol*., 65, (1) 27-32.

Ni, Y., Zhou, Y., Chen, W.Y., Zheng, M., Yu, J., Li, C., Zhang, Y., & Shi, Q.X. 2009. HongrES1, a cauda epididymis-specific protein, is involved in capacitation of guinea pig sperm. *Mol.Reprod.Dev*., 76, (10) 984-993.

Nikolopoulou, M., Soucek, D.A., & Vary, J.C. 1985. Changes in the lipid content of boar sperm plasma membranes during epididymal maturation. *Biochim.Biophys.Acta.*, 815, (3) 486-498.

Nilsson, E.E. & Skinner, M.K. 2003. Bone morphogenetic protein-4 acts as an ovarian follicle survival factor and promotes primordial follicle development. *Biol.Reprod*., 69, (4) 1265-1272.

Nishimura, H., Kim, E., Nakanishi, T., & Baba, T. 2004. Possible function of the ADAM1a/ADAM2 Fertilin complex in the appearance of ADAM3 on the sperm surface. *J.Biol.Chem*., 279, (33) 34957-34962.

Nixon, B., Asquith, K.L., & John, A.R. 2005. The role of molecular chaperones in mouse sperm-egg interactions. *Mol.Cell Endocrinol*., 240, (1-2) 1-10.

Nixon, B., Bielanowicz, A., McLaughlin, E.A., Tanphaichitr, N., Ensslin, M.A., & Aitken, R.J. 2009. Composition and significance of detergent resistant membranes in mouse spermatozoa. *J.Cell Physiol.*, 218, (1) 122-134.

Noda, Y., Kohda, H., Takai, I., Hayashi, S., Shimada, H., Mori, T., & Tojo, S. 1983. Characterization of glycoproteins isolated from porcine zonae pellucidae. J.Reprod.Immunol., 5, (3) 161-172.

O'Brien, M.J., Pendola, J.K., & Eppig, J.J. 2003. A revised protocol for in vitro development of mouse oocytes from primordial follicles dramatically improves their developmental competence. *Biol.Reprod*., 68, (5) 1682-1686.

Ohinata, Y., Payer, B., O'Carroll, D., Ancelin, K., Ono, Y., Sano, M., Barton, S.C., Obukhanych, T., Nussenzweig, M., Tarakhovsky, A., Saitou, M., & Surani, M.A. 2005. Blimp1 is a critical determinant of the germ cell lineage in mice. *Nature.*, 436, (7048) 207-213.

Oko, R. & Maravei, D. 1995. Distribution and possible role of perinuclear theca proteins during bovine spermiogenesis. *Microsc.Res Tech*., 32, (6) 520-532.

Oktay, K., Briggs, D., & Gosden, R.G. 1997. Ontogeny of follicle-stimulating hormone receptor gene expression in isolated human ovarian follicles. *J.Clin.Endocrinol.Metab.*, 82, (11) 3748-3751.

Oktay, K., Newton, H., Mullan, J., & Gosden, R.G. 1998. Development of human primordial follicles to antral stages in SCID/hpg mice stimulated with follicle stimulating hormone. *Hum.Reprod*., 13, (5) 1133-1138.

Oktem, O. & Oktay, K. 2008. The ovary: anatomy and function throughout human life. *Ann.N.Y.Acad.Sci*., 1127, 1-9.

Oktem, O. & Urman, B. 2010. Understanding follicle growth in vivo. *Hum.Reprod*., 25, (12) 2944-2954.

Olds-Clarke, P. 1989. Sperm from tw32/+ mice: capacitation is normal, but hyperactivation is premature and nonhyperactivated sperm are slow. *Dev.Biol*., 131, (2) 475-482.

Oren-Benaroya, R., Orvieto, R., Gakamsky, A., Pinchasov, M., & Eisenbach, M. 2008. The sperm chemoattractant secreted from human cumulus cells is progesterone. *Hum.Reprod*., 23, (10) 2339-2345.

Osman, R.A., Andria, M.L., Jones, A.D., & Meizel, S. 1989. Steroid induced exocytosis: the human sperm acrosome reaction. *Biochem.Biophys.Res Commun*., 160, (2) 828-833.

O'Toole, C.M., Arnoult, C., Darszon, A., Steinhardt, R.A., & Florman, H.M. 2000. Ca(2+) entry through store-operated channels in mouse sperm is initiated by egg ZP3 and drives the acrosome reaction. *Mol.Biol.Cell.*, 11, (5) 1571-1584.

Overstreet, J.W. & Cooper, G.W. 1979. Effect of ovulation and sperm motility on the migration of rabbit spermatozoa to the site of fertilization. *J.Reprod.Fertil*., 55, (1) 53-59.

Owen, D.H. & Katz, D.F. 2005. A review of the physical and chemical properties of human semen and the formulation of a semen simulant. *J.Androl.*, 26, (4) 459-469.

Pang, P.C., Chiu, P.C., Lee, C.L., Chang, L.Y., Panico, M., Morris, H.R., Haslam, S.M., Khoo, K.H., Clark, G.F., Yeung, W.S., & Dell, A. 2011. Human Sperm Binding Is Mediated by the Sialyl-Lewisx Oligosaccharide on the Zona Pellucida. *Science*.

Papi, M., Brunelli, R., Sylla, L., Parasassi, T., Monaci, M., Maulucci, G., Missori, M., Arcovito, G., Ursini, F., & De, S.M. 2010. Mechanical properties of zona pellucida hardening. *Eur.Biophys.J*., 39, (6) 987-992.

Park, J., Cho, C.H., Parashurama, N., Li, Y., Berthiaume, F., Toner, M., Tilles, A.W., & Yarmush, M.L. 2007. Microfabrication-based modulation of embryonic stem cell differentiation. *Lab Chip*., 7, (8) 1018-1028.

Park, J.Y., Ahn, H.J., Gu, J.G., Lee, K.H., Kim, J.S., Kang, H.W., & Lee, J.H. 2003. Molecular identification of Ca2+ channels in human sperm. *Exp.Mol.Med*., 35, (4) 285-292.

Parte, S., Bhartiya, D., Telang, J., Daithankar, V., Salvi, V., Zaveri, K., & Hinduja, I. 2011. Detection, characterization, and spontaneous differentiation in vitro of very small embryonic-like putative stem cells in adult mammalian ovary. *Stem Cells Dev*., 20, (8) 1451-1464.

Patel, S.S., Beshay, V.E., Escobar, J.C., & Carr, B.R. 2010. 17alpha-Hydroxylase (CYP17) expression and subsequent androstenedione production in the human ovary. *Reprod.Sci*., 17, (11) 978-986.

Patrat, C., Serres, C., & Jouannet, P. 2000. The acrosome reaction in human spermatozoa. *Biol.Cell.*, 92, (3-4) 255-266.

Pellegrini, M., Grimaldi, P., Rossi, P., Geremia, R., & Dolci, S. 2003. Developmental expression of BMP4/ALK3/SMAD5 signaling pathway in the mouse testis: a potential role of BMP4 in spermatogonia differentiation. *J.Cell Sci*., 116, (Pt 16) 3363-3372.

Pesce, M., Wang, X., Wolgemuth, D.J., & Scholer, H. 1998. Differential expression of the Oct-4 transcription factor during mouse germ cell differentiation. *Mech.Dev*., 71, (1-2) 89-98.

Publicover, S., Harper, C.V., & Barratt, C. 2007. [Ca2+]i signalling in sperm--making the most of what you've got. *Nat.Cell Biol*., 9, (3) 235-242.

Publicover, S.J., Giojalas, L.C., Teves, M.E., de Oliveira, G.S., Garcia, A.A., Barratt, C.L., & Harper, C.V. 2008. Ca2+ signalling in the control of motility and guidance in mammalian sperm. *Front Biosci*., 13, 5623-5637.

Putney, J.W. 2001. Cell biology. Channelling calcium. *Nature.*, 410, (6829) 648-649.

Qing, T., Shi, Y., Qin, H., Ye, X., Wei, W., Liu, H., Ding, M., & Deng, H. 2007. Induction of oocyte-like cells from mouse embryonic stem cells by co-culture with ovarian granulosa cells. *Differentiation.*, 75, (10) 902-911.

Rajareddy, S., Reddy, P., Du, C., Liu, L., Jagarlamudi, K., Tang, W., Shen, Y., Berthet, C., Peng, S.L., Kaldis, P., & Liu, K. 2007. p27kip1 (cyclin-dependent kinase inhibitor 1B) controls ovarian development by suppressing follicle endowment and activation and promoting follicle atresia in mice. *Mol.Endocrinol*., 21, (9) 2189-2202.

Rankin, T. & Dean, J. 2000. The zona pellucida: using molecular genetics to study the mammalian egg coat. *Rev.Reprod*., 5, (2) 114-121.

Rankin, T.L., Coleman, J.S., Epifano, O., Hoodbhoy, T., Turner, S.G., Castle, P.E., Lee, E., Gore-Langton, R., & Dean, J. 2003. Fertility and taxon-specific sperm binding persist after replacement of mouse sperm receptors with human homologs. *Dev.Cell.*, 5, (1) 33-43.

Reddy, P., Liu, L., Adhikari, D., Jagarlamudi, K., Rajareddy, S., Shen, Y., Du, C., Tang, W., Hamalainen, T., Peng, S.L., Lan, Z.J., Cooney, A.J., Huhtaniemi, I., & Liu, K. 2008. Oocyte-specific deletion of Pten causes premature activation of the primordial follicle pool. *Science.*, 319, (5863) 611-613.

Reid, A.T., Redgrove, K., Aitken, R.J., & Nixon, B. 2011. Cellular mechanisms regulating sperm-zona pellucida interaction. *Asian J.Androl.*, 13, (1) 88-96.

Richards, J.S. & Pangas, S.A. 2010. The ovary: basic biology and clinical implications. *J.Clin.Invest.*, 120, (4) 963-972.

Richardson, B.E. & Lehmann, R. 2010. Mechanisms guiding primordial germ cell migration: strategies from different organisms. *Nat.Rev.Mol.Cell Biol*., 11, (1) 37-49.

Roberts, H.E., Saxe, D.F., Muralidharan, K., Coleman, K.B., Zacharias, J.F., & Fernhoff, P.M. 1996. Unique mosaicism of tetraploidy and trisomy 8: clinical, cytogenetic, and molecular findings in a live-born infant. *Am.J.Med.Genet*., 62, (3) 243-246.

Rodgers, R.J. & Irving-Rodgers, H.F. 2010a. Formation of the ovarian follicular antrum and follicular fluid. *Biol.Reprod*., 82, (6) 1021-1029.

Rodgers, R.J. & Irving-Rodgers, H.F. 2010b. Morphological classification of bovine ovarian follicles. *Reproduction*., 139, (2) 309-318.

Rodgers, R.J., Irving-Rodgers, H.F., van Wezel, I.L., Krupa, M., & Lavranos, T.C. 2001. Dynamics of the membrana granulosa during expansion of the ovarian follicular antrum. *Mol.Cell Endocrinol*., 171, (1-2) 41-48.

Rogers, B.J., Perreault, S.D., Bentwood, B.J., McCarville, C., Hale, R.W., & Soderdahl, D.W. 1983. Variability in the human-hamster in vitro assay for fertility evaluation. *Fertil.Steril*., 39, (2) 204-211.

Russell, D.L., Ochsner, S.A., Hsieh, M., Mulders, S., & Richards, J.S. 2003. Hormone-regulated expression and localization of versican in the rodent ovary. *Endocrinology.*, 144, (3) 1020-1031.

Saitou, M., Barton, S.C., & Surani, M.A. 2002. A molecular programme for the specification of germ cell fate in mice. *Nature.*, 418, (6895) 293-300.

Salicioni, A.M., Platt, M.D., Wertheimer, E.V., Arcelay, E., Allaire, A., Sosnik, J., & Visconti, P.E. 2007. Signalling pathways involved in sperm capacitation. *Soc.Reprod.Fertil.Suppl.*, 65, 245-259.

Saling, P.M. & Storey, B.T. 1979. Mouse gamete interactions during fertilization in vitro. Chlortetracycline as a fluorescent probe for the mouse sperm acrosome reaction. *J.Cell Biol*., 83, (3) 544-555.

Saling, P.M. 1982. Development of the ability to bind to zonae pellucidae during epididymal maturation: reversible immobilization of mouse-spermatozoa by lanthanum. *Biol.Reprod*., 26, (3) 429-436.

Salustri, A., Garlanda, C., Hirsch, E., De, A.M., Maccagno, A., Bottazzi, B., Doni, A., Bastone, A., Mantovani, G., Beck, P.P., Salvatori, G., Mahoney, D.J., Day, A.J., Siracusa, G., Romani, L., & Mantovani, A. 2004. PTX3 plays a key role in the organization of the cumulus oophorus extracellular matrix and in in vivo fertilization. *Development.*, 131, (7) 1577-1586.

Sasanami, T., Ohtsuki, M., Ishiguro, T., Matsushima, K., Hiyama, G., Kansaku, N., Doi, Y., & Mori, M. 2006. Zona Pellucida Domain of ZPB1 controls specific binding of ZPB1 and ZPC in Japanese quail (Coturnix japonica). *Cells Tissues.Organs.*, 183, (1) 41-52.

Sato, T., Kinoshita, M., Kansaku, N., Tahara, K., Tsukada, A., Ono, H., Yoshimura, T., Dohra, H., & Sasanami, T. 2009. Molecular characterization of egg envelope glycoprotein ZPD in the ovary of Japanese quail (Coturnix japonica). *Reproduction*., 137, (2) 333-343.

Scholer, H.R., Dressler, G.R., Balling, R., Rohdewohld, H., & Gruss, P. 1990. Oct-4: a germline-specific transcription factor mapping to the mouse t-complex. *EMBO J*., 9, (7) 2185-2195.

Seki, Y., Yamaji, M., Yabuta, Y., Sano, M., Shigeta, M., Matsui, Y., Saga, Y., Tachibana, M., Shinkai, Y., & Saitou, M. 2007. Cellular dynamics associated with the genome-wide epigenetic reprogramming in migrating primordial germ cells in mice. *Development.*, 134, (14) 2627-2638.

Serizawa, M., Kinoshita, M., Rodler, D., Tsukada, A., Ono, H., Yoshimura, T., Kansaku, N., & Sasanami, T. 2011. Oocytic expression of zona pellucida protein ZP4 in Japanese quail (Coturnix japonica). *Anim Sci.J.*, 82, (2) 227-235.

Seytanoglu, A., Georgiou, A.S., Sostaric, E., Watson, P.F., Holt, W.V. & Fazeli, A. 2008. Oviductal cell proteome alterations during the reproductive cycle in pigs. *J.Proteome.Res.*, 7, (7) 2825-2833.

Shamsadin, R., Adham, I.M., Nayernia, K., Heinlein, U.A., Oberwinkler, H., & Engel, W. 1999. Male mice deficient for germ-cell cyritestin are infertile. *Biol.Reprod*., 61, (6) 1445-1451.

Sherard, J., Bean, C., Bove, B., DelDuca, V., Jr., Esterly, K.L., Karcsh, H.J., Munshi, G., Reamer, J.F., Suazo, G. & Wilmoth, D. 1986. Long survival in a 69,XXY triploid male. *Am.J.Med.Genet*., 25, (2) 307-312.

Shi, S., Williams, S.A., Seppo, A., Kurniawan, H., Chen, W., Ye, Z., Marth, J.D., & Stanley, P. 2004. Inactivation of the Mgat1 gene in oocytes impairs oogenesis, but embryos lacking complex and hybrid N-glycans develop and implant. *Mol.Cell Biol*., 24, (22) 9920-9929.

Shivaji, S., Kumar, V., Mitra, K., & Jha, K.N. 2007. Mammalian sperm capacitation: role of phosphotyrosine proteins. *Soc.Reprod.Fertil.Suppl.*, 63, 295-312.

Shur, B.D. & Hall, N.G. 1982. A role for mouse sperm surface galactosyltransferase in sperm binding to the egg zona pellucida. J.Cell Biol., 95, (2 Pt 1) 574-579.

Siiteri, J.E., Dandekar, P., & Meizel, S. 1988. Human sperm acrosome reaction-initiating activity associated with the human cumulus oophorus and mural granulosa cells. *J.Exp.Zool*., 246, (1) 71-80.

Silva, C., Wood, J.R., Salvador, L., Zhang, Z., Kostetskii, I., Williams, C.J., & Strauss, J.F., III 2009. Expression profile of male germ cell-associated genes in mouse embryonic stem cell cultures treated with all-trans retinoic acid and testosterone. *Mol.Reprod.Dev*., 76, (1) 11-21.

Simon, L. & Lewis, S.E. 2011. Sperm DNA damage or progressive motility: which one is the better predictor of fertilization in vitro? *Syst.Biol.Reprod.Med*., 57, (3) 133-138.

Smith, D.J., Gaffney, E.A., Gadelha, H., Kapur, N., & Kirkman-Brown, J.C. 2009. Bend propagation in the flagella of migrating human sperm, and its modulation by viscosity. *Cell Motil.Cytoskeleton.*, 66, (4) 220-236.

Smith, L.D. 1989. The induction of oocyte maturation: transmembrane signalling events and regulation of the cell cycle. *Development.*, 107, (4) 685-699.

Solc, P., Schultz, R.M., & Motlik, J. 2010. Prophase I arrest and progression to metaphase I in mouse oocytes: comparison of resumption of meiosis and recovery from G2-arrest in somatic cells. *Mol.Hum.Reprod*., 16, (9) 654-664.

Soyal, S.M., Amleh, A., & Dean, J. 2000. FIGalpha, a germ cell-specific transcription factor required for ovarian follicle formation. *Development.*, 127, (21) 4645-4654.

Spehr, M., Gisselmann, G., Poplawski, A., Riffell, J.A., Wetzel, C.H., Zimmer, R.K., & Hatt, H. 2003. Identification of a testicular odorant receptor mediating human sperm chemotaxis. *Science.*, 299, (5615) 2054-2058.

Stahlberg, A., Bengtsson, M., Hemberg, M., & Semb, H. 2009. Quantitative transcription factor analysis of undifferentiated single human embryonic stem cells. *Clin.Chem*., 55, (12) 2162-2170.

Stein, K.K., Primakoff, P., & Myles, D. 2004. Sperm-egg fusion: events at the plasma membrane. *J.Cell Sci*., 117, (Pt 26) 6269-6274.

Strunker, T., Goodwin, N., Brenker, C., Kashikar, N.D., Weyand, I., Seifert, R., & Kaupp, U.B. 2011. The CatSper channel mediates progesterone-induced Ca2+ influx in human sperm. *Nature.*, 471, (7338) 382-386.

Suarez, S.S. & Osman, R.A. 1987. Initiation of hyperactivated flagellar bending in mouse sperm within the female reproductive tract. *Biol.Reprod*., 36, (5) 1191-1198.

Suarez, S.S. 2008. Control of hyperactivation in sperm. *Hum.Reprod.Update*., 14, (6) 647-657.

Sun, F., Bahat, A., Gakamsky, A., Girsh, E., Katz, N., Giojalas, L.C., Tur-Kaspa, I., & Eisenbach, M. 2005. Human sperm chemotaxis: both the oocyte and its surrounding cumulus cells secrete sperm chemoattractants. *Hum.Reprod*., 20, (3) 761-767.

Sun, Q.Y. 2003. Cellular and molecular mechanisms leading to cortical reaction and polyspermy block in mammalian eggs. *Microsc.Res Tech*., 61, (4) 342-348.

Tarlatzis, B.C., Pazaitou, K., Bili, H., Bontis, J., Papadimas, J., Lagos, S., Spanos, E., & Mantalenakis, S. 1993. Growth hormone, oestradiol, progesterone and testosterone concentrations in follicular fluid after ovarian stimulation with various regimes for assisted reproduction. *Hum.Reprod*., 8, (10) 1612-1616.

Teves, M.E., Barbano, F., Guidobaldi, H.A., Sanchez, R., Miska, W., & Giojalas, L.C. 2006. Progesterone at the picomolar range is a chemoattractant for mammalian spermatozoa. *Fertil.Steril*., 86, (3) 745-749.

The University of Jerusalem. SPR technology. http://bio.huji.ac.il/eng/services.asp?cat=120&in=0. 2011. Accessed 1-1-2009.

Thomas, P. & Meizel, S. 1989. Phosphatidylinositol 4,5-bisphosphate hydrolysis in human sperm stimulated with follicular fluid or progesterone is dependent upon Ca2+ influx. *Biochem.J*., 264, (2) 539-546.

Thomas, P.G., Ignotz, G.G., Ball, B.A., Brinsko, S.P. & Currie, W.B. 1995b. Effect of coculture with stallion spermatozoa on de novo protein synthesis and secretion by equine oviduct epithelial cells. *Am.J.Vet.Res.*, 56, (12) 1657-1662.

Thomson, J.A., Itskovitz-Eldor, J., Shapiro, S.S., Waknitz, M.A., Swiergiel, J.J., Marshall, V.S., & Jones, J.M. 1998. Embryonic stem cell lines derived from human blastocysts. *Science.*, 282, (5391) 1145-1147.

Tollner, T.L., Yudin, A.I., Treece, C.A., Overstreet, J.W., & Cherr, G.N. 2008. Macaque sperm coating protein DEFB126 facilitates sperm penetration of cervical mucus. *Hum.Reprod*., 23, (11) 2523-2534.

Tormala, R.M., Jaaskelainen, M., Lakkakorpi, J., Liakka, A., Tapanainen, J.S., & Vaskivuo, T.E. 2008. Zona pellucida components are present in human fetal ovary before follicle formation. *Mol.Cell Endocrinol*., 289, (1-2) 10-15.

Toyooka, Y., Tsunekawa, N., Akasu, R., & Noce, T. 2003. Embryonic stem cells can form germ cells in vitro. *Proc.Natl.Acad.Sci.U.S.A.*, 100, (20) 11457-11462.

Tremblay, K.D., Dunn, N.R., & Robertson, E.J. 2001. Mouse embryos lacking Smad1 signals display defects in extra-embryonic tissues and germ cell formation. *Development.*, 128, (18) 3609-3621.

Tripathi, A., Kumar, K.V., & Chaube, S.K. 2010. Meiotic cell cycle arrest in mammalian oocytes. *J.Cell Physiol.*, 223, (3) 592-600.

Tsubamoto, H., Hasegawa, A., Nakata, Y., Naito, S., Yamasaki, N., & Koyama, K. 1999. Expression of recombinant human zona pellucida protein 2 and its binding capacity to spermatozoa. *Biol.Reprod*., 61, (6) 1649-1654.

Tulsiani, D.R., Abou-Haila, A., Loeser, C.R., & Pereira, B.M. 1998. The biological and functional significance of the sperm acrosome and acrosomal enzymes in mammalian fertilization. *Exp.Cell Res.*, 240, (2) 151-164.

Tunquist, B.J. & Maller, J.L. 2003. Under arrest: cytostatic factor (CSF)-mediated metaphase arrest in vertebrate eggs. *Genes Dev*., 17, (6) 683-710.

Turner, R.M. 2006. Moving to the beat: a review of mammalian sperm motility regulation. *Reprod.Fertil.Dev*., 18, (1-2) 25-38.

Urch, U.A. & Patel, H. 1991. The interaction of boar sperm proacrosin with its natural substrate, the zona pellucida, and with polysulfated polysaccharides. *Development.*, 111, (4) 1165-1172.

van den Berg-Bakker CA, Hagemeijer, A., Franken-Postma, E.M., Smit, V.T., Kuppen, P.J., van Ravenswaay Claasen, H.H., Cornelisse, C.J., & Schrier, P.I. 1993. Establishment and characterization of 7 ovarian carcinoma cell lines and one granulosa tumor cell line: growth features and cytogenetics. *Int.J.Cancer.*, 53, (4) 613-620.

van der Merwe, P.A. & Barclay, A.N. 1994. Transient intercellular adhesion: the importance of weak protein-protein interactions. Trends *Biochem.Sci*., 19, (9) 354-358.

van Wezel, I.L. & Rodgers, R.J. 1996. Morphological characterization of bovine primordial follicles and their environment in vivo. *Biol.Reprod*., 55, (5) 1003-1011.

van, D.M., Polman, J.E., De Breet, I.T., van, G.K., Bunschoten, H., Grootenhuis, A., Brindle, J., & Aitken, R.J. 1994. Recombinant human zona pellucida protein ZP3 produced by Chinese hamster ovary cells induces the human sperm acrosome reaction and promotes sperm-egg fusion. *Biol.Reprod*., 51, (4) 607-617.

Vazquez, M.H., Phillips, D.M., & Wassarman, P.M. 1989. Interaction of mouse sperm with purified sperm receptors covalently linked to silica beads. *J.Cell Sci*., 92 (Pt 4), 713-722.

Vignini, A., Turi, A., Giannubilo, S.R., Pescosolido, D., Scognamiglio, P., Zanconi, S., Silvi, C., Mazzanti, L., & Tranquilli, A.L. 2008. Follicular fluid nitric oxide (NO) concentrations in stimulated cycles: the relationship to embryo grading. *Arch.Gynecol.Obstet*., 277, (3) 229-232.

Villemure, M., Chen, H.Y., Kurokawa, M., Fissore, R.A., & Taketo, T. 2007. The presence of X- and Y-chromosomes in oocytes leads to impairment in the progression of the second meiotic division. *Dev.Biol*., 301, (1) 1-13.

Vincent, S.D., Dunn, N.R., Sciammas, R., Shapiro-Shalef, M., Davis, M.M., Calame, K., Bikoff, E.K., & Robertson, E.J. 2005. The zinc finger transcriptional repressor Blimp1/Prdm1 is dispensable for early axis formation but is required for specification of primordial germ cells in the mouse. *Development.*, 132, (6) 1315-1325.

Visconti, P.E. & Kopf, G.S. 1998. Regulation of protein phosphorylation during sperm capacitation. *Biol.Reprod*., 59, (1) 1-6.

Visconti, P.E., Bailey, J.L., Moore, G.D., Pan, D., Olds-Clarke, P., & Kopf, G.S. 1995. Capacitation of mouse spermatozoa. I. Correlation between the capacitation state and protein tyrosine phosphorylation. *Development.*, 121, (4) 1129-1137.

Visconti, P.E., Krapf, D., de la Vega-Beltran JL, Acevedo, J.J., & Darszon, A. 2011. Ion channels, phosphorylation and mammalian sperm capacitation. *Asian J.Androl.*, 13, (3) 395-405.

Visconti, P.E., Ning, X., Fornes, M.W., Alvarez, J.G., Stein, P., Connors, S.A., & Kopf, G.S. 1999. Cholesterol efflux-mediated signal transduction in mammalian sperm: cholesterol release signals an increase in protein tyrosine phosphorylation during mouse sperm capacitation. *Dev.Biol*., 214, (2) 429-443.

Vitt, U.A., McGee, E.A., Hayashi, M., & Hsueh, A.J. 2000. In vivo treatment with GDF-9 stimulates primordial and primary follicle progression and theca cell marker CYP17 in ovaries of immature rats. *Endocrinology.*, 141, (10) 3814-3820.

Voronina, E. & Wessel, G.M. 2003. The regulation of oocyte maturation. *Curr.Top.Dev.Biol*., 58, 53-110.

Wang, D., King, S.M., Quill, T.A., Doolittle, L.K., & Garbers, D.L. 2003. A new sperm-specific Na+/H+ exchanger required for sperm motility and fertility. *Nat.Cell Biol*., 5, (12) 1117-1122.

Wassarman, P.M. 1990. Regulation of mammalian fertilization by zona pellucida glycoproteins. *J.Reprod.Fertil.Suppl*., 42, 79-87.

Wassarman, P.M., Jovine, L., & Litscher, E.S. 2001. A profile of fertilization in mammals. *Nat.Cell Biol*., 3, (2) E59-E64.

Watanabe, H. & Kondoh, G. 2011. Mouse sperm undergo GPI-anchored protein release associated with lipid raft reorganization and acrosome reaction to acquire fertility. *J.Cell Sci*., 124, (Pt 15) 2573-2581.

Wen, X., Li, D., Tozer, A.J., Docherty, S.M., & Iles, R.K. 2010. Estradiol, progesterone, testosterone profiles in human follicular fluid and cultured granulosa cells from luteinized pre-ovulatory follicles. *Reprod.Biol.Endocrinol*., 8, 117.

White, D.R. & Aitken, R.J. 1989. Relationship between calcium, cyclic AMP, ATP, and intracellular pH and the capacity of hamster spermatozoa to express hyperactivated motility. *Gamete Res.*, 22, (2) 163-177.

Williams, S.A., Xia, L., Cummings, R.D., McEver, R.P., & Stanley, P. 2007. Fertilization in mouse does not require terminal galactose or N-acetylglucosamine on the zona pellucida glycans. *J.Cell Sci*., 120, (Pt 8) 1341-1349.

Wobus, A.M., Guan, K., Yang, H.T., & Boheler, K.R. 2002. Embryonic stem cells as a model to study cardiac, skeletal muscle, and vascular smooth muscle cell differentiation. *Methods Mol.Biol*., 185, 127-156.

Wolf, D.P., Blasco, L., Khan, M.A., & Litt, M. 1977. Human cervical mucus. II. Changes in viscoelasticity during the ovulatory menstrual cycle. *Fertil.Steril*., 28, (1) 47-52.

Wouters-Tyrou, D., Martinage, A., Chevaillier, P., & Sautiere, P. 1998. Nuclear basic proteins in spermiogenesis. *Biochimie.*, 80, (2) 117-128.

Wright, G.J. 2009. Signal initiation in biological systems: the properties and detection of transient extracellular protein interactions. *Mol.Biosyst*., 5, (12) 1405-1412.

Xia, J., Reigada, D., Mitchell, C.H., & Ren, D. 2007. CATSPER channel-mediated Ca2+ entry into mouse sperm triggers a tail-to-head propagation. *Biol.Reprod*., 77, (3) 551-559.

Yamada, O., Abe, M., Takehana, K., Hiraga, T., Iwasa, K., & Hiratsuka, T. 1995. Microvascular changes during the development of follicles in bovine ovaries: a study of corrosion casts by scanning electron microscopy. *Arch.Histol.Cytol*., 58, (5) 567-574.

Yamada, T., Yoshikawa, M., Kanda, S., Kato, Y., Nakajima, Y., Ishizaka, S., & Tsunoda, Y. 2002. In vitro differentiation of embryonic stem cells into hepatocyte-like cells identified by cellular uptake of indocyanine green. *Stem Cells.*, 20, (2) 146-154.

Yamaguchi, R., Muro, Y., Isotani, A., Tokuhiro, K., Takumi, K., Adham, I., Ikawa, M., & Okabe, M. 2009. Disruption of ADAM3 impairs the migration of sperm into oviduct in mouse. *Biol.Reprod*., 81, (1) 142-146.

Yamashita, M., Honda, A., Ogura, A., Kashiwabara, S., Fukami, K., & Baba, T. 2008. Reduced fertility of mouse epididymal sperm lacking Prss21/Tesp5 is rescued by sperm exposure to uterine microenvironment. *Genes Cells.*, 13, (10) 1001-1013.

Yanagimachi, R. 1970. The movement of golden hamster spermatozoa before and after capacitation. *J.Reprod.Fertil*., 23, (1) 193-196.

Yanagimachi, R. 1981, "Mechanisms of fertilisation in mammals," *In Fertilisation and embryonic development in vitro*, L. Mastroianni & J. D. Biggers, eds., New York: Plenum Press, pp. 81-182.

Yanagimachi, R. 1994. Fertility of mammalian spermatozoa: its development and relativity. *Zygote*., 2, (4) 371-372.

Yeung, W.S., Lee, K.F., Koistinen, R., Koistinen, H., Seppala, M., Ho, P.C., & Chiu, P.C. 2006. Roles of glycodelin in modulating sperm function. *Mol.Cell Endocrinol*., 250, (1-2) 149-156.

Yi, Y.J., Manandhar, G., Sutovsky, M., Zimmerman, S.W., Jonakova, V., van Leeuwen, F.W., Oko, R., Park, C.S., & Sutovsky, P. 2010. Interference with the 19S proteasomal regulatory complex subunit PSMD4 on the sperm surface inhibits sperm-zona pellucida penetration during porcine fertilization. *Cell Tissue Res.*, 341, (2) 325-340.

Ying, Y. & Zhao, G.Q. 2001. Cooperation of endoderm-derived BMP2 and extraembryonic ectoderm-derived BMP4 in primordial germ cell generation in the mouse. *Dev.Biol*., 232, (2) 484-492.

Ying, Y., Liu, X.M., Marble, A., Lawson, K.A., & Zhao, G.Q. 2000. Requirement of Bmp8b for the generation of primordial germ cells in the mouse. *Mol.Endocrinol*., 14, (7) 1053-1063.

Yoshinaga, K. & Toshimori, K. 2003. Organization and modifications of sperm acrosomal molecules during spermatogenesis and epididymal maturation. *Microsc.Res Tech*., 61, (1) 39-45.

Zanetti, N. & Mayorga, L.S. 2009. Acrosomal swelling and membrane docking are required for hybrid vesicle formation during the human sperm acrosome reaction. *Biol.Reprod*., 81, (2) 396-405.

Zhang, H., Vollmer, M., De, G.M., Litzistorf, Y., Ladewig, A., Durrenberger, M., Guggenheim, R., Miny, P., Holzgreve, W., & De, G.C. 2000. Characterization of an immortalized human granulosa cell line (COV434). *Mol.Hum.Reprod*., 6, (2) 146-153.

Zhao, M., Chang, C., Liu, Z., Chen, L.M., & Chen, Q. 2010. The level of vascular endothelial cell growth factor, nitric oxide, and endothelin-1 was correlated with ovarian volume or antral follicle counts: a potential predictor of pregnancy outcome in IVF. *Growth Factors.*, 28, (5) 299-305.

Zhao, M., Gold, L., Ginsberg, A.M., Liang, L.F., & Dean, J. 2002. Conserved furin cleavage site not essential for secretion and integration of ZP3 into the extracellular egg coat of transgenic mice. *Mol.Cell Biol*., 22, (9) 3111-3120.

Zhou, J., Kumar, T.R., Matzuk, M.M., & Bondy, C. 1997. Insulin-like growth factor I regulates gonadotropin responsiveness in the murine ovary. *Mol.Endocrinol*., 11, (13) 1924-1933.

Zvetkova, I., Apedaile, A., Ramsahoye, B., Mermoud, J.E., Crompton, L.A., John, R., Feil, R., & Brockdorff, N. 2005. Global hypomethylation of the genome in XX embryonic stem cells. *Nat.Genet*., 37, (11) 1274-1279.

Zwaka, T.P. & Thomson, J.A. 2005. A germ cell origin of embryonic stem cells? *Development.*, 132, (2) 227-233.